SEDIMENT BUDGET AND ESTUARINE CIRCULATION ON THE BRANTAS RIVER ESTUARY EAST-JAVA, INDONESIA

R. DIDIEK MOETARYONO

SEDIMENT BUDGET AND ESTUARINE CIRCULATION

ON THE BRANTAS RIVER ESTUARY EAST-JAVA, INDONESIA

BY

©R.DIDIEK MOETARIYONO, Civil Eng.

A THESIS SUBMITTED TO THE SCHOOL OF GRADUATE

STUDIES IN PARTIAL FULFILMENT OF THE

REQUIREMENTS FOR THE DEGREE OF

MASTER OF ENGINEERING

FACULTY OF ENGINEERING AND APPLIED SCIENCE

MEMORIAL UNIVERSITY OF NEWFOUNDLAND

AUGUST, 1992

ST. JOHN'S NEWFOUNDLAND CANADA

ISBN 0-315-82656-8

Abstract

The Brantas River with a catchment area of 12,000 sq km is the largest river in Eastern Java, Indonesia. Heavy monsoon rains create flooding and the sediment load is enhanced by fine volcanic ashes from Kelud Mountain, located in the middle of the drainage basin. Flood controls were placed on the river to minimize excessive floods Every year large quantities of sediment enter the estuary. Some settles within the estuary, particularly the deltaic region, but a significant portion flushes directly to the surf zone bordering the Madura strait. Much of this material is redistributed in estuary areas as the fresh water flow subsides.

Topographical changes caused by this sediment load became more significant after a manmade channel, the shortcut channel, was dredged to bypass the existing delta.

Field measurements and collation of existing data were carried out during the dry season of 1991. Data were collected relating to tides, sediments, waves, currents, topographical changes and fresh water discharge with a view to understanding sediment movement and budget in the estuary and any chronological sequences. Theoretical analyses were also conducted to evaluate sediment inflow by tidal and longshore currents, river mouth processes and delta growth.

The study has shown that significant changes have taken place, that the processes are ongoing and that the discharge capacity of the two main channels is decreasing. One

specific aspect of the study shows that since the dredged shortcut channel has been completed, the major delta growth has moved from the original river mouth to that of the shortcut channel. Consequently, new geometric formations of the surf zone have been developed. Now, the shortcut channel has become a main channel while the original river becomes shallower and narrower year by year.

Sedimentation in the estuary is an important aspect of flood and sediment ma· ment on the Brantas River. Further work is required to adequately determine the sediment budget and estuarine circulation to permit development in the Brantas estuary.

Acknowledgements

I wish to express my deepest gratitude to Dr. J.H. Allen and Dr.J.J Sharp, my Supervisors, by whom the supervision of this thesis and study was carried out. Without their guidance, advice and encouragement this study would not have been accomplished.

I would also like to thank Dr. C.A. Sharpe, the Associate Dean of the School of Graduate Studies and Dr.J.J Sharp, the Associate Dean of the Faculty of Engineering and Applied Science for the opportunity to study at Memorial University of Newfoundland.

Furthermore, I wish to say a special thank you to Dr. Leonard M. Lye, the Coordinator of CIDA students in Memorial University for his excellent direction of our study; and to Ir. Rusfandi Usman M.Eng and Ir.K.Marpaung Dipl.H.E, my Indonesian supervisors, for their invaluable assistance all the time during collecting data and field observation in Indonesia. And also to my wife and my children for their love and encouragement.

Finally, I wish to thank the staff of the Memorial University of Newfoundland, Huntsman Marine Science Centre and colleagues and friends in this course for their help and information.

R.Didiek Moetariyono
August 1992

Contents

List of Tables

List of Figures

List of Symbols and Abbreviations Used

Symbols/ Abbrev.	Description	Dimensions
A	Basin area	L^2
A	Cross section area	L^2
ASTM	The American Society for Testing and Materials	-
A_0	Tidal amplitude the river mouth	L
A_x	Tidal amplitude at distance x from the river mouth	L
b	Channel width	L
b_0	Channel width at the river mouth	L
b_x	Channel width at distance x from the river mouth	L
C	Chezy coefficient	$L^{1/2}/T$
C	Concentration of sediment	M/L^3
C	Wave celerity	L/T
C_g	Wave group celerity	L/T
C_{g0}	Group wave speed in deep water	L/T
C_l	Crenulation index	-
C_0	Individual wave speed in deep water	L/T
D	Discharge duration	T
d	Depth	L
d	Diameter of sediment particle	L
$d_f=d_i$	Depth of seaward limit of significant transport	L
d_{50}	Median diameter of sediment	L
E	Erosion rate	$M/L^2/T$
E	Wave energy	M/T^2
EL	Elevation	L
E_f	Energy flux of wave	ML/T^3
E_s	Estuarine Number	-
F	Ratio of tidal type	-
F_d	Densimetric Froude number	-
f	Run-off coefficient	-
g	Acceleration due to gravity	L/T^2
h	Water depth	L
h_0	Water depth from channel bed to the interface	L
h_1	Water depth from water surface to the interface	L
H	Wave height	L
HI	Hypsometric Integral	-

HHWL	High High Water Level (high water at spring tide condition)	L
H_f	Wave height after refraction and shoaling effects	L
H_{sb}	Significant breaking wave heights	L
H_{s50}	Mean significant wave height	L
H_o	Wave height at deep water	L
H'	Wave height after refraction	L
I	Rainfall intensity	L/T
I	Similarity integral for transverse velocity distribution at the jet expansion	-
I_w	Water Surface gradient	-
I_b	River bed slope	-
K	Degree of mixing	-
k	Friction coefficient	L^2/T
km	Kilometre	-
KP	Abbreviation of Kali Porong means Porong River	-
K_R	Refraction coefficient for waves	-
K_s	Shoaling coefficient for waves	-
L	Wave length	L
L_A	Intrusion length	L
L_m	Protrusion Length	L
L_s	Shoreline Length	L
LHWL	Low High Water Level (high water at neap tide condition)	L
M	Mean diameter of sediment particles	L
M	Erosion rate constant	T/L
M_d	Median diameter = d_{50} of sediment particles	L
M_ϕ	Mean phi diameter	L
MSL	Mean Sea Water Level	L
m	Meter	-
mm	Millimetre	-
m^3/s	Cubic meter per second	L^3/T
n	Manning coefficient	-
P_i	Protrusion index	-
P_l	Wave power	ML/T^3
P_{ls}	Wave power at breaking condition	ML/T^3
Q_s	Sediment discharge	L^3/T
$Q=Q_w$	Water discharge	L^3/T
Q_{max}	Maximum daily run-off	L^3/T
Q_o	Discharge at the river mouth	L^3/T
Q_f	Fresh water discharge	L^3/T
q_s	Suspended sediment rate	L^3/LT
q_w	Water discharge per unit width	L^3/LT
q_B	Bed load rate	L^3/LT
R	Hydraulic radius	L
R_d	Densimetric Reynolds number	-
R_{max}	maximum daily rainfall	L

R_n	Reynolds number	-
R_t	Stability correction factor of windspeed	-
RL	Correction factor of windspeed over land and water	-
S	Salinity (part per thousand)	ppt
SHR	Surabaya Harbour Reference	L
$SHVP$	Surabaya Horizontal Voer Peil (Reference of Height)	L
S_a	Annual sediment inflow	L^3
S_k	Degree of skewness	-
S_q	Sediment carrying capacity	L^3/T
T	Return period	T^{-1}
T	Tidal period	T
T	Temperature	°C
T_s	Significant wave period	T
$T_{s\,avg}$	Mean Significant wave period	T
t	Time	T
U	Mean tidal current	L/T
U	Wind speed	L/T
U_A	Windstress factor	L/T
$USCS$	The Unified Soils Classification System	-
$U_{max(-d)}$	Peak near-bottom velocity	L/T
$U_{(z)}$	Wind speed at elevation Z	L/T
$U_{(10)}$	Wind speed at elevation of 10 m	L/T
U_t	Windspeed at duration (t)	L/T
$U_{3,600}$	Windspeed of 1-hour duration	L/T
u_*	Shear velocity of fluid	L/T
V_d	Densimetric velocity	L/T
V_r	Mean velocity of river flow	L/T
V_r	Sediment distribution on the right side of the river mouth axis	-
V_l	Sediment distribution on the left side of the river mouth axis	-
W	Delta width	L
α	Angle between shoreline and wave crest in deep water	o
α_b	Angle between shoreline and wave crest in breaker zone	o
γ	Specific weight of water	M/L^2T^2
γ_s	Specific weight of sediment	M/L^2T^2
γ	Density difference ratio = $1-(\rho_f/\rho_s)$	-
$\Delta\rho$	Different density	M/L^3
ϵ	Rate of expansion flow	-
η	wave height above mean tidal level	L
ν	Kinematic viscosity of water	L^2/T
ϕ	Sato-Kikkawa-Ashida factor	-
ρ	Mass density	M/L^3
ρ_f	Mass density of fresh water	M/L^3
ρ_m	Average density, $(\rho_s+\rho_f)/2$	M/L^3
ρ_s	Mass density of sediment material	M/L^3

ρ_s	Mass density of saline water	M/L^3
$\rho_{s,t}$	Density of the Water at Salinity (S) and temperature (T)	M/L^3
σ	Standard deviation	-
σ_H	Standard deviation of significant wave height	-
σ_t	Density index = $(\rho_{s,t} - 1)10^3$	-
τ	Shear stress	M/LT^2
τ_o	Bed shear stress = τ_b	M/LT^2
τ_c	Critical shear stress	M/LT^2

Chapter 1

Introduction

Chapter 1

Introduction

The Brantas River is located in the East Java Province, Indonesia (figure 1.1). With a drainage area of 12,000 square kilometres and a length of 320 kilometres (figure 1.2), the river is the second largest river on the island of Java. The population in the area was more than 10 million in 1988 excluding the population in Surabaya which is the capital city of East Java Province. This city is located in the lower reach of the river and has a population of about 3 million.

Along the middle and the lower reach of the river, the large fertile area and its inhabitants have always been threatened by annual flooding. Damage is aggravated by the sediment load carried by the Brantas during floods. Much of this sediment load is derived from volcanic ash from Kelut Mountain which erupts periodically every 15 to 20 years. This active volcanic mountain is located in the middle course of the drainage area (see figure 1.2). The effects of the settling of the sediment load cause major problems when it reaches the lower part of river where the energy gradient is very low. The sediment settles in this area and a delta is formed continuously seawards.

In its lower reaches, the Brantas River splits into two branches. The "Surabaya River branch is about 55 km long, flows through Surabaya city and debouches into the Madura Strait at north and east of Surabaya city. Another river branch called the Porong River is about 51 km long, flows directly down to the Madura Strait about 15 km south

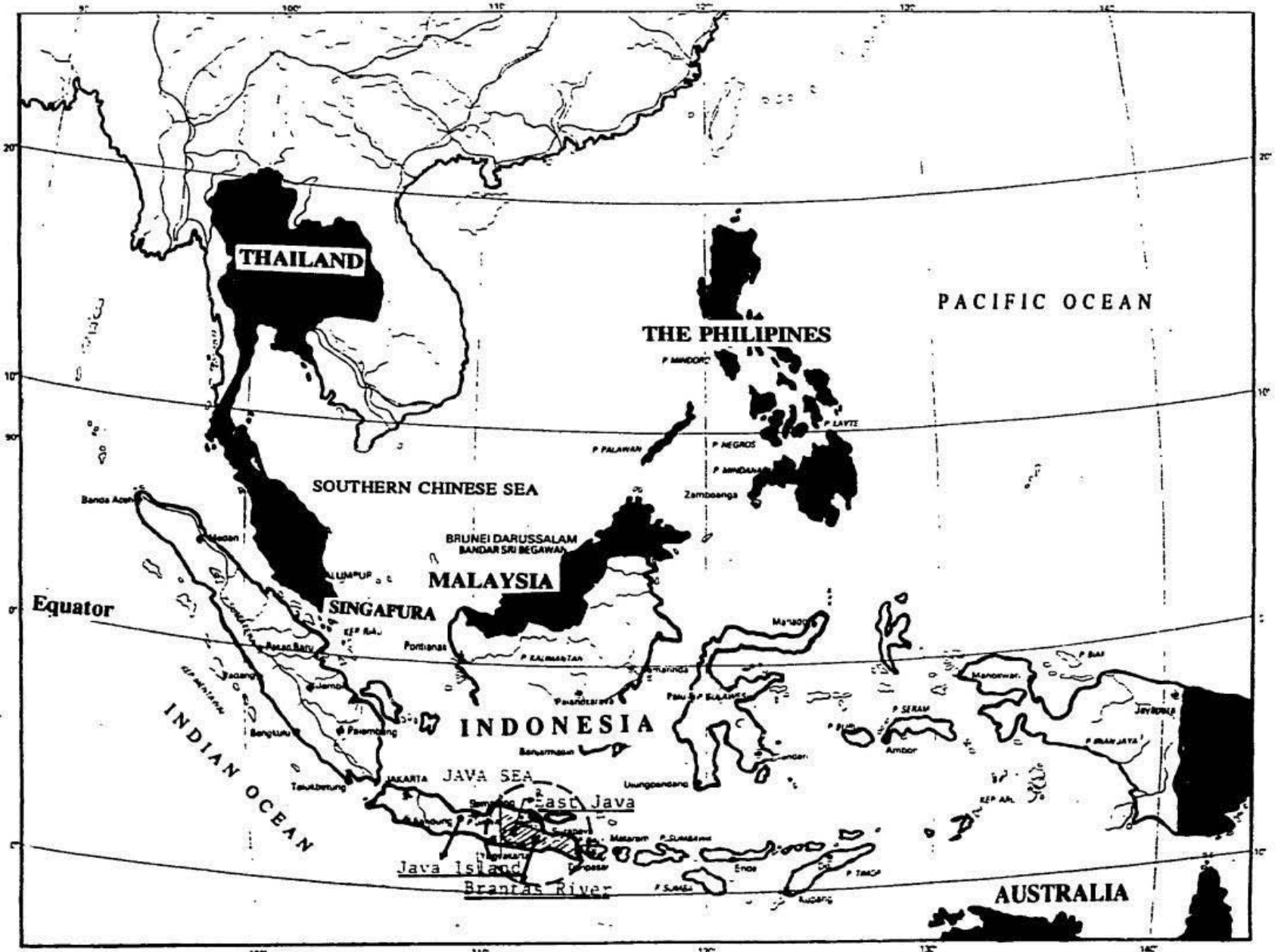

LOCATION MAP OF EAST-JAVA PROVINCE, INDONESIA

Figure 1.1

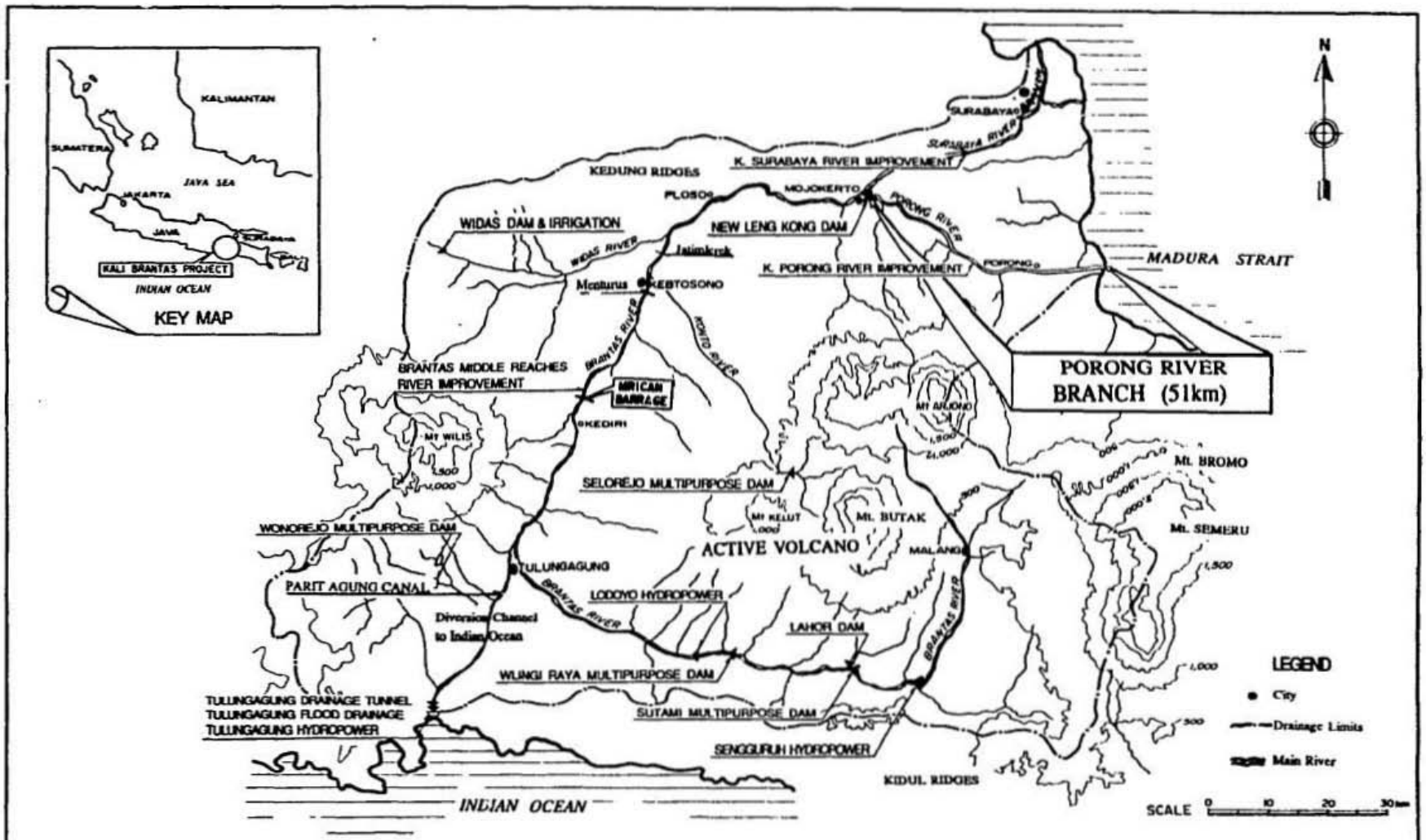

Fig.1.2 The Brantas River and Its Drainage Basin

of the Surabaya River mouth.

Originally, some control works to manage flood water and sediment discharge were carried out in the colonial age (before 1945), but these were minor compared to major control works which have been done during 1961 to 1990. The Surabaya River branch has been developed as the source of drinking and industrial water supply for Surabaya city while the Porong River branch is used as the flood diversion channel. The river discharges in both branches are regulated by the New Lengkong dam located at the point where the Brantas River splits into the Porong and the Surabaya River (see figure 1.2).

Since the function of the Porong River branch is to act as a flood control channel, the river and its estuary are extremely important. Both are affected by sedimentation. To increase the carrying capacity of the river, a shortcut channel was dredged in 1977 starting at 5 km from the coastline, to permit river water to be rapidly discharged to the sea (the Madura Strait). Since water flows continuously through this channel, the estuarine sedimentation process, the geometry of the shortcut channel and the adjacent surf zone have significantly changed. These changes have given rise to concerns about the effects of river discharge and its sediment, tide, currents and salinity intrusion.

This thesis looks at the conditions in the shortcut channel and the surf zone and what changes have taken place to date.

Chapter 2

Geographic Description of the Brantas River Basin

2.1 General Geographic Conditions

The Brantas river basin in East-Java lies between latitude 7°01' and 8°15' south and between longitude 110°30' and 112°55' east. The river is 320 kilometres in length and its basin area is 12,0000 square kilometres. The basin is bounded by Bromo Mountain (El.2,392 m) and Semeru Mountain (El.3,676 m) in the east, a series of Kidul ridges (El.300-500 m) in the south, Wilis Mountain (El.2,169 m) and its families in the west and Kedung ridges and Madura Strait in the north (see figure 1.2).

The Brantas River originates from the Arjuna Mountain complex consisting of Arjuna Mountain (El.3,339 m), Butak Mountain (2,868 m) and Kelud Mountain (El.1,731 m). These mountains are found in the centre of the basin. The river flows in a clockwise spiral course and goes down to the Madura Strait.

For most of its length, the river flows through a densely inhabited area. There are four big cities and many regency towns which had a total population of 13 million in 1988. Present land-use in the basin consists of 3,450 km^2 of rice field, 2.005 km^2 of upland field, 332 km^2 of plantations such as sugar cane, clove, and tobacco. 2,608 km^2 of forest, 2,396 km^2 of human settlement. The remaining area of 1,009 km^2 is largely unproductive forest. Since the basin is almost all very productive land, the Brantas River

production in Indonesia.

The main river course can be divided into three reaches; the upper, middle and lower reaches. In the upper reach, beginning from Arjuna Mountain, the river flows southward passing through the Malang Plateau at an elevation about 400 m SHVP (Surabaya Horizontal Voer Peil)[1]. About 20 kilometres southward from Malang, the river turns to the west and reaches the Sengguruh dam. River bed slopes to this point are generally steeper than 1/200. After Sengguruh dam, there are three dams in series: Sutami, Wlingi and Lodoyo dams. All four dams are multi purpose, used for flood control, irrigation, hydro electric power, fisheries and recreation.

After the Lodoyo dam, the river bed slope becomes much more gentle, averaging about 1/1,000. Many tributaries join the Brantas from the southern slope of Kelud Mountain. Kelud Mountain is an active volcano that erupts periodically every 15 to 20 years. A large amount of sediment will enter the Brantas River directly after the eruption of the volcano and the remainder of the volcanic material on the sloping mountain will be brought routinely by rain to the river.

The river flows continuously westward up to the Parit Agung canal, then it turns northward. Parit Agung canal is a diversion channel constructed to reduce flooding by diverting some of the discharge to the Indian Ocean to the south. This point can be judged as the beginning of the middle reaches. The river bed slope is still about 1/1000. There are three irrigation dams: Mrican Barrage, and two inflatable dams, Menturus and

[1] 0.00 m SHVP is equivalent to +0.90 m above Mean Sea Level

dam at Mojokerto city which is the beginning of the lower reaches.

The total catchment area above the New Lengkong dam site is about 8,650 Km^2 and the average riverbed slope from this place down to the sea is about 1/1,500 to 1/3,500. In this area the Brantas river divides into the Porong and Surabaya river branches. Both branches debouch into the Madura Strait. The Surabaya estuary is located at the north and east of Surabaya city while the Porong estuary is located south of the Surabaya river estuary in the corner of the Porong bay.

The Porong and Surabaya river branches flow through a very flat plain lower than 25 m, SHVP elevation. The Porong river branch is used as a flood diversion canal in the rainy season while the Surabaya river branch is maintained as a drinking and industrial water supply for Surabaya Metropolitan area throughout the year. This study of sediment problems and estuarine circulation on the Brantas river focuses on the Porong river branch and its estuary rather than the Surabaya branch.

2.2 Climatic Conditions and Water Discharge

The climatic conditions in the Brantas basin are dominated by the tropical monsoons. In normal years, the rainy season extends for about 6 months from November to April when the prevailing wind is from the west. There is also a marked dry season from May to October when the prevailing wind is from the east. There is little variation in temperature throughout the year. The yearly mean temperature in the basin ranges from 24°C in Malang to 27°C in Porong. The average annual rainfall over the basin is

2,000 mm, of which more than 80 % occurs in the rainy season.

Variation of annual rainfall is large; 2,958 mm in a wet year to 1,374 mm in a dry year. The average annual rainfall in the higher elevations is generally high. In some places the rainfall reaches 3,000 to 4,000 mm per annum especially in the southern and western slopes of Kelud Mountain. The yearly mean relative humidity over the whole basin ranges from 73 % to 82 %.

Although extremes of climate can be experienced, i.e. high rainfall intensities during the wet season and long drought periods during the dry season, there are no catastrophes resulting from weather alone. Java island, where the Brantas basin is located, does not lie in the area regularly affected by tropical cyclones and therefore very rarely experiences periods of storm activity such as occur in the Philippines.

Based on recording of discharge data carried out by the Brantas River Basin Development Office (later called the Brantas Office) from 1977 to 1988, the largest flood in the Brantas basin occurred on March 2 to 5, 1984. The peak discharges were 1,180 m^3/sec at Karangkates dam, 1,100 m^3/sec in the middle reach after the Parit Agung parit canal and 1,466 m^3/sec at Porong river. The gate of the Lengkong dam to the Surabaya river branch was closed totally to protect Surabaya city from the flood damage. The recorded discharge data of the Surabaya river at that time was 320 m^3/sec (at Perning station which is about 30 km downstream from the Lengkong dam). This discharge was obtained from the Surabaya river basin itself since eventually, the rain was distributed evenly over almost the whole of the Brantas drainage area.

Based on the gate operation guideline of the New Lengkong dam, the maximum

permitted discharge from the Brantas river to the Surabaya river branch is 115 m^3/sec. However, the actual water discharges released from the Lengkong dam to the Surabaya River branch depend largely on the flow conditions in the Surabaya River itself and also on the municipal and industrial water demand around the Surabaya metropolitan area. The schematic junction of the Brantas river at the lower reaches including the average and design discharges is shown in figure 2.1.

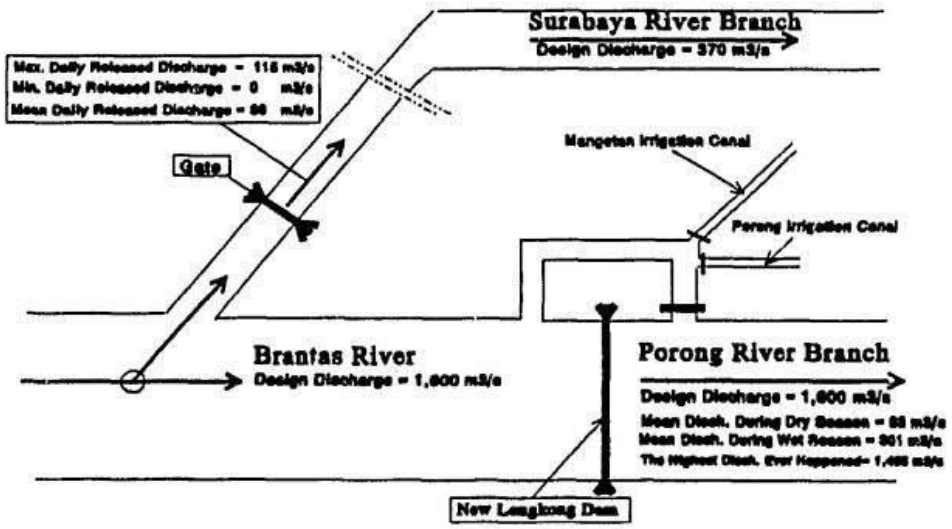

Fig.2.1 Schematic Junction of the Brantas River at the Beginning of the Lower Reaches

For determining annual sediment transport, mean and dominant discharges are also needed. The mean discharge in the Porong river branch is 301 m^3/sec in the rainy season and 63 m^3/sec in the dry season while the dominant discharge is 712 m^3/sec. The dominant discharge represents a value of the river discharge which produces the highest portion of the annual sediment rate passing through a river section. It is determined by the relationships between the annual frequency of the discharge and the carrying capacity of the sediment. A detailed explanation of this discharge is presented in section 6.2.2.

2.3 River Development and Porong Estuarine Geometry

Land and water resources development has been carried out for many years. The old Lengkong dam, for example, was constructed in 1857. Most of the existing irrigation and diking systems along the main stream, including along the Porong river, were constructed before the Dutch colonialists left in 1945. After 1960, the Brantas River Development has been promoted by the Asian Development Bank. An adequate flood control system has now been completed and can be used to maintain the 50 year probable flood along the Brantas river (1600 m^3/sec for the Porong river). River water can now be regulated effectively for irrigation, hydro power, drinking and industrial water supply.

The Porong river flows for about 51 kilometres from the New Lengkong dam to the sea and runs through the main rice growing area. Infrastructures such as highway and railway as well as many towns and villages are located along the river side. Good maintenance and improvement of the river are indispensable for the welfare of the people in the region. The basin map is shown in figure 2.2.

The whole river channel is formed with artificial levees on both banks which were improved during the period 1971 to 1977. Alignment of the river channel, in general, is fairly smooth. The minimum radius of curvature at the most sharp meander is 400 m. Based on data from measurement work in 1988, thalwegs or the deepest riverbed points were generally found in the middle of the channel. The river bed slope of Porong river was about 1/2,500 to 1/3,000 in the upper part and 1/3,500 in the lower part. The average elevation of riverbed, levee crown, and ground downstream of the

New Lengkong dam were around 13.50 m, 20.00 m, and 18.50 m, SHVP. Similar elevations at the river mouth were found to be of -3.30 m, 1.65 m and 0.50 m, SHVP, respectively.

Before 1970, the riverbed of the Porong river had shown a trend of aggradation due to sediment transported from upstream reaches year by year. The average rise in the riverbed is about 4 cm per annum. Kelud Mountain erupted recently in 1966 and provides the main source of the sediment. The river mouth of the Porong river had moved toward the sea by 300 m yearly, having formed its own delta. In the upper part of the river, the average of river width between both bank dikes is around 200 m. In the lower reach at about 14 km from the sea, the river width has become gradually wider up to about 500 m.

In 1977, an artificial channel was cut starting at about 5 km from the sea or upstream of the original river mouth. It is used as a bypass channel to accommodate rapid flood discharge to the sea. The river now branches into two: the original river and the shortcut river channel. At that time, the channel width was 80 m and the original distance from the starting point, namely the splitting point, to the existing shoreline was 1.1 km. Recently, the distance from the splitting point which is also named as KP.238 to the shortcut mouth has become much longer. It is now 3.4 km. Furthermore, the shortcut width also seems to get wider year by year. Measurements were taken in the dry season of 1991. The upper width of the shortcut channel, 1 km downstream of the split, was found to be 142 m, while the width of the channel 1 km upstream of the river mouth was 286 m.

At the same time, in 1991, the width of the original river channel was found to be narrower than that of the shortcut channel. It was found to be 70 m. In addition, sedimentation in the upper part of the original river, near the split, was found to be more significant than in the middle or lower part of the original river mouths. The sediment in the original river after the split was basically fine sand (d_{50}=0.39 mm) except in the upper area immediately after the split where the sediment was dominantly coarse sand (d_{50}=0.93 mm). At about 6 km downstream of the split, the original river split again into three branches. Naturally, they were narrower than the original main river channel and their length was less than 2 km from the split to the river mouths.

Tidal rise and fall occurs twice a day with unequal height. In the river mouth, the maximum tidal range between consecutive high and low water is about 2.02 m. The tides affect water elevations up to 27 km upstream from the river mouth.

Bathymetric features of the nearshore area show very gentle slopes, particularly in the dry season. The elevation of the nearshore area is higher than that of the shortcut or original river channel. Water depths at the estuary in the neap tide are about 0.30 m although many areas are dry. The neap tide line is found about 2.5 km from the shortcut mouth.

Delta growth is significant in the area surrounding the shortcut mouth. Briefly, the growth can be identified by comparison of the estuary topography in 1945 (figure 2.3) and estuary topography in 1977 - after the shortcut channel was completed - (figure 2.4), and a map which was made from an air photo taken in 1985 (figure 2.5 and figure 2.6).

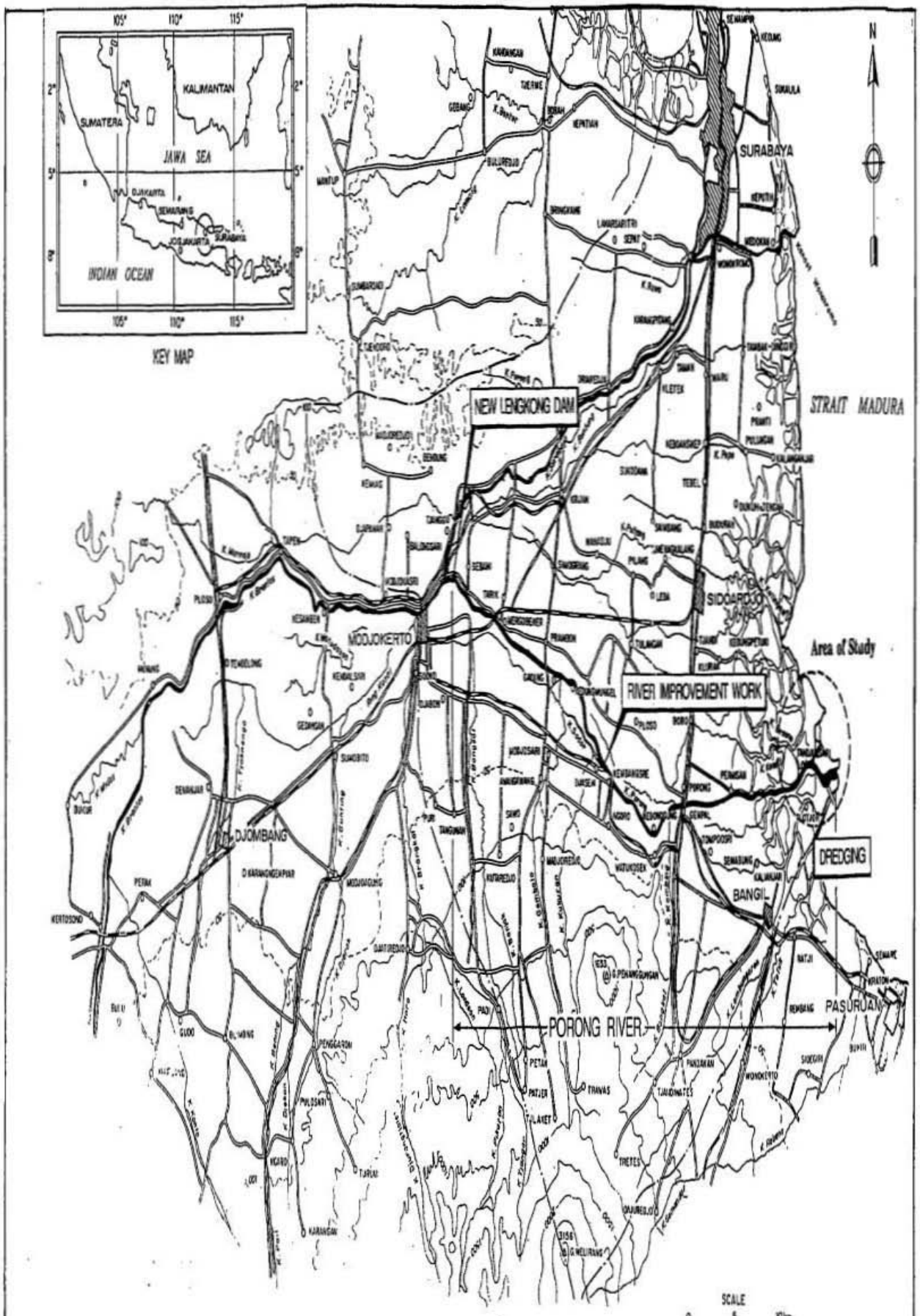

Fig. 2.2 Map of the Porong River Basin and Area of Study

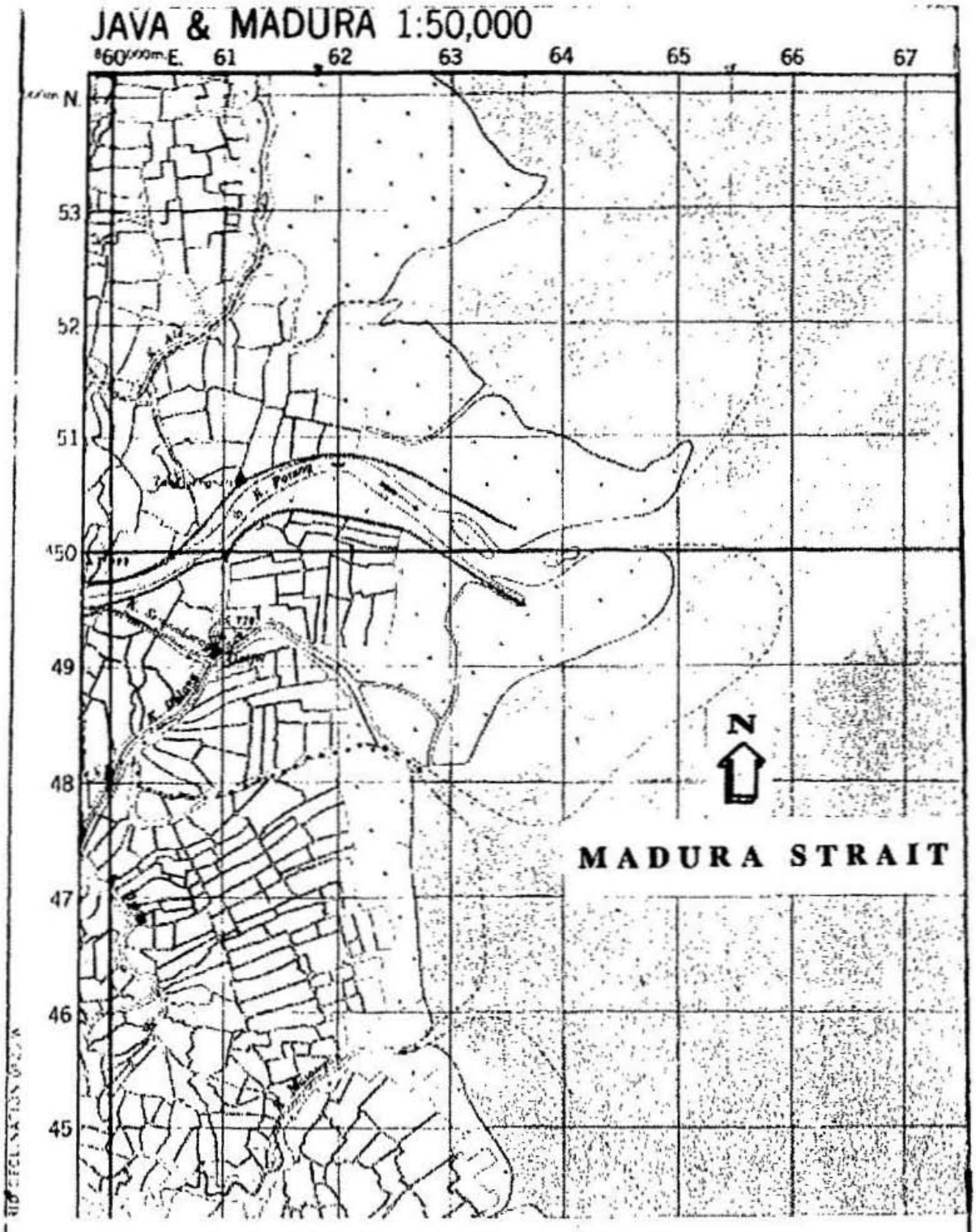

Fig. 2.3 Topographic Map of the Brantas River Delta 1945

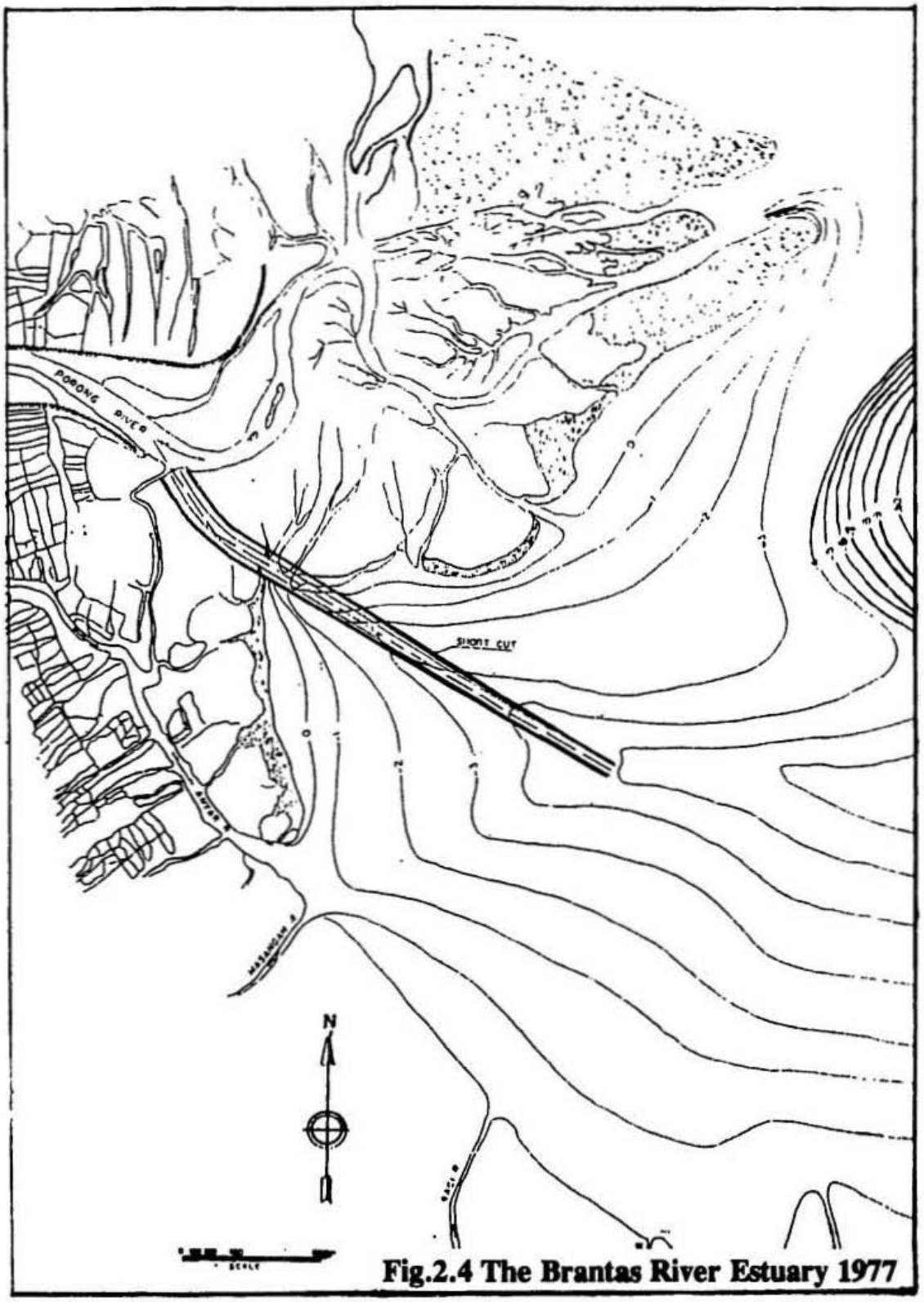

Fig.2.4 The Brantas River Estuary 1977

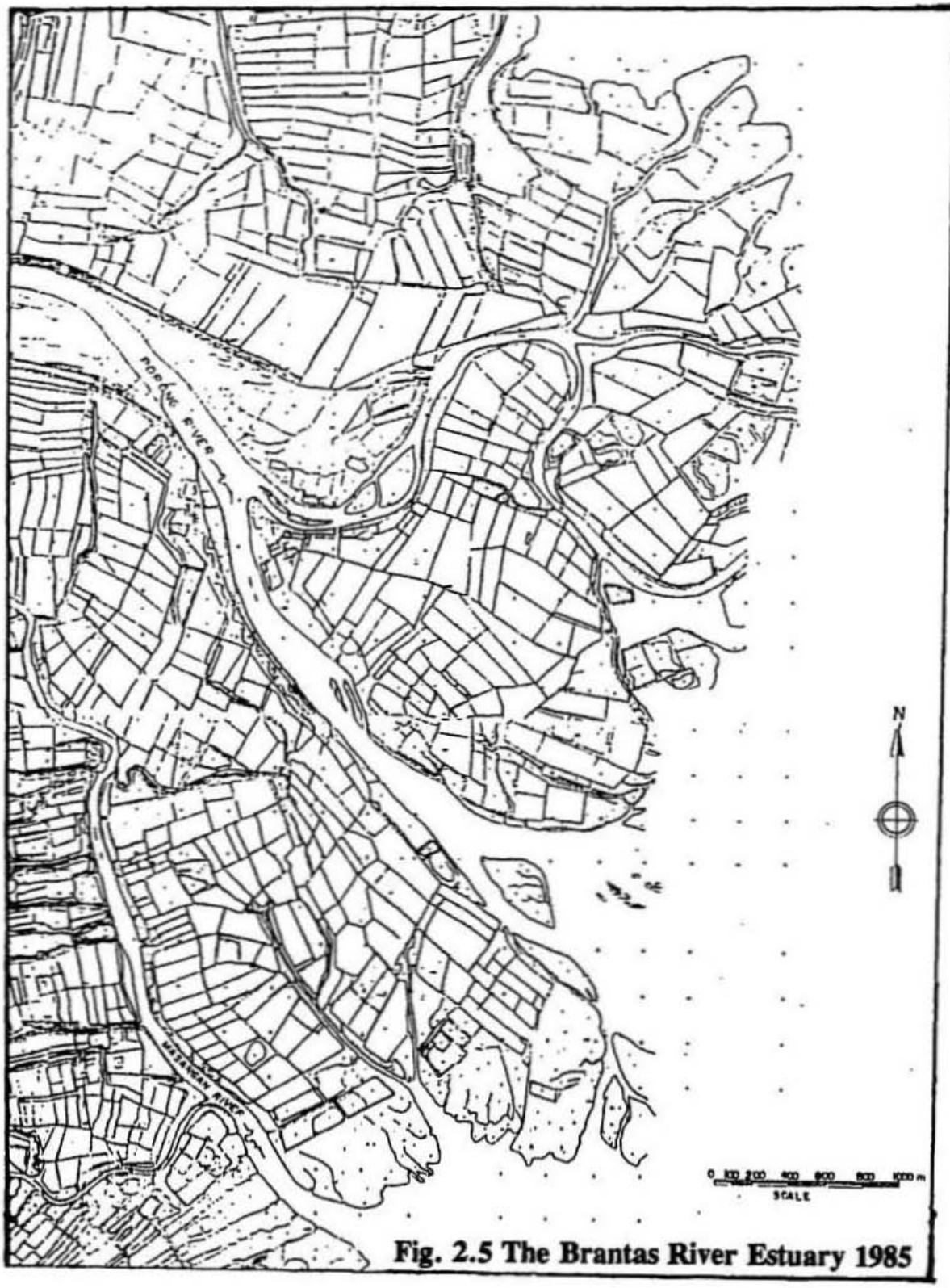

Fig. 2.5 The Brantas River Estuary 1985

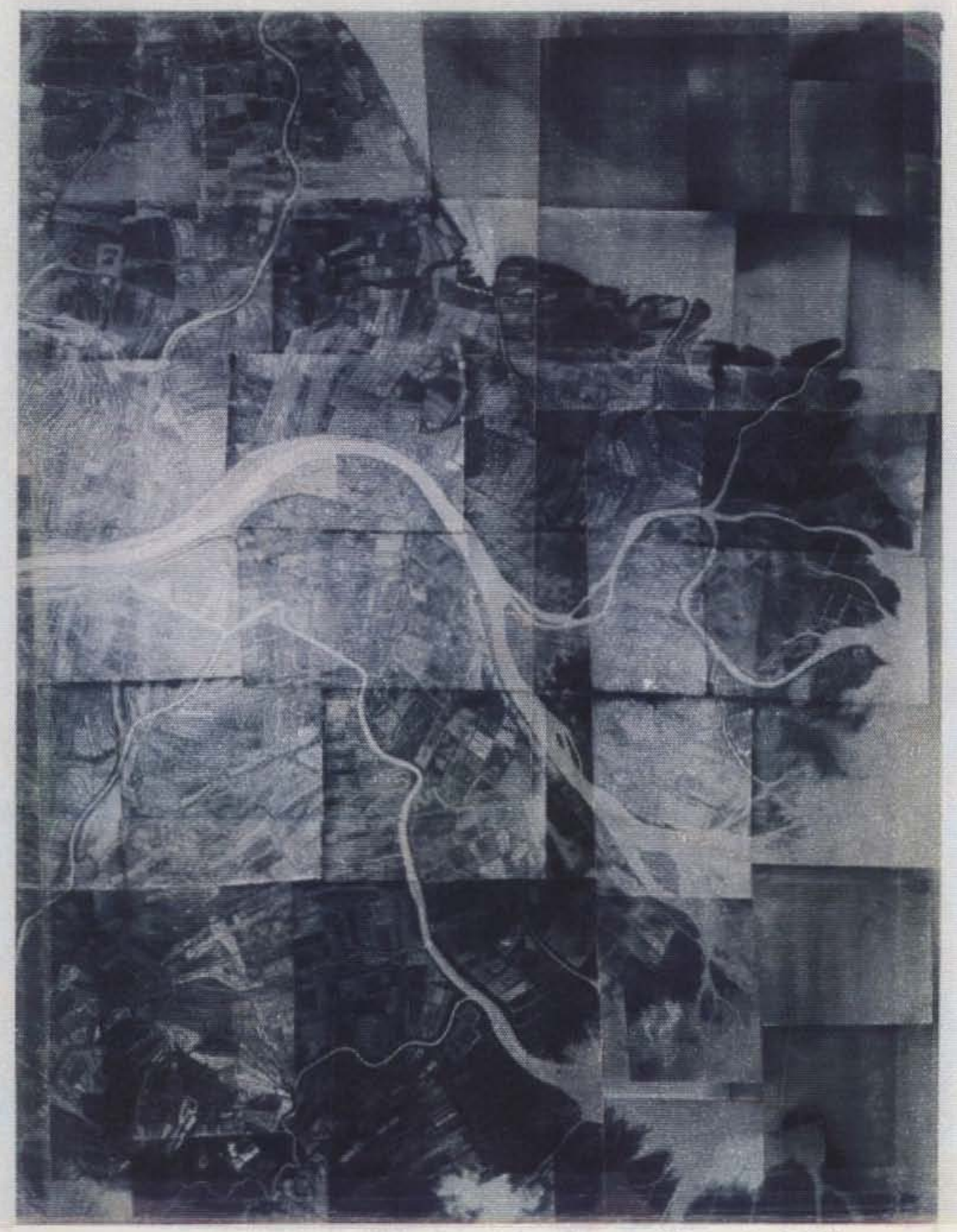

Fig. 2.6 Aero Photo Mosaic of the Brantas Delta in 1985

Chapter 3

Theoretical Background

Chapter 3

Theoretical Background

3.1 Estuaries

An Estuary can be defined as a transition zone where fresh water from the river mixes routinely with salt water from the sea. The word estuary is derived from the Latin word aestus which means tide. Since an estuary is always related to tidal influence, the landward boundary of the estuary depends on the distance of the tidal influence. The region can be divided by three zones. First, the zone where there is free connection with the open sea. It is called a lower estuary. Second, the zone where the salt and fresh water are always mixing. This part is termed the middle estuary. Finally, the zone that is characterized by fresh water but still influenced by the tide is named the upper or fluvial estuary. A schematic map showing the three zones above is presented figure 3.1.

3.1.1 Classification of Estuaries

Estuaries can be divided into many types based on different points of view; for example, geomorphology and physiography, hydrography, tidal range, salinity regime, and sedimentation behaviour.

Pritchard (1955) classified estuaries based on their morphology into four types:

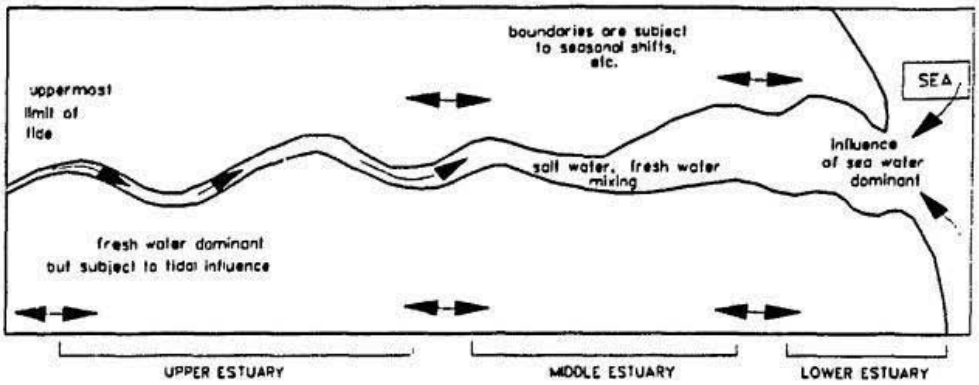

Fig.3.1 Divisions of an Estuary: Upper, Middle and Lower Estuary

drowned river valleys, lagoon type or bar-built estuaries, fjord-type estuaries and tectonically produced estuaries.

Drowned river valleys formed in the Flandrian transgression that ended approximately 5,000 years ago. They were formed about 15,000 years ago within the transgression and subsequent to the Wisconsin glaciation that drowned the existing river valleys and produced the increment of sea water level of 100 m to be the estuary system. The physiography of these estuaries can be characterized by the fact that their width is much longer than their depth, and that they are wedge-shaped, broadening and deepening seaward or are funnel-shaped in plan. These types are also called coastal plain estuaries which are mainly identified by low relief estuary. This type is illustrated in figure 3.2.

Another type of physiographic feature which has a low relief IS the Lagoon-type or bar-built estuary. These are characterized by sand bars that separate estuarine from coastal areas and form a semi-isolated estuary. Barrier beaches, that are formed mainly by the marine forces such as waves and littoral drift processes, enclose the outer embayment creating a lagoon-type environment. Narrow inlets created by a breach of

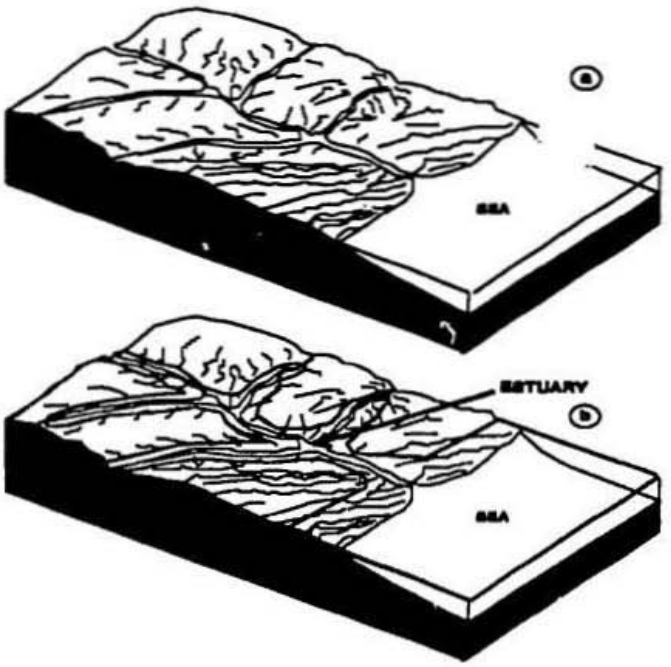

Fig.3.2 Drowned River Valleys or Coastal Plain Estuaries Formed by Eustatic Rise in Sea Level. a) Initial Condition, b) After Sea-Level Rise and Drowning of River Valley

wave forces, form the connection between the isolated estuary and the ocean water via tidal currents. This type commonly occurs along a coastal region where the slope is gentle, wave actions are considerably strong and produces active coastal sediment, and where tidal ranges are less than 4 m. Laguna Madre, Texas and Pamlico Sound, North Carolina are good examples of this type.

Sand bars that enclose the lagoon area can have multiple origins. They may be obtained from ocean sediment or river sediment. Wave action in the coastal region plays an important factor in the development of the sand barrier. As waves approach the coastline, they erode the sea floor, pick up the sediment and bring and deposit the

sediment in elongated bars. If the sediment comes mainly from a river delta, waves and currents rework the sediment particles that have settled in the shoaling area and bring them onto beaches, overwash flats, and dunes. The basic physiography of bar-built estuaries is illustrated in figure 3.3.

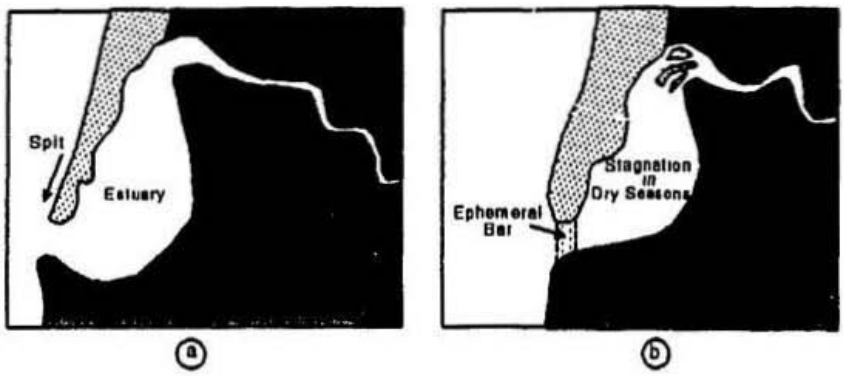

Fig.3.2 Basic Physiography of Bar Built Estuaries a.Elongating of Barrier Spit b.With Seasonal Bar (after Pritchard, 1967)

Fjord-types and tectonically produced estuaries always show high relief. Fjord-types are commonly found in high latitude coastal areas and were formed by glacier erosion. They are U-shaped with steep sides and a rock bottom. Most estuaries of this type have a sill at the mouth. Tectonically produced estuaries are identified by bays that are cut off from the ocean because of land movements: faulting, volcanism or landslide. This study deals primarily with estuaries which exhibit low relief features similar to those of the Brantas estuary. High relief features are, therefore, not considered in detail.

In the hydrographical classification, there are two important factors that can be identified to aid the classification of estuaries. Those factors are river or fresh water

discharge and tidal range. These two factors affect salinity distribution and circulation of water and sediment within the estuary in many situations. Cameron and Pritchard (1963), and Ippen (1966) have classified estuaries into three types: Salt wedge, partially mixed and well mixed.

Salt wedge or highly stratified estuaries can be obtained if the fresh water discharge is more dominant than the tidal influence. The limit would occur where the river discharge flows into a tideless sea. In the area of the river mouth, the less dense river water spreads out over the denser saltwater. Seawater penetrates upstream along the bottom in a rough wedge shape. Consequently, a sharp gradient of salinity and internal waves occur through the interface area between fresh and salt water. This area is named the halocline. The thickness of the dense water below the halocline reduces in the upstream direction and forms a salt wedge. The penetration of the wedge may increase if the fresh water discharge decreases. Upstream from the limit of salt water intrusion, the velocity distribution is always seawards but, in the interface region, the current below the interface is upstream. This case is shown in figures 3.4 and 3.5.

If the fresh water brings much sediment, fine particles which are carried in suspension will be transported in the upper layer seawards and some of them may settle within the estuary by gravitational forces. Coarse particles that move on the riverbed will settle in the area near the tip of the salt wedge. Along the bottom layer, the fine particles that have settled may be carried upstream as far as the tip of the wedge. Some particles may then enter the interfacial area and flow back seawards. A delta will be formed if

large volumes of riverborne sediment are supplied continuously.

Partially mixed or moderately stratified estuaries form if the tidal energy is significant compared to that of the fresh water discharge. Strong tidal currents can cause longer penetration than that caused by the salt wedge type. Since the tidal current is dominant, it creates the shear stress in the river bed and then produces vertical turbulent mixing. Vertical mixing, therefore, occurs easily. The mixing current which occurs during a flood or ebb tide period will exist longer than the period of flood or ebb tide itself. This current is called the residual current. Residual currents are the special identification of moderately stratified estuaries.

Well mixed or homogeneous estuaries are formed where tidal energy is very strong and where the fresh water discharge is thoroughly mixed throughout the depth giving a vertically homogeneous water body. However, salinity gradients may occur laterally and longitudinally. Sometimes, an embryo interface may occur in certain regions of the estuary as a transition zone. Based on the salinity gradient, the well mixed estuary can be divided into two kinds: first, the vertically homogenous estuary with a lateral salinity gradient and second, the vertically homogenous estuary with a longitudinal salinity gradient. If only one of the two conditions happens, the estuary is called a sectionally homogenous estuary. The three types of the hydrographical estuarine classification mentioned above are illustrated in figure 3.4.

According to Pickard's estuarine classification scheme (1975), the ratio involving fresh water discharge and tidal currents is an important factor in the mixing process.

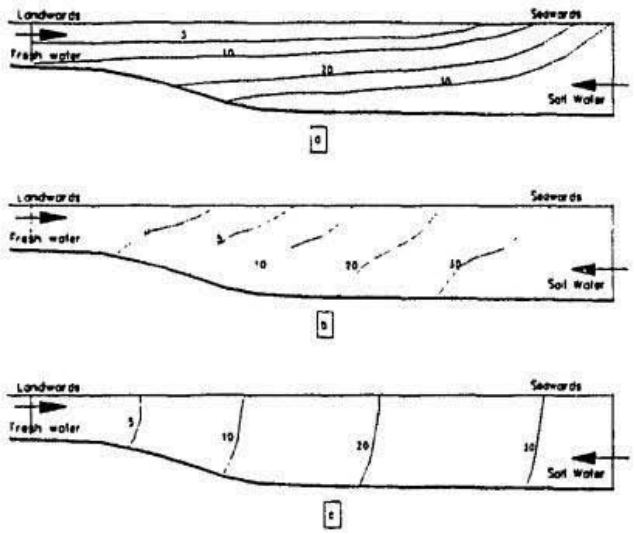

Fig.3.4. Classification of Estuaries Based on Hydrography a) Salt Wedge or Highly Stratified, b) Partially-Mixed or Moderately Stratified, and c) Well-Mixed or Homogeneous Estuaries

Increasing fresh water discharge tends to increase stratification while decreasing tidal currents tend to make the estuary well mixed. Pickard's estuarine number can be expressed as

$$E_s = \frac{U^3 b}{g\, Q_f} \qquad \textbf{(3-1)}$$

Where U = the mean tidal current during a flood tide

b = the width of the estuary

g = acceleration due to gravity

Q_f = the fresh water discharge rate

A lower value of Es means that the fresh water discharge is dominant over the tidal current, so the estuary will become stratified. If the value of E_s is less than 0.03 the estuary will be highly stratified. A transition occurs if the value of E_s is between 0.03

through 0.3, and a well mixed estuary will be obtained if E_t is more than 0.3. In the above equation, U is the mean velocity of the flood tidal current within the tidal prism.

In long estuaries, Pickard also found that the phase difference of maximum current and maximum tidal height varies from the entrance to the head of the estuary. This case should be considered in determining the estuarine number or the likely circulation pattern within the estuary.

Another method concerning the degree of mixing (K) has been introduced by Schultz and Simmons, 1957 (as quoted in Allen, 1962 and Silvester, 1974). They determined that the degree of mixing was governed by the volume ratio between fresh water per tidal cycle and salt water in a flood tide. Hence

$$K = \frac{Vol.\ Fresh\ Water\ per\ Tidal\ Cycle}{Vol.\ Salt\ Water\ During\ Flood\ Tide} \qquad (3\text{-}2)$$

The boundary of stratification was stated to be as follows

If $K = > 0.7$ highly stratified

$K = 0.2 - 0.5$ partly mixed

$K = < 0.1$ well mixed

Based on tidal range, Davis and Hayes (as quoted in Kennish, 1986) proposed that estuaries could be classified as microtidal, mesotidal and macrotidal estuaries. A microtidal estuary is identified by an average tidal range less than 2.00 meters. Waves transport sediment continuously to the shoreline and tidal currents are dominant in the river mouth only. A mesotidal estuary is characterized by an average tidal range between

2.00 to 4.00 meters. In this case, a large part of sediment is deposited by the tidal currents. A macrotidal estuary is identified by an average tidal range more than 4.00 meters. Sediment processes are dominated by the tidal currents.

Three classifications are possible from the point of view of salinity: positive, negative and neutral estuaries. An estuary is called positive if the volume of fresh water discharge to the estuary is larger than the evaporation that occurs from the entire estuarine area. The net discharge is, therefore, always towards the sea and the less dense water will flow seawards over the denser water. The opposite will happen if the inflow is less than evaporation. The water in the estuary then becomes hypersaline or denser than sea water and consequently, the estuarine water will penetrate below the sea water. Such an estuary is called a negative estuary. It is commonly found in tropical regions where tidal amplitude and fresh water inflow are low and evaporation is high. A neutral estuary occurs if the volume of water inflow is approximately equal to the evaporation.

Estuaries may also be classified depending on sediment behaviour. Sediment may be brought down by the river water or may be moved from the beach or sea-surf zone by waves or tidal currents. Rusnak (as quoted in Kennish, 1986) proposed three classifications based on sedimentation behaviour. A positive estuary occurs if the sediment comes primarily from the river. The estuary is classified as inverse-filled, if the estuary basin is filled by sediment from the sea area. A neutral-filled estuary occurs if there is a balance with little or no change in volume due to sedimentation.

3.1.2 Circulation in Estuaries

Density is an important factor which affects circulation. It depends on salinity and temperature and can be defined (Neumann and Pierson, 1966, and Crowley, 1968) as

$$\rho_{s,t}=1+10^{-3}\left[(28.14-0.0735T-0.00469T^2)+(0.802-0.002T)(S-35)\right] \quad \textbf{(3-3)}$$

Where $\rho_{s,t}$ is the density of the water affected by salinity (s) and temperature (t)

T is the water temperature in °C and

S is the salinity of the water in parts per thousand (ppt).

In hydrodynamic circulation studies, Crowley (1968) introduced the water density which was computed in the form of a density index (σ_t). This will give the value of the density to five decimal places. The sigma-t is given by

$$\sigma_t = (\rho_{s,t,o}-1)\ 10^{-3} \quad \textbf{(3-4)}$$

Circulation within the estuary varies with the condition of the tide and with fresh water discharges. Therefore, the circulation in a salt wedge, partially mixed or well mixed estuary is also different. Since the circulation is always related to the sediment behaviour, different circulations will result in different sediment dynamics and different sediment patterns in the estuary.

In a salt wedge estuary, for example, the fresh water discharge is dominant over the tidal influence. Sediment particles that are brought by fresh water will be influenced

by the density stratification. Coarse particles which move along the river bottom tend to be deposited first in the tip of the salt wedge. This region is a region of active sedimentation. Fine particles flow through the upper layer seawards. Part of them may settled along the estuary because of gravitational forces. On the other hand, the fine particles that have settled within the estuary will penetrate up the estuary by tide-density currents to the tip of the salt wedge region. Since the river discharge varies temporally, so the region will be move upstream and downstream, along the estuary.

Circulation patterns are always related to the type of estuary whether the estuary is a salt-wedge, partially-mixed or well-mixed estuary. The circulation can be identified by salinity distributions across various planes along the estuary. Ippen (1966) has introduced a rough standard for defining a well mixed estuary. They determined that an estuary can be classified as well mixed if the difference in salinity from surface to bed is less than 15 to 25 %.

For a given fresh water discharge, the estuary can reach a static condition for a short time period which occurs on the turn of the tide, either the flood or ebb. Ippen (1966) has recognized the difference between a highly stratified and a well mixed estuary based on the depth distribution of salinity, velocity and salinity transport on the arrested saline wedge. The typical forms of those parameters for the both estuaries is shown in figure 3.5.

To determine the length of the salinity intrusion (L_A), Keulegan (1966) has given an empirical formula showing the ratio between intrusion length and channel depth as

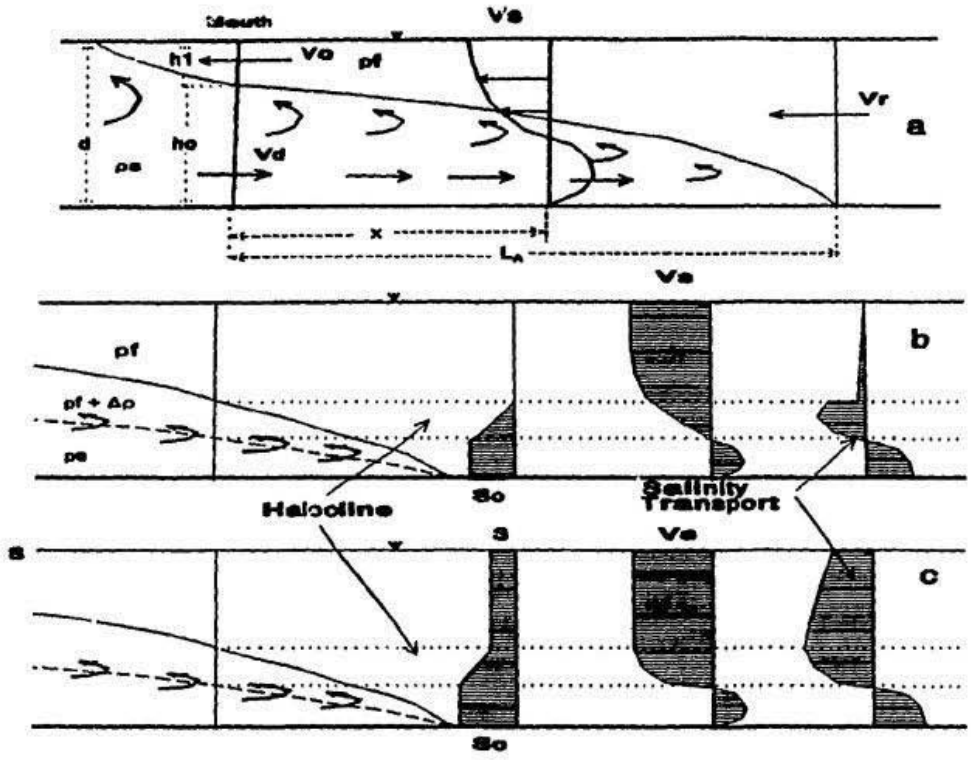

Fig.3.5.a) Velocity Vectors of an Arrested Saline Water, b) Velocity, Salinity and Salt Transport for Highly Stratified Condition, c) Well-mixed Condition

$$\frac{L_A}{d} = \left[\frac{0.88}{280(R_d)^{-1} + 0.148(R_d)^{-1/4}}\right](2F_d)^{-5/2} \qquad (3\text{-}5)$$

Where R_d is the densimetric Reynolds number that can be given by $R_d = V_d d/\nu$ (3-6)

V_d is the kinematic velocity of stratified fluid called the densimetric velocity and defined as

$$V_d = \sqrt{(\Delta\rho/\rho_m)\, g\, d} \qquad (3\text{-}7)$$

$\Delta\rho$ is the different density between salt and fresh water

ρ_m is the average density, $(\rho_s - \rho_f)/2$

F_d is the densimetric Froude number that is given by

$$F_d = \frac{V_r}{V_d} \tag{3-8}$$

V_r is the mean velocity of river flow just upstream of the toe of the wedge (see figure 3.5-a).

Stommel and Farmer, 1952 (quoted in Silvester, 1974) found that the critical flow condition of the fresh water at the mouth occurs if the densimetric Froude number is equal to one. The ratio between interface depth from the bottom (h_1) and the channel depth (d) can then be expressed as

$$\frac{h_0}{d} = 1 - \frac{V_r^{2/3}}{(gd\,\Delta\rho/\rho_m)^{1/3}} \tag{3-9}$$

3.2 Tides and Currents

Tides are characterized by rising and falling sea water levels because of the gravitational effects of the moon and sun on the earth. The gravitational effect is stronger if the moon, earth and sun are in line. The tide in this position is called a spring tide. However, if the sun and the moon are at an angle to each other, the combined gravitational effect is much less than when they are in a straight line. The tide in this position is called a neap tide. A rising tide is called a flood tide and a falling tide is

called an ebb tide. Rising and falling tides produce horizontal water motions called tidal currents.

3.2.1 Types of Tides

In some regions, the rising and falling tide occurs once a day, but at other places the rising and falling tide occurs twice a day. The tide is called a diurnal type if it has one rising and falling tide of about equal height during a lunar day (24 hours and 50 minutes). If it has two high waters and two low waters of about equal height during a lunar day, it is called a semi diurnal type. In certain places, the rising tide and the falling tide occur twice a day with unequal vertical height between rise and fall. That type is called a mixed tide.

Really, the tide is a wave that has a period (T) of about 12 hours 25 minutes, a wave length (L) of about half of the circumference of the earth and a wave height (H) about 1 to 3 m in the absence of landforms and other geometric influences. The response of every place to the tide is different. In certain places the vertical heights are about 1 to 3 m, but these may be more than 20 m in places such as the Bay of Fundy. The respond to the tide depends on the geometry of the area and the geographic position.

3.2.2 Tides in Rivers and Estuaries

Many rivers are influenced by the tide, especially if the estuary is inundated

continuously by sea water. In a rising tide condition, the sea water will propagate up river. The speed of propagation depends on the water depth and on the dimensions of the basin. Furthermore, the shape of the tidal curve is not symmetrical. The period from high water to the succeeding low water is generally longer than that of the low water to the next high water especially at the upper places. This condition becomes clear if an observation of a tidal cycles of a place at the seaward end is recorded and then the result is compared with that at the landward end of the estuary. An example of such a comparison will be presented in section 5.1.1.

In general, the propagation of tidal energy to the river or estuary is derived mainly from the ocean tide but is influenced by the geometry of the estuary or the river.

3.2.3 Tidal Propagation in Shallow Water

Theoretical analysis of tidal propagation in shallow water has been described in An Open University Course Team (1989). A tide produces water movement in the vertical and horizontal directions. In the vertical direction, the oscillation of water can be identified as a rise and fall in water level. On the other hand the horizontal movement tends to form rotation in elliptical paths. The direction of the rotation is either clockwise or anticlockwise. In a small estuary, the effect of rotation is insignificant but the frictional effect cannot be ignored.

In a shallow, funnel-shaped, estuary, the rotation of the world may influence the direction of tidal currents. In the northern hemisphere the incoming tidal current tends

to go to the left side (facing downstream), and in the southern hemisphere, the rising tidal currents tend to go to the right side while falling tidal currents swing to the left side. This phenomenon is caused by the Coriolis effect.

If the tidal currents are strong enough, frictional drag at the sea bed produces turbulence which creates a vertical component of flow. This can cause vertical mixing and can also lift sediment from the bed. This condition commonly occurs in all types of estuaries. During a rising tide, the energy of the tide is reduced by estuary bottom friction, landward constriction of the channel or convergence of the channel, and reflection of energy from a shoal or estuary head (Ippen and Harleman, 1966).

Estuary bottom friction will reduce the amplitude of the tidal wave. Amplitude decreases exponentially landward as a function of distance from the river mouth (x) and a friction coefficient (k) is given by

$$k = \frac{g}{C^2} \qquad \textbf{(3-10)}$$

Where C is the Chezy coefficient and g is the acceleration due to gravity. Decreasing amplitude landward is expressed as

$$A_x = A_0 \, e^{-kx} \qquad \textbf{(3-11)}$$

Where A_x = the amplitude at distance x from the river mouth

A_0 = the amplitude at the river mouth.

Friction also influences the symmetry of tidal rise and fall. If the water depth in the estuary is shallow compared to the tidal amplitude, the tide wave is propagated as a

shallow water wave where the wave speed is influenced by the water depth. Hence the wave speed C is given by

$$C = \sqrt{g(h+\eta)} \qquad \textbf{(3-12)}$$

Where h = the water depth (m)

g = the acceleration due gravity (m/sec^2)

and η = the local wave height of water surface above mean tidal level.

In a falling tidal period, the water depth decreases, so η/h increases and the speed of the tidal wave decreases. Consequently, the period of the rising tide is shorter than that of the falling tide. However, a funnel-shaped channel will increase the tidal amplitude.

3.3 Waves

Waves can transfer energy from one location to another or from one material to another. They are a natural phenomena and very easy to find in every day life such as, sound, light, ripples on a pond, and many other waves. Waves at sea are produced by wind blowing on the sea surface and transferring energy to the water, stretching the smooth water surface to become sinusoidal. That is one of the forms of the water waves.

There are important wind induced wave characteristics. The first is wave height (H), which is defined as a vertical distance between the crest and the bottom of the wave. The second is wave length (L). This is a horizontal distance between two successive waves. Amplitude (A) is the vertical distance from the normal elevation of water to the top of waves. It is commonly taken to be one half of the wave height. Finally, the

steepness of a wave which refers to the ratio of the wave height and the wave length.

It is important to understand that the particles of water are not transported by propagation of wind induced waves. The water particles move in circular or in elliptical orbits. Only energy is being transported. Waves also have some characteristics relating to time. Those are the period (T) and the frequency (f). Period refers to the time between two crests of waves passing through a fixed point. Frequency is the number of waves per second passing through a fixed point.

Based on the direction of the wave movement, waves can be classified into two types : progressive waves and standing waves. Progressive waves are waves which all travel in the same direction. On the other hand, standing waves are derived from the two progressive waves but moving in opposite directions.

3.3.1 Wind Generated Waves on the Oceans

If two fluid layers having differing speed or density are in contact, they will create frictional stress between them and result in a transfer of energy. At the sea surface, different velocities between wind and sea water will produce waves (external waves).

Harold Jeffreys, 1925 (as quoted in U.S. Army CERC, 1984) suggested that waves obtained energy from wind by virtue of pressure differences caused by the sheltering effect provided by wave crest. Empirically, he found that most wind generated waves in the ocean have a steepness of about 0.03 to 0.06. A fully developed sea can be achieved if the wind speed is constant for a long enough time and the area is

unobstructed. The sheltering effect will reach a maximum when the wind speed is three times the wave speed. Wave velocity can never be equal to the wind speed. The wave speed is always below the wind speed because of three reasons. (1) Some of the wind energy is transferred to the sea water to develop currents. (2) Some wind energy is dissipated by friction between wave and surface water and (3) energy may be lost by breaking waves.

Sometimes, in certain locations, no wave data is available. Wind data is, therefore, commonly used to estimate generated waves because growth and dissipation of waves are relative to the windspeed and direction. To convert wind data to wave energy, four correction factors should be considered.

The first is elevation where the wind data is measured. Commonly, windspeed is measured at an elevation of about 10 m above ground level. If the observation is not made at that elevation, a conversion is needed (U.S Army CERC, 1984 p.3-26). As long as the station is below than 20 m, the converted windspeed is stated as

$$U_{(10)} = U_{(z)}\left(\frac{10}{z}\right)^{\frac{1}{7}} \qquad \textbf{(3-13)}$$

Where $U_{(10)}$ is the wind speed at elevation of 10 m

Z is an elevation where the data was made

$U_{(z)}$ is the wind speed at elevation Z (less than 20 m)

The second factor is duration-averaged windspeed. In some locations, only maximum windspeed data are available. In fact, the fastest wind blows for only a short duration. Therefore, this data cannot be used directly for wave generation. It should be

converted to a time-dependent average windspeed with a certain period such as 10, 25 or 50 minutes. The common way is to convert the fastest windspeed to a 1-hour duration windspeed and then make a conversion again from the 1-hour duration to a decided duration. Ratio of windspeed of any duration (U_t) to the 1-hour windspeed was found by Simiu and Scanlan (1978) as

$$\frac{U_t}{U_{3,600}} = 1.277 + 0.296 \tanh\left(0.9 \log_{10} \frac{45}{t}\right) \quad for\ 1 < t < 3{,}600 sec. \tag{3-14}$$

$$\frac{U_t}{U_{3,600}} = -0.15 \log_{10} t + 1.5334 \quad for\ 3{,}600 < t < 36{,}000 sec. \tag{3-15}$$

Where U_t = windspeed at duration (t) in ft/sec or m/sec

$U_{3,600}$ = windspeed of 1-hour duration in ft/sec or m/sec

The third correction factor is related to the temperature difference between air and sea water. This is called the stability correction. If the air temperature is the same as or higher than the water temperature, the boundary layer is unaffected. However, if the sea water temperature is higher than that of the air, the windspeed is more effective in causing wave growth. This stability correction factor, R_t, was presented by Resio and Vincent (1977) and is illustrated in figure 3.6. The result from equation 3-13, 3-14 or 3-15 should be multiplied by this factor (R_t).

The fourth factor is the location effect. In many locations, there are no overwater wind data. Therefore, overland wind data is always recorded and needs to be converted to overwater wind data. This conversion is possible as long as the air pressure gradients

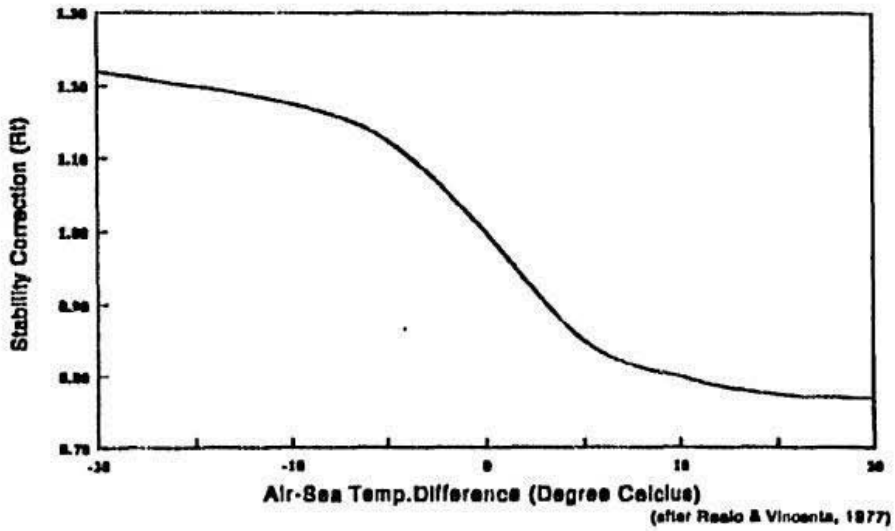

Fig 3.6 Stability Correction, Rt, Accounting For Effects of Air-Sea Temperature Difference

on land and water are equal. The correction is necessary because of the difference between surface roughness of land and sea. This factor was also illustrated by Resio and Vincent (1977) and is presented in figure 3.7. Like the R_t factor, this factor (RL) should also be used to multiply by the result of equation 3-13, 3-14 or 3-15.

Finally, after the windspeed has been corrected by the four factors above, the wind stress factor can be determined by using the following equation

$$U_A = 0.71\ U^{1.23} \qquad (3\text{-}16)$$

Where U is the windspeed after correction by the factors (m/s)

U_A is the windstress factor (m/s)

By using the nomograms in figure 3.8 (quoted in U.S Army CERC, 1984, p.3-49) the wind stress factor (U_A) calculated above and a fetch length based on the wind

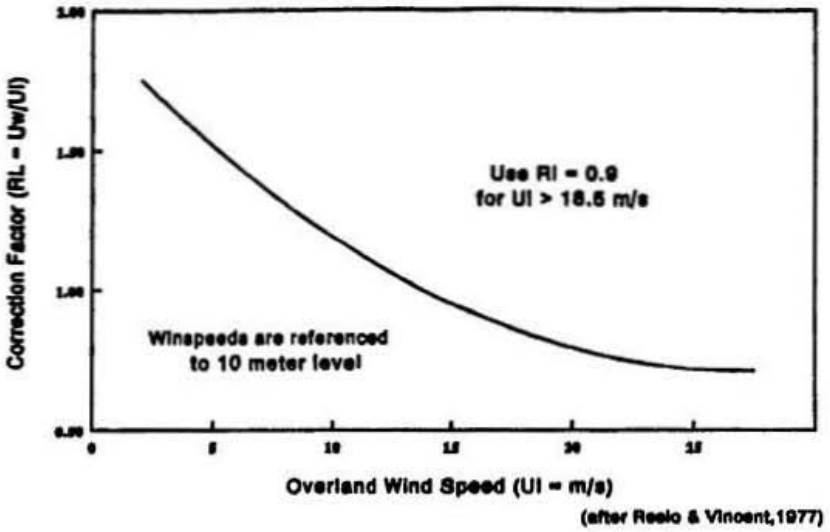

Fig 3.7 Ratio (RL) of Windspeed Over Water (U_w) and Over Land (U_l) as Function of Windspeed Over Land (U_l)

direction and an oceanographic map, a prediction of the deep water significant wave height and duration can be made. Significant wave height is defined as the average height of the one-third highest waves. That is about equal to the average height of the waves as estimated by an experienced observer. The significant wave height would represent the characteristic of the real sea wave (Munk, 1944, qouted in U.S Army CERC, 1984, p.3-2)

3.3.2 Waves in Shallow Water

In deep water, the wave speed is related to the wave the wave length (L). The greater the wave length the higher the wave speed. In shallow water an important factor relating to wave speed is the water depth (d).

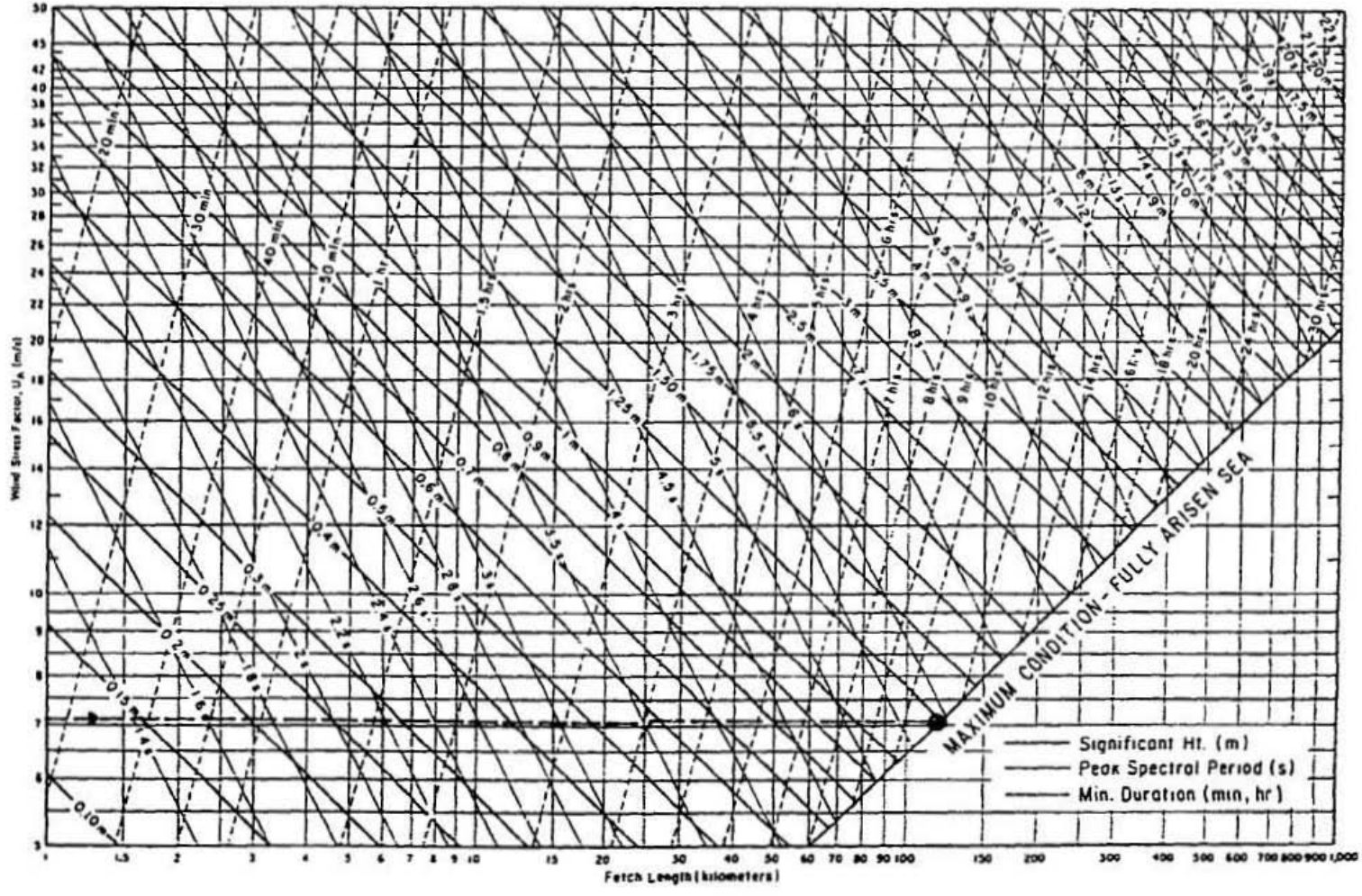

Figure 3 . 8. Nomograms of deepwater significant wave prediction curves as functions of windspeed, fetch length, and wind duration (metric units). Source : "Shore Protection Manual", 1984, by U.S Army Corps and Engineers.

To determine whether wave motion occurs in deep or shallow water, the ratio of the water depth to the wave length (d/L) is important. If $d/L > 0.5$, the sea is considered to be deep water and the motion of water particles is generally circular. The diameter of the circular path will decrease with increasing depth. The orbits will be negligible if the depth reaches more than 1.5 of the wave length. In transitional and shallow water, where the values of d/L are found from 0.05 through 0.5 ($0.5 < d/L < 0.05$) and less than 0.05 ($d/L < 0.05$), respectively, the orbitals are elliptical at the surface and become progressively flattened with increasing depth. The orbital form near the bottom is relatively flat. Wave speed (C) can be presented as the ratio between wave length (L) and period (T), so, $C = L/T$. In general, the formula of wave speed can be written as

$$C = \sqrt{\frac{gL}{2\pi}\tanh(2\pi\frac{d}{L})} \qquad (3\text{-}17)$$

If k is identified as the wave number, equal to $2\pi/L$, equation 3-17 can be written as

$$C^2 = \frac{g}{k}\tanh kd \qquad (3\text{-}18)$$

In shallow water ($d/L < 0.05$), the wave speed is influenced by the water depth. For values $d/L < 0.05$ $\tanh(2\pi d/L)$ is equal to $2\pi d/L$ and the wave speed in equation 3-17 can be written as

$$C = \sqrt{g\,d} \quad or \quad C^2 = g\,d \qquad (3\text{-}19)$$

Waves usually appear in groups. Therefore, the wave speed of a group of waves must be considered. This is called the group speed (C_g). From visual observation it can

be seen that each wave moves through the group to die out in the front as a new wave is formed in the rear. The group speed is approximately equal to one half of the individual wave speed in deep water (C_0), i.e

$$C_{g0}=\frac{1}{2}\ C_0 \qquad for\frac{d}{L}>0.5 \qquad (3\text{-}20)$$

Where C_{g0} = group wave speed in deep water

C_0 = individual wave speed in deep water

In shallow water (d/L < 0.05) the group velocity is equal to the wave velocity. Hence

$$C_g = C = \sqrt{g\ d} \qquad for\frac{d}{L}< 0.05 \qquad (3\text{-}21)$$

Wave energy can be divided into two forms. The first is kinetic energy which relates to the water particle velocities associated with wave motion. The second is potential energy which refers to the movement of fluid mass from the trough to the wave crest. The total of both energies per meter of wave crest, E, is proportional to the square of the wave height and can be expressed as

$$E =\frac{1}{8}\ \rho\ g\ H^2 \qquad (3\text{-}22)$$

Where ρ = fluid density

g = acceleration due to gravity

H = the wave height

In the ocean, waves travel in many directions. If the bottom slopes so gently that reflection and energy dissipation can be neglected, the wave energy between two stations can be assumed to he constant. The energy flux (E_f) at both stations is stated as

$$E_{f1} = E_{f2} = \frac{1}{8}\rho g\ H_1^2 C_{g1} = \frac{1}{8}\rho g\ H_2^2 C_{g2} \qquad (3\text{-}23)$$

Where the subscript 1 and 2 represent the variable factors at stations 1 and 2, while the other variables are as mentioned above.

Energy spreads out along the wave front and as the length of waves increase, the energy per unit length decreases. If the waves travel into shallow water near the shoreline, the speed and height will be changed because of the reduced depth. There are two important factors that cause wave energy dissipation.

Firstly, wave height changes due to shoaling. The water depth and the wave height at station 1 and station 2 are unequal ($d_1 \neq d_2$ and $H_1 \neq H_2$). If both observed stations are located in shallow water where $C_g = (gd)^{1/2}$, it can be substituted in equation 3-23 which can then be written as

$$\frac{H_2}{H_1} = \left(\frac{d_1}{d_2}\right)^{1/4} \qquad (3\text{-}24)$$

If one station is located in deep water which was identified by subscribe 0 and another station is located in shallow water which will be identified by no subscribe, equation 3-23 can be written as

$$\frac{H}{H_0} = \left(\frac{C_{g0}}{C_g}\right)^{1/2} \qquad (3\text{-}25)$$

By using equations 3-20 and 3-21 for C_{g0} and C_g, respectively, equation 3-25 can be rewritten as

$$\frac{H}{H_0} = \left(\frac{C_0}{2\,C_g}\right)^{1/2} = K_s \qquad (3\text{-}26)$$

Where C_0 = wave speed in deep water

C_g = wave speed in shallow water

K_s = the shoaling coefficient.

Secondly, waves that travel from deep water to the shore are influenced by their angle of approach to the sea bottom contour. This effect is called refraction. Refraction occurs if there is an angle between the direction of the incident waves and the bottom contours, so waves tend to bend themselves parallel to the bottom contours. Refraction causes a reduction of wave speed that is comparable to the difference of water depth as

$$\frac{C_1}{C_2} = \frac{\sqrt{gd_1}}{\sqrt{gd_2}} = \sqrt{\frac{d_1}{d_2}} \qquad (3\text{-}27)$$

In deep water, a wave propagates in a direction perpendicular to the wave crest. The wave directions are indicated by lines known as orthogonal lines which change because of refraction. An illustration of a refracted wave is shown in figure 3.9.

In figure 3.9, C_1 and C_2 are the wave speeds in the region with the depths are equal to d_1 and d_2 respectively while b_1 and b_2 are the distances between the orthogonal lines. θ_1 and θ_2 are the angles of the wave propagation between the orthogonal lines and the x axis. Based on this figure, geometrical relationships can be obtained as

$$\sin\theta_1 = \frac{C_1\,\delta_t}{l_c} \qquad \textit{and} \qquad \sin\theta_2 = \frac{C_2\,\delta_t}{l_c} \qquad (3\text{-}28)$$

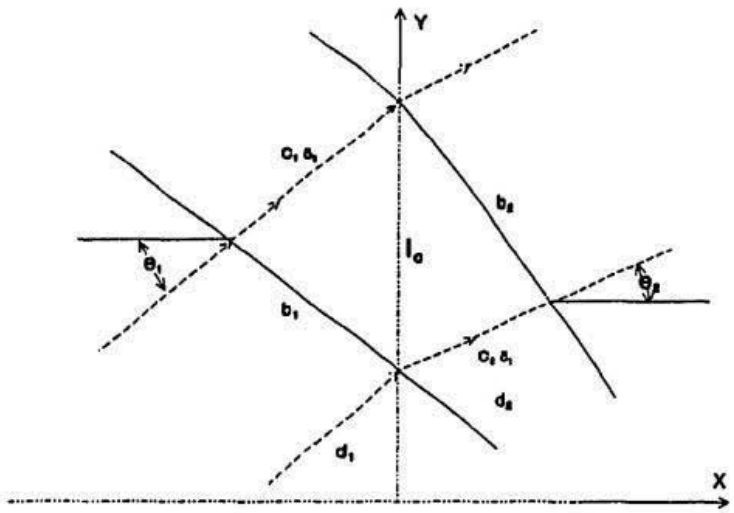

Fig.3.9 **Wave Refraction. Waves Crests, Full lines; Wave Orthogonals, Dashed Lines with Arrows to indicate Direction of Propagation (after Madsen, O.S, 1976)**

Where l_c is the ordinate y of the two wave crests and then

$$\frac{C_1}{\sin\theta_1} = \frac{C_2}{\sin\theta_2} \tag{3-29}$$

Equation 3-29 is commonly called Snell's Law. To evaluate the change in wave height caused by refraction, the energy between the two wave crests in figure 3.9 is assumed to be constant. The constancy of the energy flux between the two orthogonals can be presented as

$$E_{f1}b_1 = E_{f2}b_2 = \frac{1}{8}\rho g\, H_1^2\, C_{g1} b_1 = \frac{1}{8}\rho g\, H_2^2\, C_{g2}\, b_2 \tag{3-30}$$

then

$$\frac{H_2}{H_1} = \left(\frac{C_{g1}}{C_{g2}}\right)^{1/2}\left(\frac{b_1}{b_2}\right)^{1/2} \tag{3-31}$$

If station 1 is found in deep water, equation 3-31 can be written as

$$\frac{H}{H_0} = K_s \left(\frac{b_0}{b}\right)^{1/2} \tag{3-32}$$

And the refraction coefficient (K_r) is given by

$$K_r = \left(\frac{b_0}{b}\right)^{1/2} \tag{3-33}$$

The effect of refraction can be shown clearly if the bottom form where the waves pass is a submarine ridge or canyon, even though the shoreline is almost straight. Refraction also happens within a bay with an irregular shoreline and bottom contours almost parallel to the shoreline. Refraction processes within those regions are presented in figure 3.10.

The orthogonals within a submarine ridge (figure 3.10.a) are more closely spaced, so the refraction coefficient will be more than 1 and the waves are also higher than in the previous area. Consequently, wave energy will increase near the shoreline. The opposite will happen if there is a submarine canyon (figure 3.10.b). The orthogonals will diverge and the wave energy will decrease as the waves approach the shore. In a bay, both things may happen (figure 3.10.c). The orthogonals will converge around the headland and diverge within the bay.

3.4. Sediment Transport

Estuarine sediments are materials that originate from weathering and erosion

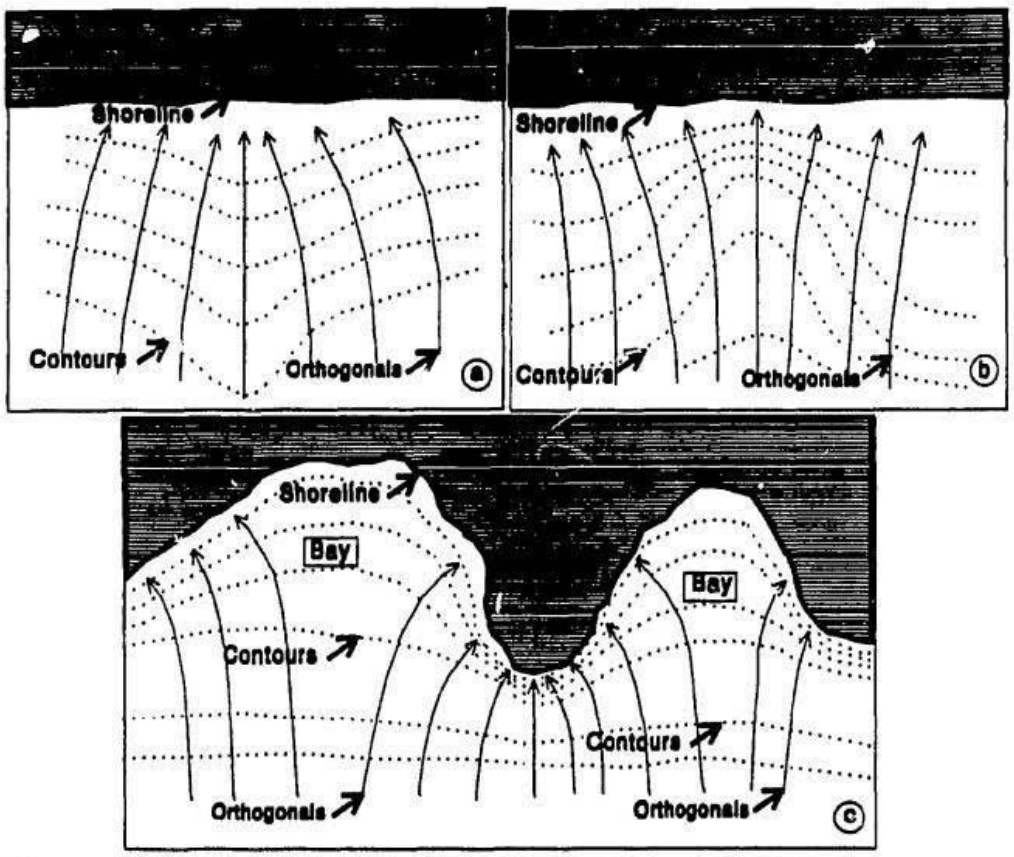

Figure 3.10. a. Refraction by a Submarine Ridge
b. Refraction by a Submarine Canyon
c. Refraction along an Irregular Shoreline

processes. Materials are brought into the estuarine area by river discharge, by the waves and tidal currents or by a combination. The sediments that are so significant to many problems of estuarine studies are mineral particles. This study, therefore, concentrates on particle grain size rather than other properties of the sediments such as chemical and organic composition.

3.4.1 General Classification of Sediment Transport

Sediments are classified into three kinds : Bed load, suspended load and wash load. Bed load is defined as sand or gravel rolling on the river bed by the tractive force of water flow. Suspended load is sand or silt picked up from the river bed, moving in a suspended condition in the water. Wash load is very fine sand or other material supplied and transported always throughout the water core and not found in the river bed materials. In sediment discharge calculations, sediment particles smaller than 0.1 mm in diameter are dealt with as wash load. The boundaries of particle size in every classification depend largely on the hydraulic condition of their transportation.

Sugiura, 1982 (quoted in Brantas River Development Executing Agency, 1989) identified some factors which influence sediment transport. The capacity depends largely on the hydraulic characteristics of the river which mainly produces the scouring force, transportation of the sediment and deposition. He also made classifications of the river based on the quantity of sediment inflow and outflow at two cross sections. If sediment inflow passing through a certain cross section in a given time is greater than sediment outflow at another cross section, that means the river section is affected by deposition of sediment. On the other hand, if the sediment inflow is less than sediment outflow, scouring occurs in the river section. Finally, if sediment inflow is equal to the sediment outflow, this means that the river is in a balanced condition.

For field measurements, bed load samples are taken by a bed load sampler, while

suspended and wash load sediment are collected by a suspended load sampler.

3.4.2 Grain-Size Distribution of Sediment

Particle grain size is commonly used to describe the differences in sediments throughout the estuary and coastal areas. Based on grain size, sediment materials can be divided into clay, silt, sand, gravel, pebbles, cobbles and boulders. There are two systems of grain size classification commonly used in engineering. The first is the Unified Soils Classification (USCS) and the second is the Wentworth- classification.

The Unified Soils Classification is based on the U.S. Standard sizes using the American Standard of Testing Materials (ASTM) sieve sizes which are commonly identified by mesh numbers. A mesh number refers to the total holes in one square centimetre of the mesh. One series or set of ASTM mesh consists of ten meshes that are arranged from number 4 for the largest to 230 for the smallest. The Wentworth classification uses the logarithm (to the base 2) of the particle size as a standard. For example, a material having a particle size range from 0.062 to 2 mm would have a range on the Wentworth classification from -4 ($\log_2 0.062$) to 1 ($\log_2 2$). Krumbein (1936) proposed a phi unit for the Wentworth classification as

$$\text{Phi unit } (\phi) = -\log_2 (\text{diameter in mm}) \qquad (3\text{-}34)$$

By using the definition of equation 3-34, the different limits between both systems can be illustrated. This is shown in table 3.1. The table shows that better values are

obtained for fine particles by the Wentworth system because the larger numbers make it easier to differentiate among the fine sands, silts and clays of very small particle size. This is very important to distinguish one sediment sample from others. Therefore, the Wentworth system seems more advantageous than the USC system.

The general distribution of sediment materials can be described by well sorted, well graded, mean and median diameter. A sediment is called well sorted if a large part of the sediment is of the same size. The sediment is well graded if the quantity of the particle in every range size is almost equal or, in other words, if the particle sizes are distributed evenly over a wide range. Median diameter (M_d)is the sediment diameter that divides the sediment particles into two parts. A half weight of the whole sediment is coarser than the median diameter and another half part is finer than the median diameter. Hence

$$M_d = d_{50} \tag{3-35}$$

Mean diameter (M) is the average diameter of the whole size distribution. Folk and Ward (1957) proposed the mean diameter as

$$M_\phi = \frac{\phi_{16} + \phi_{50} + \phi_{84}}{3} \tag{3-36}$$

Where $\phi_{subscript}$ is the particle size in phi units that is exceeded by the subscript percent total dry weight of the sediment. The most commonly used term is the median diameter (d_{50}).

Table 3.1 Grain-size scales of USCS and Wentworth System

USC System		ASTM Mesh	mm size	Phi Value		Wentworth System
Cobble			256.0	-8.0		Boulder
			76.0	-6.25		Cobble
Coarse Gravel			64.0	-6.0		
			19.0	-4.25		Pebble
Fine Gravel		4	4.76	-2.25		
Coarse Sand		5	4.0	-2.0		
		10	2.0	-1.0		Gravel
Medium Sand		18	1.0	0.0		Very CoarseSand
		25	0.5	1.0		Coarse Sand
		40	0.42	1.25		Medium Sand
Fine Sand		60	0.25	2.0		
		120	0.125	3.0		Fine Sand
		200	0.074	3.75		Very Fine Sand
Silt		230	0.062	4.0		
			0.0039	8.0		Silt
Clay			0.0024	12.0		Clay
						Colloid

3.4.3 Sediment Movements

Sediment can be moved by the energy of tidal currents and wave currents. The direction of sediment movement depends on the direction of these currents. Sediment will be moved if the force of the current flowing over it is capable of overcoming both the

force of gravity acting on sediment grains and the friction between the grains and the surface on which the sediment is resting. Therefore the water flow must give rise to adequate drag and lift forces. The lower part of the flow which experiences friction is called the boundary layer. The boundary layer in estuaries normally extends between 0.1 and 1.0 meters.

The frictional force that is responsible for sediment movement is the shearing force. This causes a shear stress usually designated by τ. The value of shear stress at the bottom is τ_0. The value of τ_0 is related to the velocity (u) of moving water which increases with height (z) above the bed. The shear stress is proportional to the rate of charge of velocity with distance above the bed. The coefficient of proportionality is known as the dynamic viscosity. Thus

$$\tau_0 = \mu \times \frac{du}{dz} \qquad (3\text{-}37)$$

Where μ = dynamic viscosity and d_u/d_z = rate of change of velocity

To make a relationship between velocity and bed shear stress, it is usual to convert shear into a term that has the dimensions of velocity. This term is called the shear velocity or friction velocity, u_* as

$$u_* = \sqrt{\frac{\tau_0}{\rho}} \quad \textit{then} \quad \tau_0 = \rho u_*^2 \qquad (3\text{-}38)$$

By measurement of the actual velocity at any given depth, the value of mean velocity ($d\bar{u}$) over a certain depth (dz), $d\bar{u}/dz$, can be known. When the velocity gradient was plotted using a logarithmic on the depth scale, V`n Karman (quoted in Dyer, 1986, p.58) found

that

$$5.75\, u_* = \frac{d\bar{u}}{d\log z} \qquad \text{and} \qquad u_* = \frac{d\bar{u}}{5.75 d\log z} \tag{3-39}$$

By using equation (3-39) above u_* and τ_0 can be determined. To determine whether or not the sediment will move with a given value of τ_0, the value of critical shear stress of the sediment (τ_c) must be found. If τ_0 exceeds τ_c, the sediment particles will move and, on the other hand, if $\tau_c > \tau_0$, the sediment particles will remain stable. Several equations have been used for determining the value of τ_c. Shields, 1936 (quoted in Chadwick and Morfett, 1986, p.250) has proposed an equation as

$$\tau_c = 0.056\, (\rho_s - \rho)\, g\, d_{50} \tag{3-40}$$

Where γ_s = specific weight of sediment

γ = specific weight of water

g = acceleration due to gravity

d_{50} = median diameter of the sediment.

3.4.4 Movement of Sediment by Tidal Currents

Since tidal currents have two directions, a repeated cycle occurs. Inward currents will fluctuate over a flood tidal cycle and then slack water happens at high tide. After the slack period, seaward currents will be obtained during ebb tide and a slack water period again happens in low water and so forth. Sediment movements will follow the cycle, particularly suspended sediments. Erosion, suspension and inland transport of sediment

happens during the flood tide. A settling process then occurs at the slack period. Re-erosion, resuspension and seaward transport will occur during the ebb tide and so on. As a result, accretion or scouring as net transport may happen within certain sections of the estuary.

Erosion takes place if the value of shear stress at the bed (τ_b) exceeds the resistance of the bed sediment (τ_c). For cohesive sediments, the resistance depends on interparticle bond strength rather than the diameter of sediment particles. The strength may be obtained either from electrochemical forces or biochemical forces or both.

Results of laboratory studies by Owen (1976), Sheng and Lick (1979), and Lavelle at al (1984) show that the rate of erosion increases linearly with excess bottom shear stress as

$$E = M (\tau_b - \tau_c) \qquad (3\text{-}41)$$

Where E = the erosion rate (g/cm^2/sec)

M = the erosion rate constant (sec/cm)

τ_b = the bottom shear stress (dyne/cm^2)

τ_c = the critical shear stress (dyne/cm^2)

3.4.5 Movement of Sediment by Longshore Currents

Waves arriving at the shore will produce currents and cause sediment transport in the littoral zone. The currents are mainly parallel to the shoreline and are called longshore currents. The currents create energy to lift and carry the sediment along the

coast. This is called littoral drift. The amount of sediment passing through a certain cross section per unit time is called the longshore transport rate.

The longshore current speed is proportional to the energy of waves, particularly in the breaker zone and is affected by the oblique angle of their crest to the shoreline, and also by longshore components such as bottom percolation and wave reflection.

Various formulae for estimating sediment transport by littoral drift have been published. The rate is estimated generally using the wave power (P_l) which depends on wave energy (E) and wave group speed (C_g). Both factors have been explained in section 3.3.2. Power of waves parallel to coast is given by

$$P_l = C_g\left(\frac{1}{8}\rho g H^2\right) \tag{3-42}$$

If the angle between the wave crest and the shoreline is equal to α, the wave power can be written as

$$P_l = C_g\left(\frac{1}{8}\rho g H^2\right)\cos\alpha\sin\alpha \tag{3-43}$$

Where ρ is the density of sea water, g is the acceleration due of gravity and C_g is the group speed of waves in shallow water. Since $\cos\alpha \sin\alpha = 1/2 \sin 2\alpha$, equation 3-43 can be written as

$$P_l = \frac{\rho g}{16} H^2 C_g \sin 2\alpha \tag{3-44}$$

If wave data is available as significant breaking heights (H_{sb}), the energy flux can be presented as

$$P_{ls} = \frac{\rho g}{16} H_{sb}^2 C_{gb} \sin 2\alpha_b \tag{3-45}$$

U.S Army CERC (1984), in Littoral Environmental Observation (LEO), has introduced an energy flux factor based on the collection of field data. Using LEO data, difficulties in measuring the angle of the wave crest to the shoreline can be ignored. The important factor is the length of the surf zone. The equation of energy flux is given by

$$P_{ls} = \frac{\rho g\, H_{sb}\, V_{LEO}\, C_f}{(\frac{5\,\pi}{2})\,(\frac{V}{V_o})_{LH}} \qquad (3\text{-}46)$$

Where $(V/V_o)_{LH}$= dimensionless longshore current based on Longuet-Higgins (1970).

$$(\frac{V}{V_o})_{LH} = 0.2\,(\frac{X}{W}) - 0.714\,(\frac{X}{W})\ln(\frac{X}{W}) \qquad (3\text{-}47)$$

and ρ = fluid density

g = acceleration due to gravity

H_{sb} = breaking wave height

W = Width of surf zone

V_{LEO}= average longshore current due to breaking waves

C_f = friction factor (assumed 0.01)

X = distance to dye patch from shoreline

The LEO breaking wave height is a good approximation of the significant breaking wave height. Definition of the significant wave height can be found in section 3.3.1.

3.4.6 Seaward Limit of Significant Transport

The seaward limit can be defined as an outer boundary at which waves should

have neither strong nor negligible effects on the sand bottom during a typical year. This area is called the subaqueous buffer zone. As mentioned in the previous section, sediment motion depends largely on the characteristics of the waves. Wave climate is, therefore, a significant factor in determining the seaward limit. Another important factor is the characteristic of the sediment itself. In fact sediment which is commonly found near the shoreline is finer and better sorted than at some distance seaward. The seaward limit is usually determined by a certain depth at which bottom water particle velocities for high tide waves cannot have a significant influence on the bottom sediment. The empirical relationship can be expressed as (U.S Army CERC, 1984, p. 4-73)

$$\left[U_{max\,(-d)}\right]_{0.137} = \left[0.03\left(\frac{\gamma_s}{\gamma} - 1\right) g\, d_l\right]^{0.5} \qquad (3\text{-}48)$$

Where $U_{max\,(-d)}$ = the peak near-bottom velocity

0.137 = period of the peak near-bottom velocity that is exceeded 12 hours per year (0.137 % per year)

γ_s = specific weight of sediment

γ = specific weight of water

g = acceleration due to gravity

d_l = the depth of seaward limit

For quartz sand and small amplitude wave theory, equation (3-48) can be approximated by the equation below (U.S Army CERC, 1984, p. 4-73)

$$d_l \approx 2\, H_{s50} + 12\, \sigma_H \qquad (3\text{-}49)$$

Where d_l = the depth of seaward limit

H_{s50} = mean significant wave height

σ_H = standard deviation of significant wave height

Another determination of seaward limit depth can be stated by an equation of initiation of sand motion which depends strongly on the median diameter (d_{50}) of the sediment. Hallermeier, 1981 (quoted in U.S Army CERC, 1984, p.4-73) has introduced the equation as

$$\left[U_{max\,(-d)}\right]_{s50} = \left[8\left(\frac{\gamma_s}{\gamma} - 1\right) g\, d_{50} \right]^{0.5} \qquad (3\text{-}50)$$

Where s_{50} is related to the peak near-bottom velocity that influences the sediment.

d_{50} is median diameter of the sediment

For quartz sand and small amplitude wave theory, equation (3-50) can be approximated by the equation below (U.S Army CERC, 1984, p.4-73)

$$d_l \approx H_{s50}\, T_s \left(\frac{g}{5000\, d_{50}}\right)^{0.5} \qquad (3\text{-}51)$$

Where H_{s50} is a significant wave height that can influence sediment movement. This significant wave height is approximately equal to $H_{s(mean)}$-0.307 σ_H. Where σ_H is the standard deviation of the distribution wave height and is equal to 0.62 $H_{s(mean)}$.

3.5 Sediment Budget and Delta Formation

Sediment budget is always related to a certain volume of sediment which is

continually cycled from one part of the coast to another with small amounts of material being added from the rivers and the sea. Therefore, the sediment budget is always evaluated using possible sources and sinks relative to a control volume.

Since the main source of the sediment deposition on a delta is riverborne, the annual sediment outflow from the river is an important factor in calculating the sediment budget that enters the sea-zone. Within this area, sediment particles may settle as final deposition to a sink. However, they may settle as temporary deposition and then re-erode as a source. In between, other particles may come from other sources and accumulate within the same place to become a delta. The mechanism and outflow pattern of dispersion will determine the pattern distribution of the sediment on the delta area. The theoretical background of this process will be discussed briefly in the following section.

3.5.1 Sediment Budget

Sediment budgets have been studied by many coastal engineers. They said that in a complete sediment budget, the difference between the sediment volume added by all sources and the volume removed by all sinks should be zero (U.S Army CERC, 1984, p.4-114). Hence

$$\sum \textit{ of Sources} - \sum \textit{ of Sinks} = 0 \qquad \textbf{(3-52)}$$

In many cases, the estimated volume of known sources is unequal to that of known sinks. The remaining volume is identified as coming from unknown sources or sinks. Therefore

$$\sum \textit{Known Sources} - \sum \textit{Known Sinks} = \sum \textit{Unknown Source(Sink)}$$

(3-53)

Possible sources of littoral materials are rivers, erosion of shores and cliffs, transport from offshore slope, beach replenishment and many others. On the other hand, the possible sinks are river inlets and lagoons, overwash during storms, mining and dredging, and also many other possibilities. Summation of all factors within a certain boundary will result in the sediment budget.

3.5.2 Deita Formation and River Mouth Processes

In general terms, a delta can be defined as those coastal and nearshore features that have been built mainly by riverborne sediments. In deltaic processes, the physical dynamics of the ocean regime, such as wave forces and tidal action, and river discharge regime are important factors in determining deltaic morphology.

Based on the differences in the relative influences of fresh water discharge, tidal action and wave forces, Wright and Coleman (1971), and Coleman (1982) have divided delta processes into three types: river-dominated deltas, tide dominated deltas and wave-dominated deltas.

River-dominated deltas are formed if the tidal currents and wave energy are weak compared to river forces. Expansion and diffusion depend on outflow velocity and determine the relative contributions of inertia, bottom friction and buoyancy. For a simple

case, with no density difference (i.e homopycnal), the expansion depends on the velocity of the fresh water relative to the dimension of the river mouth. Wright and Coleman (1971) concluded that the jet structure in that condition is controlled by the ratio of inertial to viscous forces indexed by the Reynold's number (R_n) expressed as

$$R_n = \frac{u_0 \left([h_0(b_0/2)]^{1/2}\right)}{\nu} \qquad (3\text{-}54)$$

Where u_0 = the mean velocity at the river mouth (m/s)

h_0 = the depth of the river mouth (m)

b_0 = the width of the river mouth (m)

ν = the kinematic viscosity. In general order of magnitude, this value is 0.01 cm^2/s.

Three conditions can be identified. If the velocity is low or moderate and the estuary mouth is deep enough, density stratification will occur and buoyant expansion prevails. Pearce, 1966, (quoted in Wright and Coleman, 1974) found that when the value of R is less than 500 the flow will be laminar. The presence of stratification will cause fine-grained sediments to flow out on the surface layer while coarse-grained sediment will settle in front of the estuary mouth. This circulation is the same as in a salt wedge estuary. If the velocity of fresh water is high and the estuary mouth is deep enough, turbulent mixing processes occur rather than stratification. The effect of the river discharge is felt over an area that is longer and thinner than for the previous condition, so the spreading angle is narrow. The value of R in this condition is about 1,500 to 2,500. The last condition occurs if the river discharge is high and enters shallow water.

Deceleration of water flow happens immediately and fully turbulent mixing also occurs with the value of R being more than 3,000. The deceleration causes lateral spreading. Therefore, the spreading angle is wide and a delta bar is formed near the mouth. Sometimes the mouth is blocked totally. Then, new bifurcating channels will be established on the deposition area to make a form which is called a bird-foot.

In the case of stratified outflows, buoyancy effects depend largely on the ratio between inertial and buoyant forces. This ratio can be expressed as the densimetric Froude number (F_d) as

$$F_d = \frac{u}{(\gamma\ g\ h_0)^{1/2}} \qquad \textbf{(3-55)}$$

Where u = mean outflow velocity in the upper layer (m/s)

γ = density difference ratio between effluent and ambient fluids given by

$$\gamma = 1 - (\rho_f/\rho_s) \qquad \textbf{(3-56)}$$

ρ_f and ρ_s are the densities of effluent and ambient fluid (kg/m^3), respectively.

g = acceleration due to gravity (m/s^2)

h_0 = the depth of the density interface (m)

Hayashi and Shuto (1967 and 1968) determined three conditions of the outflow governed by the value of the densimetric Froude number. If it is greater than 16.1, the outflow is fully turbulent. In the case of a homopycnal outflow, the γ value will be zero and the densimetric Froude number is infinite. If the value lies between 1 and 16.1 varying degrees of turbulence will occur. Bates (1953) introduced his jet model and concluded that the inertial forces are dominant if F_d is high and this outflow is turbulent.

When F_d decreases, turbulence will decrease and the buoyant outflow prevails. Two types of turbulent jet have been introduced by Bates. The first is the plane jet. It occurs if the bottom form of the receiving basin restricts expansion of lateral movement. The turbulent form is then called a plume. The second type is an axial jet which occurs if the depth immediately after the outflow is deeper, allowing vertical as well as transverse expansion.

In the turbulent jet model, Bates (1953) dealt with homopycnal outflows and proved that turbulent eddies cause exchange and mixing between effluent and ambient fluids. Decelerated velocities and transporting capacity cause deposition of a large part of the sediment. The concentration will also decrease seawards. Basically, Bates divided the turbulent region into two zones; the zone of flow establishment and the zone of established flow (see figure 3.11).

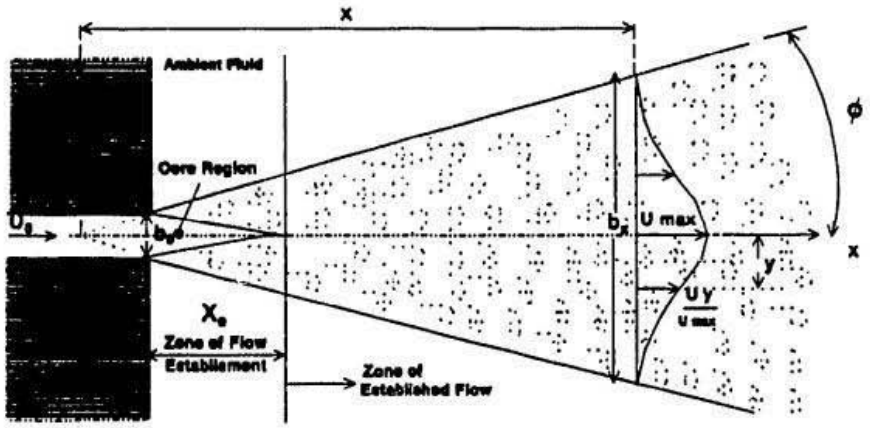

Figure 3.11 Schema of a Turbulent Jet Model (After Bates, 1953)

The zone of flow establishment is found by a distance (X_e) from the river mouth seawards to a point where the turbulent eddies within the boundary of the expansion

penetrate to the centreline of the jet. The area from the outflow to this point is called the core region and is identified by constant velocity throughout the region. The length of the zone of flow establishment, X_e for any given outlet geometry is inversely proportional to the rate of expansion, ε, (i.e the tangent of half the spread angle ϕ), and to the similarity integral for transverse velocity distribution. Based on an investigation by Wright and Coleman (1974), the angle between the centreline and the jet boundary (ϕ) is 12° 24' and the value of ε is equal to 0.22. Hence

$$\varepsilon = \frac{d\ (b/2)}{dx} = 0.22 \qquad \textbf{(3-57)}$$

Where x is the distance from the virtual source (see figure 3.11). Stolzenbach and Harleman, 1971 (quoted in Wright and Coleman, 1974), found that the similarity integral (I) has a constant value of 0.316 in fully turbulent jets.

In the zone of established flow, the maximum velocity is found in the centreline. The velocity distribution decreases in longitudinal and transverse directions because of the ambient water forces. The form of the decelerated velocity in this zone seems to be a Gaussian probability distribution as shown in figure 3.11. Progressive longitudinal decrease of the velocity can be given as

$$\frac{U\ \max}{U_0} = \frac{b_0/2}{\varepsilon\ I\ x} \qquad \textbf{(3-58)}$$

Under non stratified conditions, friction effects between outflow water and bottom friction should be considered. Borichansky and Mikhailov (1966) suggested that interaction between inertial forces and bottom friction in a river mouth tends to yield a balanced

condition between them. Therefore, the deceleration of the mean velocity ($U_{x\,mean}$) at a certain distance seaward relative to the mean velocity at the river mouth (U_0), should have an exponential function of the friction coefficient (K), distance (x) and mean water depth (h_{mean}) over the distance. These relationships can be given by

$$\frac{U_{x_{mean}}}{U_0} = e^{-K(x/h_{mean})} \tag{3-59}$$

Where K is a function of the Chezy coefficient (C) as

$$K = \frac{g}{C^2} \tag{3-60}$$

g is the acceleration due to gravity.(see also eqn 3.10)

The width of the lateral expansion at a distance x from the river relative to the river mouth width (b_x/b_0) is also influenced by those factors. The expansion width can be expressed as

$$\frac{b_x}{b_0} = \frac{h_0}{h_x\, e^{K(x/h_{mean})}} \tag{3-61}$$

Another significant feature of expansion and diffusion in a river mouth is the presence of buoyancy effects. As mentioned in equation 3-55, if the densimetric Froude number decreases, turbulence will also decrease and buoyant expansion prevails. Bondar (1968) assumed that the lateral expansion is caused by the hydrostatic pressure of fresh water that is obtained from different elevations or superelevation (Δh) created by the buoyancy of the lighter fluid. The value of Δh is equal to the thickness of fresh water (h') multiplied by the density ratio (γ) which has been mentioned in equation 3-56. Hence :

$$\Delta h = h' \gamma \tag{3-62}$$

This can be illustrated in figure 3.12.

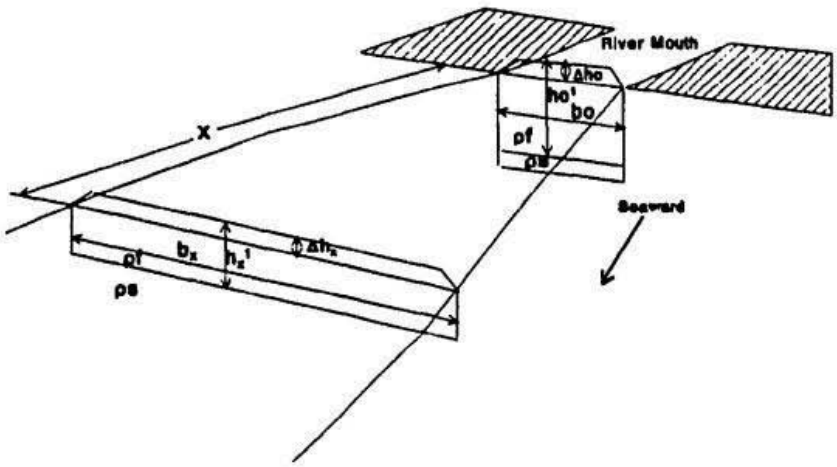

Fig.3.12 Mouth Model Showing Expansion of Buoyant Effluents (after Bondar, 1968)

At any distance (x) seaward, the expansion width (b_x) and depth (h'_x) relative to the river mouth width (b_0) and depth (h_0), respectively, are expressed as

$$\frac{b_x}{b_0} = (1 + ax)^{2/3} \tag{3-63}$$

$$\frac{h'_x}{h'_o} = \frac{1}{(1 + ax)^{2/3}} \tag{3-64}$$

Where a is the dynamic expansion coefficient which is given by

$$a = \frac{3}{2}\left[\frac{K\, h'_0 (h'_o)^{1/2}}{Q_0}\right] \tag{3-65}$$

K represents the buoyant expansion coefficient which is presented as

$$K = \frac{4}{3}(2g\gamma)^{\frac{1}{2}} \frac{1-\gamma}{2} \qquad (3\text{-}66)$$

Tide-dominated deltas are formed in the regions where tidal range is more than 4.00 m. Tidal currents are, therefore, strong enough to affect the delta formation. This process can be identified by a series of depositions generally in line with the main river flow direction. These occur at the mouth of the estuary and develop in a seaward direction. Deposition will extend above the water level and vegetation will accelerate the delta growth.

Wave-dominated deltas can be found in the sea region where wave propagation can counter the strength of river discharge. The influence of waves becomes more significant if they can propagate upstream during an ebbing tide and bring back a large part of the sediment to the river mouth area. This delta can be identified by the formation of a sand bar surrounding the river distributary mouth and running almost parallel to the wave crest.

3.5.3 Morphology of deltas

As mentioned in the previous section, deltas are consequences of the conflict between rivers and the sea. Marine forces and river discharges are, therefore, major factors in the morphology of deltas. In tide-dominated deltas and wave dominated deltas, for example, marine forces are more dominant than river forces. To evaluate the relative contribution of river and marine forces, it is possible to consider the effect of river

discharge relative to marine power. An alternative evaluation can be based on an investigation of different river deltas, such as the Mississippi (U.S.A), the Danube (Rumania), the Ebro (Spain) and many others.

Since waves sort and redistribute sediments that enter the sea zone by river discharge, wave power is one of the sources of energy for delta formation. An explanation of wave energy has been given in section 3.3.2, equations 3-22 and 3-23, while shoaling and refraction processes have been described in equations 3-24 through 3-32. Wave attenuation because of refraction and shoaling has been studied by Bretschneider and Reid (1954) who showed that the reduction of wave height because of bottom friction over a distance (Δx) is given by

$$H_f = \frac{H'}{\frac{fH^2\phi\Delta x}{K_s T^4}+1} \qquad (3\text{-}67)$$

Where H' = the wave height after refraction

f = the friction coefficient. This can be assigned of 0.02 if sediment particles are low roughness and mainly consist of silt and clay

K_s = the shoaling coefficient

T = the wave period

and ϕ is given by

$$\phi = \frac{64\pi^3}{3g^2}\left[\frac{K_s}{\sinh 2\pi(d/L)}\right]^3 \qquad (3\text{-}68)$$

Where g is acceleration due to gravity, d is the water depth and L is the wave length. To

know the degree to which wave power is reduced by the offshore slope, an attenuation ratio (A_p) should be stated as

$$A_p = (P_0/P_s)K_r^2 \qquad (3\text{-}69)$$

Where P_0 is the deep water wave power per unit width, P_s is the nearshore wave power also per unit width and K_r is the refraction coefficient. If A_p is equal to 1.0 there is no reduction in wave power owing to friction. If A_p is 100, wave power is reduced by 1 percent and so on.

The magnitude and frequency of wave forces should be considered in determining the relative strength of the marine forces upon the river forces. River discharges should be compared to the wave climate over the same time periods. If a high discharge, for example, coincides with a high wave power, the sediment volume that is supplied by the river may be balanced by the wave power to redistribute the material to become a spit or barrier beach along the coast. However, if both forces are out of phase, either the river forces or the wave forces are dominant. The river dominated delta will result in a delta having a fairly regular and continuous growth with an irregular shoreline. A wave dominated delta, however, will produce a regular shoreline and sand bars which are mostly parallel to wave directions. In a low marine energy area, for another example, the river may be totally dominant and an irregular delta shoreline will develop.

To evaluate the relative strength between the two forces, Wright and Coleman (1973) did a comparison of seven deltas using a discharge effectiveness index. The discharge effectiveness index is given by

$$\frac{\textit{River Discharge/Unit Width at the River Mouth}}{\textit{Wave Power/Unit Width at the Coast}} \qquad (3\text{-}70)$$

The deltas studied by Wright and Coleman ranged from a fluvial-dominated delta (Mississippi) to a wave-dominated delta (Senegal). Both factors are calculated in the same month and the average distribution of the index can be determined annually. The shape of a longitudinal section through the seaward end of the delta can also be used for tracing fluvial and marine processes. The deltaic configuration will indicate the dominant power that forms the morphology of the delta as long as the deltaic configuration can be described quantitatively whether perpendicular or parallel to the shoreline. Maps of the delta provide basic data for this purpose and, in order to get a comparison, the result should be compared to the deltas that have been observed. Wright and Coleman (1973) have described some factors or indices that can be used to indicate the deltaic process.

The first is the protrusion index (P_i). Typically, any delta has a protrusion that extends seaward from the adjacent shoreline and is spread out around the centreline of the river mouth. This index is defined as the ratio between the length of the protrusion (L_m), normal to the coast, and the maximum width of the protrusion or as it sometimes is called, the delta width, (W). Hence

$$\textit{Protrusion Index } (P_i) = \frac{\textit{Protrusion Length } (L_m)}{\textit{Delta Width } (W)} \qquad (3\text{-}71)$$

This index will show the domination of the river forces relative to marine power if the delta protrusion is long relative to the delta width.

The second index is the crenulation index. It is obtained from comparisons of the

shoreline length and the delta width. This index is given by

$$Crenulation\ Index\ (C_i) = \frac{Shoreline\ Length\ (L_s)}{Delta\ Width\ (W)} \qquad (3\text{-}72)$$

The higher the value, the greater the coastline irregularity which means that the river forces are dominant.

The third is the degree of skewness (S_k). This factor is expressed as

$$S_k = V_r / V_l \qquad (3\text{-}73)$$

Skewness happens if there is a pronounced littoral drift that dominantly comes from one direction. Sediment volume distribution on the left (V_r) and the right side (V_l) of the protrusion coastline is likely to be unbalanced and the down-drift part will have the largest volume. Typically, the distribution volume is greatest in the zone adjacent to the protrusion axis. It decreases with increasing distance from the axis. To calculate the distribution, the delta area is divided into several segments parallel or perpendicular to the shoreline. The trend of the distribution will be shown based on the volume in every segment.

According to the discharge effectiveness index mentioned in equation 3-70, the power of the river discharge relative to the wave power will be reflected in the configuration of the front of the delta . If wave power is more dominant than discharge, waves will form a concave delta front. If the deposition process is dominantly determined by the discharge the deposition form tends to be convex. This is the fourth factor that can be used for examining the deltaic processes. It is called the subaqueous hypsometric integral (HI) and is given by

$$HI = \int_{-40}^{0} \left(\frac{a_s}{A_s}\right) d\left(\frac{z}{Z}\right) \qquad (3\text{-}74)$$

Where a_s = the area between any given depth contour around the deltaic protrusion and the shoreline

A_s = the area between the basalt (40 ft) depth contour and the shoreline

z = the vertical distance of the given contour above the basalt contour

Z = the total vertical distance from the basalt to the shoreline

If the value of HI is more than 0.5, the form of the delta front tends to be convex and if it is less than 0.5, the form tends to be concave.

The four factors above have been calculated by Wright and Coleman (1973) for seven deltas. Results are shown in table 3.2. This table can be used as a standard for determining whether river or marine forces are dominant in the Brantas delta formation.

Table 3.2 Morphometric Properties of Seven Deltas

Rivers	$C_i = L_s/W$	$P_i = L_m/W$	$S_k = V_r/V_t$	HI	Dominant Forces
Mississippi	5.20	0.35	0.85	0.59	River
Danube	1.46	0.30	1.13	0.51	River
Ebro	3.51	0.64	1.05	0.50	River & Marine
Niger	1.29	0.34	1.39	0.48	River & Marine
Nile	1.22	0.23	1.21	0.37	Marine
Sao Francisco	1.08	0.26	0.74	0.34	Marine
Senegal	1.02	None	None	0.26	Marine

Chapter 4

Existing Data Information and Analysis

Chapter 4

Existing Data Information and Analysis

Existing data is very valuable in many ways. First, by using existing data, the chronology of river and estuary changes can be evaluated, especially if the changes can be related to men's activities. At the Brantas river, for example, a shortcut channel was dredged at the estuarine area in 1977 for flushing flood discharge rapidly to the sea. The physical conditions have been changing since that time. A study of the original design and present conditions should be done to evaluate the geometrical changes in the channel, estuary mouth and the delta growth over the years. Topographic maps are needed for examining natural behaviour besides river discharges, tidal currents, wave climates and other data.

Second, by using existing data, natural phenomena can be understood. The data are useful for supporting analysis. Wind, wave and tidal data, for example, are very important for understanding the characteristic forces that influence the sediment budget and estuarine circulation. In this chapter, all of the existing data and analysis which have relevance to the sediment budget and circulation within the estuary will be examined. The basic features of this study are presented in figure 4.1.

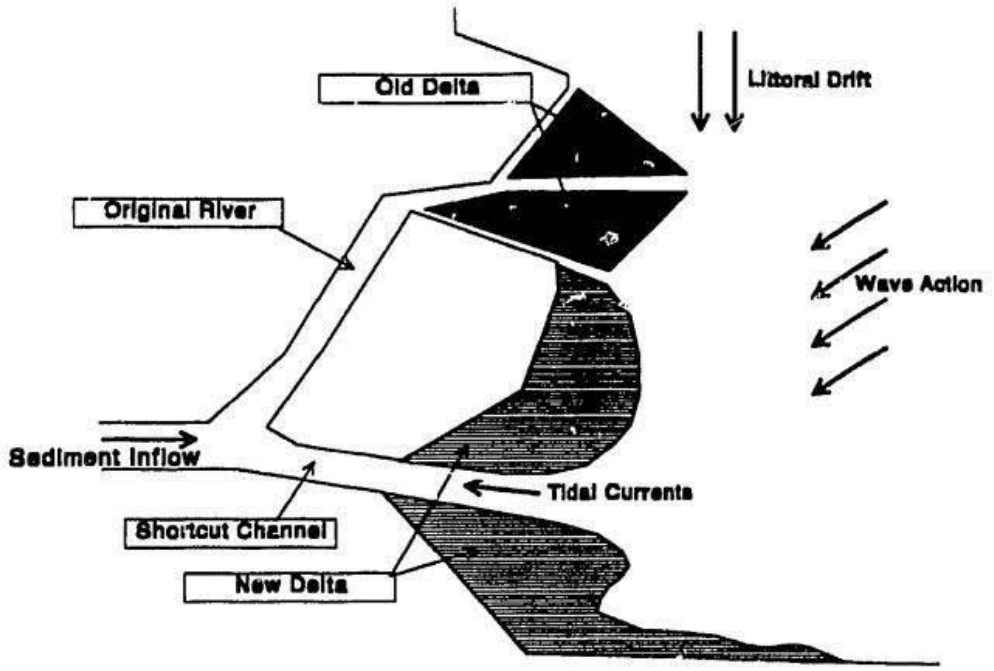

Fig.4.1 Schema of the Brantas Rivermouth Showing Influential Factors in Sediment Budget

4.1 Waves, Wind and Tidal Data

4.1.1 Wave Data

No wave data were available in the Madura Strait. For analysis, wind data were used to predict the waves and then they were then compared to a few wave data sets which were taken by field observation. This is the best way of approaching the real conditions of waves and wave climate. Wind and wave observations will be discussed in chapter 5.3.

4.1.2 Wind Data

As mentioned above, wind data is fundamental data in calculating the characteristics and climate of the waves. Existing wind data were taken from Juanda airport which is located at about 10 kilometres north of the Porong estuary and about 3 km from the shoreline of the Madura Strait. Only mean daily windspeed data including mean direction is available. Monthly mean windspeed and the directions is summarized in table 4.1. This is based on the daily data during two years, 1989 and 1990.

The table shows that the mean daily wind-speed is about 6.5 m/s and the dominant wind direction during the dry season and rainy season are from the east (70^0N) and from the west (270^0N) respectively. It is important to stress that the fluctuation of windspeeds and the changing directions are insignificant throughout each season. These changes are caused by the tropical climate of the Brantas area. There is a marked wet season from November to April when the prevailing wind is from the west and a marked dry season for the remaining months when the prevailing wind is from the north east or south east. Furthermore, Java island does not lie in the area regularly affected by tropical cyclones. Therefore, the area very rarely experiences periods of prolonged storm activity as occur in the Philippines or other tropical countries. The Brantas area has little variation in windspeed throughout the year.

During the wet season, the wind comes from the west or the main island, so it has no significant influence on the coastal environment and it can be ignored.

Referring to section 3.3.1 it can be seen that windspeed data should be corrected

Table 4.1 Daily Mean Wind-speed and Direction during Two Years

No:	Month	Average wind speed (m/s) '89	'90	Average Wind Direction '89	'90	Note
1	January	6	7	W /	W	Dominant Dir.during
2	February	6	7	W /	NE	wet season is west
3	March	6	7	W /	W	(270°N - azimuth)
4	April	5	6	E /	E	
5	May	6	6	E /	E	Dominant Dir.during dry
6	June	6	7	E /	E	dry season is east
7	July	7	7	E /	E	(70°N - azimuth)
8	August	8	8	E /	E	
9	September	8	8	E /	E	
10	October	7	8	E /	E	
11	November	6	6	E /	E	
12	December	6	6	W /	W	

Average speed : 6.8 - 6.4 m/s. Wind direction during the dry season is 70°N and during wet season is 270°N.

before being used for predicting waves. Wind data from Juanda airport is measured 10 m above ground, so the correction factor mentioned in equation 3-13 is unnecessary. The stability factor (Rt) (see figure 3.6) is also not needed since the temperature difference between the water and air is small. In addition, there is a little variation in temperature throughout the year. One of the correction factors which might have been necessary is RL (see figure 3.7). This is the factor caused by the differences in surface roughness between water and air. However, field observations showed that mean windspeeds over

water are almost equal to windspeeds measured in Juanda airport 4 km inland from sea (see table 5.15). Therefore, conversion from the wind data to windstress factor (U_A) can be done directly using equation 3-16 and no correction factors are necessary.

Assuming that the mean daily wind blows for 24 hours and that all the correction factors are equal to 1, the wind stress factor is $U_A = 0.71 \times 6.5^{1.23} = 7.09$ m/s. Then, from the oceanographic map (see figure 4.2), using the wind direction 70° N, the fetch length from the river mouth through the Madura Strait can be found to be 136 kilometres. Finally, the significant wave height in deep water, wave duration and wind duration can be found by using figure 3.8. The results are stated in table 4.2.

Table 4.2 Significant Wave Height, Wave Period in the Deep Water and Wind Duration

Significant Wave Height (m)	Wave Duration (sec)	Wind Duration (hours)	N o t e :
1.20	5.8	11	Fully arisen sea

4.1.3 Tidal data

Existing tidal data was taken from the Surabaya Harbour Department. Data are measured hourly based on a certain elevation that is called the Surabaya Harbour Reference (SHR). Zero elevation is placed at 1.50 m below mean sea level (MSL).

The SHR is different from the provincial levelling standard which is commonly used by projects in East-Java Province. This common standard is called the Surabaya

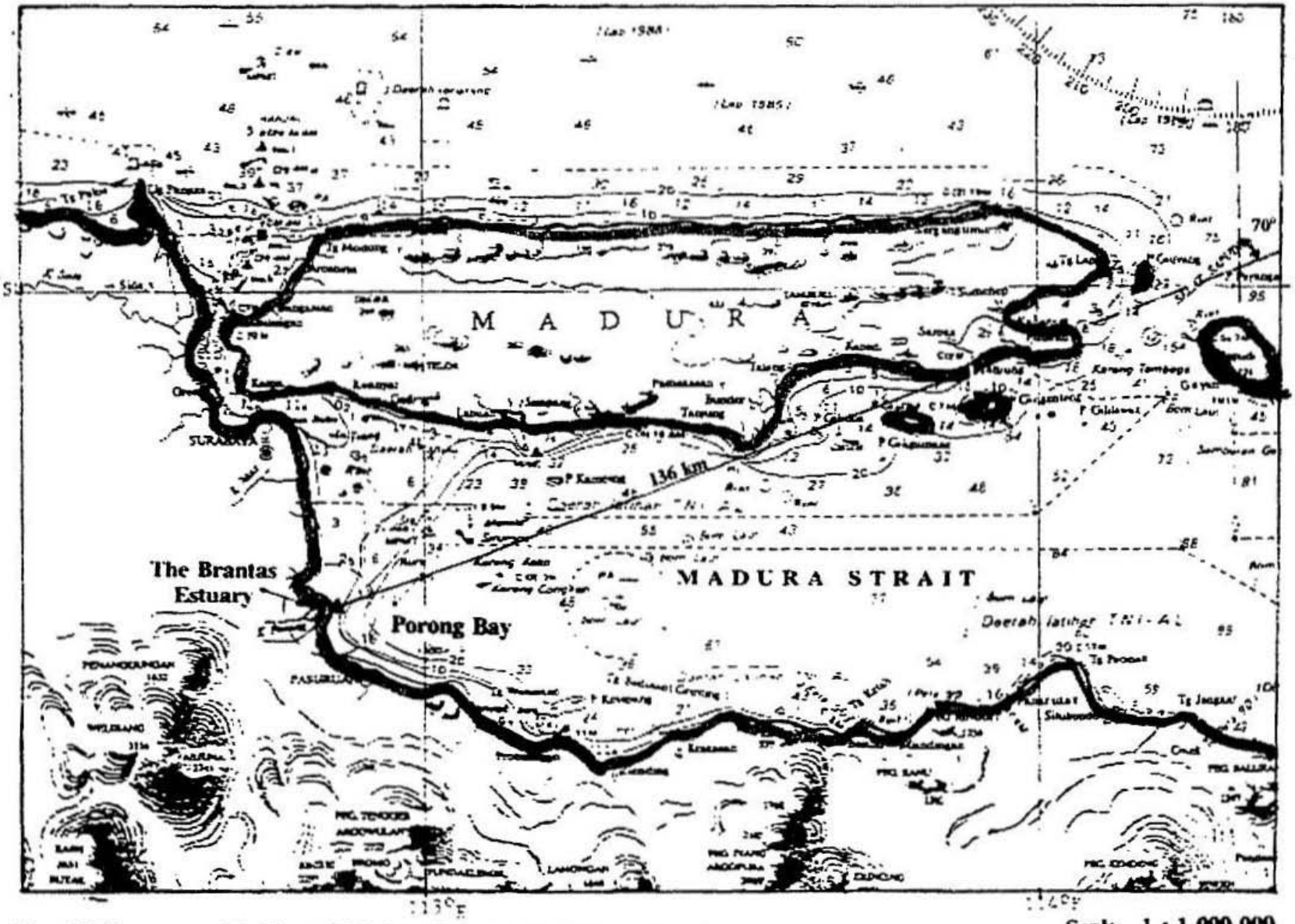

Fig. 4.2 Oceanographic Map of Madura Strait, East Java, Indonesia

Scale 1 : 1,000,000

Horizontal Voer Peil (SHVP) which is 2.40 m above the Harbour Reference. To avoid the confusion, elevation data hereafter, will be transferred to SHVP.

Tidal data in the harbour is very useful for comparison with the tidal data of the Brantas estuary which is obtained from the field measurements. This will be done in chapter 5. Summarized data from June 6 through July 12 is shown in table 4.3.

Some important features can be identified from the table. First, the rise and fall of the water occurs twice a day with unequal height. Every month, there are two spring and two neap tides. According to the type of tides (see section 3.2.1), the tide of Surabaya Harbour or Madura Strait is characterized as a mixed diurnal tide with bimonthly spring and neap tides. The period of one tidal cycle is about 24 to 25 hours (lunar day = 24 hours and 50 minutes). Consequently, the period of rise and fall moves forward periodically. For example, if on one day the fall and rise of the tide begins at 7 a.m and 1.00 p.m respectively, in the next two or three days, the time will change to 8.00 a.m and 2.00 p.m., and so forth. Unfortunately, the data is recorded hourly, so details of moving time cannot be explained in detail. Second, from table 4.3, the mean duration of the flood and ebb tides are 6.25 and 6.13 hours respectively (see table 4.3). The values are almost equal and they tend to have the same period of mean tidal rise and fall and mean tidal range.

Finally, in order to make the tidal fluctuation of Surabaya Harbour clear, data in table 4.3 have been transformed to figure 4.3.

Table 4.3 Tidal Data of Surabaya Harbour

Location : Karang Kleta (07.3 South - 112.8 East)
Recording period : From June 6, 1991 to July 12,1991

Date		High Water		Low Water		Duration		Range	
		Time	El. m,SHR	Time	El. m,SHR	Fall	Rise	Fall	Rise
						hrs		m	
June	6	7	2.00	13	1.40	6.0	5.0	0.60	0.20
		18	1.60	24	1.00	6.0	7.0	0.60	0.98
	7	7	2.20	14	1.10	7.0	5.0	0.99	0.50
		19	1.60	1	1.10	6.0	6.0	0.50	1.30
	8	7	2.40	15	0.80	8.0	5.0	1.60	0.80
		20	1.60	2	1.10	6.0	6.0	0.50	1.50
	9	8	2.60	16	0.50	8.0	5.0	2.10	1.20
		21	1.70	2	1.10	5.0	6.0	0.60	1.70
	10	8	2.80	16	0.20	8.0	6.0	2.60	1.60
		22	1.80	3	1.20	5.0	6.0	0.60	1.80
	11	9	3.00	17	0.00	8.0	6.0	3.00	1.80
		23	1.80	4	1.20	5.0	5.0	0.60	1.90
	12	9	3.10	17	-0.10	8.0	7.0	3.20	2.00
	13	24	1.90	4	1.20	4.0	6.0	0.70	1.90
		10	3.10	18	-0.20	8.0	7.0	3.30	2.20
	14	1	2.00	5	1.30	4.0	6.0	0.70	1.70
		11	3.00	19	-0.20	8.0	6.0	3.20	2.20
	15	1	2.00	6	1.30	5.0	6.0	0.70	1.60
		12	2.90	19	-0.10	7.0	7.0	3.00	2.10
	16	2	2.00	7	1.40	5.0	6.0	0.60	1.30
		13	2.70	20	0.00	7.0	6.0	2.70	2.00
	17	2	2.00	8	1.50	6.0	6.0	0.50	0.90
		14	2.40	21	0.30	7.0	6.0	2.10	1.70
	18	3	2.00	9	1.50	6.0	5.0	0.50	0.70
		14	2.20	22	0.50	8.0	6.0	1.70	1.50
	19	4	2.00	10	1.40	6.0	5.0	0.60	0.50
		15	1.90	23	0.70	8.0	6.0	1.20	1.50
	20	5	2.20	11	1.20	6.0	6.0	1.00	0.50
		17	1.70	24	0.90	7.0	5.0	0.80	1.40
	21	5	2.30	11	0.90	6.0	7.0	1.40	0.80
		18	1.70	1	1.10	7.0	5.0	0.60	1.30
	22	6	2.40	12	0.60	6.0	7.0	1.80	1.10
		19	1.70	2	1.20	7.0	5.0	0.50	1.30
June	23	7	2.50	13	0.40	6.0	7.0	2.10	1.40
		20	1.80	3	1.40	7.0	5.0	0.40	1.20

(next page)

Table 4.3 (Continued)

Date		High Water		Low Water		Duration		Range	
		Time	El. m,SHR	Time	El. m,SHR	Fall hrs	Rise	Fall m	Rise
June	24	8	2.60	14	0.20	6.0	7.0	2.40	1.70
		21	1.90	4	1.40	7.0	4.0	0.50	1.30
	25	8	2.70	14	0.10	6.0	7.0	2.60	1.80
		21	1.90	5	1.50	8.0	5.0	0.40	1.20
	26	10	2.70	15	0.00	5.0	7.0	2.70	1.90
		22	1.90	6	1.50	8.0	4.0	0.40	1.30
	27	10	2.80	16	0.00	6.0	7.0	2.80	1.80
		23	1.80	6	1.50	7.0	5.0	0.30	1.20
	28	11	2.70	17	0.10	6.0	7.0	2.60	1.70
	29	24	1.80	6	1.50	6.0	5.0	0.30	1.20
		11	2.70	17	0.20	6.0	7.0	2.50	1.50
	30	24	1.70	6	1.50	6.0	5.0	0.20	1.10
		11	2.60	18	0.30	7.0	7.0	2.30	1.50
July	1	1	1.80	7	1.50	6.0	5.0	0.30	1.00
		12	2.50	19	0.40	7.0	7.0	2.10	1.40
	2	2	1.80	7	1.40	5.0	6.0	0.40	0.90
		13	2.30	20	0.60	7.0	6.0	1.70	1.20
	3	2	1.80	8	1.40	6.0	6.0	0.40	0.60
		14	2.00	20	0.80	6.0	7.0	1.20	1.20
	4	3	2.00	9	1.40	6.0	6.0	0.60	0.40
		15	1.80	21	0.90	6.0	7.0	0.90	1.20
	5	4	2.10	9	1.20	5.0	7.0	0.90	0.30
		16	1.50	22	1.10	6.0	6.0	0.40	1.10
	6	4	2.20	10	1.00	6.0	7.0	1.20	0.50
		17	1.50	23	1.20	6.0	6.0	0.30	1.20
	7	5	2.40	10	0.60	5.0	8.0	1.80	1.00
		18	1.60	24	1.30	6.0	6.0	0.30	1.30
	8	6	2.60	11	0.30	5.0	8.0	2.30	1.40
		19	1.70	1	1.30	6.0	6.0	0.40	1.50
	9	7	2.80	12	0.10	5.0	8.0	2.70	1.80
		20	1.90	2	1.30	6.0	6.0	0.60	1.60
	10	8	2.90	13	-0.10	5.0	8.0	3.00	2.10
		21	2.00	3	1.30	6.0	6.0	0.70	1.70
	11	9	3.00	14	-0.20	5.0	8.0	3.20	2.20
		22	2.00	4	1.20	6.0	6.0	0.80	1.80
July	12	10	3.00	16	-0.20	6.0	-	3.20	-
Average :			2.19		0.82	6.25	6.13	1.36	1.36
Equal to SHVP			-0.21*)		-1.58				

*)0.00 m, SHVP is equivalent to + 0.90 m above mean sea level (MSL). 0.00 m, SHR (Surabaya Harbour Reference) is located at 1.50 m below the MSL. Therefore, 0.00 m, SHVP is equal to +2.40 m, SHR.

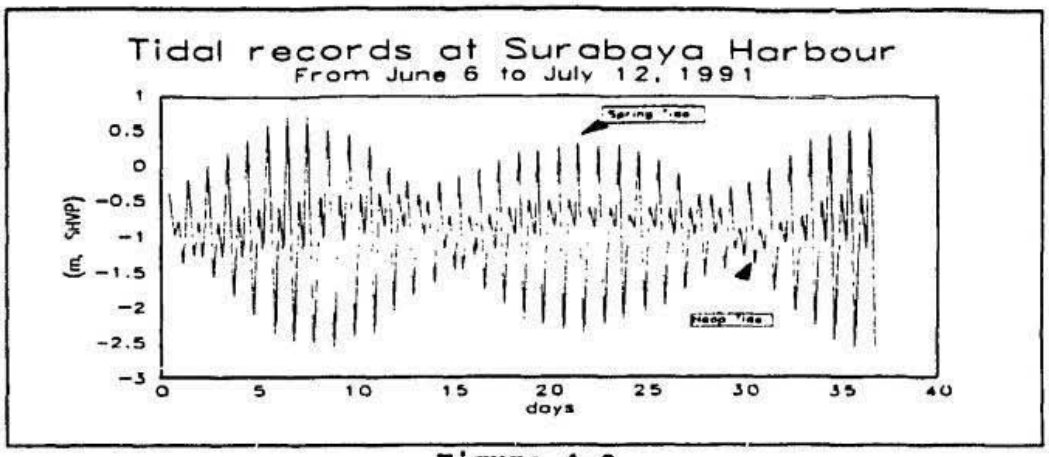

Figure 4.3

4.1.4 River Discharge

Prior to identification of fixed points along the Porong River, the Brantas River Basin Development Executing Agency (later called the Brantas Project or Brantas Office) has installed concrete piles on the levee crown on both banks. The distance between two piles is 200 m. The piles are named KP which is an abbreviation of Kali Porong. Pile numbers are given to identify the distance from the New Lengkong dam downwards to the estuary multiplying by 200 m. There are 255 piles from KP.1L (left) and KP.1R (right), at the dam, to KP.255 (L and R), at the shortcut river mouth. The approximate length of the Porong River is 51 km. All locations along the river, hereafter, will be indicated by KP and its number.

There are three water level and discharge gauge stations. The first is Porong station which is located at KP.154. It is about 30.8 km downstream of the New Lengkong Dam or 20.2 km upstream of the estuary mouth. The second is Permisan station which is found

at KP.183 (36.60 Km downstream of the New Lengkong Dam or 14.40 km from the estuary mouth). The last station is Tanjungsari which is found at KP.230. That is about 46 00 km downstream of the dam or 5 km from the river mouth. The locations of the three stations are shown figure 4.4. Daily water level data from 1977 through 1988 is

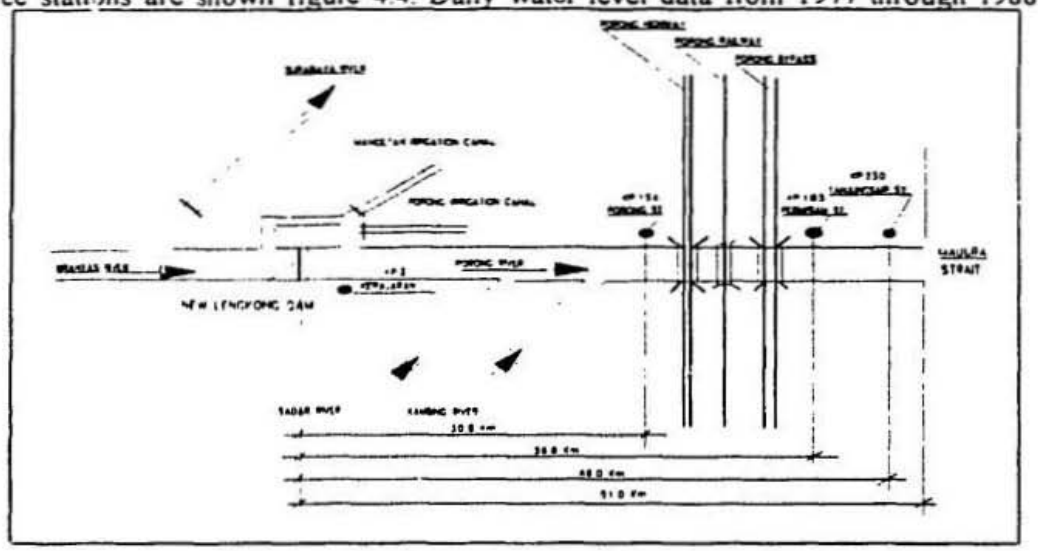

Fig.4.4 Schema of the Porong River and Locations of Water Gauging Stations

available for each station. Monthly mean discharge at Porong during that period is listed in table 4.4 and illustrated in figure 4.5.

Table 4.4 Monthly Mean Discharge at Porong Station (m^3/sec)

Year	Jan	Feb	Mar	Apr	May	Jun	Jul	Aug	Sep	Oct	Nov	Dec
1977	243	313	462	279	60	63	22	23	20	19	21	95
1978	377	391	391	189	291	384	338	85	91	74	142	332
1979	662	575	379	454	499	269	24	18	9	6	18	133
1980	365	415	251	328	82	7	5	6	3	2	59	259
1981	409	429	345	212	265	88	121	18	31	52	140	364
1982	575	606	540	312	39	4	4	2	1	1	0	40
1983	241	438	414	376	567	96	17	3	1	16	137	115
1984	449	798	597	600	121	17	5	2	59	39	17	212
1985	248	383	448	294	33	115	2	2	14	30	10	89
1986	374	474	561	588	29	85	43	4	10	21	82	63
1987	371	683	294	32	12	3	1	1	1	1	2	191
1988	333	301	214	87	96	27	18	17	18	23	47	68

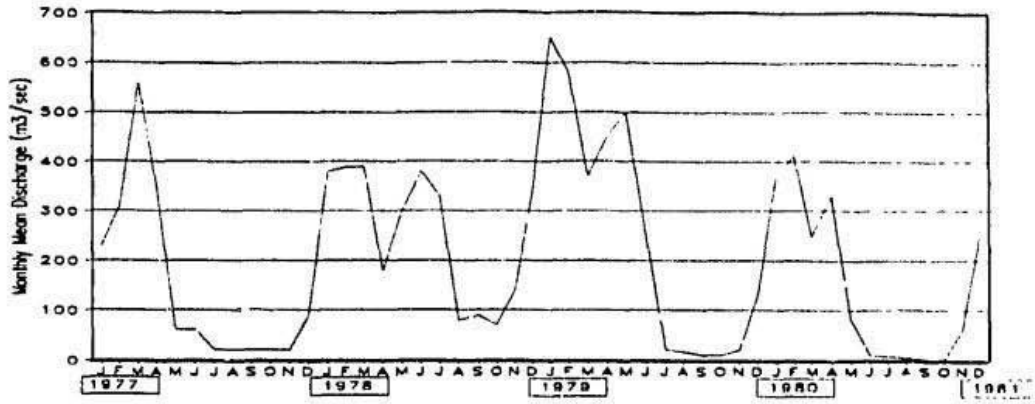

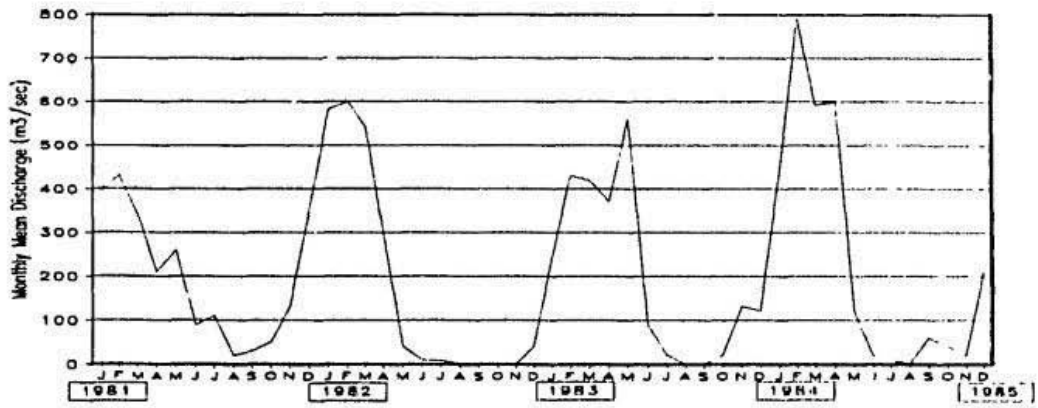

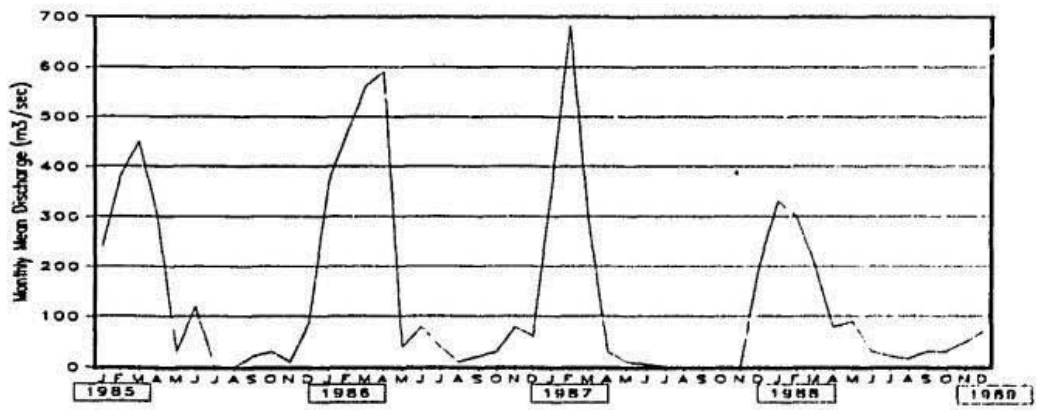

Fig.4.5 Hydrograph of Monthly Mean Discharge at Porong River

According to table 4.4 and figure 4.5, the mean river discharge at the Porong river is 301 m^3/sec in the rainy season and 63 m^3/sec in the dry season. Eight high discharges have been recorded during the period of 1977 to 1988. The instantaneous flood discharges at the Porong station in those flood conditions were around 1,100 to 1,300 m^3/sec and the highest discharge was 1,466 m^3/sec. It happened on April 7 and 8, 1986.

4.2 Design of the Shortcut River Channel

The shortcut river channel was designed and constructed in 1966 by the Brantas Project associated with Nippon Koei Consulting Engineers, Japan. The size and shape of the channel was based on the general standard design of the Porong River improvement but there was no special design of the shortcut channel. Basically, the shortcut channel and the old or the original river branch must enable the flood discharge of 1,600 m^3/sec, 50 year probable flood, to flow rapidly down to the sea.

4.2.1 Hydrology

In 1966, there were three water level stations and only one run-off and water level station. The three water level stations are those mentioned in the previous section (Porong, Permisan and Tanjungsari station) but the Permisan and Tanjungsari were originally located on the right bank of the river. Now, they are found on the left bank. The run-off and water level station, namely Kepajaran, is located immediately downstream from the Lengkong dam. At this site, the river bed changes seasonally. As a result, the relations between water stage and discharge are different every year and a

fixed stage-discharge rating curve cannot be obtained.

To calculate the 50 year flood (probability = 0.02) rainfall data was analyzed from stations surrounding the Porong river. The Maximum daily run-off (Q_{max}) was computed by

$$Q_{max} = 11.6x10^{-3} R_{max} A f \quad (4\text{-}1)$$

Where Q_{max} = maximum daily run-off (m^3/sec)

R_{max} = maximum daily rainfall (mm) with probability of 0.02

A = basin area in km^2

11.6 = a constant found by observation on the Brantas river.

f = run-off coefficient of individual flood (f = 0.27 is reasonable for Brantas river basin)

The maximum daily rainfall R_{max} was obtained by the Theissen method (quoted in Brantas River Basin Development Executing Agency, 1966, and Roberson et al., 1988) and was given by

$$R_{max} = \frac{\sum A_i R_i}{\sum A_i} = \frac{A_1R_1+A_2R_2+\ldots+A_nR_n}{A_1+A_2+\ldots+A_n} \quad (4\text{-}2)$$

Where R = average rainfall over a given area (mm)

. A_i = area represented by each rain gauge station (Km^2)

R_i = rainfall at each rain-gauge station (mm)

The catchment area of the Porong River is about 406.7 km^2. By using equation 4-2, the mean annual rainfall can be calculated. It was found to be 2,517 mm/year. Flood discharge probabilities were calculated by Gumbel's method (Brantas River Basin Development Executing Agency, 1966) and were found to be as shown in table 4.5. The

same calculation was done also at Djabon area, upper Porong river, and the result was 1,570 m^3/sec for a return period of 50 years. This was rounded to 1,600 m^3/sec.

Table 4.5 Probability of Flood Discharge in the Porong River

Probability	Porong Station (m3/sec)	N o t e :
Once in 5 years	1,300	
Once in 10 years	1,380	
Once in 25 years	1,490	
Once in 50 years	1,570	Recommended
Once in 100 years	1,650	

4.2.2 Sediment Discharges

According to section 3.4.1, sediment load can be classified into three kinds : Bed load, suspended load, and wash load. In this design calculation, a sediment grain size below 0.1 mm is dealt with as wash load.

In 1966, prior to commencement of the design river improvements on the Porong River, some observations of sediment transport were carried out at four places during three months. The annual bed load was then calculated using Sato-Kikkawa-Ashida's formula, 1958 (quoted in Brantas River Basin Development Agency, 1966 and 1990 or Bogardi, 1978, p.257). The formula is expressed as

$$\frac{q_B \left(\frac{\rho_s}{\rho} - 1\right) g}{\left(\frac{\tau_0}{\rho}\right)^{\frac{3}{2}} F\left(\frac{\tau_0}{\tau_c}\right)} = \phi \qquad \textbf{(4-3)}$$

Where q_B = bed load per unit time per unit width of section ($m^3/sec/m$)

ρ_s = density of riverbed material (kg/m^3)

ρ = density of water (kg/m^3)

g = acceleration due to gravity (m/sec^2)

τ_0 = shear stress on bed (N/m^2)

τ_c = critical shear stress on bed (N/m^2)

ϕ = Sato-Kikkawa-Ashida factor which depends on the bottom friction refers to Manning's roughness coefficient (n). If $n < 0.025$, $\phi = 0.623$ and if $n \geq 0.025$, $\phi = 0.623\ (40n)^{3.5}$

F = function of (τ_0/τ_c) which is presented in figure 4.6. For the Brantas river, this value was taken as 1, because the actual value was found to vary from 0.99 to 1.

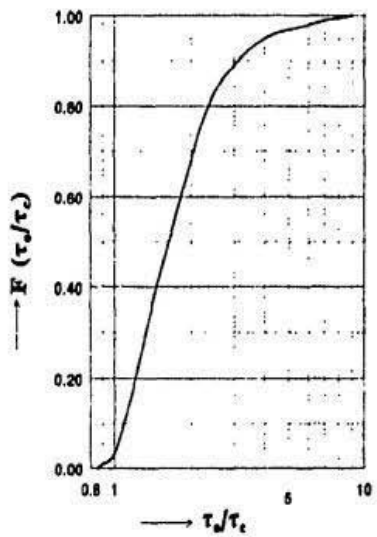

Fig.4.6 Relationships between $F(\tau_0/\tau_c)$ & τ_0/τ_c

Although the value of ϕ can be taken directly from the basic formula, in order to get the exact value, the Brantas Project has corrected the value by the least squares method based on measurements of q_b. The original formula can be assumed as

$y = a\,x$. Where

$$y = q_B \tag{4-4}$$

$$a = \frac{\phi}{(\frac{\rho_s}{\rho} - 1)} \tag{4-5}$$

$$x = \frac{\tau_0 U_*}{\rho\, g} \tag{4-6}$$

If $y = a\,x$ is written in logarithmic form, the equation is $Y = X + A$, where $Y = \log y$, $A = \log a$, and $X = \log x$. The constant A can be obtained by the method of least squares as follows

$$A = -\frac{Y - X}{n} \tag{4-7}$$

Where n is the total of samples considered. Based on observations carried out by the Brantas Project, the value of A was found to be -1.3182. Hence $a = 0.04806$ and $\phi = 0.09180$. Sato-Kikkawa-Ashida's formula (equation 4-3) can thus be presented as

$$\frac{q_B \left(\frac{\rho_s}{\rho} - 1\right) g}{\left(\frac{\tau_0}{\rho}\right)^{\frac{3}{2}}} = 0.0918 \tag{4-8}$$

The value of the critical tractive force (τ_c) can be found by Iwagaki's formula (quoted in Brantas River Basin Development Executing Agency, 1990), as

$$\tau_c = \rho\, U^2\, c \tag{4-9}$$

Where the value of $U.^2\, c$ depends on $R.$ while

$$R_* = \left[\left(\frac{\rho_s}{\rho} - 1\right) g\right]^{\frac{1}{2}} \frac{d^{\frac{3}{2}}}{\nu} \tag{4-10}$$

Where d : median diameter of river bed material (d_{50})

ν : kinematic viscosity of water

If the value of $R. \geq 671$; $U.^2\, c = 0.05\,(\rho_s/\rho - 1)\, g\, d$

$162.7 \leq R. \leq 671$; $U.^2\, c = \{0.01505\,(\rho_s/\rho - 1)g\}^{25/22}\, \nu^{-3/11}\, d^{31/22}$

$54.2 \leq R. \leq 162.7$; $U.^2\, c = 0.034\,(\rho_s/\rho - 1)\, g\, d$

$2.14 \leq R. \leq 54.2$; $U.^2\, c = \{0.1235\,(\rho_s/\rho - 1)g\}^{25/32}\, \nu^{7/16}\, d^{11/32}$

and if $R. \leq 2.14$; $U.^2\, c = 0.14\,(\rho_s/\rho - 1)\, g\, d$.

By using mean monthly water discharge (Q_w) the hydraulic parameters such as water depth (h) width of channel (b) and energy gradient (I_e) can be found. Finally, the rate of the sediment discharge can be calculated.

Suspended load was measured at the same places and the same time as bed sediments were taken. The sample obtained by the suspended load sampler is divided into suspended load and wash load based on the particle size. As mentioned in the beginning of this section sediment with a grain size below 0.1 mm is dealt with as wash load.

This suspended load is the main quantity of sediment causing deposition whether within the estuary or in the surf zone. Comparisons among three cases were, therefore, made to select the appropriate formula. The first case was an examination of the relationships between friction velocity (U_*) and sediment discharge per unit width and time (q_b) of a section. The second was to calculate the unknown factors of Kalinske-formula (quoted in Brantas River Basin Development Executing Agency, 1966 and Bogardi, 1978, p.712). The equation is presented as

$$\frac{q_s}{U_* d_{50}} = A_s \left[\frac{U_*^2}{(\frac{\rho_s}{\rho} - 1)\, g\, d_{50}} \right]^p \qquad \textbf{(4-11)}$$

Where d_{50} = median diameter of sediment (m)

ρ_s = density of riverbed material (kg/m^3)

ρ = density of water (kg/m^3)

A_s & p = constant value

Using Brown's formula (quoted in Brantas River Basin Development Executing Agency, 1966) $A_s = 10$ and $p = 2$. The third was to get the relationships between water

depth (H), square of the friction velocity (U_*^2), $H U_*^2$, and sediment discharge (q_s). By plotting data and application of the least squares method, the results of the three cases above was found as follows

$$q_s = 1.357 U_*^{4.764} \tag{4-12}$$

$$\frac{q_s}{U_* d_{50}} = 4.051 \left[\frac{U_*^2}{(\frac{\rho_s}{\rho} - 1) g\, d_{50}} \right]^{2.135} \tag{4-13}$$

$$q_s = 6.62 \times 10^{-2} (H U_*)^{1.479} \tag{4-14}$$

Based on an accuracy test to the three above equations by an index correlation, the last equation (4-14) has the best approximation. Therefore, the suspended sediment rate was calculated using equation 4-14.

The rate of wash load was calculated directly by an equation obtained from an examination of the relationships between water discharge (q_w) and sediment discharge (q_s). By the same process, the results can be presented as

$$q_s = 1.54\ 10^{-4}\ q_w^{1.88} \tag{4-15}$$

The annual sediment rate was divided into two conditions: mean annual sediment rate before and after river improvement. The main difference between the two conditions is the difference of the hydraulic gradient because of dredging works and shortcut channel at the river mouth. Consequently, the sediment rate will be also changed. The final result of both calculations is summarized in table 4.6.

Table 4.6 Annual Sediment Transport of the Porong River

Condition	Bed Load (m^3/year)	Suspended load (m^3/year)	Wash Load (m^3/year)	Total sediment (m^3/year)
Before Improvement				
Mean Rate	10,700	567,000	3,698,000	4,276,000
After Improvement				
1 - 20 km	11,700	1,031,000	5,864,000	6,907,000
20 - 30 km	12,000	1,070,000	6,148,000	7,230,000
30 - 41 km	11,300	1,152,000	7,308,000	8,471,000
41 - 48 km	10,900	991,000	6,570,000	7,572,000
Mean Rate	11,500	1,061,000	6,472,000	7,545,000

This result shows that most of the sediment consisted of suspended and wash load. A large part of these sediments will be flushed directly to the sea area and should be considered as important for the delta growth. The total annual sediment is the main source of sediment which will be distributed within the estuary and seawards.

From the table, it can be seen that the annual transport of bed sediment is very small compared to the amount of suspended and wash load sediment. This condition can be explained easily since the bed gradient of the Porong river is very gentle, so the tractive force is relatively small. In percentage, the bed, suspended and wash sediment after improvement are 0.15%, 14.06% and 85.79 % respectively .

In fact, after the shortcut channel was completed in 1977, the river bed of the Porong River exhibited very rapid degradation up to 1989. In view of this condition, the Brantas Project decided to rehabilitate and improve the river by doing some construction such as foot protection of the artificial levee as well as building new revetments and groundsills which were made while re-investigation of the sediment transport was

undertaken.

The sediment carrying capacity of the bed and suspended loads were estimated for each river cross section using the same formula as mentioned in the previous part of this section (see equations 4-3 to 4-11). The calculated values of discharge and sediment carrying capacity from KP.150 - KP.230 are illustrated in figure 4.7.

Annual sediment inflow (S_s) for each stretch was estimated by multiplying the sediment carrying capacity (S_q)

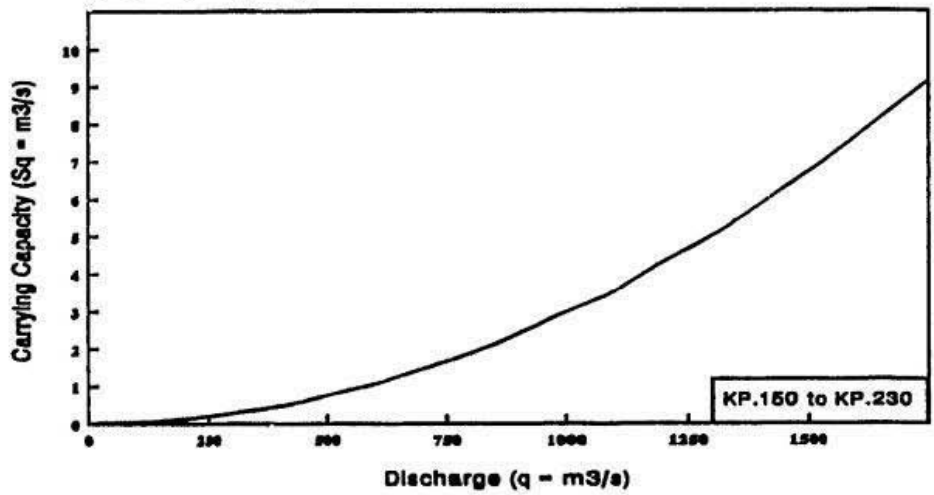

Fig 4.7 Relationships Between Water Discharge and Suspended Sediment Carrying Capacity of the Porong River

for each discharge with the duration of the discharge (D) over one year. It is, therefore, necessary to know the distribution of water discharges or to have discharge duration curves. Based on data from 1977 through 1988, the distribution of discharges can be calculated. The range of the discharge duration during one year was divided into 8 sections from 0 m^3/s through maximum discharge 1,466 m^3/sec . This curve is presented in figure 4.8.

Sediment carrying capacity corresponding to the 8 scales of discharge in figure 4.8

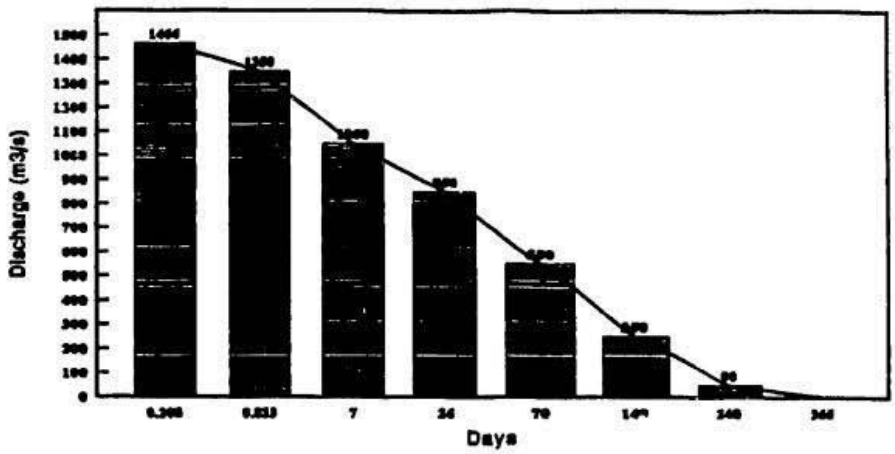

Fig.4.8 Discharge Duration Curve of the Porong River

can be read from figure 4.7. The estimated total annual rate was estimated by the following expression

$$S_a = \sum_{0}^{1466} S_q \; D \; 86400 \qquad \textbf{(4-16)}$$

Results are shown in table 4.7.

Table 4.7 Annual Suspended Sediment Transport

Section	KP.0-30	KP.30-80	KP.80-150	KP150-230
Annual S. Transport (1000 m^3)	20,500	16,100	18,100	11,200

4.2.3 Dimension of the Shortcut River channel

Design of the Porong river improvement was based on the data described in sections 4.2.1 and 4.2.2. However, no detailed information was available regarding the design of the shortcut channel and Brantas Office staff indicated that the dimension of the channel was determined approximately based on the average discharge of the Porong river at the

last confluence during the rainy season. This discharge is 301 m^3/sec. Typical dimensions are presented in figure 4.9.

4.2.4 Dredging Maintaining Work

In order to maintain the water-route at the estuary, the Brantas Project has organized continuous maintenance dredging at the estuary from 1978 up to 1989. The maintenance dredging volume each year can be found in table 4.8. Other routine dredging work was also done along the middle reach of the Porong river from 1980 to 1987. The annual volume of the dredging work is presented in table 4.9. The mean annual volume of the dredging work at the estuary was about 141,000 m^3/year.

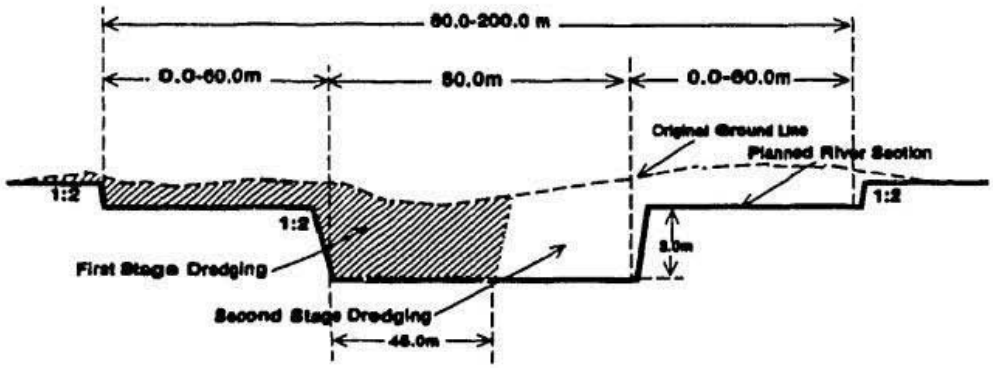

Fig.4.9 Cross-Sectional Design of Shortcut Channel

Table 4.8 Maintenance Dredging Work Along the Shortcut Channel
(Unit : 10^3 m^3)

Year	1978	1979	1980	1981	1982	1983
Volume	230	464	154	159	77	48
Year	1984	1985	1986	1987	1988	1989
Volume	168	95	108	50	85	55

Table 4.9 Maintenance Dredging Work in the Middle Reach of Porong River
(Unit : 10^3 m^3)

Year	1980	1981	1982	1983	1984	1985	1986	1987
Vol.	971	1,873	1,930	1,950	1,589	1,307	1,124	507

4.3 Geometrical Measurement Data of Porong Estuary

In order to understand the physical changes of the estuary since the shortcut channel was completed in 1977 up to now, some measurements of geometric data are used. Furthermore, details of the geometry can be evaluated by cross and longitudinal sections of the channel.

4.3.1 Physical Changes in the Estuary

Figure 2.3 shows the estuary topography in 1945 and figure 2.4 shows the plan view and topography of the estuary in 1977 when the shortcut channel was completed. Figure 2.5 and figure 2.6 show the plan view of the delta and an aerial photo taken in 1985. The difference between them can be made clear if the three figures (figures 2.3, 2.4 and 2.5) with the same scale are put on a tracing paper.

The estuary continues to grow offshore with sediment transported from upstream as the main resource. Growth is especially remarkable on the right bank of the shortcut mouth. On the basis of the three figures above, general features of
the delta growth is presented in figure 4.10.

This figure shows that from 1945 to 1977 significant delta growth happened in the

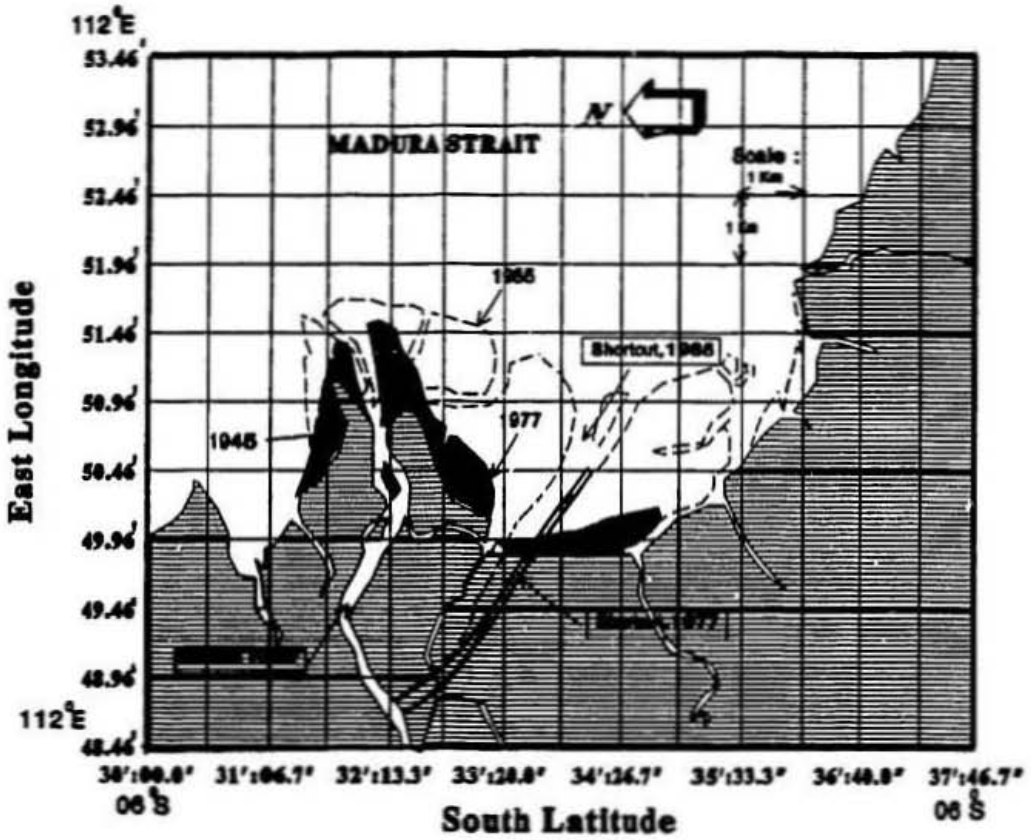

Fig.4.10 The Growth of the Brantas Delta, 1945 - 1985

area surrounding the original river mouth. This occurred in the northern and southern parts of the mouth but the deposition in the southern part was more dominant than that in the northern part. Since the shortcut channel was completed in 1977, delta growth has been changing to the area around the shortcut mouth or the southern part of the original river mouth. To know the present geometric condition of the delta area, the Brantas Project carried out topographic measurements in 1989 at the area in front of the shortcut

river mouth (see appendix B, figures B.5-1 to B.5-9). The area covered 3.25 km from the estuary mouth seawards and about 3.00 km of the shoreline length with the centre placed at the axis of the shortcut river mouth. Based on this topographical measurement, the mean gradient of the delta area was found to be 0.00112. This was taken from the mean gradient of 5 lines on the area seawards with 750 m distance between the lines. The result is illustrated in figure 4.11.

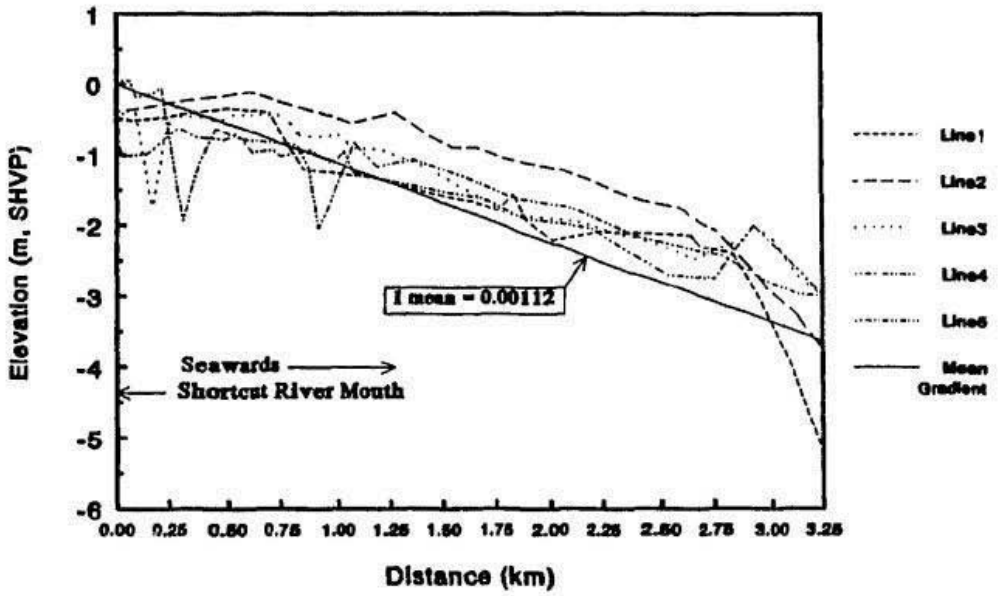

Fig.4.11 Mean Gradient on the Delta Area

Along the shortcut channel, the downstream half of the channel is now mostly buried with sediment particularly at the right side (facing downstream), so the water-route tends to go to the left side, making a meander, between the middle reach and the shortcut mouth. This process will be more clear by doing some comparisons of cross and longitudinal sections of the shortcut channel including the estuary. The comparisons will be discussed in the following section.

4.3.2 Cross and Longitudinal Sections

Some cross sectional surveys carried out on the Brantas river show that, in general, the width of the river sections have not changed considerable except for the cross sections along the shortcut channel. Cross sectional comparisons of the shortcut channel between the original design (1977) and the present condition (1990) as well as the measurements carried out in the dry season 1991 are presented in figure 4.12.

In longitudinal section, the river bed fluctuation from 1977 to 1988 was analyzed on the basis of a cross sectional survey with around 200 m intervals beginning from the Lengkong Dam (KP.0) to KP.237, about 45 km downstream from the dam. This study has been done by the Brantas Project. As a result, the degradation of the deepest riverbed along the water route has been found to vary between +0.221 m/year (from 1977 through 1986) and -0.034 m/year. Detailed drawings of the riverbed fluctuation are shown in figure 4.13 and the average amount of the degradation in every river section is shown in table 4.10.

Table 4.10 Average Riverbed Degradation

Dura-tion	River Stretch (KP.No)					Average	
	0- 50	50-100	100-150	150-200	200 - 237	All year	per Stretch
1977-1986	2,41	1,91	1,90	1,78	1,97	1,99	0,22
1986-1988	0.04	0.03	-0.07	-0.02	-0.31	-0.07	-0.03

Degradation happened continuously from 1977 through 1986. Slight deposition has

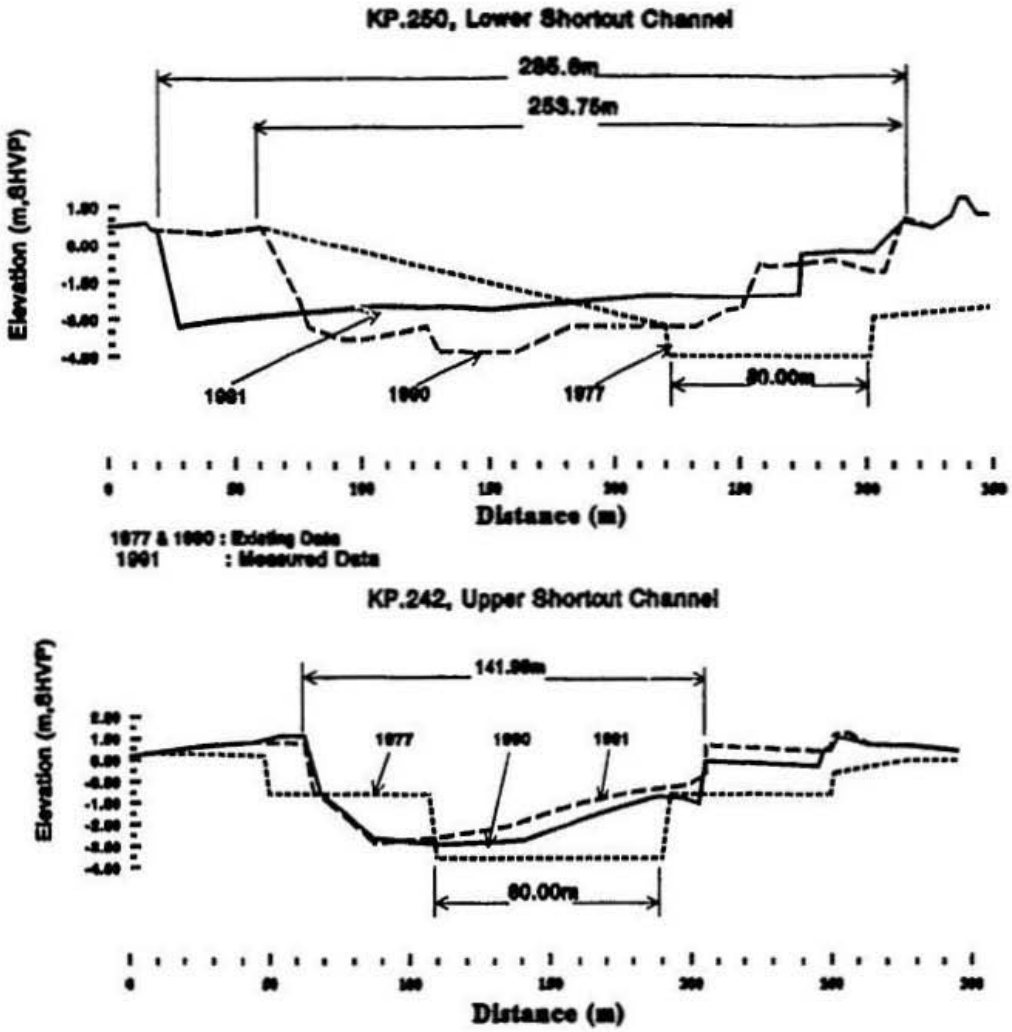

Fig.4.12 Cross Sectional Changes of the Shortcut Channel

been occurring since then. The effect of a sediment trap by the dam constructed in the upstream area and manual sand mining by people may be considered as conceivable causes of the degradation. However, regardless of the degradation of the channel, the deposition in the area surrounding the shortcut mouth happens continuously. Another possible reason is, therefore, that the hydraulic condition enables sediment to be flushed directly to the surf zone. Detailed discussions will be presented in chapter 6.

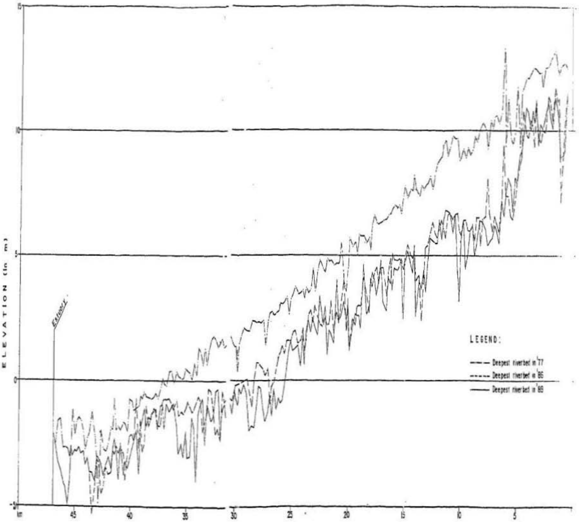

DISTANCE FROM NEW LENGKONG DAM	46,940	45,686	43,640	41,631	39,949	37,959	35,962	33,942	31,980	30,100	28,142	26,141	24,238	22,247	20,255	18,271	16,319	14,266	12,273	10,277	8,273	6,272	4,341	2,310	0,431	0
DISTANCE FROM ESTUARY	0	1,254	3,046	5,109	6,994	8,981	10,978	12,976	14,960	16,840	18,798	20,799	22,702	24,693	26,685	28,669	30,621	32,674	34,667	36,663	38,667	40,668	42,599	44,630	46,509	46,947
KP. PILE NO.	237	230	220	210	200	190	180	170	160	150	140	130	120	110	100	90	80	70	60	50	40	30	20	10	1	435

Fig.4.13 Fluctuation of the Deepest River Bed, Ta

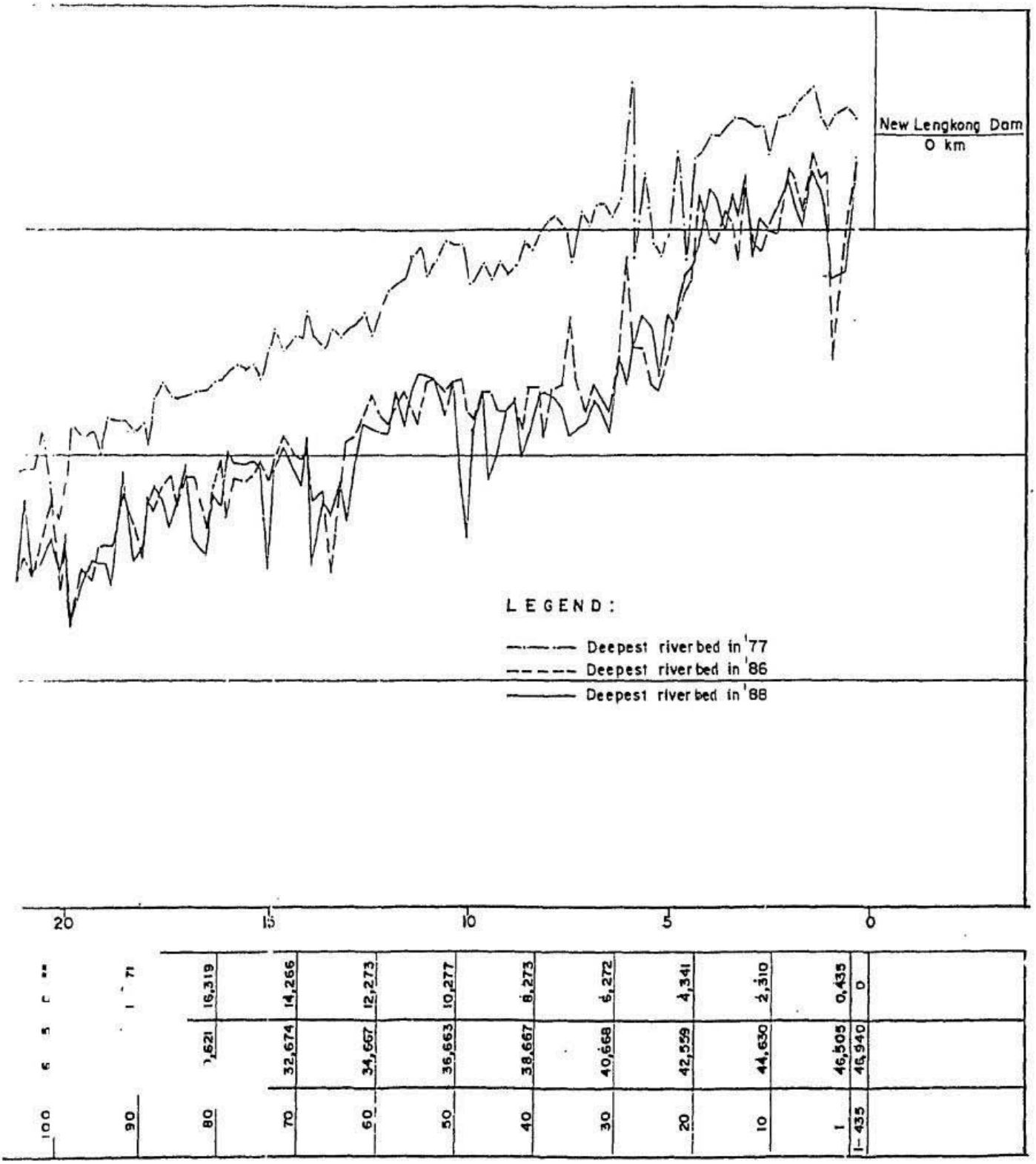

Fig.4.13 Fluctuation of the Deepest River Bed, Talwegs (1977 - 1988)

Chapter 5

Field Measurement Data and Analysis

Chapter 5

Field Measurement Data and Analysis

Field measurements of the Brantas Estuary were carried out during the dry season of 1991. Data such as duration of flood and ebb tides, tidal ranges, tidal currents during tidal cycles, sediments, salinity and temperature distributions within longitudinal and cross sections of the estuary have been taken. Observation of waves, wind and longshore currents were also observed. Data and analysis will be presented in this chapter.

5.1 Tidal Measurement Data

According to the recorded tide data at Surabaya harbour (see chapter 4.1.3), the typical tide at Surabaya harbour is mixed diurnal with bimonthly spring and neap tides. The flood and ebb tides occur twice per day with different ranges at high and low water. The spring and neap tides happen twice a month. In order to determine tidal penetration within the estuary, tidal measurements were taken within the estuarine regions.

5.1.1 Tidal Measurement

Tidal water levels were measured using the simplest tidal gauge or peil schaal, a simple staff graduated in meters and read manually by an observer. The tidal gauges were

installed on the right bank of the river and the zero elevations of the gauges were placed below the low low water level (LLWL). The main reason for this was so that the water level could be identified continuously even in the neap tidal condition.

Five tidal gauges were installed. The stations were placed to measure the different tidal ranges, their periods and mean tidal elevations. Location of the stations is shown in figure 5.1.

The first station was located 1 km upstream from the shortcut channel mouth (KP.250[1]). The second station was placed 2.6 km from the mouth. Both stations are in the shortcut channel. Tidal data obtained from both stations were used for analyzing the tidal behaviour along the channel. A branch between the old river or original river and the shortcut channel is found at KP.238. The third station was located 400 m upstream from the branch (KP.236). This means that the station was placed 3.8 km from the shortcut mouth or about 6.2 km from the original river mouth. Data obtained from this station were used for determining whether the tidal influence comes from the shortcut channel or from the original river. The fourth station was placed on the original river about 0.75 km downstream from the tributary or 5.0 km from the original river mouth. The abbreviation of Sembilangan River is, SB, which is taken from one name of an original branch river before the original river reaches the sea. Observations at this station were used for analyzing the tidal influence that comes through the original river. The last tidal station was placed 15 km upstream from the shortcut channel mouth. These data were useful for analyzing the limit of the tidal penetration.

[1] "KP" is abbreviation of "Kali Porong". See section 4.1.4

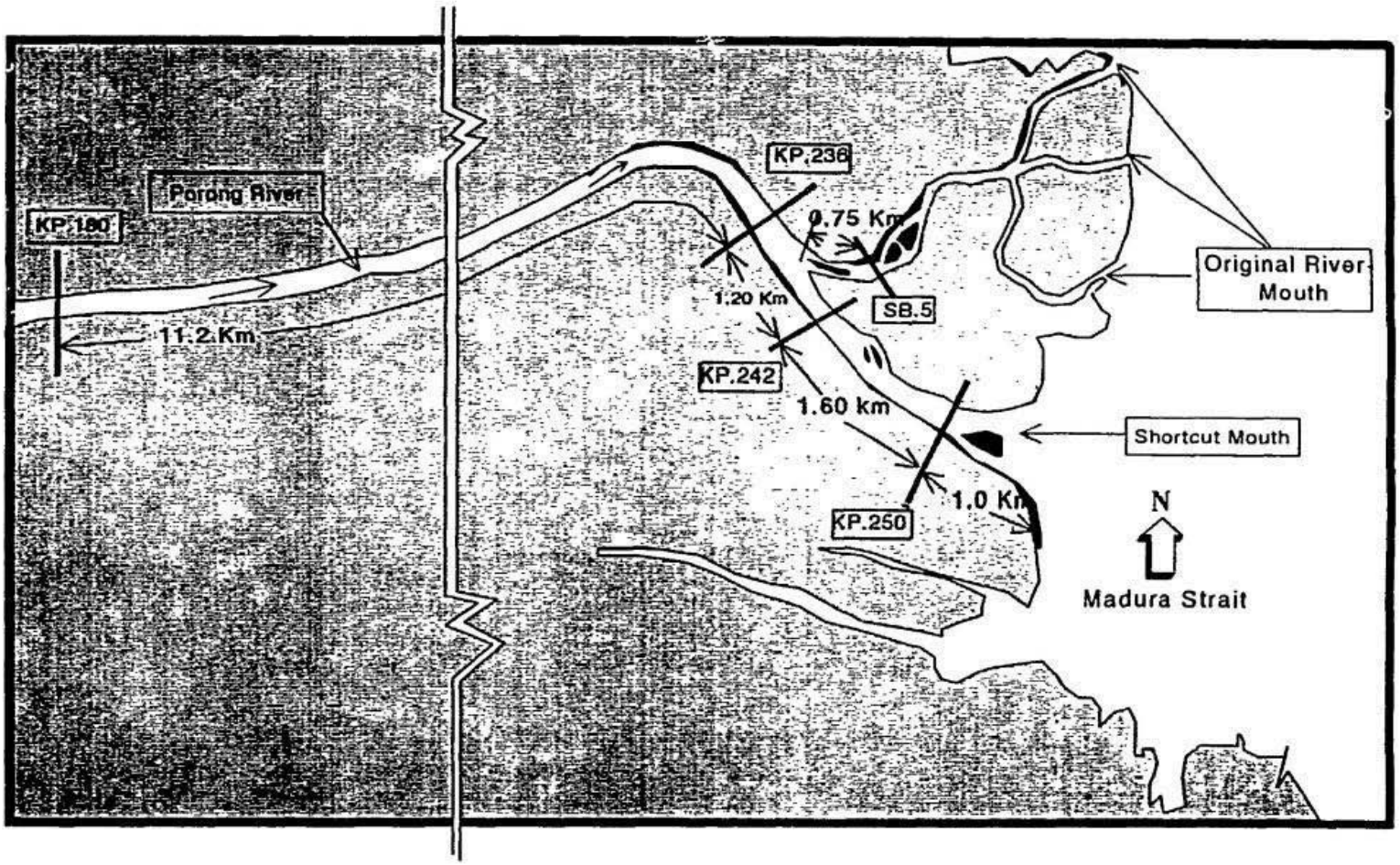

Fig.5.1 Locations of Field Observations

Data were recorded hourly from June 6 to July 12, 1991. Recorded data relating to water levels at KP.250 are presented in table 5.1, while data for other stations are given in appendix A, tables A.1-1 to A.1-4. The tidal fluctuations at the five stations during field observations will be clearer if they are also compared to the tidal data recorded at Surabaya Harbour (see table 4.3) which is located about 25 km northward of the river mouth. This comparison is presented in figure 5.2.

The tables (table 5.1 and appendix A, table A.1-1 through table A.1-4) show that the mean durations of the tidal rise and fall among the stations are different. Generally, the ebb or falling tide has a longer period than the rising or flood tide at every station. The difference becomes significant at the upper station (KP.180) where the ebb period is much longer than the flood period. At KP.242, KP.236 and SB.5, the rise and fall happen almost in the same time. This is because there is little distance between them. One significant factor which should be noted is that the ebb period at those stations is shorter than that of the upstream station but the flood period is longer than that of the upstream station. In addition, the ebb and flood periods at the most downstream station (KP.250) are almost equal.

The mean tidal ranges at the stations are all different. The upper stations have less mean tidal range than the lower stations. Tidal range at KP.180, for example, is smaller than that of KP.236, but it is still larger than the tidal range at KP.242. The tidal range decreases gradually landward. This is caused by the reduction in energy of the tide because of the estuary bottom friction and other geometric factors. This condition will be discussed in greater detail in chapter 6. The mean tidal periods and ranges are

Taole 5.1
TIDAL DATA

Location : Shortcut channel
Tidal Gauge : KP.250 (1 km Upstream the Shortcut Mouth)
Recording period : From June 6, 1991 to July 12,1991

Date	High Water		Low Water		Duration		Range		Mean Level	
	Time	Elevation m,SHVP	Time	Elevation m,SHVP	Fall hrs.	Rise hrs.	Fall m	Rise m	m,SHVP	
June 6	8	-0.396	14	-0.936	6.0	4.0	0.54	0.43	-0.666	-0.721
	18	-0.506	1	-1.126	7.0	6.0	0.62	1.10	-0.816	-0.576
7	7	-0.026	14	-1.136	7.0	5.0	1.11	0.63	-0.581	-0.821
	19	-0.506	1	-1.066	6.0	7.0	0.56	1.12	-0.786	-0.505
8	8	0.056	15	-1.186	7.0	5.0	1.24	0.69	-0.565	-0.841
	20	-0.496	2	-1.106	6.0	6.0	0.61	1.38	-0.801	-0.415
9	8	0.276	15	-1.245	7.0	7.0	1.52	0.76	-0.4845	-0.8655
	22	-0.486	3	-1.116	5.0	5.0	0.63	1.53	-0.801	-0.35
10	8	0.416	16	-1.246	8.0	7.0	1.66	0.83	-0.415	-0.831
	23	-0.416	4	-1.106	5.0	5.0	0.69	1.71	-0.761	-0.25
11	9	0.606	17	-1.296	8.0	6.0	1.90	0.97	-0.345	-0.811
	23	-0.326	4	-1.096	5.0	5.0	0.77	1.79	-0.711	-0.2
12	9	0.696	18	-1.306	9.0	6.0	2.00	0.98	-0.305	-0.816
13	24	-0.326	4	-1.086	4.0	6.0	0.76	1.80	-0.706	-0.185
	10	0.716	18	-1.326	8.0	7.0	2.04	1.11	-0.305	-0.771
14	1	-0.216	5	-1.026	4.0	6.0	0.81	1.74	-0.621	-0.155
	11	0.716	19	-1.245	8.0	6.0	1.96	1.05	-0.2645	-0.7205
15	1	-0.196	6	-0.896	5.0	5.0	0.70	1.60	-0.546	-0.095
	11	0.706	19	-1.216	8.0	7.0	1.92	1.16	-0.255	-0.636
16	2	-0.056	8	-0.926	6.0	4.0	0.87	1.43	-0.491	-0.21
	12	0.506	20	-1.166	8.0	6.0	1.67	1.08	-0.33	-0.626
17	2	-0.086	7	-0.825	5.0	7.0	0.74	1.25	-0.4555	-0.2
	14	0.425	21	-1.125	7.0	6.0	1.55	1.14	-0.35	-0.555
18	3	0.015	8	-0.805	5.0	7.0	0.82	1.03	-0.395	-0.29
	15	0.225	22	-1.085	7.0	6.0	1.31	1.14	-0.43	-0.515
19	4	0.055	9	-0.835	5.0	7.0	0.89	0.63	-0.39	-0.52
	16	-0.205	23	-1.005	7.0	6.0	0.80	1.04	-0.605	-0.485
20	5	0.035	10	-0.855	5.0	8.0	0.89	0.54	-0.41	-0.585
	18	-0.315	24	-0.985	6.0	5.0	0.67	1.09	-0.65	-0.44
21	5	0.105	11	-0.995	6.0	7.0	1.10	0.61	-0.445	-0.69
	18	-0.385	1	-0.935	7.0	5.0	0.55	1.15	-0.66	-0.36
22	6	0.215	12	-1.205	6.0	7.0	1.42	0.88	-0.495	-0.765
	19	-0.325	2	-0.925	7.0	5.0	0.60	1.21	-0.625	-0.32
23	7	0.285	13	-1.285	6.0	7.0	1.57	0.98	-0.5	-0.795
	20	-0.305	3	-0.905	7.0	5.0	0.60	1.23	-0.605	-0.29
June 24	8	0.325	14	-1.285	6.0	7.0	1.61	0.98	-0.48	-0.795
	21	-0.305	4	-0.925	7.0	5.0	0.62	1.31	-0.615	-0.27

(next page)

(Table 5.1 Continued)

Date		High Water		Low Water		Duration		Range		Mean Level	
		Time	Elevation m,SHVP	Time	Elevation m,SHVP	Fall hrs.	Rise hrs.	Fall m	Rise m	m,SHVP	
June	25	9	0.385	15	-1.305	6.0	6.0	1.69	1.06	-0.46	-0.775
	26	21	-0.245	4	-0.905	7.0	6.0	0.66	1.34	-0.575	-0.235
		10	0.435	15	-1.315	5.0	7.0	1.75	1.07	-0.44	-0.78
	27	22	-0.245	5	-0.915	7.0	6.0	0.67	1.42	-0.58	-0.205
		11	0.505	16	-1.315	5.0	7.0	1.82	1.08	-0.405	-0.775
	28	23	-0.235	5	-0.935	6.0	6.0	0.70	1.37	-0.585	-0.25
		11	0.435	17	-1.285	6.0	7.0	1.72	1.03	-0.425	-0.77
	29	24	-0.255	6	-0.965	6.0	5.0	0.71	1.31	-0.61	-0.31
		11	0.345	18	-1.285	7.0	6.0	1.63	1.00	-0.47	-0.785
	30	24	-0.285	7	-0.965	7.0	5.0	0.68	1.28	-0.625	-0.325
		12	0.315	19	-1.235	7.0	6.0	1.55	0.90	-0.46	-0.785
July	1	1	-0.335	8	-0.965	7.0	5.0	0.63	1.17	-0.65	-0.38
		13	0.205	20	-1.205	7.0	6.0	1.41	0.81	-0.5	-0.8
	2	2	-0.395	8	-0.945	6.0	6.0	0.55	0.95	-0.67	-0.47
		14	0.005	21	-1.115	7.0	5.0	1.12	0.70	-0.555	-0.765
	3	2	-0.415	9	-0.935	7.0	6.0	0.52	0.73	-0.675	-0.57
		15	-0.205	21	-1.005	6.0	6.0	0.80	0.77	-0.605	-0.62
	4	3	-0.235	10	-0.925	7.0	5.0	0.69	0.50	-0.58	-0.675
		15	-0.425	22	-0.955	7.0	6.0	0.53	0.83	-0.69	-0.54
	5	4	-0.125	10	-0.925	6.0	6.0	0.80	0.60	-0.525	-0.625
		16	-0.325	22	-1.055	6.0	6.0	0.73	1.04	-0.69	-0.535
	6	4	-0.015	11	-1.205	7.0	6.0	1.19	0.80	-0.61	-0.805
		17	-0.405	23	-1.015	6.0	7.0	0.61	1.09	-0.71	-0.47
	7	6	0.075	12	-1.275	6.0	6.0	1.35	0.93	-0.6	-0.81
		18	-0.345	24	-1.035	6.0	7.0	0.69	1.24	-0.69	-0.415
	8	7	0.205	13	-1.345	6.0	6.0	1.55	0.98	-0.57	-0.855
		19	-0.365	1	-1.035	6.0	7.0	0.67	1.30	-0.7	-0.385
	9	8	0.265	14	-1.345	6.0	6.0	1.61	1.00	-0.54	-0.845
		20	-0.345	2	-1.035	6.0	7.0	0.69	1.42	-0.69	-0.325
	10	9	0.385	15	-1.365	6.0	6.0	1.75	1.00	-0.49	-0.865
		21	-0.365	3	-1.065	6.0	7.0	0.70	1.57	-0.715	-0.28
	11	10	0.505	16	-1.375	6.0	6.0	1.88	1.02	-0.435	-0.865
		22	-0.355	4	-1.015	6.0	7.0	0.66	1.65	-0.685	-0.19
July	12	11	0.635	17	-1.365	6.0	-	2.00	-	-0.365	-
Average :			-0.01013		-1.09527	6.34	6.04	1.09	1.09	-0.55	-0.55

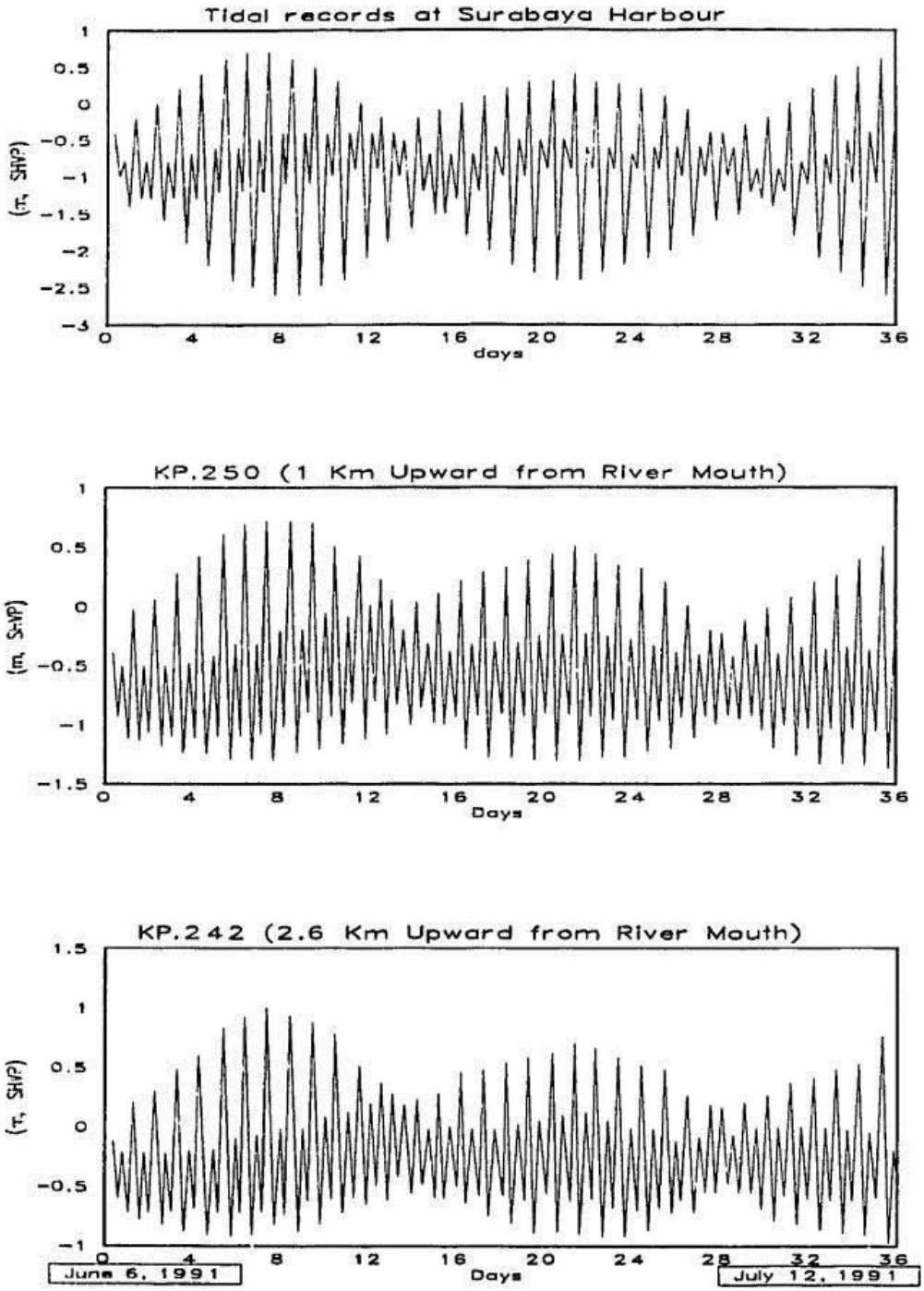

Fig.5.2 Recorded Tidal data at Surabaya Harbour and Five Stations along the Estuary during June 6, 1991 to July 12, 1991

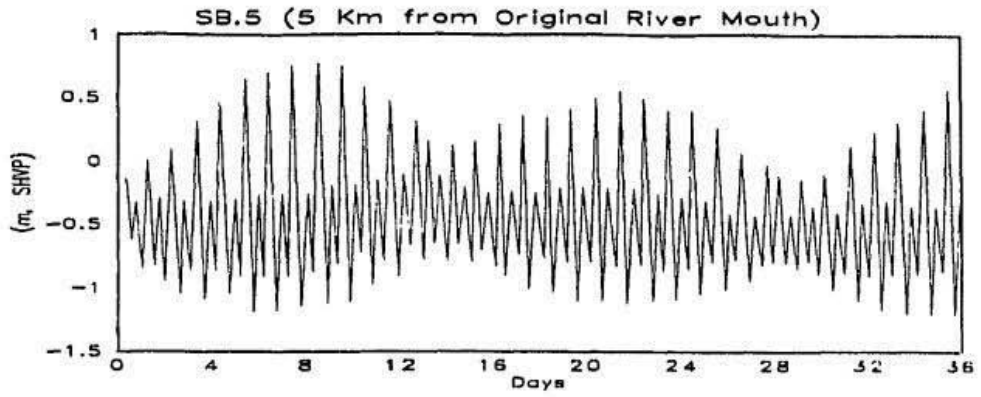

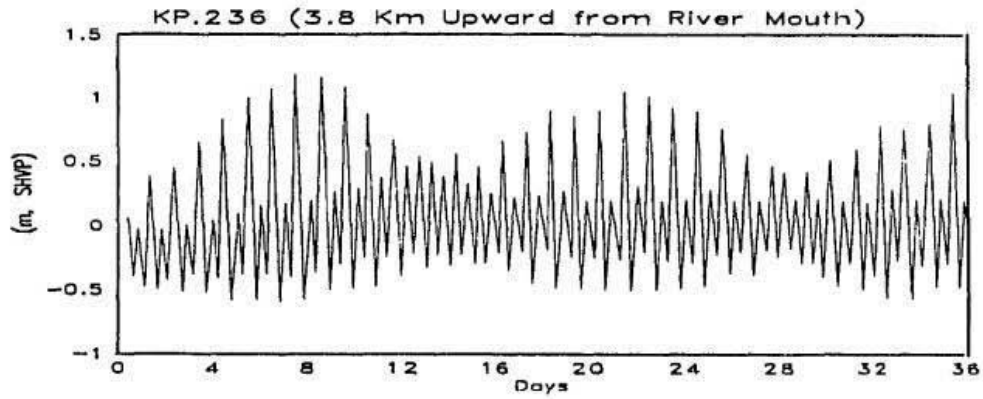

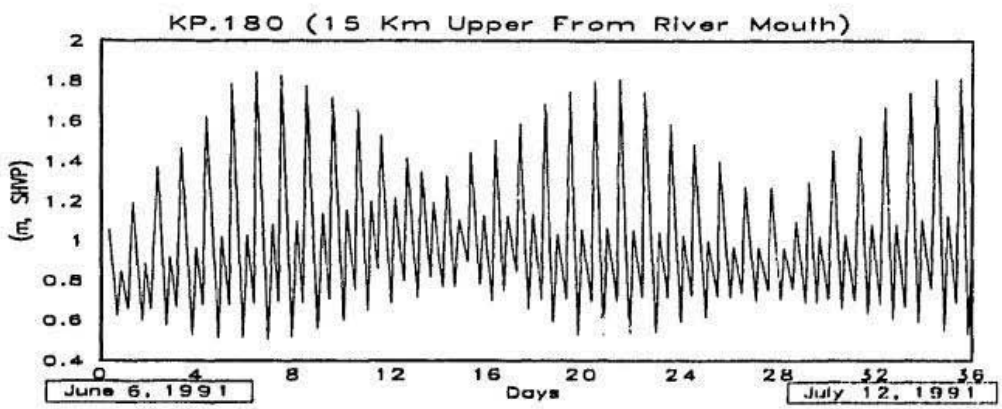

Fig.5.2 Continued for SB.5, KP.236 and KP.180

summarized in table 5.2

Table 5.2 Mean Tidal Period and Range along the Estuary

Station Number	Mean Tidal Period		Mean Tidal Range		Remarks
	Ebb (hrs)	Flood (hrs)	Ebb (m)	Flood (m)	
KP.250	6.34	6.04	1.09	1.09	Shortcut River mouth
KP.242	6.93	5.46	0.95	0.95	Downstream of the shortcut branch
KP.236	6.93	5.46	0.86	0.86	Upstream of the shortcut branch
SB.5	6.93	5.46	0.97	0.96	Original river
KP.180	8.68	3.71	0.65	0.65	15 km upper from the river mouth

5.1.2 Tidal Limit

Based on the above tidal data, the extreme limit of the tidal rise can be determined using two methods. The first is obtained from the mean high water elevation at every station. The mean water elevation at one station is connected to the other stations and then the average water surface slope along the estuary can be found. The point of intersection between the mean surface water slope and the mean river bed slope is assumed to be the extreme limit of the tidal rise. The significant limit of tidal rise must be identified in the spring tide and neap tide condition. Referring to data in table 5.1 and appendix A, tables A.1-1 to A.1-4, the calculation is presented in table 5.3.

Table 5.3 Tidal Limit

Station (1)	Mean High Water *) (m,SHVP) (2)	Distance from KP.250 (km) (3)	Mean Slope of Water Surface (I_w) (4) = (Δ2)/(3)	Mean River Bed Slope (I_b) (5) = **)
KP.250	-0.01	-	-	-
KP.242	0.245	1.60	0.00016	0.00029
KP.236	0.487	2.80	0.00018	
KP.180	1.316	14.00	0.00009	
Average:			0.00014	0.00029
KP.250	Date	Time	Water level	Reference Point ***)
HHWL	June 13	10.00	0.716	-3.415
LHWL	June 21	18.00	-0.385	
Upper Distance from KP.250		$H/(I_b-I_w)$		
Spring Tide (HHWL)		= (3.415 + 0.716) / (0.00015) = 27 54 km		
Neap Tide (LHWL)		= (3.415 - 0.385) / (0.00015) = 20.20 km		

*) see table 5.1 and appendix A, tables A.1-1 to A.1-4

**) see figure 5.3

***) the deepest point at KP.250 based on field measurement data in the dry season of 1991.

The second method to determine the extreme limit of tidal rise uses the fundamental understanding that the tidal amplitude varies in a landward direction because of friction and constriction. By using water elevations at the mouth (KP.250) in the spring tide (HHWL) and then connecting to the water elevation at the other stations at the same time, the water surface curve can be obtained by exponential regression. The break point between the water surface curve and the mean river bed slope is assumed to be the extreme limit of the tidal rise. The water elevation at that time is shown in table 5.4 and the tidal limit is presented in figure 5.3.

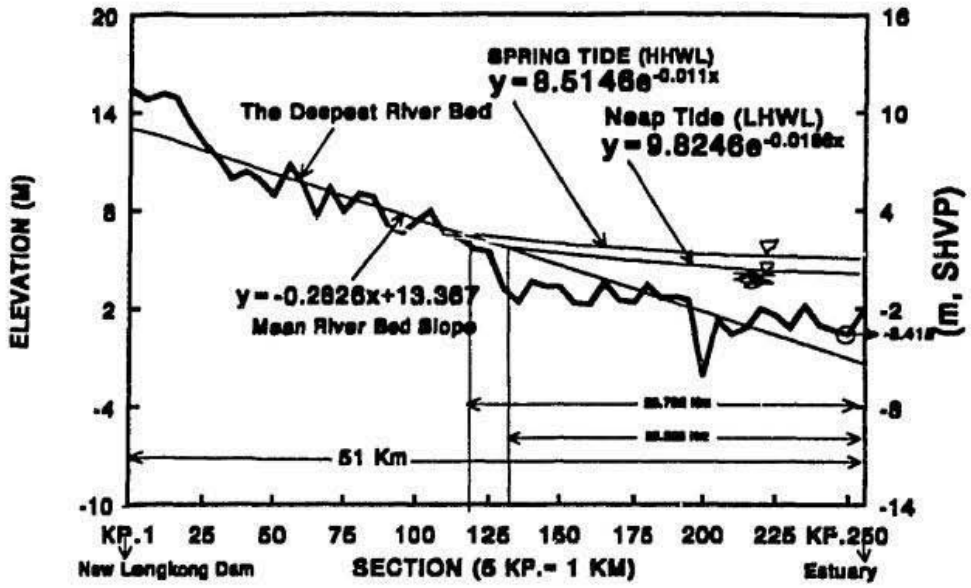

Fig.5.3 Longitudinal Section and Surface Water Profile for Determining the Tidal Limit.

Table 5.4 High Water Elevation of Spring and Neap Tide

Tide	Condition	Date	Time	Water Elevation (m, SHVP)			
				KP.250	KP.242	KP.236	KP.180
Spring	HHWL	June13	10.00	0.716	1.002	1.181	1.626
Neap	LHWL	June21	18.00	-0.385	0.000	0.251	0.926

The result shows that the extreme limit of the tidal rise is 26.8 km from the shortcut mouth on the Spring tide and 25.2 km on the neap tide. Estimates using the first method were 27.5 km and 20.2 km, respectively. Therefore, determination of the tidal limit 27.50 km and 25.2 km from the shortcut mouth are reasonable.

5.1.3 Observations at Particular Points

Observations at particular points were carried out in order to examine the characteristics of tidal currents, sediment transport, temperature and salinity distributions during tidal cycles. Devises used in these observations were current meter, bed load sampler, suspended sediment sampler, and salinometer (see appendix B, figures B.4-1 through B.4-4). This observation is needed because these factors have a close relationship to the circulation type within the estuary. Two basic observations have been made: cross sectional or lateral survey and longitudinal survey along the estuary.

The cross sectional survey was taken at the same four stations where tidal data were observed (KP.250, KP.242, KP.236, SB.5). However, no observations were made at KP.180 because the tidal effects at this point seem insignificant except for the influence of the tidal water level.

Regardless of the salinity distribution, the relationships between current velocity, water discharge and sediment discharge will be examined by the cross sectional survey. The records were made during a tidal cycle and were taken at the middle and two quarter points across the estuary at the stations. Velocity measurement and suspended sediment load measurements were taken every one sixth of the water depth if the depth was more than 2.00 m and taken every one fourth if the depth was less than 2.00 m. Water discharge can be estimated by multiplication between the mean velocity, represented by the three points above, and the cross section area in that water level condition. Suspended discharges were calculated by mean sediment content multiplied by

the water discharge. The calculations are summarized in table 5.5-1 through 5.5-4.

The tables show that there are certain relationships between hydraulic conditions and suspended sediment discharges. If the mean velocity in every measurement is used as a basic reference, it can be seen that there is no obvious relationship between velocity and sediment discharge. At KP.250, for example, mean velocity and suspended sediment discharge during the rising tide are not directly related to the velocity, particularly near

Table 5.5-1 Cross Sectional Survey Data - Relationships Between Hydraulic and Suspended Sediment Discharges at KP.250

Date : June 15, 1991
Location : Porong river mouth
Station : KP.250

No	Time	Water Elevation (m,SHVP)	Mean Vel. m/s	Discharge		Note
				Water m3/s	Suspended kg/s	
1	06:00	-0.896	0.00	0.00	0.00	Rising
2	06:30	-0.886	0.11	45.94	8.07	tide
3	07:00	-0.846	0.13	55.27	9.80	
4	07:30	-0.766	0.33	142.44	24.51	
5	08:00	-0.406	0.40	209.17	34.02	
6	08:30	-0.276	0.46	256.62	42.96	
7	09:00	-0.036	0.44	275.04	63.18	
8	09:30	0.284	0.40	285.22	76.06	
9	10:00	0.554	0.20	161.09	65.06	Falling
10	11:00	0.564	0.12	97.04	40.03	tide
11	11:30	0.704	0.07	59.83	20.32	
12	11.45	0.704	0.00	0.00	0.00	
13	12.00	0.644	0.11	91.84	8.04	
14	12.30	0.574	0.19	154.27	12.11	
15	14:00	0.106	0.35	233.29	26.55	
16	14:30	-0.156	0.33	195.04	27.50	
17	15:30	-0.256	0.29	163.37	23.26	
18	16:10	-0.406	0.25	130.73	20.49	
19	16:50	-0.526	0.19	93.41	14.26	
20	19:00	-1.216	0.00	0.00	0.00	

Table 5.5-2 : at KP.242

Date : June 11, 1991
Location : Upper Shortcut Channel
Station : KP.242

No	Time	Water Elevation (m,SHVP)	Mean Vel. m/s	Discharge		Note
				Water m3/s	Suspended kg/s	
1	04:00	-0.722	0.00	0.00	0.00	Rising
2	04:30	-0.682	0.11	28.94	7.05	tide
3	05:00	-0.642	0.13	34.69	8.39	
4	06:00	-0.562	0.32	85.83	20.94	
5	07:00	-0.072	0.45	151.37	37.41	
6	08:00	0.488	0.40	165.27	67.51	Falling
7	08:30	0.758	0.14	64.84	48.59	tide
8	09:00	0.828	0.00	0.00	0.00	
9	09:30	0.478	0.30	124.74	9.61	
10	10:00	-0.012	0.41	140.78	11.05	
11	11:00	-0.502	0.25	69.20	8.34	
12	12:00	-0.582	0.19	50.64	6.01	
13	13:30	-0.622	0.12	31.37	4.54	
14	14:30	-0.762	0.11	26.83	4.07	
15	18:00	-0.922	0.00	0.00	0.00	

Table 5.5-3 : at KP.236

Date : July 1, 1991
Location : Porong river
Station : KP.236 (3.8 km Upward from the Shortcut Mouth)

No:	Time	Water Elevation(m,SHVP)	Mean Vel. m/s	Discharge		Note
				Water m3/s	Suspended kg/s	
1	08:00	-0.231	0.00	0.00	0.00	Rising
2	08:15	-0.071	0.08	25.28	0.41	tide
3	09:25	0.199	0.16	60.19	0.89	
4	10:00	0.339	0.20	80.44	1.50	
5	11:00	0.609	0.24	109.14	2.59	
6	11:50	0.679	0.13	60.96	2.49	
7	12:30	0.731	0.08	38.36	1.58	Falling
8	13:00	0.761	0.00	0.00	0.00	tide
9	14:00	0.601	0.23	104.23	2.76	
10	15:20	0.321	0.37	146.37	3.67	
11	16:00	0.131	0.33	120.07	3.95	
12	17:00	-0.029	0.20	67.11	3.15	
13	18:00	-0.099	0.16	51.76	2.46	
14	21:00	-0.376	0.00	0.00	0.00	

Table 5.5-4 : at SB.5

Date : July 3,1991
Location : Original River
Station : SB.5 (750 m downstream of tributary)

No.	Time	Water Elevation (m,SHVP)	Mean Vel. m/s	Discharge		Note
				Water m3/s	Suspended kg/s	
1	09:00	-0.825	0.00	0.00	0.00	Rising
2	09:30	-0.705	0.12	2.26	0.06	tide
3	10:00	-0.545	0.14	3.43	0.10	
4	10:30	-0.405	0.17	5.08	0.16	
5	11:00	-0.365	0.20	6.31	0.23	
6	11:30	-0.255	0.23	8.32	0.27	
7	12:00	-0.175	0.24	9.52	0.32	
8	12:30	-0.115	0.23	7.75	0.33	
9	13:00	-0.085	0.14	6.13	0.28	
10	14:00	-0.075	0.07	3.10	0.13	
11	15:00	-0.025	0.00	0.00	0.00	Falling
12	15:30	-0.065	0.07	2.91	0.06	Tide
13	16:00	-0.182	0.28	11.02	0.22	
14	17:00	-0.375	0.27	8.40	0.24	
15	17:30	-0.455	0.24	6.70	0.20	
16	18:00	-0.515	0.22	5.64	0.16	
17	21:00	-0.805	0.00	0.00	0.00	

the high water. The velocity decreases but the sediment load increases. Table 5.5 may be used to average the mean values of velocity and suspended sediment discharge over the flood and ebb tides. During the flood tide, the average of the mean velocities is 0.24 m/sec while the average of the suspended sediment discharge is 35.40 kg/sec. The tidal range is 1.91 m. During the ebb tide the corresponding values are 0.30 m/sec and 9.63 kg/sec. Comparisons of flood and ebb values show no correlation between velocity and sediment discharge. This is true at all four stations and means that measurements of mean velocity cannot be directly used for calculation of sediment discharge. The durations and ranges of any flood or ebb tide among the stations are also different (see chapter 5.1.1). Therefore, the best way of evaluating sedimen discharge is to evaluate the tidal volume

which is correlated to the tidal range, mean water discharge and suspended sediment discharge at every station. This case will be discussed in more detail in following sections (5.2.1 and 5.2.2).

In longitudinal observations, the main concern is with distributions of salinity, velocity and temperature along the estuary for flood and ebb tides. These measurements were begun at the river mouth (KP.250) and continued upstream to 15 km from the river mouth (KP.180) during a flood tide and beginning from KP.180 downstream to KP.250 in an ebb tide. Observations were done twice during flood and ebb tides.

As in the cross sectional surveys discussed above, salinity, velocity, and temperature were measured every one sixth of the depth for two meter depths and more, and every one fourth of the depth for depths less than two meters. The distance between two observed points was 1 km and the observed points were located along the axis of the river. One section of the data is presented in table 5.6. This includes calculation of density and density index using equation 3-3 and 3-4.

Table 5.6 Longitudinal Observed Data: Salinity, Velocity and Temperature Distribution Including Calculation of Density and Density Index. (During a Flood Tide, First Observation)

Date : June 25, 1991
Location : Porong River, From the Shortcut Mouth to 15 Km upward
Survey Station: KP.250 to KP.180

No	Time	Stations & Water Depth	Depth m	Velocity m/s	Salinity ppt	Temp °C	Density g/cm³	Density Index	Note
1	07.15 a.m.	KP.250	0.00	0.544	24.1	26.0	1.0149	14.9	The tide is rising
			0.38	0.553	24.1	26.0	1.0149	14.9	
		2.28 m	0.76	0.512	24.3	26.0	1.0150	15.0	
			1.14	0.520	24.4	26.0	1.0151	15.1	
			1.52	0.459	24.5	26.0	1.0152	15.2	
			1.90	0.397	25.0	25.9	1.0156	15.6	
			2.28	0.000	25.9	25.7	1.0163	16.3	

Table 5.6 continued

2	07.30 a.m.	KP.245 2.20 m	0.00 0.37 0.73 1.10 1.47 1.83 2.20	0.416 0.426 0.484 0.505 0.498 0.416 0.000	23.6 23.6 23.8 24.0 24.2 24.3 24.4	26.2 26.2 26.1 26.0 25.8 25.6 25.4	1.0144 1.0144 1.0146 1.0148 1.0150 1.0152 1.0153	14.4 14.4 14.6 14.8 15.0 15.2 15.3	
3	07.45 a.m.	KP.240 3.40 m	0.00 0.57 1.13 1.70 2.27 2.83 3.40	0.391 0.387 0.297 0.260 0.292 0.260 0.000	22.3 22.3 22.7 22.8 22.8 22.8 22.8	26.4 26.4 26.4 26.2 26.0 25.8 25.6	1.0134 1.0134 1.0137 1.0138 1.0139 1.0140 1.0140	13.4 13.4 13.7 13.8 13.9 14.0 14.0	
4	08.00 a.m.	KP.235 2.70 m	0.00 0.45 0.90 1.35 1.80 2.25 2.70	0.272 0.337 0.266 0.269 0.228 0.212 0.000	16.7 16.7 17.7 18.3 19.2 20.0 20.4	26.7 26.7 26.7 26.5 26.4 26.4 26.4	1.0091 1.0091 1.0099 1.0104 1.0111 1.0117 1.0120	9.1 9.1 9.9 10.4 11.1 11.7 12.0	
5	08.10 a.m.	KP.230 3.45 m	0.00 0.58 1.15 1.73 2.30 2.88 3.45	0.230 0.319 0.292 0.237 0.156 0.136 0.000	15.4 15.4 16.0 16.4 16.7 17.0 17.6	27.0 27.0 26.8 26.7 26.7 26.7 26.7	1.0081 1.0081 1.0086 1.0089 1.0091 1.0094 1.0098	8.1 8.1 8.6 8.9 9.1 9.4 9.8	The tide is still rising
6	08.25 a.m.	KP.225 2.40 m	0.00 0.40 0.80 1.20 1.60 2.00 2.40	0.224 0.221 0.244 0.176 0.215 0.149 0.000	13.8 13.8 14.2 14.5 14.7 14.8 14.8	27.5 27.5 27.5 27.2 27.1 27.1 27.1	1.0067 1.0067 1.0070 1.0073 1.0075 1.0076 1.0076	6.7 6.7 7.0 7.3 7.5 7.6 7.6	
7	08.35 a.m.	KP.220 3.35 m	0.00 0.56 1.12 1.68 2.23 2.79 3.35	0.160 0.170 0.144 0.130 0.123 0.152 0.000	12.0 12.0 12.0 12.5 13.0 13.5 13.6	27.9 27.9 27.9 27.8 27.5 27.3 27.3	1.0053 1.0053 1.0053 1.0057 1.0061 1.0066 1.0066	5.3 5.3 5.3 5.7 6.1 6.6 6.6	Almost high water
8	08.55 a.m.	KP.215 3.40	0.00 0.57 1.13 1.70 2.27 2.83 3.40	0.000 0.000 0.000 0.000 0.000 0.000 0.000	7.9 7.9 8.9 9.3 9.7 10.4 10.7	28.3 28.3 28.0 27.8 27.8 27.8 27.7	1.0021 1.0021 1.0029 1.0029 1.0033 1.0036 1.0041	2.1 2.1 2.9 3.3 3.6 4.1 4.4	High water
9	09.05 a.m.	KP.210	-	-	-	-	-	-	Slack water -> Unmeasured

All other calculations are given in appendix A, table A.2-1 to table A.2-3.

In order to clarify salinity, velocity and temperature distributions, data was transferred into figure 5.4-1 to figure 5.4-4. They show that salinity distributions were slightly stratified at the mouth region and up to 8 km upstream (KP.215). After that region, the water is homogeneous and the density is almost equal to 1.0 g/cm^3 The salinity difference between bottom and surface layer was less than 10 %. In other words local salinity distributions vary little from surface to bottom over the entire intrusion length. According to Ippen (1966), see section 3.1.2, a well mixed estuary can be identified by salinity differences between bottom and surface layer less than 15 to 25 %. Therefore, the estuarine mixing process at that time was classified as a well-mixed type. The vertical salinity gradient found during the observation can be categorized as an embryo interface that always moves during the tidal process up to the slack water period, high or low tide (figures 5.4-2, 5.4-3 and 5.4-4). In the high tide condition (figure 5.4.1) - this is an important requirement for a reliable observation - the vertical salinity gradient is less than that of the progressing tide (figure 5.4-2). In that condition the salinity difference at the river mouth (KP.250) was about 7.5 %.

Another supporting reason that the estuary type at that time was well mixed, is the velocity distribution. Undistorted velocity profiles at all depths were found along the estuary. The currents at all depths were predominantly landward during flood tides and seaward during ebb tides. The river discharge at that time was relatively low and the Lengkong dam gates for flushing water to the Porong river were closed. The fresh water discharge came mainly from the Porong basin itself including discharge from the Sadar

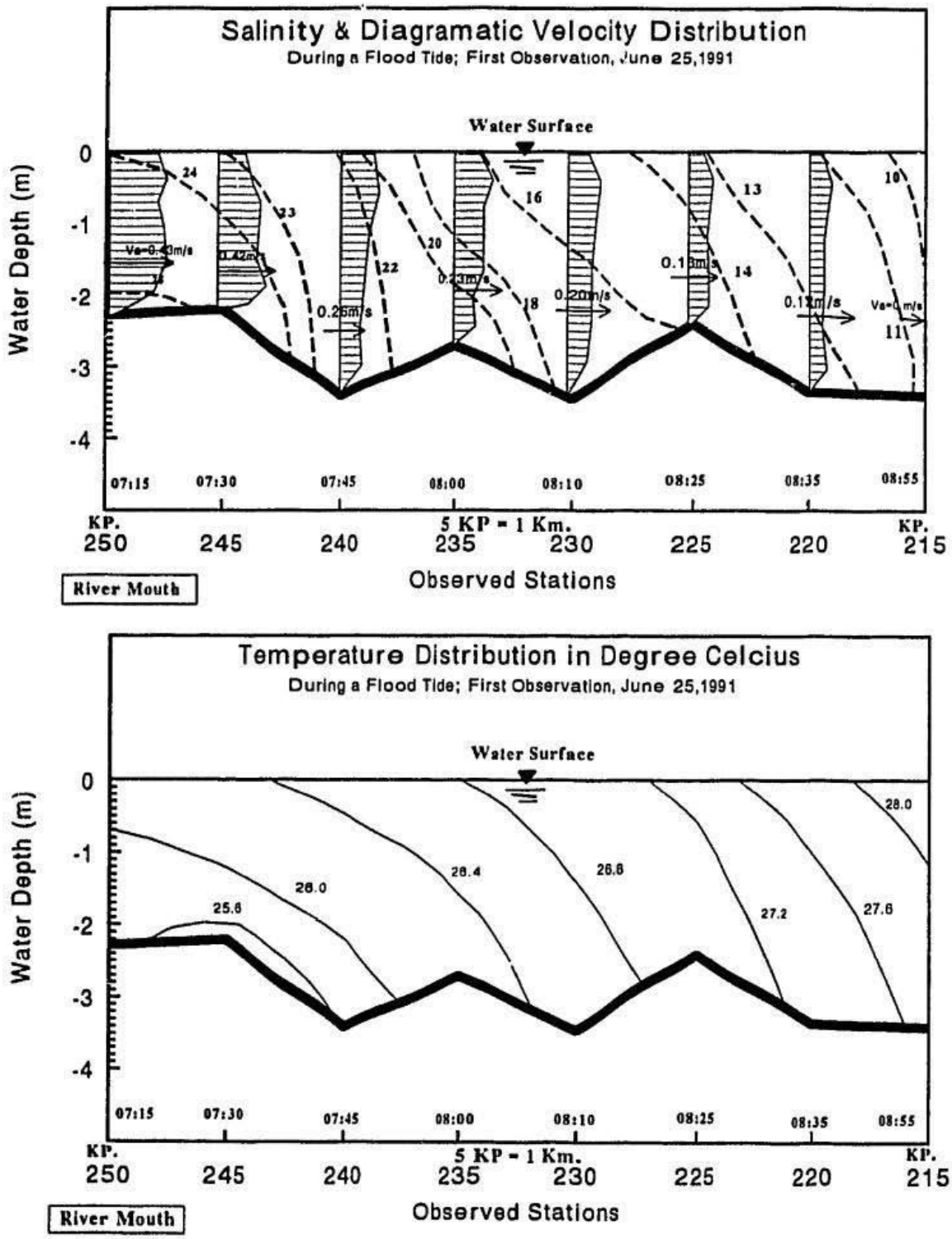

Fig.5.4-1 Salinity, Velocity & Temperature Distribution During a Flood Tide

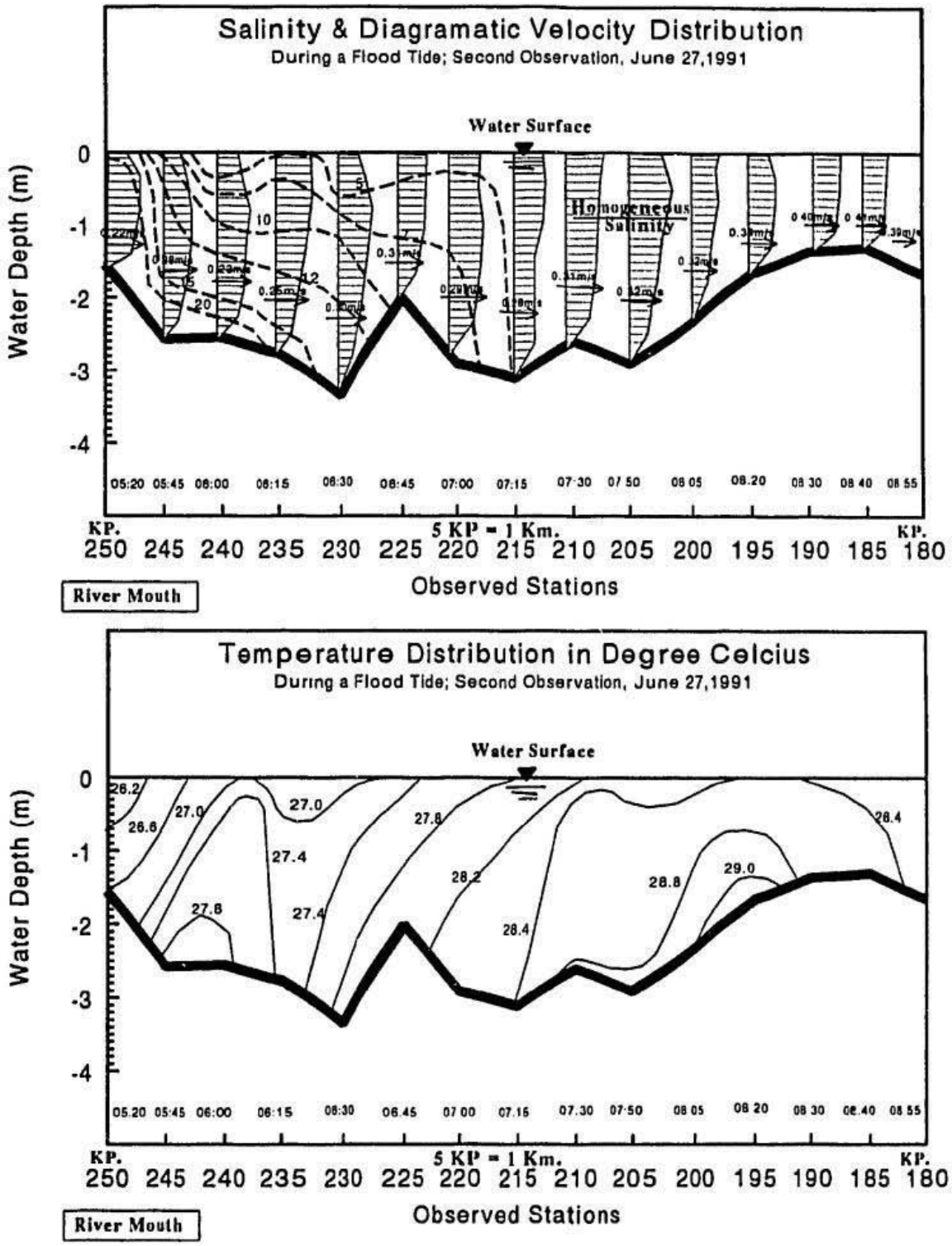

Fig.5.4-2 Salinity, Velocity & Temperature Distribution During a Flood Tide

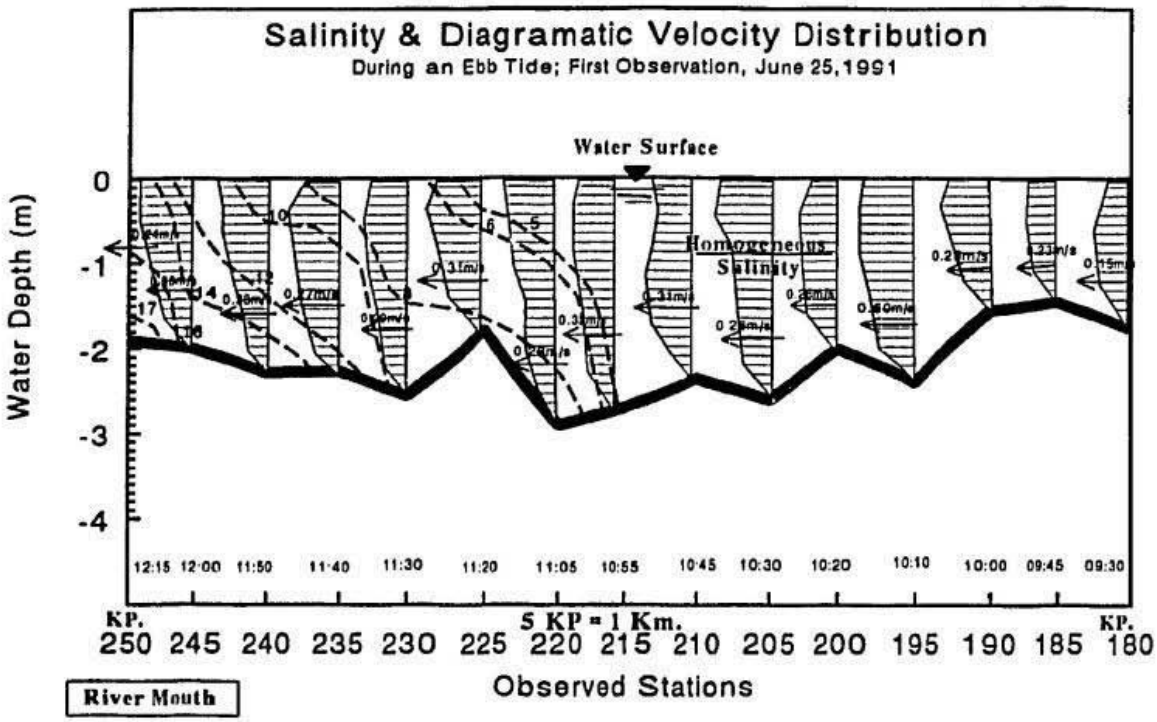

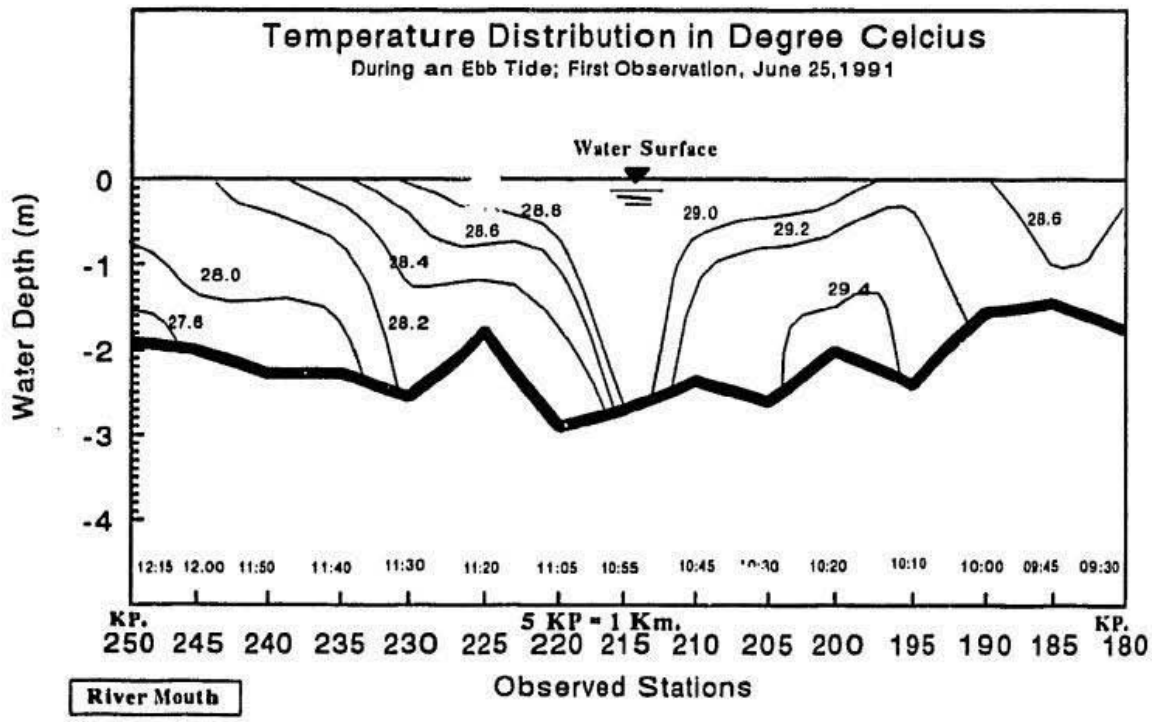

Fig.5.4-3 Salinity, Velocity & Temperature Distribution During an Ebb Tide

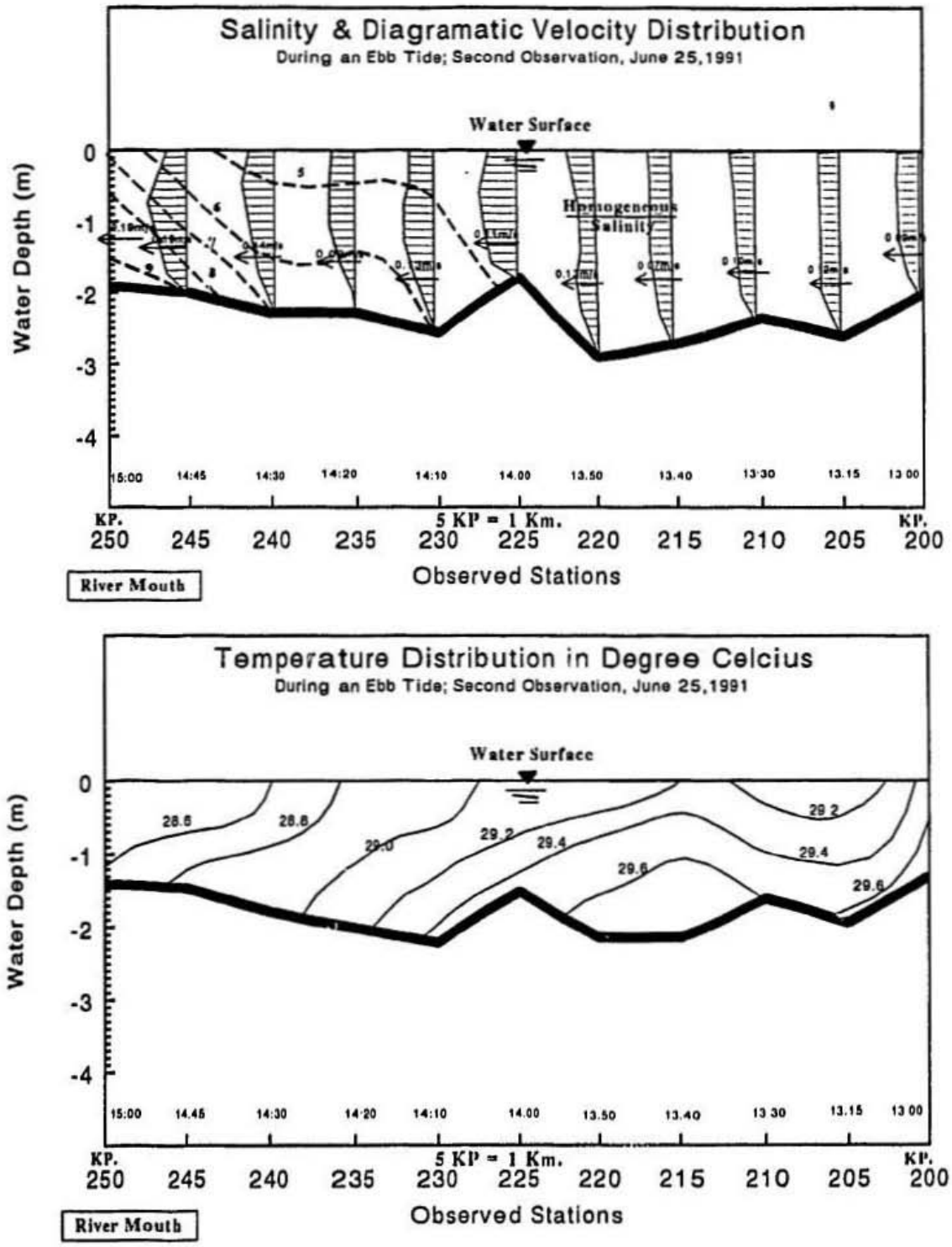

Fig.5.4-4 Salinity, Velocity & Temperature Distribution During an Ebb Tide

and Kambing rivers (see figure 4.4). Under these conditions, the water level was below the zero elevation of the Porong water level recorder. Since the zero of the recorder corresponded to 25 m^3/sec, it is possible only to say that the flow at that time was less than 25 m^3/sec. Further discussion about discharge limits of circulation pattern within the Porong River will be explained in chapter 6.

5.1.4 Directions of Surface Tidal Currents

As mentioned in chapter 5.1.3, observations at particular points are important to know how the behaviour of tidal currents relates to the sediment load and salinity distribution. However, it is also important to understand the changing current directions during a tidal cycle. These will contribute to the sedimentation process in the estuary.

The direction of currents can be observed by using a current-meter and floats. At the river mouth (KP.250), for example, the current directions always change considerably during a tidal cycle. At the beginning of a flood tide, the tidal currents tend to go to the left side of the channel (if viewers look upstream from the sea). Then, with increasing velocity, the current direction moves slowly to the right side and becomes parallel to the channel line. Near the end of the flooding period, i.e at slack water, the surface currents decrease gradually and switch their direction from parallel to the right side of the channel. Then, beginning from the right side, the ebb tide currents show up and move gradually leftward and go straight to the sea. This process is illustrated in figure 5.5. The same phenomena can be seen clearly along the shortcut channel and for short distances upstream of the branch between the shortcut channel and the original river. In the upper

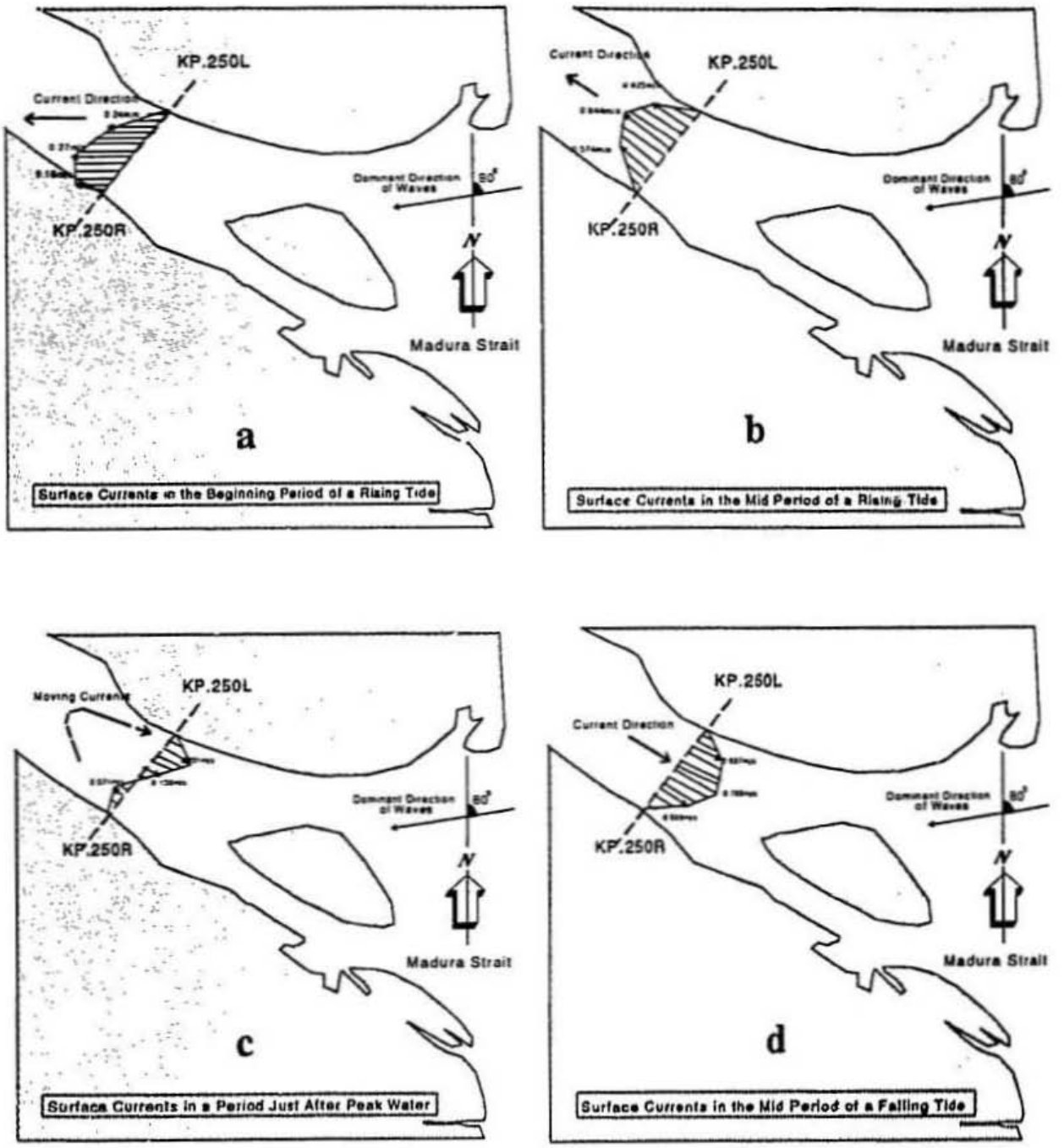

Fig.5.5.Surface Current Movement During a Tidal Cycle
at KP.250 (River Mouth); June 15, 1991

location, the influence of tidal currents is not significant relative to the influence of fluctuating water levels.

5.1.5 Estimation of Tidal Volume

Tidal volume is always related to the water volume contained in the estuary for the various tidal conditions. The volumes obtained in this way refer to the volume of water that must pass into or out of the estuary or through a section in the estuary. Estimation of tidal volume and mean velocity can be made from tidal data which have been obtained at the five stations from June 6 to July 12, 1991 (see chapter 5.1.1). There are two important factors which must be considered: tidal range and tidal period. Since these factors are different in every tidal cycle, the sequence of calculation of tidal volume and mean velocity should follow the process below.

Firstly, the relationships between water elevation and cross section area can be defined using measured data that have been obtained during the field observations at the stations. These relationships can be found by regression or by elevation-cross section area curves. The best approximate equation was found to be a polynomial of second degree. The resulting curves are shown in figure 5.6.

Secondly, tidal ranges and water elevations at every station in the same cycle and time can be obtained from the data discussed in section 5.1.1. Therefore, the tidal area or area between flood tide and ebb tide consecutively in cycles can be calculated. One sample of the calculation is presented in table 5.7 and the others can be found in appendix A, tables A.3-1 to A.3-4.

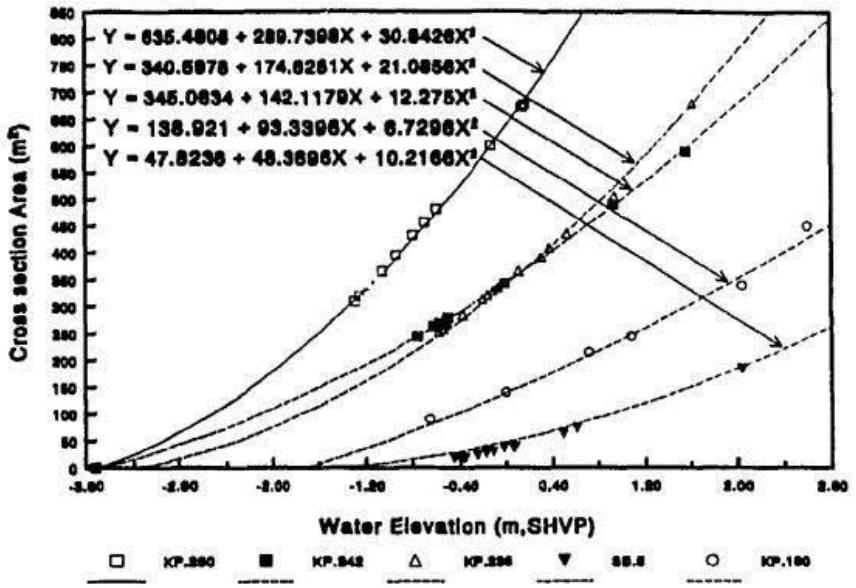

Fig.5.6 Water Elevation and Cross Area Curves at the Observed Stations Including Their Equations

Thirdly, tidal volume can be calculated simply by taking the average of tidal area between two stations and multiplying by the distance between the two stations. Calculation of tidal volume between KP.250 and KP.242 is presented in table 5.8 and other calculations for KP.242, KP.236 and so forth are shown in appendix A, tables A.4-1 to A.4-5.

An important note should be made regarding the calculation of the tidal volume between KP.180 and the tidal limit (see appendix A, table A.4-3). The distance of the tidal limit from the station changes with the difference of the tidal range. This case is approached by using an assumption that the tidal volume is a prism. The distance between KP.180 and the tidal limit depends on the tidal height at KP.180. It may be calculated from the tidal range (R) divided by the difference of the mean water surface slope

Table 5.7

Calculation of Tidal Area at KP.250

Location : 7.1 Km Upward from the [illegible]
Tidal Gauge : Nigaseo
Recording period : From June 6, 1991 to July 12, 1991

Date		Elevation		Cross Area		Tidal Area	
		HWL m,SHVP	LWL m,SHVP	HWL m2	LWL m2	Fall m2	Rise m2
June	6	-0.396	-0.936	525.58	391.31	134.28	105.46
		-0.506	-1.126	496.77	348.34	148.43	279.63
	7	-0.026	-1.136	627.97	346.14	281.83	150.63
		-0.506	-1.066	496.77	361.67	135.10	290.14
	8	0.056	-1.186	651.80	335.23	316.57	164.13
		-0.496	-1.106	499.36	352.76	146.60	365.04
	9	0.276	-1.245	717.80	322.56	395.24	179.39
		-0.486	-1.116	501.95	350.54	151.41	410.81
	10	0.416	-1.246	761.35	322.35	439.00	197.94
		-0.416	-1.106	520.29	352.76	167.53	469.63
	11	0.606	-1.296	822.39	311.78	510.61	232.52
		-0.326	-1.096	544.30	354.97	189.33	497.11
	12	0.696	-1.306	852.08	309.69	542.39	234.62
	13	-0.326	-1.086	544.30	357.20	187.10	501.55
		0.716	-1.326	858.75	305.52	553.23	268.82
	14	-0.216	-1.026	574.34	370.68	203.66	488.07
		0.716	-1.245	858.75	322.56	536.18	257.32
	15	-0.196	-0.896	579.88	400.63	179.24	454.78
		0.706	-1.216	855.41	328.76	526.65	290.59
	16	-0.056	-0.926	619.35	393.63	225.72	396.36
		0.506	-1.166	789.99	339.58	450.41	271.21
	17	-0.086	-0.825	610.79	417.44	193.35	346.75
		0.425	-1.125	764.19	348.56	415.63	291.28
	18	0.015	-0.805	639.83	422.23	217.61	280.01
		0.225	-1.085	702.23	357.42	344.81	294.09
	19	0.055	-0.835	651.51	415.05	236.46	162.33
		-0.205	-1.005	577.38	375.44	201.94	270.22
	20	0.035	-0.855	645.66	410.30	235.36	136.97
		-0.315	-0.985	547.27	380.01	167.26	286.23
	21	0.105	-0.995	666.24	377.72	288.52	150.78
		-0.385	-0.935	528.50	391.54	136.97	307.66
	22	0.215	-1.205	699.20	331.13	368.07	213.44
		-0.325	-0.925	544.57	393.86	150.71	326.70
	23	0.285	-1.285	720.56	314.09	406.47	235.89
		-0.305	-0.905	549.98	398.53	151.45	334.38
June	24	0.325	-1.285	732.90	314.09	418.81	235.89
		-0.305	-0.925	549.98	393.86	156.12	357.74

(next page)

(Table 5.7 Continued)

Date		Elevation		Cross Area		Tidal Area	
		HWL	LWL	HWL	LWL	Fall	Rise
		m,SHVP	m,SHVP	m2	m2	m2	m2
June	25	0.385	-1.305	751.60	309.90	441.71	256.45
	26	-0.245	-0.905	566.35	398.53	167.82	368.83
		0.435	-1.315	767.35	307.81	459.55	258.54
	27	-0.245	-0.915	566.35	396.19	170.15	393.47
		0.505	-1.315	789.67	307.81	481.86	261.29
	28	-0.235	-0.935	569.10	391.54	177.56	375.82
		0.435	-1.285	767.35	314.09	453.26	249.51
	29	-0.255	-0.965	563.60	384.60	179.00	354.51
		0.345	-1.285	739.11	314.09	425.02	241.32
	30	-0.285	-0.965	555.41	384.60	170.81	345.21
		0.315	-1.235	729.81	324.69	405.12	217.19
July	1	-0.335	-0.965	541.88	384.60	157.28	311.57
		0.205	-1.205	696.17	331.13	365.05	194.72
	2	-0.395	-0.945	525.85	389.22	136.63	247.71
		0.005	-1.115	636.93	350.77	286.17	169.79
	3	-0.415	-0.935	520.55	391.54	129.01	185.84
		-0.205	-1.005	577.38	375.44	201.94	193.65
	4	-0.235	-0.925	569.10	393.86	175.23	124.05
		-0.425	-0.955	517.91	386.91	131.00	212.84
	5	-0.125	-0.925	599.75	393.86	205.88	150.71
		-0.325	-1.055	544.57	364.13	180.44	267.01
	6	-0.015	-1.205	631.14	331.13	300.01	192.07
		-0.405	-1.015	523.20	373.17	150.03	284.22
	7	0.075	-1.275	657.38	316.20	341.18	222.99
		-0.345	-1.035	539.19	368.64	170.55	327.53
	8	0.205	-1.345	696.17	301.58	394.60	232.26
		-0.365	-1.035	533.83	368.64	165.20	345.79
	9	0.265	-1.345	714.43	301.58	412.85	237.62
		-0.345	-1.035	539.19	368.64	170.55	382.96
	10	0.385	-1.365	751.60	297.45	454.15	236.38
		-0.365	-1.065	533.83	361.89	171.94	427.77
	11	0.505	-1.375	789.67	295.40	494.26	241.11
		-0.355	-1.015	536.51	373.17	163.34	458.73
July	12	0.635	-1.365	831.90	297.45	534.45	-
Average :		-0.010	-1.095	636.67	355.92	280.76	281.51

Table : 5.8

Calculation of Tidal Volume (KP.250 - KP.242)

Location : Between KP.250 and KP.242
Distance : 1.6 km
Recording period : From June 6, 1991 to July 12,1991

Date	Tidal Area				Tidal Volume	
	KP.250		KP.242		KP.250 --> KP.242	
	Fall m2	Rise m2	Fall m2	Rise m2	Fall m3	Rise m3
June 6	134.28	105.46	63.95	50.16	158,581	124,500
	148.43	279.63	65.27	126.30	170,957	324,746
7	281.83	150.63	133.72	72.68	332,441	178,652
	135.10	290.14	65.27	139.65	160,294	343,831
8	316.57	164.13	151.97	77.58	374,831	193,365
	146.60	365.04	64.02	165.70	168,497	424,595
9	395.24	179.39	186.54	88.00	465,418	213,915
	151.41	410.81	64.67	181.84	172,864	474,120
10	439.00	197.94	208.78	91.74	518,224	231,745
	167.53	469.63	68.55	222.30	188,866	553,546
11	510.61	232.52	246.69	106.23	605,836	271,001
	189.33	497.11	81.84	237.02	216,937	587,300
12	542.39	234.62	260.21	109.23	642,083	275,080
13	187.10	501.55	84.80	249.69	217,521	600,991
	553.23	268.82	263.25	105.41	653,187	299,381
14	203.66	488.07	95.57	241.15	239,387	583,377
	536.18	257.32	258.26	113.24	635,552	296,448
15	179.24	454.78	81.09	217.89	208,269	538,133
	526.65	290.59	242.77	119.69	615,533	328,221
16	225.72	396.36	92.27	199.10	254,392	476,369
	450.41	271.21	214.21	113.15	531,694	307,493
17	193.35	346.75	96.77	156.74	232,101	402,797
	415.63	291.28	164.35	114.59	463,989	324,696
18	217.61	280.01	95.40	120.70	250,407	320,566
	344.81	294.09	134.83	122.84	383,714	333,539
19	236.46	162.33	98.25	83.47	267,762	196,641
	201.94	270.22	101.68	109.03	242,892	303,400
20	235.36	136.97	99.21	63.05	267,656	160,018
	167.26	286.23	76.71	120.29	195,178	325,217
21	288.52	150.78	120.80	80.34	327,455	184,896
	136.97	307.66	67.47	135.14	163,549	354,239
22	368.07	213.44	153.85	83.06	417,534	237,203
	150.71	326.70	75.43	149.29	180,917	380,794
23	406.47	235.89	170.67	95.96	461,709	265,478
	151.45	334.38	73.31	157.29	179,806	393,332
June 24	418.81	235.89	187.32	110.44	484,904	277,060
	156.12	357.74	85.51	168.62	193,303	421,092

(next page)

(Table 5.8 Continued)

Date		Tidal Area				Tidal Volume	
		KP.250		KP.242		KP.250 -> KP.242	
		Fall m2	Rise m2	Fall m2	Rise m2	Fall m3	Rise m3
June	25	441.71	256.45	203.25	124.43	515,963	304,700
	26	167.82	368.83	83.42	168.51	200,988	429,870
		459.55	258.54	208.32	128.98	534,290	310,013
	27	170.15	393.47	96.83	188.83	213,585	465,841
		481.86	261.29	223.38	134.27	564,192	316,450
	28	177.56	375.82	97.18	179.93	219,788	444,601
		453.26	249.51	219.43	128.02	538,149	302,025
	29	179.00	354.51	98.64	177.46	222,110	425,575
		425.02	241.32	206.84	117.48	505,489	287,035
	30	170.81	345.21	90.60	170.63	209,123	412,667
		405.12	217.19	191.50	111.47	477,295	262,926
July	1	157.28	311.57	88.09	161.95	196,296	378,818
		365.05	194.72	166.95	79.05	425,594	219,018
	2	136.63	247.71	65.22	119.86	161,479	294,058
		286.17	169.79	133.69	83.24	335,887	202,420
	3	129.01	185.84	61.74	100.39	152,601	228,990
		201.94	193.65	100.39	98.93	241,865	234,066
	4	175.23	124.05	91.17	56.78	213,126	144,666
		131.00	212.84	64.54	103.33	156,435	252,933
	5	205.88	150.71	103.33	74.42	247,371	180,109
		180.44	267.01	92.18	129.95	218,098	317,567
	6	300.01	192.07	142.34	105.00	353,883	237,653
		150.03	284.22	79.97	132.28	184,000	333,199
	7	341.18	222.99	160.98	108.67	401,730	265,328
		170.55	327.53	81.25	141.13	201,441	374,934
	8	394.60	232.26	174.62	112.89	455,375	276,119
		165.20	345.79	80.67	153.12	196,696	399,123
	9	412.85	237.62	187.74	112.47	480,473	280,066
		170.55	382.96	79.11	162.11	199,732	436,057
	10	454.15	236.38	197.86	112.04	521,609	278,742
		171.94	427.77	72.47	194.61	195,535	497,908
	11	494.26	241.11	242.50	100.89	589,412	273,599
		163.34	458.73	56.81	209.74	176,124	534,776
July	12	534.45	-	244.29	-	622,994	-
Average :		280.76	281.51	130.74	131.16	329,197	330,138

between tidal fall (I_1) and tidal rise (I_2). Hence, $X = R/(I_1-I_2)$ and the prism volume is equal to the value of X multiplied by the difference in area between tidal rise and fall consecutively. The mean slope of the water surface of the flood and ebb tides is taken from the water level relation between KP.250 and the other stations at high water and low water during the observations. The estimation is presented in table 5.9.

Table 5.9 Mean water surface slope

Stations	Mean High Water (m,SHVP)	Mean Low Water (m,SHVP)	Distance from KP.250 (km)	Mean Slope of Water Surface	
				Flood (If)	Ebb (Ie)
KP.250	-0.01	-1.095	-	-	-
KP.242	0.245	-0.705	1.60	0.00016	0.00024
KP.236	0.487	-0.376	2.80	0.00018	0.00026
KP.180	1.316	0.666	14.00	0.00009	0.00013
Average:				0.00014	0.00021

Finally, from data which were recorded continuously from June 6 to July 12,1991, the relationships between various tidal ranges and tidal volumes can be determined (see table 5.10).

By using the relationships between tidal range and tidal volume, the average discharge during the tide was calculated by dividing the tidal volume to the duration of the tide (see table 5.11). An additional result is the average velocity during the tidal cycle. In the estimation of the tidal volume, the most important thing is to know the relationship between the tidal range and tidal discharge. These factors are important for examining the quantity of the sediment discharge.

In summary, the distribution of sediment within the Brantas Estuary, calculated

Table : 5.10

Relationships Between
Tidal Range and Tidal Volume at KP.250
Recording period : From June 6, 1991 to July 12,1991

Date		High Water		Low Water		Duration		Range		Tidal Volume *)	
		Time	El. m,SHVP	Time	El. m,SHVP	Fall hrs	Rise hrs	Fall m	Rise m	Fall m3	Rise m3
June	6	8	-0.396	14	-0.936	6.0	4.0	0.54	0.43	948,348	638,917
		18	-0.506	1	-1.126	7.0	6.0	0.62	1.10	776,792	1,701,717
	7	7	-0.026	14	-1.136	7.0	5.0	1.11	0.63	1,785,020	863,624
		19	-0.506	1	-1.066	6.0	7.0	0.56	1.12	740,855	1,965,185
	8	8	0.056	15	-1.186	7.0	5.0	1.24	0.69	2,198,224	984,509
		20	-0.496	2	-1.106	8.0	6.0	0.61	1.38	769,084	2,389,557
	9	8	0.276	15	-1.245	7.0	7.0	1.52	0.76	2,750,355	1,132,528
		22	-0.486	3	-1.116	5.0	5.0	0.63	1.53	857,737	2,903,664
	10	8	0.416	16	-1.246	8.0	7.0	1.66	0.83	3,343,453	1,303,010
		23	-0.416	4	-1.106	5.0	5.0	0.69	1.71	948,222	3,479,241
	11	9	0.606	17	-1.296	8.0	6.0	1.90	0.97	3,990,709	1,441,412
		23	-0.326	4	-1.096	5.0	5.0	0.77	1.79	1,048,809	3,693,903
	12	9	0.696	18	-1.306	9.0	6.0	2.00	0.98	4,262,450	1,541,145
	13	24	-0.326	4	-1.086	4.0	6.0	0.76	1.80	1,121,065	3,795,144
		10	0.716	18	-1.326	8.0	7.0	2.04	1.11	4,328,661	1,594,852
	14	1	-0.216	5	-1.026	4.0	6.0	0.81	1.74	1,161,019	3,643,597
		11	0.716	19	-1.245	8.0	6.0	1.96	1.05	4,063,750	1,600,423
	15	1	-0.196	6	-0.896	5.0	5.0	0.70	1.60	1,141,325	3,315,514
		12	0.706	19	-1.216	8.0	7.0	1.92	1.16	3,779,008	1,651,597
	16	2	-0.056	8	-0.926	6.0	4.0	0.87	1.43	1,176,941	2,756,298
		12	0.506	20	-1.166	8.0	6.0	1.67	1.08	3,198,318	1,672,310
	17	2	-0.086	7	-0.825	5.0	7.0	0.74	1.25	1,159,875	2,120,521
		14	0.425	21	-1.125	7.0	6.0	1.55	1.14	2,564,020	1,694,762
	18	3	0.015	8	-0.805	5.0	7.0	0.82	1.03	1,315,145	1,765,192
		15	0.225	22	-1.085	7.0	6.0	1.31	1.14	2,062,373	1,833,744
	19	4	0.055	9	-0.835	5.0	7.0	0.89	0.63	1,530,454	1,123,537
		16	-0.205	23	-1.005	7.0	6.0	0.80	1.04	1,317,798	1,737,047
	20	5	0.035	10	-0.855	5.0	8.0	0.89	0.54	1,601,113	969,291
		18	-0.315	24	-0.985	6.0	5.0	0.67	1.09	1,003,151	1,684,384
	21	5	0.105	11	-0.995	6.0	7.0	1.10	0.61	1,801,863	1,001,667
		18	-0.385	1	-0.935	7.0	5.0	0.55	1.15	980,010	2,163,285
	22	6	0.215	12	-1.205	6.0	7.0	1.42	0.88	2,326,934	1,162,226
		19	-0.325	2	-0.925	7.0	5.0	0.60	1.21	854,924	2,187,035
	23	7	0.285	13	-1.285	6.0	7.0	1.57	0.98	2,786,169	1,384,792
		20	-0.305	3	-0.905	7.0	5.0	0.60	1.23	973,248	2,681,976
June	24	8	0.325	14	-1.285	6.0	7.0	1.61	0.98	3,264,110	1,425,915
		21	-0.305	4	-0.925	7.0	5.0	0.62	1.31	987,078	2,842,203

(next page)

(Table 5.10 Continued)

Date		High Water		Low Water		Duration		Range		Tidal Volume *)	
		Time	El. m,SHVP	Time	El. m,SHVP	Fall hrs	Rise hrs	Fall m	Rise m	Fall m3	Rise m3
June	25	9	0.385	15	-1.305	6.0	6.0	1.69	1.06	4,200,908	1,891,136
	26	21	-0.245	4	-0.905	7.0	6.0	0.66	1.34	1,235,309	3,616,309
		10	0.435	15	-1.315	5.0	7.0	1.75	1.07	4,420,017	1,919,722
	27	22	-0.245	5	-0.915	7.0	6.0	0.67	1.42	1,274,873	3,910,301
		11	0.505	16	-1.315	5.0	7.0	1.82	1.08	4,736,486	2,042,927
	28	23	-0.235	5	-0.935	6.0	6.0	0.70	1.37	1,318,275	3,616,751
		11	0.435	17	-1.285	6.0	7.0	1.72	1.03	4,420,001	1,853,406
	29	24	-0.255	6	-0.965	6.0	5.0	0.71	1.31	1,275,977	3,255,696
		11	0.345	18	-1.285	7.0	6.0	1.63	1.00	3,855,745	1,752,021
	30	24	-0.285	7	-0.965	7.0	5.0	0.68	1.28	1,235,979	3,055,395
		12	0.315	19	-1.235	7.0	6.0	1.55	0.90	3,544,306	1,665,823
July	1	1	-0.335	8	-0.965	7.0	5.0	0.63	1.17	1,186,921	2,646,881
		13	0.205	20	-1.205	7.0	6.0	1.41	0.81	2,942,797	1,314,038
	2	2	-0.395	8	-0.945	6.0	6.0	0.55	0.95	957,309	1,997,987
		14	0.005	21	-1.115	7.0	5.0	1.12	0.70	2,326,740	1,257,307
	3	2	-0.415	9	-0.935	7.0	6.0	0.52	0.73	920,230	1,696,780
		15	-0.205	21	-1.005	6.0	6.0	0.80	0.77	1,817,847	1,459,729
	4	3	-0.235	10	-0.925	7.0	5.0	0.69	0.50	1,320,387	984,742
		15	-0.425	22	-0.955	7.0	6.0	0.53	0.83	1,157,436	1,871,870
	5	4	-0.125	10	-0.925	6.0	6.0	0.80	0.60	1,845,055	1,164,495
		16	-0.325	22	-1.055	6.0	6.0	0.73	1.04	1,347,703	2,396,345
	6	4	-0.015	11	-1.205	7.0	6.0	1.19	0.80	2,630,197	1,489,164
		17	-0.405	23	-1.015	6.0	7.0	0.61	1.09	1,170,826	2,606,315
	7	6	0.075	12	-1.275	6.0	6.0	1.35	0.93	3,049,727	1,682,060
		18	-0.345	24	-1.035	6.0	7.0	0.69	1.24	1,367,691	3,262,311
	8	7	0.205	13	-1.345	6.0	6.0	1.55	0.98	3,745,204	1,879,633
		19	-0.365	1	-1.035	6.0	7.0	0.67	1.30	1,360,753	3,353,707
	9	8	0.265	14	-1.345	6.0	6.0	1.61	1.00	3,960,758	1,866,624
		20	-0.345	2	-1.035	6.0	7.0	0.69	1.42	1,272,208	3,523,990
	10	9	0.385	15	-1.365	6.0	6.0	1.75	1.00	4,265,528	1,864,511
		21	-0.365	3	-1.065	6.0	7.0	0.70	1.57	1,340,676	4,078,059
	11	10	0.505	16	-1.375	6.0	6.0	1.83	1.02	4,755,041	1,835,918
		22	-0.355	4	-1.015	6.0	7.0	0.66	1.65	1,166,398	4,175,161
July	12	11	0.635	17	-1.365	6.0	-	2.00	-	5,040,722	-
Average :			-0.010		-1.095	6.338	6.043	1.09	1.09	2,160,344	2,126,186

*) Assumed 70 % of the total volume flows through the shortcut channel and 30 % flows through the original river

Table 5.11

Relationships Between
Tidal Range, Duration, Tidal Volume, Mean Discharge, and Mean Velocity at KP 280
Recording period : From June 6, 1991 to July 12,1991

Date	Range		Duration		Cross Area		Tidal Volume		Mean Discharge		Mean Velocity	
	Fall	Rise	Fall	Rise	Fall	Rise	Fall	Rise	Fall	Rise	Fall	Rise
	m	m	hrs	hrs	m2	m2	m3	m3	m3/s	m3/s	m/s	m/s
June 6	0.54	0.43	6.0	4.0	525.58	391.31	948,348	638,917	43.90	44.37	0.08	0.11
	0.62	1.10	7.0	6.0	496.77	348.34	776,792	1,701,717	30.83	78.78	0.06	0.23
7	1.11	0.63	7.0	5.0	627.97	346.14	1,785,020	863,624	70.83	47.98	0.11	0.14
	0.56	1.12	6.0	7.0	496.77	361.67	740,855	1,965,185	34.30	77.98	0.07	0.22
8	1.24	0.69	7.0	5.0	651.80	335.23	2,198,224	984,509	87.23	54.69	0.13	0.16
	0.61	1.38	6.0	6.0	499.36	352.76	769,084	2,389,557	35.61	110.63	0.07	0.31
9	1.52	0.76	7.0	7.0	717.80	322.56	2,750,355	1,132,528	109.14	44.94	0.15	0.14
	0.63	1.53	5.0	5.0	501.95	350.54	857,737	2,903,664	47.65	161.31	0.09	0.46
10	1.66	0.83	8.0	7.0	761.35	322.35	3,343,453	1,303,010	116.09	51.71	0.15	0.16
	0.69	1.71	5.0	5.0	520.29	352.76	948,222	3,479,241	52.68	193.29	0.10	0.55
11	1.90	0.97	8.0	6.0	822.39	311.78	3,990,709	1,441,412	138.57	66.73	0.17	0.21
	0.77	1.79	5.0	5.0	544.30	354.97	1,048,809	3,693,903	58.27	205.22	0.11	0.58
12	2.00	0.98	9.0	6.0	852.08	309.69	4,262,450	1,541,145	131.56	71.35	0.15	0.23
13	0.76	1.80	4.0	6.0	544.30	357.20	1,121,065	3,795,144	77.85	175.70	0.14	0.49
	2.04	1.11	8.0	7.0	858.75	305.52	4,328,661	1,594,852	150.30	63.29	0.18	0.21
14	0.81	1.74	4.0	6.0	574.34	370.68	1,161,019	3,643,597	80.63	168.69	0.14	0.46
	1.96	1.05	8.0	6.0	858.75	322.56	4,063,750	1,600,423	141.10	74.09	0.16	0.23
15	0.70	1.60	5.0	6.0	579.88	400.63	1,141,325	3,315,514	63.41	153.50	0.11	0.38
	1.92	1.16	7.0	7.0	855.41	328.76	3,779,008	1,651,597	149.96	65.54	0.18	0.20
16	0.87	1.43	6.0	4.0	619.35	393.63	1,176,941	2,756,298	54.49	191.41	0.09	0.49
	1.67	1.08	8.0	6.0	789.99	339.58	3,198,318	1,672,310	111.05	77.42	0.14	0.23
17	0.74	1.25	5.0	7.0	610.79	417.44	1,159,875	2,120,521	64.44	84.15	0.11	0.20
	1.55	1.14	7.0	6.0	764.19	348.50	2,564,020	1,694,762	101.75	78.46	0.13	0.23
18	0.82	1.03	5.0	7.0	639.83	422.23	1,315,145	1,765,192	73.06	70.05	0.11	0.17
	1.31	1.14	7.0	6.0	702.23	357.42	2,062,373	1,833,744	81.84	84.90	0.12	0.24
19	0.89	0.63	5.0	7.0	651.51	415.05	1,530,454	1,123,537	85.03	44.58	0.13	0.11
	0.80	1.04	7.0	6.0	577.38	375.44	1,317,798	1,737,047	52.29	80.42	0.09	0.21
20	0.89	0.54	5.0	8.0	645.66	410.30	1,601,113	969,291	88.95	33.66	0.14	0.08
	0.67	1.09	6.0	5.0	547.27	380.01	1,003,151	1,684,384	46.44	93.58	0.08	0.25
21	1.10	0.61	6.0	7.0	666.24	377.72	1,801,863	1,001,667	83.42	39.75	0.13	0.11
	0.55	1.15	7.0	5.0	528.50	391.54	960,010	2,163,285	38.89	120.18	0.07	0.31
22	1.42	0.88	6.0	7.0	699.20	331.13	2,326,934	1,162,226	107.73	46.12	0.15	0.14
	0.60	1.21	7.0	5.0	544.57	393.86	854,924	2,187,035	33.93	121.50	0.06	0.31
23	1.57	0.98	6.0	7.0	720.56	314.09	2,786,169	1,384,792	128.99	54.95	0.18	0.17
	0.60	1.23	7.0	5.0	549.98	398.53	973,248	2,681,976	38.62	149.00	0.07	0.37
June 24	1.61	0.98	6.0	7.0	732.90	314.09	3,264,110	1,425,915	151.12	56.58	0.21	0.18
	0.62	1.31	7.0	5.0	549.98	393.86	987,078	2,842,203	39.17	157.90	0.07	0.40

(next page)

(Table 5.11 Continued)

Date	Range		Duration		Cross Area		Tidal Volume		Mean Discharge		Mean Velocity	
	Fall	Rise	Fall	Rise	Fall	Rise	Fall	Rise	Fall	Rise	Fall	Rise
	m	m	hrs	hrs	m2	m2	m3	m3	m3/s	m3/s	m/s	m/s
June 25	1.69	1.06	6.0	6.0	751.60	309.90	4,200,908	1,891,136	194.49	87.55	0.26	0.28
26	0.66	1.34	7.0	6.0	566.35	398.53	1,235,309	3,616,309	49.02	167.42	0.09	0.42
	1.75	1.07	5.0	7.0	767.35	307.81	4,420,017	1,919,722	245.56	76.18	0.32	0.25
27	0.67	1.42	7.0	6.0	566.35	396.19	1,274,873	3,910,301	50.59	181.03	0.09	0.46
	1.82	1.08	5.0	7.0	789.67	307.81	4,736,486	2,042,927	263.14	81.07	0.33	0.26
28	0.70	1.37	6.0	6.0	569.10	391.54	1,318,275	3,616,751	61.03	167.44	0.11	0.43
	1.72	1.03	6.0	7.0	767.35	314.09	4,420,001	1,853,406	204.63	73.55	0.27	0.23
29	0.71	1.31	6.0	5.0	563.60	384.60	1,275,977	3,255,696	59.07	180.87	0.10	0.47
	1.63	1.00	7.0	6.0	739.11	314.09	3,855,745	1,752,021	153.01	81.11	0.21	0.26
30	0.68	1.28	7.0	5.0	555.41	384.60	1,235,979	3,055,395	49.05	169.74	0.09	0.44
	1.55	0.90	7.0	6.0	729.81	324.69	3,544,306	1,665,823	140.65	77.12	0.19	0.24
July 1	0.63	1.17	7.0	5.0	541.88	384.60	1,186,921	2,646,881	47.10	147.05	0.09	0.38
	1.41	0.81	7.0	6.0	696.17	331.13	2,942,797	1,314,038	116.78	60.84	0.17	0.18
2	0.55	0.95	6.0	6.0	525.85	389.22	957,309	1,997,987	44.32	92.50	0.08	0.24
	1.12	0.70	7.0	5.0	636.93	350.77	2,326,740	1,257,307	92.33	69.85	0.14	0.20
3	0.52	0.73	7.0	6.0	520.55	391.54	920,230	1,696,780	36.52	78.55	0.07	0.20
	0.80	0.77	6.0	6.0	577.38	375.44	1,817,847	1,459,729	84.16	67.58	0.15	0.18
4	0.69	0.50	7.0	5.0	569.10	393.86	1,320,387	984,742	52.40	54.71	0.09	0.14
	0.53	0.83	7.0	6.0	517.91	386.91	1,157,436	1,871,870	45.93	86.66	0.09	0.22
5	0.80	0.60	6.0	6.0	599.75	363.86	1,845,055	1,164,495	85.42	53.91	0.14	0.14
	0.73	1.04	6.0	6.0	544.57	364.13	1,347,703	2,396,345	62.39	110.94	0.11	0.30
6	1.19	0.80	7.0	6.0	631.14	331.13	2,630,197	1,489,164	104.37	68.94	0.17	0.21
	0.61	1.09	6.0	7.0	523.20	373.17	1,170,826	2,606,315	54.20	103.43	0.10	0.28
7	1.35	0.93	6.0	6.0	657.38	316.20	3,049,727	1,682,060	141.19	77.87	0.21	0.25
	0.69	1.24	6.0	7.0	539.19	368.64	1,367,691	3,262,311	63.32	129.46	0.12	0.35
8	1.55	0.98	6.0	6.0	696.17	301.58	3,745,204	1,879,833	173.39	87.03	0.25	0.29
	0.67	1.30	6.0	7.0	533.83	368.64	1,360,753	3,353,707	63.00	133.08	0.12	0.36
9	1.61	1.00	6.0	6.0	714.43	301.58	3,960,758	1,866,624	183.37	86.42	0.26	0.29
	0.69	1.42	6.0	7.0	539.19	368.64	1,272,208	3,523,990	58.90	139.84	0.11	0.38
10	1.75	1.00	6.0	6.0	751.60	297.45	4,265,528	1,864,511	197.48	86.32	0.26	0.29
	0.70	1.57	6.0	7.0	533.83	361.89	1,340,676	4,078,059	62.07	161.83	0.12	0.45
11	1.88	1.02	6.0	6.0	789.67	295.40	4,755,041	1,835,918	220.14	85.00	0.28	0.29
	0.66	1.65	6.0	7.0	536.51	373.17	1,166,398	4,175,161	54.00	165.68	0.10	0.44
July 12	2.00	-	6.0	-	831.90	297.45	5,040,722	-	233.37	-	0.28	-
Average	1.09	1.09	6.3	6.1	636.67	355.92	3,086,206	3,037,409	95.03	99.79	0.14	0.28

from tidal currents, was examined using a correlation between distribution of tidal range and mean water discharge rather than distribution of velocity. The main reason for this was that the effect of resuspension and redeposition of sediment in the estuary which creates the distribution of the sediment during the tidal process is not correlated to the velocity. This case is shown in table 5.5 and will be evaluated in detail in section 5.2.2.

5.2 Sediment Measurement Data

Sediment data were measured at many places within the estuarine and nearshore area under various current conditions. Suspended transport was measured by a suspended sediment sampler while bed load transports were measured by bed load samplers. Photos of both devices can be seen in appendix B, figure B.4-1 and figure B.4-2. Sediment concentration found in the suspended sediment sampler can be classified into suspended and wash load sediment. In the case of sediment load influenced by tidal currents, both classifications are identified as suspended sediment.

Bed sediment samples were also taken. The samples were derived from the upper station (KP.180) to the shortcut river mouth station with 3 km distance between two points. Some samples were also taken at some points along the shoreline. Two points were located in the sea area about 4 and 6 km from the river mouth and some points were located along the original river and its mouth. This data is useful for evaluating the difference in the sediment characteristics from the upper region of the estuary to the river mouth and the surf zone.

5.2.1 Suspended Sediment Transport

Capacity of suspended sediment transport is mostly determined by hydraulic conditions and sediment characteristics. During the rainy season, for example, the sediment discharge rate in the Brantas estuary is mainly determined by the outflow velocity of the fresh water discharge. On the other hand, during the dry season when the fresh water discharge is low or may be zero, the sediment inflow to the estuary is determined by tidal currents.

Measurement of sediment was referred to in section 5.1.3. Data showing the correlation between hydraulic conditions and suspended sediment are given in table 5.5. If the water discharge and suspended sediment discharge are plotted, an approximate water-sediment discharge curve can be obtained. Four curves are presented in figures 5.7-1 and 5.7-2. These are the curves for KP.250, KP.242, KP.236 and SB.5.

In general, those four curves show that the sediment and water discharges will increase continuously from beginning to end of the duration of a flood tide. Occasionally, before high water, both discharges will decrease gradually to become zero. Alternatively, before the zero point is reached, the discharge may increase again due to the ebb currents. The same behaviour will occur during the ebb tide. The discharges will increase rapidly during the ebb period and decrease gradually in the slack period and so forth.

Preliminary predictions can be obtained from the differences among the four curves discussed above. The increment rates of the sediment discharge during the flood and ebb tide are different at each station. Sediment discharge at KP.250 and KP.242 during ebb

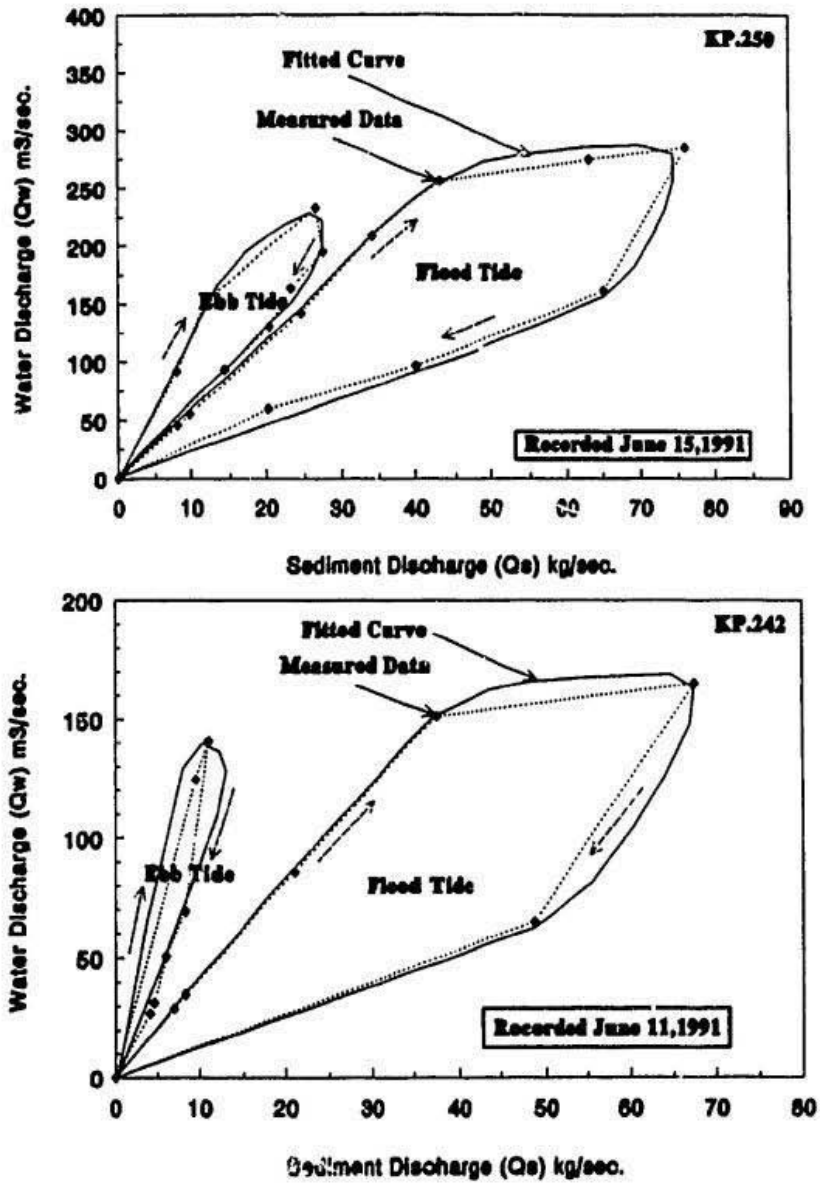

Fig.5.7-1 Relationships Between Water Discharge and Suspended Sediment Discharge During a Tidal Cycle at KP.250 and KP.242

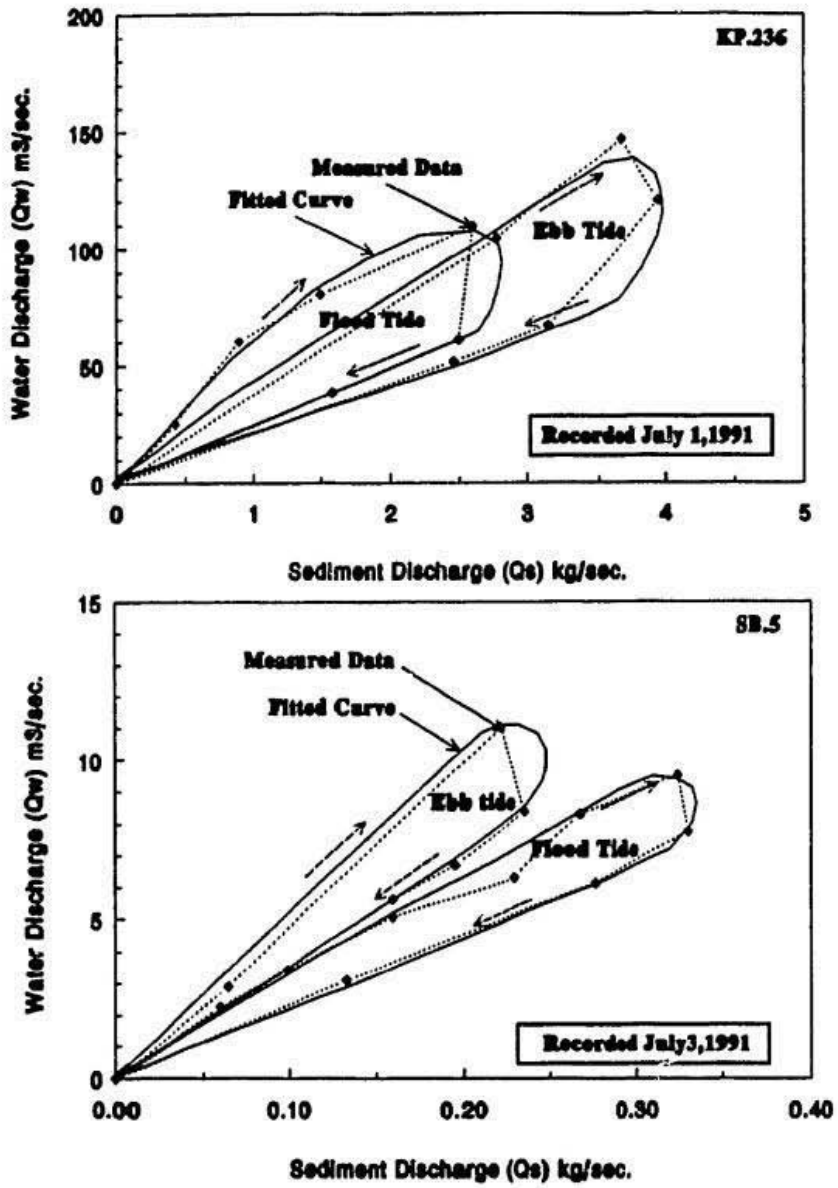

Fig.5.7-2 Relationships Between Water Discharge and Suspended Sediment Discharge During a Tidal Cycle at KP.236 and SB.5

tide is much lower than during the flood tide. This means that the mean velocity of the ebb currents are less than those of the flood currents. An inference can be drawn that, at both stations, the net sediment deposition is positive. Sediment inflow by flood tide currents is larger than sediment outflow by ebb tide currents Consequently, the deposit of sediment particles will occur continuously in the region between the two stations

Those phenomena are completely different from that shown at KP 236 There, the ebb tide sediment discharge is higher than that of the flood tide. Therefore, the mean velocity during a flood tide is lower than that of an ebb tide. Degradation will occur in this region.

At SB.5, the water-sediment discharge curve is almost the same as at KP 242 but sediment discharge during the flood tide seems only a little higher than that during the ebb tide. Deposition may also occur in this region and along the downstream channel from this station. This is one reason why the original river is always shallower year by year.

A quantitative estimation should be obtained from the tidal and the sediment data in order to develop a discussion of the approximate deposition trends and the accretion caused by tidal currents. A detailed estimation will be presented in section 6 2 3.

5.2.2 Effects of Suspension and Deposition within the Porong Estuary

Suspended sediment supplied to the estuary is influenced by repeated cycles of sedimentation and resuspension caused by tidal currents This also happens in the Porong estuary. If the velocity and sediment are evaluated in detailed observations, the behaviour

of sediment shows significant features near the slack period. The suspended sediment concentrations as a function of velocity are nonlinear. Normally, concentration of sediment will decrease with decreasing velocity. But in fact, measurements show that the sediment concentrations increase for some time after the velocity goes down (see figure 5.8).

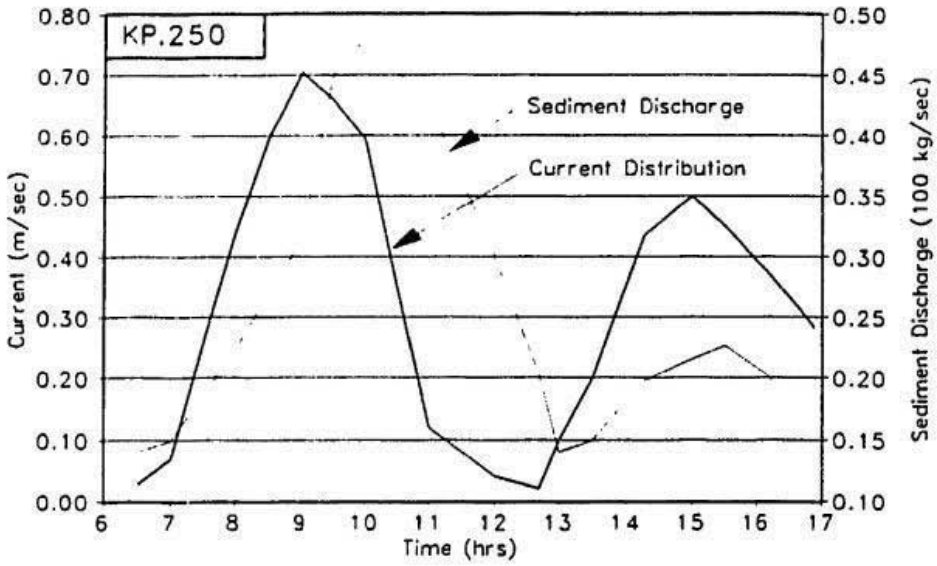

Fig.5.8 Current and Sediment Distribution During a Tidal Cycle at KP.250

Based on this figure, the sediment concentration is still increasing for about half an hour after the velocity maximum is reached. This condition is a very important consideration in calculating the distribution of sediment inflow to the estuary.

It was previously mentioned (see section 5.2.1, figure 5.7 and figure 5.8), that sediment discharge is correlated with the water discharge rather than with the velocity distribution. Therefore, the suspended discharge to the Porong estuary will be calculated based on its distribution pattern in the flood or ebb process using the mean water

discharge calculated from the tidal volume.

5.2.3 Bed Sediment Transport

Bed sediment transport was also measured at the four stations previously described. The measurement used the bed load sampler. Similar to the measurement of suspended sediment load, bed load samples were taken during a tidal cycle at 1 hour intervals. For every measurement, the bed sampler was put in the river bed for 5 minutes and the concentration of bed sediment was evaluated in the Brantas laboratory. Therefore, to calculate the bed sediment discharge per second, the sediment concentration obtained from the laboratory must be divided by the duration of measurement (300 seconds). Then, the result must be multiplied by the river width and divided by the width (20 cm) of the sediment sampler. One of the results, for KP.250, is presented in table 5.12.

The table shows that bed load transport is much smaller than that of suspended sediment (compared to table 5.5). If the mean percentage is taken as an approximation, the bed load discharge would be about 10 % of suspended load.

The most important feature obtained from the table is that the concentration of bed sediment has a certain correlation to the currents. Like suspended load, the bed sediment loads depends on the current velocity. However, since the quantity represents an insignificant contribution to the sediment budget within the estuary, the percentage of bed sediment load to suspended sediment is reasonable.

Table 5.12 Cross Sectional Survey - Relationships Between Hydraulic Condition and Bed Load Sediment

Date : June 15, 1991
Location : Porong river mouth
Station : KP.250

No	Time	Water Elevation (m,SHVP)	Mean Vel. m/s	Discharge		Note
				Water m^3/s	Bed Load kg/s	
1	06:00	-0.896	0.00	0.00	0.000	Rising
2	06:30	-0.886	0.11	45.94	1.465	tide
3	07:00	-0.846	0.13	55.27	1.815	
4	07:30	-0.766	0.33	142.44	2.680	
5	08:00	-0.406	0.40	209.17	3.100	
6	08:30	-0.276	0.46	256.62	6.327	
7	09:00	-0.036	0.44	275.04	11.073	
8	09:30	0.284	0.40	285.22	9.929	
9	10:00	0.554	0.20	161.09	2.911	
10	11:00	0.564	0.12	97.04	0.698	
11	11:30	0.704	0.07	59.83	0.612	
12	11.45	0.704	0.00	0.00	0.000	
13	12.00	0.644	0.11	91.84	0.911	Falling
14	12.30	0.574	0.19	154.27	0.929	tide
15	14:00	0.106	0.35	233.29	2.699	
16	14:30	-0.156	0.33	195.04	1.627	
17	15:30	-0.256	0.29	163.37	0.934	
18	16:10	-0.406	0.25	130.73	0.910	
19	16:50	-0.526	0.19	93.41	0.764	
20	19:00	-1.216	0.00	0.00	0.000	

5.2.4 Sieve Analysis

As mentioned in the introduction of this sub-chapter, bed sediment samples were taken along the estuary from KP.180 to KP.250 every 3 km distance. Some samples were also taken at near shore points, 4 and 6 km from the river mouth, and at some points located along the original river including its mouth. The observed locations are shown in figure 5.9.

The purpose of this sampling was to determine the differences of the grain size characteristics or their distributions between one and the other places. The samples were analyzed by sieving using the ASTM system. Eleven ASTM meshes were arranged from 0.063 mm to 6.3 mm in diameter. The largest diameter of mesh (6.3 mm) was put on the top and they were arranged consecutively to the smallest diameter (0.063 mm) on the bottom. The weight of retained sediment in each mesh was converted to a percentage of the total weight of the sediment used in the analysis. Data were then presented in a graphical form with diameter of mesh as the horizontal axis and commutative percentage as the vertical axis. One sample of graphs is shown in figure 5.10. It shows that the percentages of gravel, sand, silt and clay are 1.98, 96.96, 1.02 and 0.04 %, respectively. However, the sediment is classified as sand. Besides those specifications, the median and mean diameter are also important for identifying sediment characteristics within the estuary and the surf zone. The results are presented in table 5.13. It shows that in all points, the percentages of silt and clay are generally low. The highest content of silt and clay is about 5.66% to 6.05% and the locations are found nearby the shoreline, KN.1, KN.2 and KN.3 - see figure 5.9.

According to the longitudinal survey of salinity intrusion (see table 5.6, appendix A tables A.2-1 through A.2-3 and figures 5.4-1 to 5.4-4), the tip of salinity intrusion is located around KP.210 to KP.220. On the basis of the median diameter (table 5.13), the greatest median diameter along the estuary (from KP.180 to KP.255) was found to be 0.56 mm at KP.210. It then decreases gradually to the river mouth : 0.31 at KP.255 left or 0.35 at KP.255 right. If the circulation type in the estuary is salt

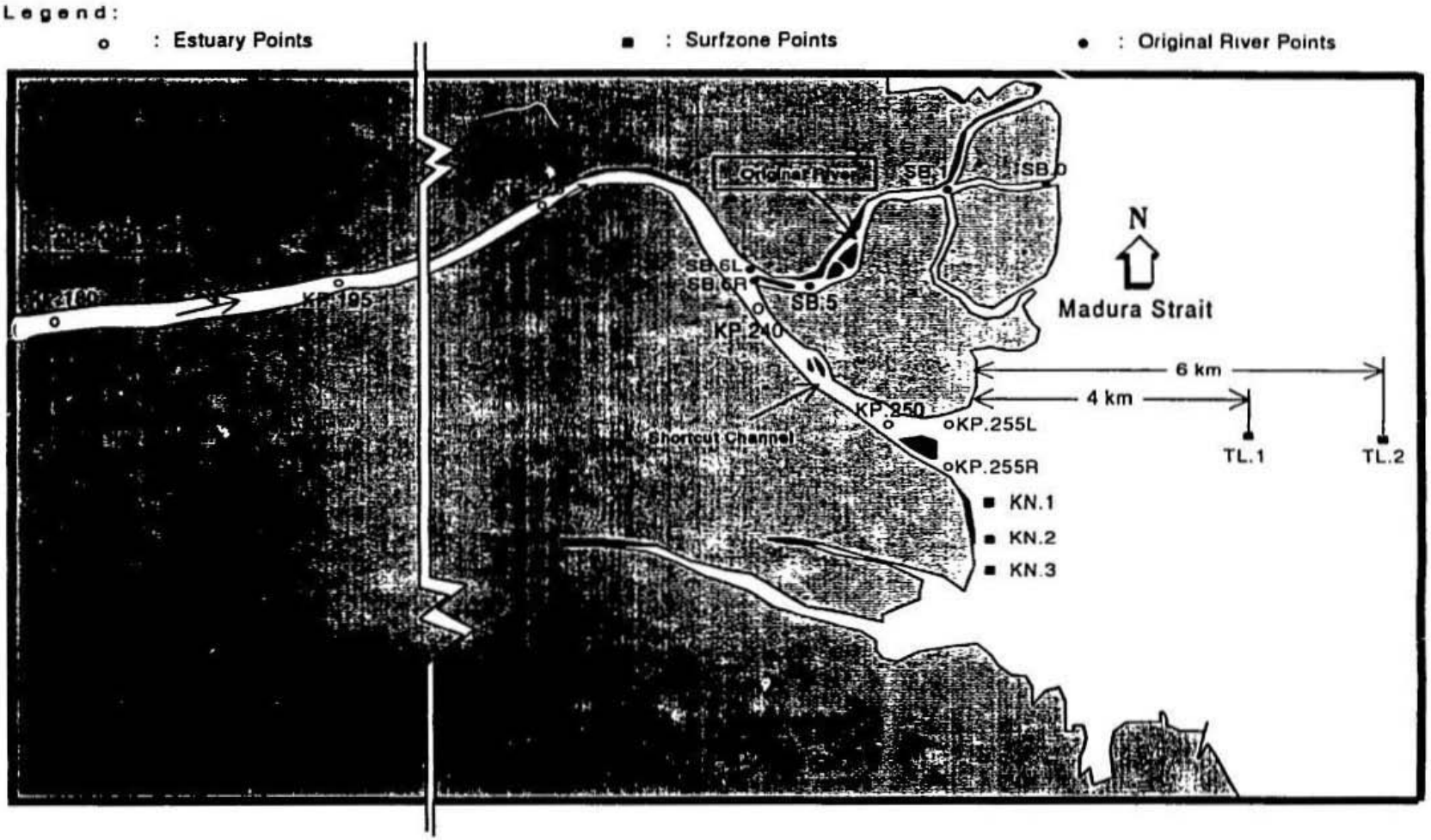

Fig. 5.9 Locations of Bed Sediment Samples

Fig.5.10 Mechanical Analysis of a Sediment Sample

Location KP. 180

Soil classification of grain size (Sample of passed 2000 μ sieve)

a CLAY
b SANDY CLAY
c SILTY CLAY
d SANDY CLAY LOAM
e CLAYEY LOAM
f SILTY CLAY LOAM
(g) SAND
h SANDY LOAM
i LOAM
j SILTY LOAM

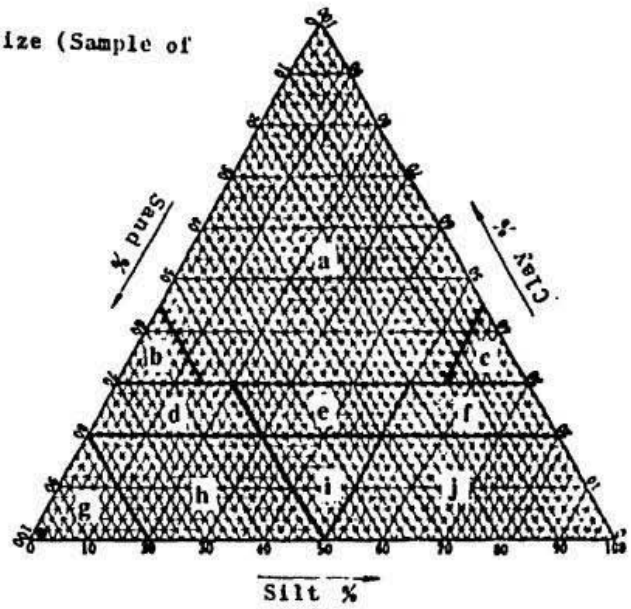

Sample No.	Gravel %	Sand %	Silt %	Clay %	Max. size	φD60	D10	Uniformity Coeff.	2000μ sieve Passed	420μ sieve Passed	74μ sieve Passed	Percentage	Classification	Remarks
1	1.98	96.96	1.02	0.04									Sand	

Grain size accumulation curve

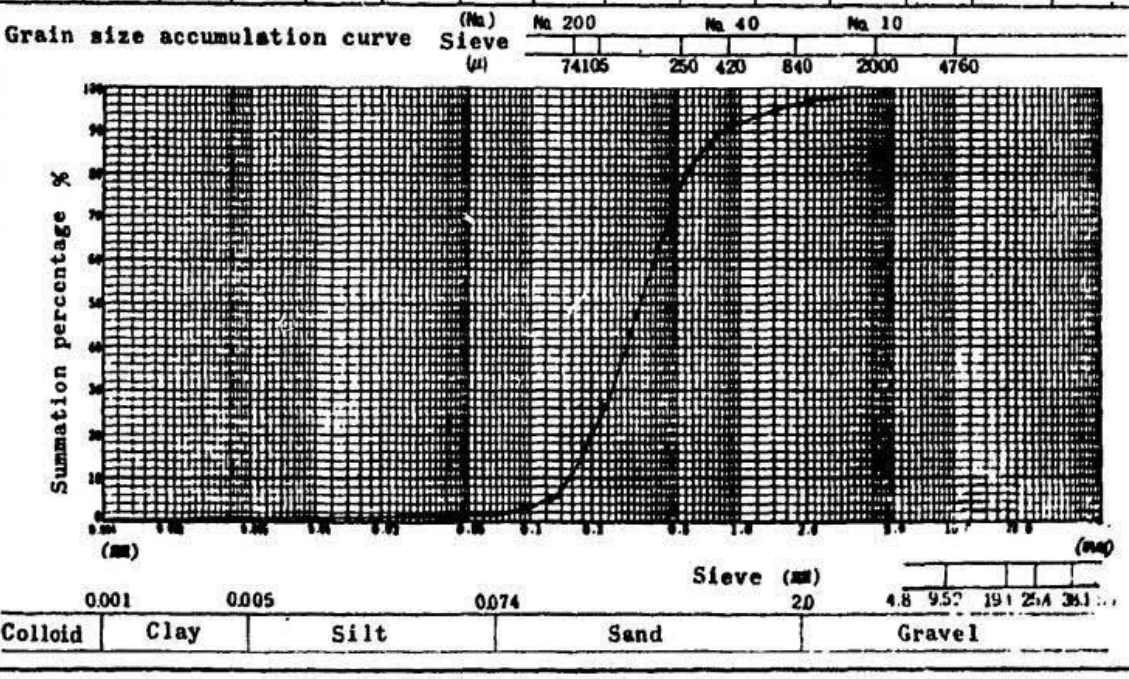

N.K. Frame No.

Table 5.13

Grain Size Distribution of Bed Sediment

(Along the Estuary, Shoreline and the Surf Zone)

No.	Location	USCS						Phi Unit	
		Fine Gravel (%)	Sand			Silt &Clay (%)	Median Diamt. Md=d50	Median Diamt. Md(phi)	Mean Diamt. M(phi)
			Coarse (%)	Med. (%)	Fine (%)				
1	KP.180 (Upper Station : 15 Km from the Shorcut Mouth)	1.98	1.73	48.17	47.14	1.06	0.43	0.44	2.41
2	KP.195 (3 Km downward KP.180; 12 Km from the Shortcut Mouth)	0.02	0.10	47.73	51.75	0 40	0.41	0.41	2.76
3	KP.210 (6 Km downward KP.180; 9 Km from the Shortcut Mouth)	2.96	3.74	62.21	30.87	0.22	0.56	0.57	1.29
4	KP.225 (9 Km downward KP.180 6 Km from the Shortcut Mouth)	0 56	1.10	60.34	37.73	0.27	0.49	0.47	2.09
5	KP.240 (12 Km downward KP.180 3 Km from the Shortcut Mouth)	1.00	2.05	53.84	42.76	0.35	0.45	0.44	2.19
6	KP.250 (14 Km downward KP.180 1 Km from the Shortcut Mouth)	0.00	0.25	51.04	48.35	0.36	0.42	0.41	2.35
7	KP.255R (The Shortcut Mouth ; Paralel to the Shoreline & the right-side of the Channel)	0.48	0.32	29.15	69.88	0.17	0.35	0.35	2.89
8	KP.255L (The Shortcut Mouth ; Paralel to the Shoreline & the left-side of the Channel)	0.00	0.62	21.63	76.28	1.47	0.31	0.31	3.40
9	KN.1 (1 km southward of the Shortcut River Mouth; on the shoreline)	0.00	0.00	17.20	76.75	6.05	0.16	0.15	5.28
10	KN.2 (2 km southward of the Shortcut River Mouth; on the shoreline)	0 00	0.00	36.09	58.72	5.19	0.34	0.35	2.70
11	KN.3 (3 km southward of the Shortcut River Mouth; on the shoreline)	0.00	0.00	32.91	61.43	5.66	0.24	0.23	3.82
12	TL (6 km eastward of the shoreline; in the Surf Zone)	0 00	0.42	33.13	64.95	1.50	0.25	0.25	3.03
13	SB.6L (Tributary between Origininal & Shortcut River; left-side)	17 52	13.11	59.34	9.96	0.07	0.92	0.93	0.74
14	SB.6R(Tributary between Origininal & Shortcut River; right-side)	4 23	5.32	65.53	24.92	0.00	0.59	0.57	1.38
15	SB.5 (750 m downward of the Tributary; in the Original River; 5 Km from the Original Mouth)	3.52	4.21	61.06	30.16	1.04	0.53	0.52	1.75
16	SB.1 (1 km upward from the Original River Mouth)	0.32	1.86	49.38	47.51	0.93	0.43	0.44	2.24
17	SB.0 (the Original River - Mouth)	0.18	0.95	42.10	55.11	1.66	0.39	0.41	2.70

wedge (see section 3.1.1), the coarse sediments of the fresh water entering the estuary will be transported as bed-load material to the tip of the salinity intrusion, where they will be deposited since the bottom currents between fresh and salt water become equal at that place. This agrees with the measured sediment distribution along the Brantas estuary. The median diameter decreases gradually down to the estuary mouth (KP.255). Another fact to strengthen this case is the percentage of the medium sand. It was found to be 62.21 % at KP.210. This is also the largest value of the medium sand along the estuary. On the other hand, the highest content of the fine sediment was located at KP.195. This means that the fine sediment particles which settle through the saline (KP.250 - KP.255), landward-flowing lower layer, get transported up the estuary as far as KP.195. If KP.180, KP.210 and KP.250 represent the upper estuary, the tip of the wedge and the lower estuary respectively, a figure showing the difference of the diameter distribution can be presented in figure 5.11.

The explanation above seems to be contrary to the results of the longitudinal field observations which have shown that the salinity distributions tended to be of the well mixed type. This case should be referred to the determinant factors that influence the form of the salinity distribution (see section 3.1.1). The stratification depends dominantly on the relative magnitude of the contribution between tidal action and fresh water inflow. In fact, during the observations, the fresh water discharges were very low and therefore, the tidal actions were more dominant than the fresh water inflow. The water discharge came only from the Porong drainage basin, while water from the Brantas river was totally diverted to the Surabaya river branch for municipal

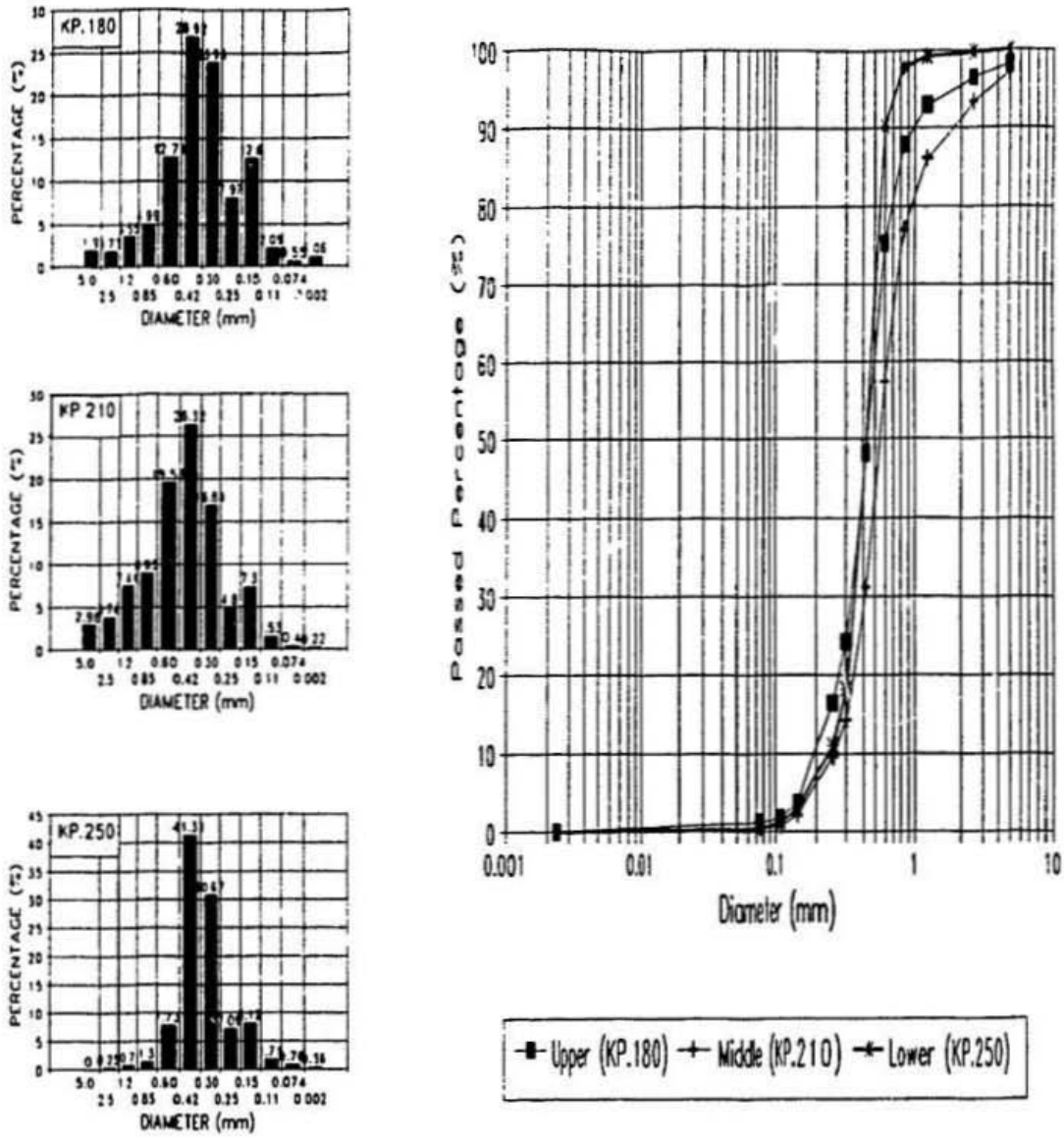

Fig.5.11 Mechanical Analysis of Sediment along the Estuary

and industrial water purposes facilitated by the New Lengkong dam. As a result, the water discharge to the Porong river varies greatly throughout the year particularly

during the dry season. The variable discharges of the Porong river during that time depend strongly on the available discharge of the Surabaya river which derives from the drainage basin itself. Additional discharges also come from the upper area of the New Lengkong dam. If the discharge of the Surabaya river is sufficient for fulfilment of the Surabaya metropolitan water requirement, the excessive water then will be discharged to the Porong River. Consequently, the variability of the water discharges will alternate the stratification forms within the estuary. A discharge limit that will change the highly stratified condition into a partly stratified or well mixed estuary for the Porong river will be discussed in section 6.1.1.

If variations in sediment characteristics between the shoreline and the surf-zone are evaluated, the significant difference between them seems unclear using only the results of the sieve analyses, together with median or mean diameters. Additional work is needed to verify their characteristics. This can be obtained by a decantation test to determine washed material percentages.

Briefly, the procedure of the decantation test can be explained as follow. A certain amount of a dry observed sediment, for example 200 grams, is put in the ASTM mesh no. 200 (size = 0.074 mm). Then, the sediment is washed until the water coming out from the mesh is quite clear. After the remaining sediment is dried by an oven, the weight of the sediment is compared to its original weight before testing. The difference in weight gives the weight of the material washed. The results of the tests for shoreline and surf zone materials are presented in table 5.14.

As shown in table 5.14, the highest content of material washed is on the

locations near the shoreline (KN.1, KN.2, KN.3). Then, the content decreases gradually seaward. This condition may be valid only during the dry season and the opposite may happen in the wet season where the fine sediment which is brought by the river is flushed directly to the surf-zone rather than to the shoreline. Furthermore, the dominant wind during the wet season is the west-monsoon which comes from the mainland and causes calm waves. Unfortunately, no decantation test data during the wet season are available, so the condition cannot be proved.

Table 5.14 Decantation Test Data of Sediment near the shoreline and the Surf-Zone

(Weight in grams)

SECTION	KN.1	KN.2	KN.3	TL.1	TL.2
BEFORE TESTING					
Weight of Sample+ Container	289.4	275.0	274.9	289.4	269.5
Weight of Container	89.4	75.0	74.90	89.4	69.5
Weight of Sample	200.0	200.0	200.0	200.0	200.0
AFTER TESTING					
Weight of sample + container	104.0	79.2	79.2	122.8	118.7
Weight of Container	89.4	75.0	74.9	89.4	69.5
Weight of Sample	14.6	4.2	4.3	33.4	49.5
DECREASED AMOUNT	185.4	195.8	195.7	166.6	150.8
PERCENTAGE (%)	92.7	97.9	97.8	83.3	75.4

A significant feature of sediment characteristics can also be found along the original river from the branch of the shortcut channel, SB.6L and SB.6R, to the original river mouth, SB.0 (see figure 5.9). The median diameter of the sediment

decreases gradually downward. In contrast, the content of fine sediment increases, also in that direction. This trend means that sediment particles are brought continuously by flood tidal currents upward from the original river mouth to the branch (SB.6) and part of them are brought back by ebb tidal currents seaward. Flood currents are higher than ebb currents (see explanation in section 5.2.1 and figure 5.7-2 for SB.5). Therefore, only certain diameters of the fine sediment will be brought backward by the ebb currents while the larger diameters will be left. This is the main reason why the median diameter decreases while the content of fine sediment increases downward from the tributary to the original river mouth.

5.3 Waves And Longshore Currents

This section deals with the littoral processes and sediment motion in the surf-zone, nearshore and along the shoreline. Wind, waves and longshore currents are the main environmental factors for determining the littoral processes. Therefore, the field observations are very useful to compensate for the unavailability of wave data in this area. Moreover, the observations will be used for determining a seaward limit of the significant transport and an approximation of the longshore transport rate.

5.3.1 Wind, Waves And Currents Along the Shoreline

Wind, waves and currents were observed at the shoreline and surf zone points where the bottom materials were taken. There were seven points: KN.1, KN.2, KN.3, KP.355R, KP.355L, TL.1 and TL.2 (see figure 5.9). Equipment used in this observation included a point gauge, current meter, anemometer and compass. Observations coped with three major factors of the marine forces particularly within the surf zone: wind, waves and currents. At each point, several kinds of the measurements were carried out such as, water depth, velocity and direction of the longshore currents, wave height, wave period, and wave direction, wind speed and its direction. The results of the observed data are presented in table 5.15.

Table 5.15-1 Currents, Waves and Wind observation near the shoreline

Date : June 29, 1991
Equipment : Point Gauge, Current meter, Anemometer and Compass
Location : KN.1, Shoreline (1 km southward of the Shortcut River Mouth)
Time : 10.20 a.m (20 minutes)

Currents			Waves			Wind	
Water Depth (m)	Vel. Distribution (m/s)	Mean Direction (°N)	Wave Height (m)	Mean Period (Sec)	Direction (°N)	Speed (m/s)	Direction (°N)
0.00 0.17 0.34 0.51 0.68 0.85	0.24 0.22 0.20 0.18 0.14 0.00	10° (Compass azimuth)	0.30 0.25 0.20 0.15	4	E (90° Compass azimuth)	4.5	ENE (70° Compass azimuth)
Avg.:	0 16	10°N	0.23	4	90°N	4.5	70°N

(Continued)

Table 5.15-2 : at KN.2

Date : June 29, 1991
Equipment : Point Gauge, Current meter, Anemometer and Compass
Location : KN.2, Shoreline (2 km southward of the Shortcut River Mouth)
Time : 11.20 a.m (20 minutes)

Current			Wave			Wind	
Water Depth (m)	Vel. Distribution (m/s)	Mean Direction (°N)	Wave Height (m)	Mean Period (Sec)	Direction (°N)	Speed (m/s)	Direction (°N)
0.00 0.20 0.40 0.60 0.80 1.00	0.14 0.10 0.16 0.12 0.11 0.11	10° (Compass azimuth)	0.35 0.20 0.30 0.25	4	ESE (110° Compass azimuth)	5.5	ENE (75° Compass azimuth)
Avg.:	0.12	10°N	0.28	4	110°N	5.5	75°N

Table 5.15-3 : at KN.3

Date : June 29, 1991
Equipment : Point Gauge, Current meter, Anemometer and Compass
Location : KN.3, Shoreline (3 km southward of the Shortcut River Mouth)
Time : 11.50 a.m (20 minutes)

Currents			Waves			Wind	
Water Depth (m)	Vel. Distribution (m/s)	Mean Direction (°N)	Wave Height (m)	Mean Period (Sec)	Direction (°N)	Speed (m/s)	Direction (°N)
0.00 0.22 0.44 0.66 0.88 1.10	0.16 0.13 0.11 0.09 0.08 0.08	70° (Compass azimuth)	0.30 0.25 0.20 0.15	5	ESE (100° Compass azimuth)	7.5	ENE (70° Compass azimuth)
Avg.:	0.11	70°N	0.23	5	100°N	7.5	70°N

Continued

Table 5.15-4 : at KP.355R

Date : June 29, 1991
Equipment : Point Gauge, Current meter, Anemometer and Compass
Location : KP.355R, Shoreline (Right side of the Shortcut River Mouth)
Time : 13.10 p.m (20 minutes)

Current			Wave			Wind	
Water Depth (m)	Vel. Distribution (m/s)	Mean Direction (°N)	Wave Height (m)	Mean Period (Sec)	Direction (°N)	Speed (m/s)	Direction (°N)
0.00 0.38 0.76 1.14 1.52 1.90	0.39 0.29 0.27 0.25 0.25 0.00	100° (Compass azimuth)	0.20 0.20 0.15 0.15	6	ENE (80° Compass azimuth)	7.5	ENE (70° Compass azimuth)
Avg.:	0.24	100°N	0.18	6	80°N	7.5	70°N

Table 5.13-5 : at KP.355L

Date : June 29, 1991
Equipment : Point Gauge, Current meter, Anemometer and Compass
Location : KP.355L, Shoreline (Left side of the Shortcut River Mouth)
Time : 14.00 p.m (20 minutes)

Currents			Waves			Wind	
Water Depth (m)	Vel. Distribution (m/s)	Mean Direction (°N)	Wave Height (m)	Mean Period (Sec)	Direction (°N)	Speed (m/s)	Direction (°N)
0.00 0.26 0.52 0.78 1.04 1.30	0.51 0.13 0.11 0.04 0.03 0.00	110° (Compass azimuth)	0.15 0.15 0.15 0.15	6	ENE (85° Compass azimuth)	7.5	ENE (80° Compass azimuth)
Avg.:	0.14	110°N	0.15	6	85°N	7.5	80°N

Tables 5.13-1 through 5.13-5 above show that the windspeeds were about 4.5 to 7.5 m/sec and the dominant wind direction was from the east-northeast (ENE), between 70° and 80° from the north. This data is almost the same as existing data taken from the Juanda International Airport, Surabaya, Indonesia (mentioned in table 4.1 in section 4.1.2). The average wind speed was about 6.5 m/s throughout the year and the wind directions during the dry and wet season were about 70° and 270° from the north, respectively. It is important to note that the dominant directions of the longshore current represented by stations KN.1, KN.2 and KN.3 are to the south (in those tables, the direction means from). This movement was identified more clearly by releasing some floats at area near the shoreline.

An estimation of longshore transport rates based on field data can be made using equation 3-41 and the Littoral Environmental Observations (LEO) method. Actually, several methods were available for calculation or prediction of the longshore transport rate but since this method is more related to results of the field data such as the distribution of the longshore currents, the high crest of the nearest breaking waves from the shoreline so, the estimation will be better. The result is shown in table 5.16. The longshore transport rate along the southern part of the shortcut mouth (KN.1, KN.2, KN.3) is 150,812 m^3 per annum while that within the surrounding area of the shortcut mouth itself is about 150,245 m^3 per annum.

5.3.2 Wind and Waves in the Surf-zone

Like the observations of wind and waves near the shoreline, observations in the

Table 5.16 Estimation of Mean Annual Longshore Transport Rate

Observation Points	Mean longshore Current (m/s)	H_{sb} Wave Height (m)	W Width of Surf-zone (m)	X Dist. from shoreline (m)	$(V/V_0)_{LH}$ Longuet-Higgins factor	P_{ls} Energy Flux N/s	Longsh. Transp. Rate m^3/year
KN.1	0.16	0.23	100	50	0.35	136	175,766
KN.2	0.12	0.28	100	50	0.35	125	161,319
KN.3	0.11	0.23	100	50	0.35	90	115,690
KP.255 (R)	0.24	0.18	100	50	0.35	157	202,959
KP.255 (L)	0.14	0.15	100	50	0.35	76	97,533

Note: $(V/V_0)_{LH}$ is the dimensionless longshore current based on Longuet - Higgins (1970). The approximate value of this factor is 0.40. Based on field observations, the mean width of the surf-zone (W) is about 100 m and the mean distance of the nearest breaking waves from the shoreline is about 50 m, so the Longuet-Higgins factor is 0.35 (see section 3.4.5).

surf zone were done at two main points: TL.1 and TL.2 which are located at about 4 km and 6 km, respectively, from the shoreline. Measurements of wind and waves were done hourly and the duration of every measurement is 20 minutes. This data is shown in table 5.17.

The seaward limit of significant transport within the surf zone can be determined from wave and sediment data at those points. The seaward limit or subaqueous buffer zone is a critical parameter in the calculation of sedimentation within the region. By using the limits, the sediment volume within the active zone can be determined and, based on the geometric historical maps, the volume of sediment during certain years can be examined.

To locate the subaqueous buffer zone, some important factors must be known, such as mean significant wave height (H_{s50}), standard deviation of significant wave height (σ_H), average significant wave period ($T_{s\,avg}$) and mean diameter (d_{50}). The main factor to be obtained from this calculation is the water depth at the seaward limit. It can be approximated by two methods mentioned in section 3.4.5. Using the wave characteristic (equation 3-44) and sediment characteristic (equation 3-46), the calculation can be presented as follows.

Table 5.17-1 Wave and Wind Observation Data in the Surf-Zone at TL.1

Date : June 30,1991
Equipment : Point gauge, Current meter, Anemometer and Compass
Location : 4 km eastward from the shoreline

No.	Time	Water depth (d)=m	Wave			Wind	
			Height (Hs) (m)	Period (T) (sec)	Direction (°N)	Wind speed m/sec	Direction (°N)
1	08.20	0.70	0.20	8.0	83	4.5	70
2	09.20	1.10	0.20	7.5	79	5.0	73
3	10.20	1.80	0.40	6.0	85	6.5	77
4	11.20	2.60	0.45	6.5	87	7.0	75
5	12.10	2.80	0.45	5.5	93	7.5	80
6	13.20	2.40	0.35	5.5	81	7.5	74
7	14.20	2.00	0.40	6.0	90	6.5	84
8	15.20	1.90	0.30	6.0	95	6.0	89
9	16.20	1.60	0.35	7.0	80	6.0	75
10	17.00	1.20	0.30	7.0	82	5.0	72

Table 5.17-2 : at TL.2

Date : July 1,1991
Equipment : Point gauge, Current meter, Anemometer and Compass
Location : 6 km eastward from the shoreline

No.	Time	Water depth (d)=m	Wave			Wind	
			Height (Hs) (m)	Period (T) (sec)	Direction (°N)	Wind speed m/sec	Direction (°N)
1	08.50	0.85	0.40	7.0	82	4.5	65
2	09.50	1.15	0.35	6.0	79	5.0	73
3	10.50	1.80	0.40	6.0	85	6.0	72
4	11.50	2.50	0.50	5.0	89	7.0	75
5	12.40	2.70	0.55	5.0	85	7.5	74
6	13.50	2.10	0.60	4.5	81	7.5	70
7	14.50	2.00	0.65	5.0	85	7.0	72
8	15.50	1.80	0.60	5.0	80	6.5	72
9	16.50	1.50	0.50	5.0	79	6.5	70
10	17.30	1.50	0.40	6.0	85	6.0	70

(a) Based on wave characteristic,

$d_i = 2 H_{s50} + 12 \sigma_H$

From table 5.15, $H_{s\,avg}$ is 0.42 m, $T_{s\,avg}$ = 5.98 sec. and

$H_{s50} = H_{s\,avg} - 0.307 \sigma_H$ where $\sigma_H = 0.62 H_{s\,avg}$. Hence,

$\sigma_H = (0.62)(0.42) = 0.26$ m and

$H_{s50} = 0.42 - (0.307)(0.26) = 0.34$ m. Therefore,

$d_i = 2 (0.34) + 12 (0.26) = 3.80$ m

From figure 4.11, the mean gradient of the surf-zone is 0.00112. Thus the seaward limit of significant transport, which is located at 1.5 d_i, is equal to (1.5)(3.80) / 0.00112 = 5.09 km. from Low Water Level. Since LWL is found at 2.25 km from the shoreline, the seaward limit is thus given by 5.09 + 2.25 km = 7.34 km from the shoreline.

(b) Based on sediment characteristic,

$d_s = (H_{s50})\ (T_{s\ avg})\ (g/(5000\ d_{50}))^{0.5}$. Where d_{50} is taken from table 5.13 and is equal to 0.25 mm. Hence,

$d_s = (0.34)\ (5.98)\ (9.81/(5000 * 0.25))^{0.5} = 5.06$ km. Thus the seaward limit is located at 5.06 + 2.25 km = 7.31 km.

Both methods are approximate and the longer length, rounded to 7.35 km was taken as the seaward limit for significant sediment transport.

Chapter 6

Results and Discussions

Chapter 6

Results and Discussions

The newly measured and existing field data obtained within the Brantas river estuary have been explained and discussed briefly in chapters 4 and 5. Referring to those chapters and the theoretical background, chapter 3, a number of results that are applicable to the Brantas river, or even to any river delta, may be obtained. These discussions will be presented in this chapter.

The explanation in this chapter deals with three basic discussions. First, the discussion of circulation and sedimentation in the estuary, particularly in the shortcut channel and the original river. Second, the discussion of circulation in the estuary and in the surf zone from the shoreline to the seaward limit of significant sediment transport. Finally, from both discussions, interconnections can be sought to provide a pattern of the sediment budget within the entire estuary.

6.1 The circulation pattern in the estuary

The circulation in the estuary depends strongly on the fresh water discharge from the river. As mentioned in section 4.1.4 river discharges entering the Porong river are regulated by the New Lengkong dam 50 km upstream in the estuary. During the dry

season, the Porong river discharges are generally low because the river water will be diverted to the Surabaya river branch for municipal and industrial purposes within the Surabaya Metropolitan area. The mean and maximum daily discharge released to the Surabaya branch from the Lengkong dam's gate are 30 m^3/s and 115 m^3/sec, respectively. The discharge depends on the water level on the Surabaya river derived from its drainage basin. As a result, the discharge of the Porong river during the dry season is relatively low compared to that during the rainy season where the excessive water of the Brantas river will be flushed continuously to the Porong river. Varying river discharges cause the salinity, circulation and sedimentation within the Brantas estuary to vary considerably between the two seasons.

Mean discharges of the Porong river during the rainy season and the dry season are 301 m^3/sec and 63 m^3/sec, respectively. The hydrograph of the monthly mean discharges during 1977 - 1988 (see section 4.2.1, figure 4.5 and table 4.4), shows that the maximum monthly mean discharge occurred in February 1984. It was about 798 m^3/sec and, from the discharge records, the highest discharge was 1,466 m^3/s on April 7 and 8, 1986.

Field measurements of salinity distribution, carried out along the estuary in the dry season of 1991 (see table 5.6 figure 5.4 and explanation in section 5.1.3), showed that the salinity distributions were generally well mixed during those measurements because the fresh water inflow was relatively low at that time. To have confidence in discussions regarding the likely circulation patterns in the Brantas estuary, it is necessary to know the limiting discharges that alter the circulation of the estuary. The distribution discharge

of the Porong river during the whole year, mentioned in section 4.1.4, can be evaluated based on those discharge limits.

6.1.1 Pattern of Water Circulation in Dry Season

Mean water discharge during the dry season is 63 m^3/s but sometimes the daily discharge released from the New Lengkong dam to the Porong river branch will be zero because all water discharges coming from the Brantas river are diverted into the Surabaya river branch. In this condition, the effect of discharge water derived from the Porong drainage basin, including two tributary rivers, the Sadar and Kambing rivers, is lower than the effect of the tide. Mean flood tidal current measurements carried out during June 6 to July 12, 1991, covered two tidal springs and neaps, at the shortcut mouth (KP.250). These were found to be about 0.58 m/s during the spring tide, and 0.11 m/s during the neap tide (see table 5.11, on June 11). On June 25. 1991 when the longitudinal salinity distribution survey was done, the velocity of the mean flood tidal current was 0.28 m/s. Fresh water discharge at that time was very low and the water level was below the zero elevation of the water level recorder of the Porong station. Thus, at that time, the water discharge was less than 25 m^3/sec. By using the approximate equation of the estuarine number, E, (equation 3-1) suggested by Pickard (1975), the fresh water discharge during that time can be estimated as follows

$$E_s = \frac{U^3\ b}{g\ Q_f} \quad or \quad Q_f = \frac{U^3\ b}{g\ E_s} \tag{3-1}$$

Where U is the mean tidal current during the flood tide (=0.28 m/s). b is the width of

the estuary (at KP.250 the width is equal to 256.00 m), g is the acceleration due to gravity (= 9.81 m/sec^2) and the value of E_z is 0.03 or 0.3 depending on whether the estuary is well mixed or slightly stratified. As a result, the fresh water discharge (Q_f)is equal to 19.1 m^3/s for a slightly stratified estuary or 1.9 m^3/s for a well mixed estuary.

If the mean spring tidal current (0.58 m/s) is used in the estimation above, the estuarine circulation will apparently be well mixed. The value of E_z is then about 0.3. The fresh water discharge will be equal to 17.0 m^3/s. Another approximation can be taken by using the degree of mixing (K) that was introduced by Schultz and Simmons, 1957 (quoted in Allen, 1962 and Silvester, 1974) mentioned in equation 3-2 as

$$K = \frac{Vol.\ Fresh\ Water\ per\ Tidal\ Cycle}{Vol.\ Salt\ Water\ During\ Flood\ Tide} \qquad (3\text{-}2)$$

The volume of the salt water during the flood tide can be taken from the tidal volume calculation that has been summarized in table 5.11. On June 25, 1991, the tidal volume was found to be 4,200,908 m^3. If the factor K is taken as 0.1, the volume of fresh water discharge should be about 420,090 m^3. In fact that the tidal cycle period at that day was 12 Hours. Hence, the fresh water discharge was found to be 9.72 m^3/s.

On the basis of the all the above estimations, an inference can be drawn that the Brantas estuary will be well of the mixed or slightly stratified type, when the fresh water inflow is less than about 20 m^3/s. Table 6.1 shows the results of the calculation for Pickard's estuarine number using a flow of 63 m^3/sec (mean discharge during the dry season) and different river widths measured during the field work. It was found that the that the value of the mean estuarine number is less than 0.03. This implies that the Brantas estuarine type is generally highly stratified during the dry season but will be

slightly stratified or well mixed when the flow drops below 20 m^3/sec.

If the estuary is highly stratified with a salt wedge, the bed sediment characteristics must be such as to agree with the circulating system of this type. This case has been discussed in detail in section 5.2.4 and an inference was drawn that the Brantas river estuary during the dry season is usually highly stratified. The maximum distance of the tip wedge was found to be 9 km from the shortcut mouth. It is located around KP.210. Bed load sediment, which moves along the river bottom, will be deposited in the tip of the salt wedge (KP.210) while suspended sediment can flow through the surface layer of the water seawards. Part of the sediment that has settled on the bottom of the lower part of the estuary will move upward through the bottom layer as far as the tip of the salt wedge. KP.210 can be identified as a place of active sedimentation.

The discussion above seems to agree with the observations of the stratification that have been built up by systematic measurement over two flood and ebb tides (refer to figures 5.4-1 to 5.4-4). Even though the estuary at that time tended to be well mixed, the intrusion of salt water reached KP.215 in the two flood tide observations (figure 5.4-1 and figure 5.4-2). This means that the intrusion length was found to be about 8 km from the shortcut mouth. Apparently, the intrusion length is not stationary. It will oscillate backwards and forwards with the tide. In the spring tide condition, for example, the tip may be found upstream from KP.210. On the other hand, it may be found below KP.215 in the neap tide condition. However based on the two measurements above, the intrusion will, on average, reach KP.210 and KP.215.

Table 6.1 Estimation of Estuarine Number

Date : June 25, 1991 & June 27, 1991
Mean Discharge : 63 m^3/sec.(during dry season)

Section	U (m/sec) Current distrib.		B River width (m)	S_e Estuarine number	
	*)	**)		*)	**)
KP.250	0.426	0.219	253	0.03165	0.00430
KP.245	0.392	0.286	183	0.01784	0.00693
KP.240	0.270	0.227	134	0.00427	0.00254
KP.235	0.226	0.248	151	0.00282	0.00373
KP.230	0.163	0.306	123	0.00086	0.00570
KP.225	0.176	0.305	168	0.00148	0.00771
KP.220	0.126	0.272	123	0.00040	0.00400
KP.215		0.288	116		0.00448
KP.210		0.308	125		0.00591
KP.205		0.319	103		0.00541
KP.200		0.324	123		0.00677
KP.195		0.391	159		0.01538
KP.190		0.401	154		0.01607
KP.185		0.414	186		0.02136
KP.180		0.390	127		0.01219
			Average :	0.00847	0.00816

Note : *) First observation June 25,1991
**) Second observation June 27,1991

Another fact found from the longitudinal survey is that water and sediment movement during low fresh water inflow is dominated by the rise and fall of the Madura Strait at the river mouth. The normal vertical velocity profiles of the ebb and flood currents in the estuary were undistorted by the density stratification. The forms of the velocity distribution were typically parabolic. This means that the velocity throughout the depth is dominantly in an upstream direction during the flood tides and downstream during the ebb tides.

Temperature profiles are also given in figure 5.4. They show that during the flood or ebb tide the temperature distribution is insignificant. The vertical temperature difference is less than 2°C as is the longitudinal temperature difference along 15 km upstream from the shortcut mouth. In addition, there is little variation in temperature throughout the year. Mean temperature is 26°C and mean daily maximum and minimum temperatures are 30°C and 22°C, respectively. the density difference influenced by changing temperature, therefore, can be ignored.

6.1.2 Pattern of Water Circulation During Rainy Season

From discussion of the previous section it is apparent that the Brantas estuary is highly stratified with a salt wedge during the rainy season. However, during this season, fresh water discharge is much larger than that during the dry season. The mean discharge during the rainy season is 301 m^3/sec (section 4.1.4) while the discharge limit that alters salinity distribution from well mixed to stratified category was found to be 20 m^3/s. Hence, the fresh water discharge will be much more dominant than tidal action and the estuary will be highly stratified during the whole of the rainy season. The tip of the salt wedge, which is located around KP.210 to KP.215 during the dry season, will be pushed down as far as the shortcut mouth or even behind it.

Since there are no measurements of the length of the saline wedge, the approximate location of the saline wedge during the rainy season will be estimated by Keulegan's empirical formula (see equation 3-5). The sequential calculation was made as follows. On the basis of figure 5.6, the relationships between water elevation and cross sectional area

at KP.250, the river mouth, were found. In order to get the mean length of the saline wedge, the mean discharge during the rainy season was evaluated under various tide conditions: spring tide, mean flood tide, and neap tide. In table 5.1, the water elevation at the three conditions above are given as +0.385, -0.010, and -0.385 m,SHVP, respectively. Water depth (d) and cross sectional area were obtained from figure 5.6. Then, by using equations 3-6 to and 3-8, the length of the wedge was found. Results are presented in table 6.2.

Table 6.2 Estimation the Length of the Saline Wedge

Data :
River discharge : 301 m^3/sec
Mean temperature : 29 °C
Salinity of sea water : 32 ppt
Density of salt water (ρ_s) : 1020 kg/m^3
Density of fresh water (ρ_f) : 1000 kg/m^3
$\Delta\rho = \rho_s - \rho_f$ = 20 kg/m^3
Average density $=(\rho_s-\rho_f)/2$ = 1010 kg/m^3

Tide condition	Spring Tide	Mean Tide	Neap Tide
Elevation (m,SHVP)	+0.385	-0.010	-0.385
Water depth (m)	3 985	3.590	3.215
Cross area (m^2)	751 6	632.6	528.5
Fresh w.velocity(V_r=m/s)	0.400	0.476	0.570
Densimetric vel.(V_d=m/s)	0 88	0.83	0.79
Densimetric Froude number ($F_d = V_r/V_d$)	0.457	0.572	0.724
Densimetric Reynolds number ($R_d = V_d d/\nu$)	4268415	2649772	3093111
Intrusion length / water depth (L_A/d)	332	181	96
Intrusion length (L_A=m)	1321	723	384

KP.250 is located 1 km from the actual river mouth, so the mean of the intrusion length should be located between 1.4 to 2.3 km upstream from the river mouth. Two important things should be noted. The tip of the wedge may be moved seawards from the

river mouth to reach an equilibrium length if the fresh water discharge is higher than 301 m^3/s. Also, Keulegan's formula was derived originally from extensive laboratory measurements on straight rectangular channels. However, natural forms of the channel, as well as meanders, will reduce the velocity of both river and tidal current. That should be considered to be a correction factor but more field measurements are needed to get an exact formula. Ozturk (1970), as quoted in Silvester, R.(1974), has derived an empirical relationship based on Keulegan's formula (1966) for an estuary in Norway and on the Mississippi River where tidal action is negligible. The formulae are given by

$$\frac{L_A}{d} = 6.018\,(R_d)^{0.82}\,(F_d)^{-5/2}$$ For the Mississippi River **(6-1)**

$$\frac{L_A}{d} = 1.062\,(R_d)^{1/4}\,(2F_d)^{-5/2}$$ For an estuary in Norway **(6-2)**

Keulegan's formula is likely to be suitable for the Brantas river if the densimetric Froude number (F_d) is higher than 0.16 or the fresh discharge is higher than 105 m^3/s. Determination of these factors were based on the measurements taken during the dry season of 1991 as mentioned in section 6.1.1. It was found that the mean intrusion length (L_A) reaches about 9 km from the river mouth on the mean river discharge of 63 m^3/s and the circulation is still highly stratified. Therefore, the formula should be applicable to that condition. Attempts were made to fit the Brantas river to the form of the formulae shown in tables 6.2 and 6.3. Calculations based on measured discharges (105 and 63 m^3/sec) and associated measured elevation are shown in table 6.3. Cross sectional areas were

calculated from figure 5.6 and various constants in Keulegan's formula were tried in an attempt to obtain agreement between measured and calculated values of the intrusion length. The best approximation gave the formula as

$$\frac{L_A}{d} = 1.435 (R_d)^{1/4} (2F_d)^{-5/2} \qquad \textbf{(6-3)}$$

This formula is suitable for the Brantas River if the densimetric Froude number (F_d) < 0.16 and fresh water discharge (Q_f) lies between 63 and 105 m^3/s.

Table 6.3 Estimation of the Length of the Saline Wedge for Determination of Suitable Limits of Densimetric Froude Number and Discharge, and Keulegan's Factor

Data :		
Condition : Mean High Water		
Elevation : -0.010 m,SHVP		
Mean temperature : 29 °C		
Salinity of sea water : 32 ppt		
Density of salt water (ρ_s) : 1020 kg/m^3		
Density of fresh water (ρ_f) : 1000 kg/m^3		
$\Delta\rho = \rho_s - \rho_f$ = 20 kg/m^3		
Average density $=(\rho_s-\rho_f)/2$ = 1010 kg/m^3		
Discharge	105.00	63.00
Water depth (m)	3.590	3.590
Cross area (m^2)	632.6	632.6
Fresh w.velocity(V_f=m/s)	0.166	0.120
Densimetric vel.(V_d=m/s)	0.83	0.83
Densimetric Froude number ($F_d = V_f/V_d$)	0.200	0.120
Densimetric Reynolds number ($R_d = V_d d/\nu$)	3649772	3649772
Intrusion length / water depth (L_A/d)	2524	2234
Intrusion length (L_A=m)	9062	8020
L_A from the River Mouth	10062	9020

The general inference can be drawn that the different factors in the Keulegan formula represent the difference of the relative force between tidal and river currents

including all variables involved, such as geometry, density, velocity and friction. For various water discharges during the rainy season, especially if the fresh water discharge is higher than 301 m^3/s, the intrusion will be located at a certain pseudo mouth seawards from the river mouth with varying degrees of turbulent development. This case will discussed in a following section (6.2.4).

6.2 The Sedimentation Pattern in the Estuary

As mentioned in the theoretical background and the previous section, sediment patterns in the estuary are mostly determined by the circulation pattern in the estuary. In this section, the estimated quantity of the sediment and river mouth processes and their effects will be presented.

6.2.1 Effects of Fresh Water Sediment Inflow

Sedimentation during the rainy season is mainly determined by the river discharge velocity distribution within the estuary. Part of the sediment will settle along the estuary, along the shortcut channel and the original river as well. Another part will be flushed directly to the sea-surf zone. The Brantas Project measured the annual sediment transport entering the estuary on two occasions (see section 4.2.2).

In 1966, the first observation was done. The measured sediment inflows before and after river improvements are shown in table 4.6. This showed that, after the river was improved, the rate of sediment discharge increased. This trend was apparent since

the energy gradient became steeper after the shortcut channel was completed. The dominant sediment inflow is suspended and wash load. Annual sediment inflow to the lower part of the river (41 through 48 km downstream from the New Lengkong Dam or 3 km upstream from the shortcut river mouth) is about 7,572,000 m^3. It consists of bed load around 0.14 %, suspended load 13.09 %, and wash load (diameter particles less than 0.1 mm) 86.77% .

In 1989, another investigation was carried out, also by the Brantas Project. This investigation was concerned only with the rate of the suspended sediment which mainly contributed to the depositional process within the estuary. The measurement showed that the annual suspended sediment transport was much larger than that of the previous investigation. The rate was found in table 4.6. The table showed that the volume of the suspended sediment passing KP.230 was 11.20 million m^3/year. This is at a location 46 km downstream from the New Lengkong dam or 5 km upstream from the mouth. The value means that the suspended sediment discharge rate is about 11.3 times the value of that which was estimated in 1966. If percentages of bed, suspended and wash load are taken in the same manner as the previous observation, the results can be summarized in table 6.4.

Table 6.4 Annual Sediment Rate

Section	Bed Load	Suspended load	Wash Load	Total Sediment
Annual S. Transport (1000 m^3)	123	11,200	74,250	85,573

The total sediment transport indicated in table 6.4 was used as a fundamental

inflow budget of the sediment to the estuary mouth and surf zone. Another result of sediment behaviour can be taken from table 4.7. Referring to Sugiura's opinion (see section 3.4.1), the scouring and depositional processes can be traced along the Porong river In the upper section, the suspended sediment inflow is about 20.5 million m^3/year. The sediment will settle between KP.30 and KP.80 in the amount of 4.1 million m^3/year, so the sediment particles passing KP.80 is about 16.1 million m^3/year. From KP.80 to KP 150, scouring happens and the sediment amount increases to 18.1 million m^3/year that is delivered to KP.150. Still, a part of the sediment is deposited along the estuary between KP.150 and KP.230. Finally, sediment that flows through KP.230, 5 km upstream from the river mouth is 11.2 million m^3/year. In summary, the percentage of the sediment settled along the estuary is about 45.36 % of the sediment inflow to the Porong River.

6.2.2 Dominant Discharge

During the rainy season, there is considerable fluctuation of water discharge through the Porong river. This fluctuation depends on the distribution of rain and on water management along the middle and upper reaches. As mentioned in chapter 2, part of the excessive discharge in the middle reach is flushed to the Indian ocean through the South Tulungagung channel (see figure 1.2) and the remaining flood discharge flows to the Porong River. The Porong River discharge varies from an average of 63.0 m^3/sec during the dry season to 1,466.0 m^3/sec in the maximum flood condition. This happened on April 7, 1986.

Dominant discharge in this case means the river discharge that provides the highest contribution to the annual sediment inflow. This can be obtained by the relationships between variations of water discharges and suspended sediment carrying capacity (see figure 4.7). The variation of water discharges must be evaluated throughout the year based on a sufficiently long record. Considering discharge data from 1977 through 1988 the duration curve can be found. This was illustrated in figure 4.8. The annual sediment rate can then be calculated by multiplying the sediment carrying capacity (S_q) and the duration of the discharge (D).

Dominant discharge can be obtained from two methods. The first uses the intersection between the duration curve and the sediment carrying capacity curve and then combines the result with the annual sediment curve as mentioned above. The process is illustrated in figure 6.1. The second method uses the following relationships

$$\bar{Q} = \frac{\Sigma(Q\ S_a)}{\Sigma S_a} \qquad (6\text{-}4)$$

Where, $\bar{Q}$ = dominant discharge (m^3/sec)

Q = discharge (m^3/sec)

S_a = annual sediment transport corresponding to each discharge (m^3)

The estimation of the dominant discharge is presented in table 6.5.

The dominant discharge is 711.62 m^3/sec and the duration is about 33 days per year.

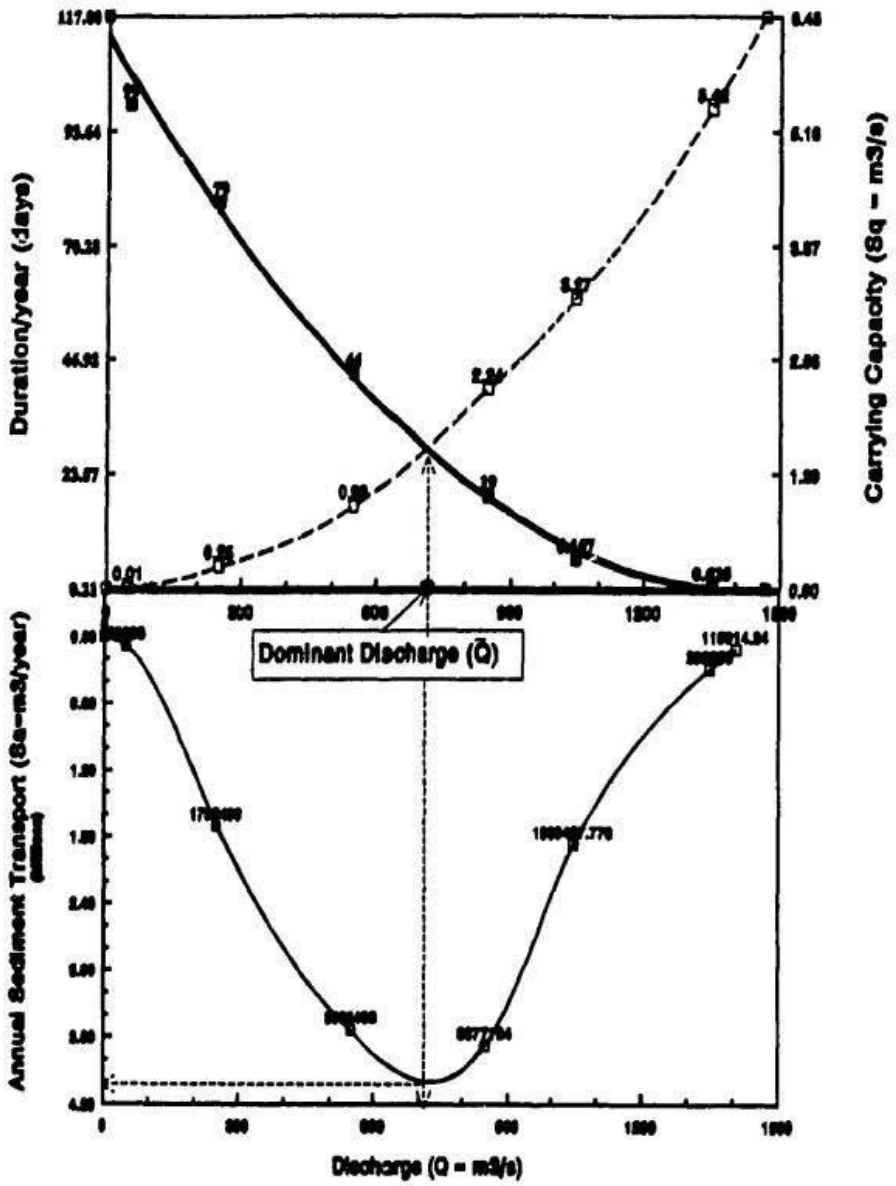

Fig.6.1 Relationships Between Duration, Discharge, Suspended Sediment Carrying Capacity and Annual Suspended Sediment Transport

Table 6.5 Estimation of the Dominant Discharge

Water Discharge Q_w=m³/s	Duration per year D=days	Sediment Carrying Capacity S_q=m³/s	Annual Sediment(S_s) $S_s=S_q \times D$ (m³)	
0	117	0	0	
50	99	0.01	85,536	
250	79	0.25	1,706,400	
550	44	0.93	3,535,488	
850	19	2.24	3,677,184	
1050	6.167	3.27	1,869,488	
1350	0.625	5.42	292,680	
1466	0.208	6.45	115,914	
Total:	365		11,282,690	
			Dominant Discharge(m³/sec):	711.

6.2.3 Effect of Tide and Its Currents

In the previous chapter discussion indicated that tidal currents causes the transportation of substantial quantities of estuarine sediments (see chapter 5). This is one matter that must be accounted for in a sediment budget within the Brantas estuary. Here, sediments are affected by the bidirectional flow of the tidal currents caused by the rise and fall of the water level, so the estimation of the budget should also consider the movement of sediment back and forth relative to any particular place. In section 5.2.1, the predicted net quantity of the suspended sediment at every observed station was discussed. Now, the actual sediment quantity during the flood and ebb tides will be calculated separately.

The quantity will be estimated by using a method developed for this thesis and called the integration method in a unit tidal range. This means that every stage during the

rise and fall of the tide is considered with regard to accumulation of the sediment. The calculation is based on the results of the field observations (see figure 5.7 and table 5.5) which show that the accumulation of the sediment during tidal rise and fall was the same at every measuring station. If a tidal range is used as a unit of the accumulation, either flood or ebb tidal range, the sediment discharges (Q_s) can be assumed to be a function of the tidal range (T_r) instead of the time period, hence $Q_s = F(T_r)$. This is primarily because the tidal range is related to the mean water discharge and mean current velocity (see table 5.11). Higher tidal ranges will produce higher mean water discharges and velocities. Both factors are also related to the quantity of the sediment discharge. Therefore, the integration method in unit tidal range is reasonable and appropriate.

The behaviour of the sediment discharge can be described as follows. In the beginning of a flood tide the sediment discharge increases gradually up to nearly one fifth of the tidal range. Then, from one fifth to one half of the tidal range, the concentration of sediment seems less than that in the previous stage. After that, around the one half stage, it increases markedly up to 80 % or 85 % of the tidal stage. Finally, the sediment concentration decreases during the remaining stage and throughout the slack water period. The behaviour is different during ebb tide. In the beginning of the ebb tide, the sediment discharge increases markedly and continuously up to about 30 % and 35 % of the tidal range. Then, it decreases gradually up to the ebb slack water period. Both conditions were observed at all stations so the magnitude is assumed to be valid for any flood or ebb tide.

The above explanation indicates that suspended sediment concentration is not

always linearly related to increasing velocity. To obtain a better understanding of this trend, the flood tide period is divided by four stages. The first stage represents the starting time up to one fifth of a flood tide period. The current velocity creates a bottom shear stress (τ_b) which exceeds the critical shear stress (τ_c) of the bottom material and erosion takes place from the surface of the bed. In the next stage, between 20 % through 50 % of the flood tide period, the current velocity increases gradually but the increase of concentration is less than during the first stage. This is because the cohesion of the sub surface layer of bottom material is higher than that of the surface layer, so a higher velocity is necessary to erode the particles below the top of the bed than the previous velocity needed to pick up unconsolidated material in the surface layer. Another possibility is that the diameter of the remaining particles is larger than that of the upper layer, so the critical shear stress in this layer (τ_c) is larger than that of the surface layer. A time delay will occur before the particles are actually suspended in the water. This delay is called scour lag. In the third stage, from one half to about 85% of the flood tide period, the velocity still increases and the bottom shear stress becomes much larger than the critical stress of the bottom material. Therefore, the shear stress can break the interparticle bond strength of the cohesive sediments and the sediment concentration increases gradually during this stage. In the last stage, from 85 % to the end of the flood period, the current velocity decreases continuously and the sediment concentration also decreases.

One important thing to be noted is that the sediment concentration is still rising for a short period after the current velocity begins to fall (see section 5.2.2). This

indicates that, when the minimum transport velocity is reached, the settling process is not fully established. The particles are moving as individual particles rather than groups of particles bonded together on the river bed. They stay in an equilibrium condition for a short period before the settling process is begun. This period is called settling lag.
In the ebb tide process, the current velocity increases rapidly after the starting period and continues to increase up to 25 or 30 % of the period. Then, the current will decrease gradually to the end of the ebb period. Unlike the sediment discharges during the flood tide, the sediment concentration seems to be proportional to the velocity distribution, except that settling lag also occurs during the time of decreasing current velocity. The sediment that just settled on the turn of the tide at high water will be resuspended easily by the ebb current. The sediment concentration will increase gradually up to a certain period after the current velocity begins to decrease and later the settling particles will be established.

Equation 3-41 indicates that the rate of erosion (E) will increase linearly with excess bottom shear stress (τ_b) given by $E = M (\tau_b - \tau_c)$, where M is the constant of the erosion rate. Based on the previous explanation, it can be inferred that the difference in critical shear stress (τ_c) between the surface and lower layers enables scour lag to occur and this coincides with the increasing bottom shear stress due to increasing current velocity. In addition, various factors may influence the erosion rate. These include, sediment composition and texture, temperature, salinity, bed structure, consolidation rate and many other factors. The three factors in equation 3-41 vary temporally and spatially.

To simplify the calculation, the quantity of sediment will be calculated on the

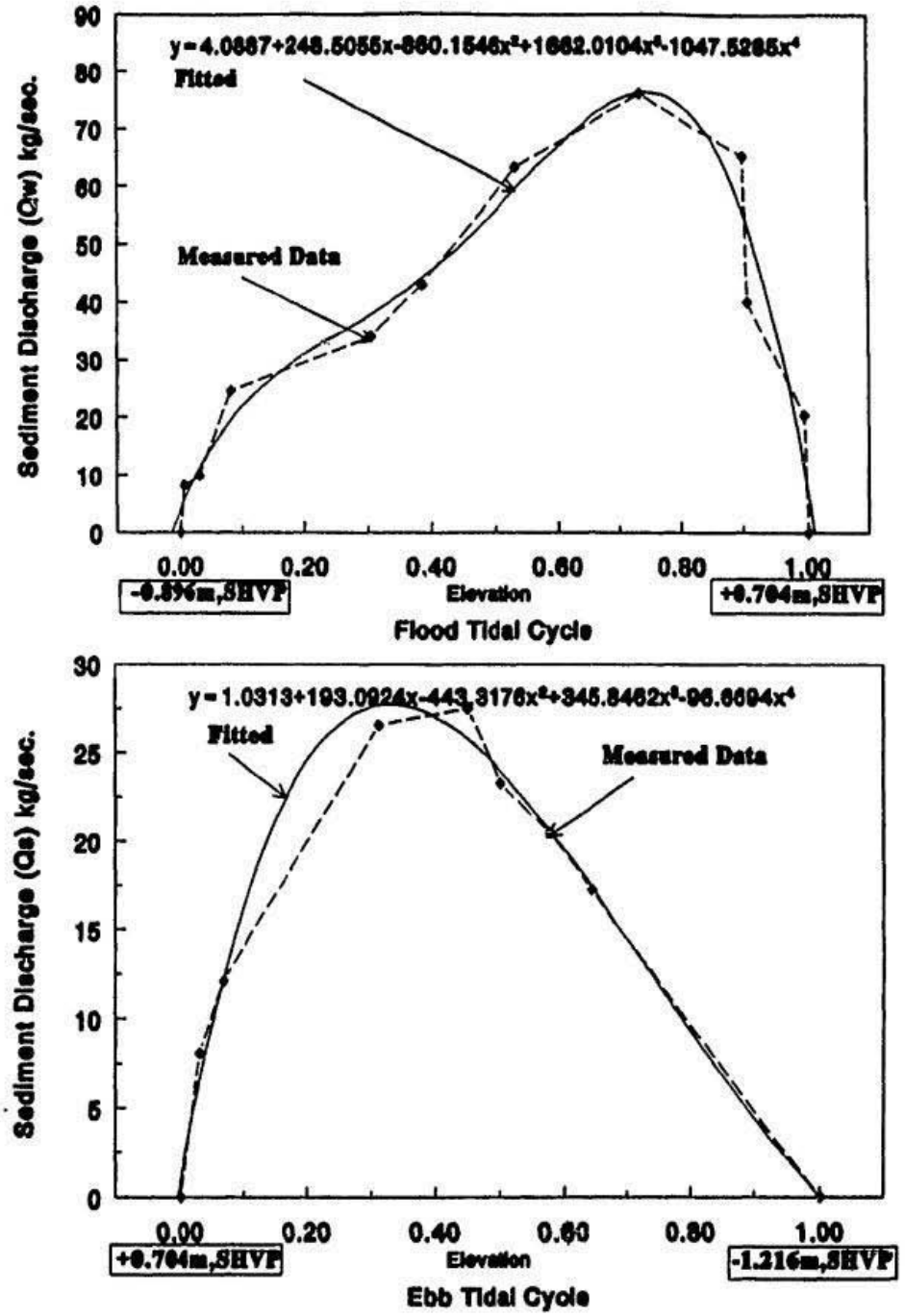

Fig.6.2 Phenomena of Suspended Sediment Discharge at KP.250 During a Tidal Cycle

basis of the entire sediment behaviour during a tidal cycle separately for rising or falling tide. The best approximate equation of the tide is a polynomial of the fourth degree (see figure 6.2). This equation was determined for every observed station by curve fitting. One of the samples is presented in figure 6.2 and the others can be found in appendix B figure B.1-1 to B.1-3. The integration of the equation represents the sediment discharge inflow and outflow due to tidal currents through the cross sectional area within a certain tidal range. Hence

$$S=\int Y\ d(x) \qquad 6\text{-}5$$

Where Y :instantaneous sediment discharge

x : time represents the tidal process

Using the equation given for the flood tide cycle in figure 6.2, as an example, this leads to the sediment discharge within the flood tidal range

$$S=\int_0^1 (4.0887+248.5055x-860.1546x^2+1662.0104x^3-1047.5285x^4)\,dx$$

S = 47.62 kg/sec ; for tidal range = 1.60 m. Then, the sediment volume can be found by multiplication between the sediment discharge (S) and the duration of the tide (D). Hence

$$V = S \times D \qquad 6\text{-}6$$

Similar methods can be used for calculating sediment volume within the ebb tide. Thus, for any tidal range, the quantity can be estimated by doing a direct comparison with the unit quantity. This is an appropriate method for calculating the net sediment entering the

estuarine area without considering the detail of various factors involved. However field observations are required to get a proper curve.

Table 6.6 shows the calculation of sediment volume through KP.250 using the above calculation. Volumes were calculated for every day, June 6 to July 12 1991 together with total and mean sediment inflow and also the mean bulk volume of the sediment. Similar tables for other stations can be found in appendix A, table A.5-1 to A.5-3.

As a final result, in figure 6.3, valuable curves can be produced based on table 6.6, to show the relationship between tidal range, sediment discharge and mean water discharge within the tidal volume. These curves are very useful for quickly estimating the quantity of net sediment entering the estuary on the tidal currents. On the Brantas estuary, this method can be made easily since the tidal type is a mixed diurnal having bimonthly spring and neap tides with approximately equal height (see figure 4.3). Similar curves at other locations not covered in this thesis can be developed using a short and inexpensive observation. This will permit sediment calculation to be made easily and will, therefore, provide guidance regarding channel maintenance.

Mean bulk volume of sediment presented in table 6.6 and appendix A, table A.5-1 through table A 5-3, will be used in the calculation of deposition or erosion of sediment along the shortcut channel throughout the year, so the general tendency for geometric changes along the channel can be known. This estimation will be explained in the following paragraph. It is important to note that this calculation is valid only if the fresh water discharge is lower than 20 m^3/sec where the circulation within the estuary is slightly

Table 6.6

Estimation of Sediment Transport through KP.250 &
Relatioships between Sediment Deposit, Tidal Range & Water Discharge
Recording period : From June 6, 1991 to July 12,1991

Date	Range		Duration		Mean Discharge		Sediment Discharge		Sediment
	Fall	Rise	Fall	Rise	Fall	Rise	Fall	Rise	Deposit
	m	m	hrs	hrs	m3/s	m3/s	Kg	Kg	Kg
June 6	0.54	0.43	6.0	4.0	43.90	44.37	102,866	184,290	81,424
	0.62	1.10	7.0	6.0	30.83	78.78	137,789	707,159	569,370
7	1.11	0.63	7.0	5.0	70.83	47.98	246,687	337,508	90,820
	0.56	1.12	6.0	7.0	34.30	77.98	106,676	841,519	734,844
8	1.24	0.69	7.0	5.0	87.23	54.69	276,023	369,651	93,628
	0.61	1.38	6.0	6.0	35.61	110.63	116,200	888,449	772,249
9	1.52	0.76	7.0	7.0	109.14	44.94	338,028	569,263	231,235
	0.63	1.53	5.0	5.0	47.65	161.31	100,008	820,733	720,725
10	1.66	0.83	8.0	7.0	116.09	51.71	422,131	622,514	200,384
	0.69	1.71	5.0	5.0	52.68	193.29	109,533	917,164	807,631
11	1.90	0.97	8.0	6.0	138.57	66.73	483,088	623,586	140,498
	0.77	1.79	5.0	5.0	58.27	205.22	122,232	960,022	837,790
12	2.00	0.98	9.0	6.0	131.56	71.35	572,048	630,015	57,967
13	0.76	1.80	4.0	6.0	77.85	175.70	96,516	1,158,455	1,061,939
	2.04	1.11	8.0	7.0	150.30	63.29	518,647	832,519	313,873
14	0.81	1.74	4.0	6.0	80.63	168.69	102,866	1,119,883	1,017,017
	1.96	1.05	8.0	6.0	141.10	74.09	498,074	674,373	176,299
15	0.70	1.60	5.0	6.0	63.41	153.50	111,120	1,029,881	918,761
	1.92	1.16	7.0	7.0	149.96	65.54	427,147	870,020	442,873
16	0.87	1.43	6.0	4.0	54.49	191.41	165,728	613,728	448,000
	1.67	1.08	8.0	6.0	111.05	77.42	424,671	694,302	269,631
17	0.74	1.25	5.0	7.0	64.44	84.15	117,311	937,522	820,210
	1.55	1.14	7.0	6.0	101.75	78.46	344,473	732,874	388,401
18	0.82	1.03	5.0	7.0	73.06	70.05	130,170	772,518	642,348
	1.31	1.14	7.0	6.0	81.84	84.90	291,136	732,874	441,739
19	0.89	0.63	5.0	7.0	85.03	44.58	141,282	472,511	331,229
	0.80	1.04	7.0	6.0	52.29	80.42	177,793	668,587	490,794
20	0.89	0.54	5.0	8.0	88.95	33.66	141,282	462,868	321,586
	0.67	1.09	6.0	5.0	46.44	93.58	127,630	583,942	456,312
21	1.10	0.61	6.0	7.0	83.42	39.75	209,541	457,511	247,969
	0.55	1.15	7.0	5.0	38.89	120.18	122,232	616,086	493,853
22	1.42	0.88	6.0	7.0	107.73	46.12	270,499	660,015	389,516
	0.60	1.21	7.0	5.0	33.93	121.50	133,345	648,229	514,885
23	1.57	0.98	6.0	7.0	128.99	54.95	299,073	735,017	435,944
	0.60	1.23	7.0	5.0	38.62	149.00	133,345	658,944	525,599
June 24	1.61	0.98	6.0	7.0	151.12	56.58	306,692	735,017	428,325
	0.62	1.31	7.0	5.0	39.17	157.90	137,789	701,802	564,013

(next page)

(Table 6.6 Continued)

Date	Range		Duration		Mean Discharge		Sediment Discharge		Sediment
	Fall	Rise	Fall	Rise	Fall	Rise	Fall	Rise	Deposite
	m	m	hrs	hrs	m3/s	m3/s	Kg	Kg	Kg
June 25	1.69	1.06	6.0	6.0	194.49	87.55	321,932	681,444	359,513
26	0.66	1.34	7.0	6.0	49.02	167.42	146,679	861,449	714,770
	1.75	1.07	5.0	7.0	245.56	76.18	277,801	802,519	524,718
27	0.67	1.42	7.0	6.0	50.59	181.03	148,901	912,878	763,977
	1.82	1.08	5.0	7.0	263.14	81.07	288,913	810,019	521,106
28	0.70	1.37	6.0	6.0	61.03	167.44	133,345	880,735	747,390
	1.72	1.03	6.0	7.0	204.63	73.55	327,647	772,518	444,871
29	0.71	1.31	6.0	5.0	59.07	180.87	135,249	701,802	566,553
	1.63	1.00	7.0	6.0	153.01	81.11	362,253	642,872	280,619
30	0.68	1.28	7.0	5.0	49.05	169.74	151,124	685,730	534,606
	1.55	0.90	7.0	6.0	140.65	77.12	344,473	578,585	234,111
July 1	0.63	1.17	7.0	5.0	47.10	147.05	140,012	626,800	486,788
	1.41	0.81	7.0	6.0	116.78	60.84	313,360	520,726	207,367
2	0.55	0.95	6.0	6.0	44.32	92.50	104,771	610,728	505,958
	1.12	0.70	7.0	5.0	92.33	69.85	248,910	375,009	126,099
3	0.52	0.73	7.0	6.0	36.52	78.55	115,565	469,297	353,731
	0.80	0.77	6.0	6.0	84.16	67.58	152,394	495,011	342,618
4	0.69	0.50	7.0	5.0	52.40	54.71	153,346	267,863	114,517
	0.53	0.83	7.0	6.0	45.93	86.66	117,788	533,584	415,796
5	0.80	0.60	6.0	6.0	85.42	53.91	152,394	385,723	233,329
	0.73	1.04	6.0	6.0	62.39	110.94	139,059	668,587	529,528
6	1.19	0.80	7.0	6.0	104.37	68.94	264,467	514,298	249,831
	0.61	1.09	6.0	7.0	54.20	103.43	116,200	817,519	701,319
7	1.35	0.93	6.0	6.0	141.19	77.87	257,164	597,871	340,707
	0.69	1.24	6.0	7.0	63.32	129.46	131,440	930,022	798,582
8	1.55	0.98	6.0	6.0	173.39	87.03	295,263	630,015	334,752
	0.67	1.30	6.0	7.0	63.00	133.08	127,630	975,023	847,393
9	1.61	1.00	6.0	6.0	183.37	86.42	306,692	642,872	336,180
	0.69	1.42	6.0	7.0	58.90	139.84	131,440	1,065,025	933,585
10	1.75	1.00	6.0	6.0	197.48	86.32	333,361	642,872	309,511
	0.70	1.57	6.0	7.0	62.07	161.83	133,345	1,177,527	1,044,183
11	1.88	1.02	6.0	6.0	220.14	85.00	358,125	655,729	297,604
	0.66	1.65	6.0	7.0	54.00	165.68	125,725	1,237,529	1,111,804
July 12	2.00	-	6.0	-	233.37	-	380,984	-	-
Total Suspended Sediment Inflow During 36.88 days (Kg)									33,793,096
Mean Sediment Inflow / day (kg/day)									916,299
Spesific Gravity = 2,600 kg/m3									
Volume of Sediment inflow (m3/day)									327
Bulk Volume = Volume of Particles /(1-Porosity)									
Porosity = 0.4									
Bulk Volume (m3/day)									545

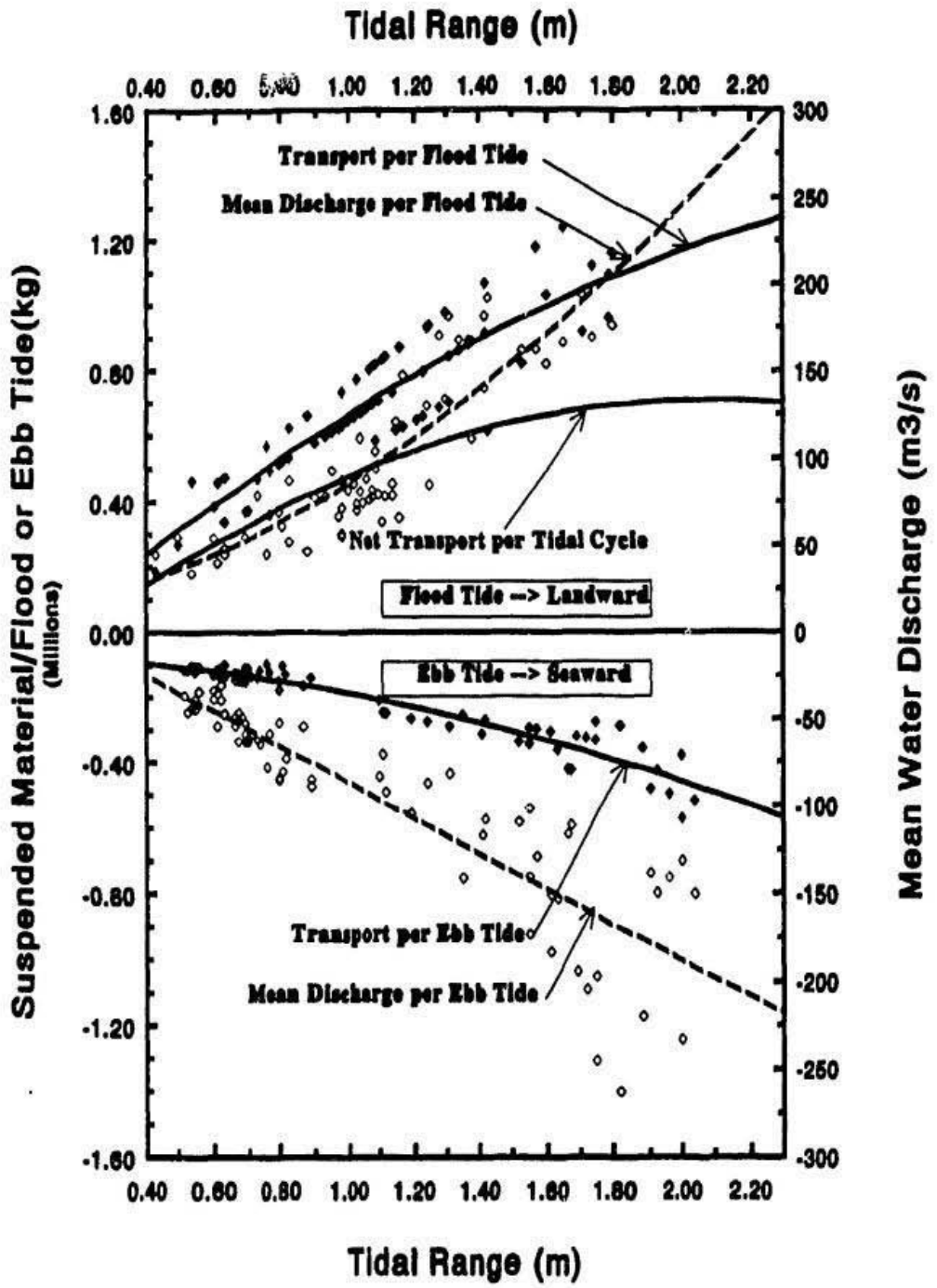

Fig.6.3 Suspended Sediment as a Function of Tidal Range and Water Discharge within Tidal Prism (at KP.250, Shortcut River Mouth)

stratified through well mixed and the tidal action is dominant.

Mean monthly discharges of the Porong river were presented in table 4.4. The data showed that mean discharges less than 20 m^3/sec commonly occur from June through November. From 144 events of monthly mean discharges inspection shows that 42 events are equal to or less than 20 m^3/sec. Thus, the probability of fresh water discharge being less than 20 m^3/sec is about 29.17 %. The result has been summarized in table 6.7.

Table 6.7 Probability Discharge on the Porong River

Discharge (m^3/sec)	Events	Probability (%)	Days per year
1 - 20	42	29.17	106
20 - 50	17	11.81	43
50 - 100	19	13.19	48
100 - 200	10	6.94	25
200 - 300	14	9.72	36
> 300	42	29.17	106

Using bulk volume of sediment found in table 6.6, and appendix A, table A.5-1 through A.5-3, the scouring and deposition per annum within the shortcut channel can be estimated. The result is presented in table 6.8 and the region of deposition is presented in figure 6.4.

Table 6.8 Deposition and Erosion within the Shortcut Channel and the Original River

Station	Suspended Sediment		Bed Sediment		Total	
	m^3/day	m^3/yr	m^3/day	m^3/yr	m^3/day	m^3/yr
KP.250	+545	+57750	+54.5	+5775	+600	+63525
KP.242	+451	+47806	+45.1	+4781	+496	+52587
KP.236	-34	-3604	- 3.4	- 360	- 37	- 3964
SB.5	- 1.3	- 133	- 0.1	- 14	- 1.4	- 147

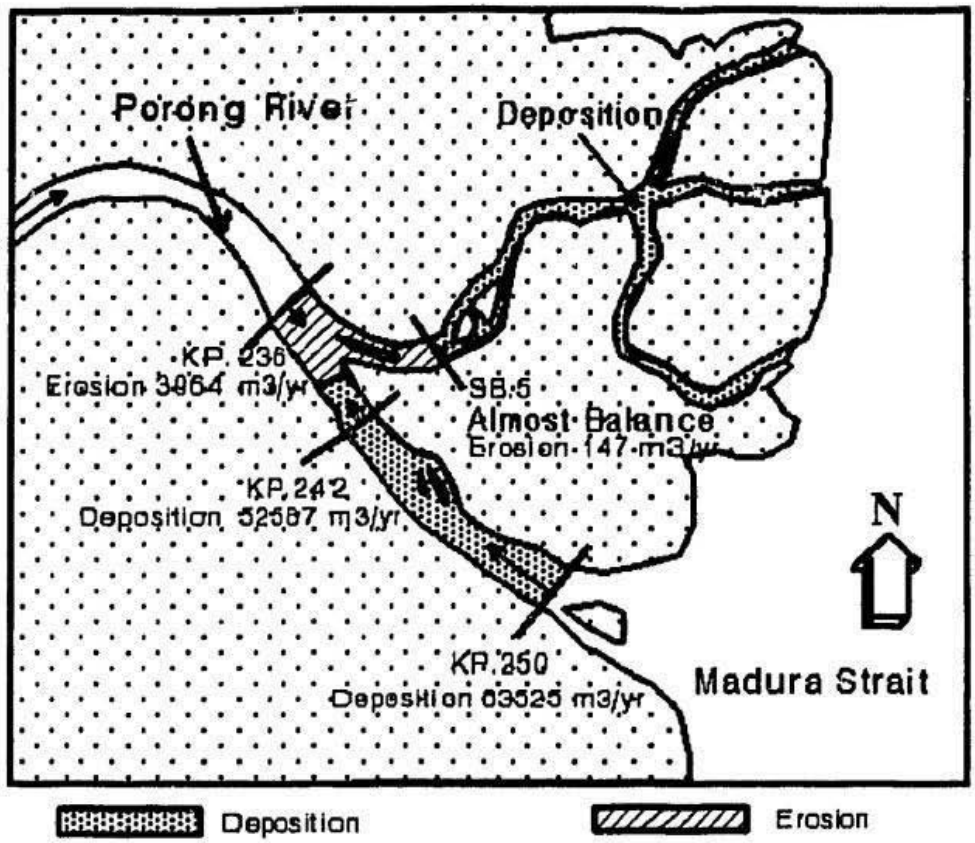

Fig.6.4 Area of Deposition and Erosion Because of Tidal Currents

6.2.4 Deposition within the Delta Area

Brief discussions about the Brantas-Delta growth have been presented in section 4.3.1. However, it is also important to know the actual quantity of sediment that has settled on the delta area. In order to obtain the real quantity, the best approximation is to make a comparison of geometric data of the delta between 1977, when the shortcut channel was made, and the recent geometric data. At the end of 1989, the Brantas Project

carried out a topographic measurement on the delta. Unfortunately, since the budget was limited, the measurement covered only 3.25 x 3.00 km. This area was located at the axis of the shortcut river mouth, 3.00 km parallel to the shoreline and 3.25 km perpendicular to the shoreline. The location is shown in figure 6.5. and the original copy of this measurement can be found in appendix B, figure B.5-1 through B.5-9. The area is divided

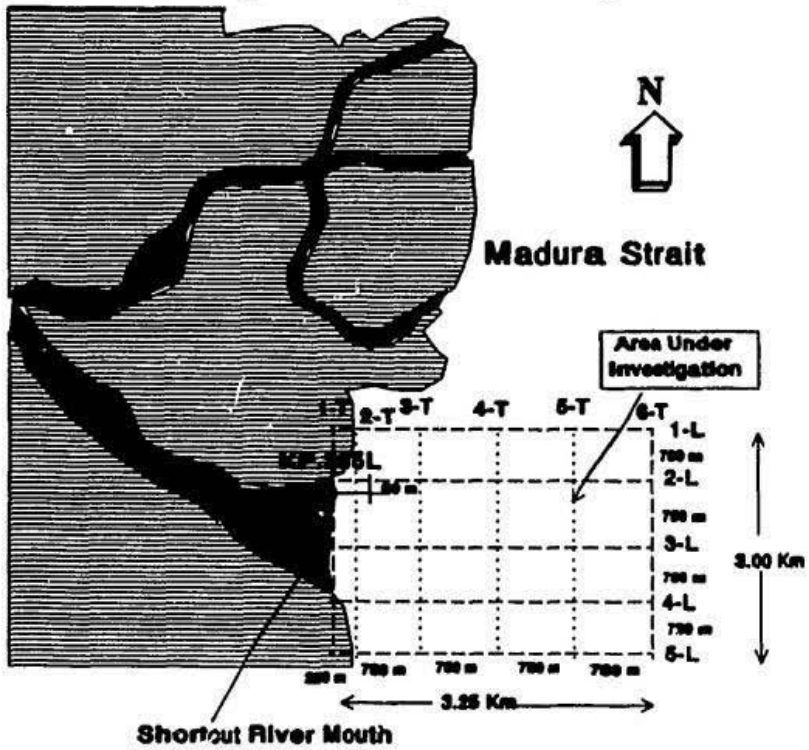

Fig.6.5 Investigated Area of Depositional Process within the Brantas Delta

into 5 lines that are perpendicular to the shoreline and 6 lines parallel to the shoreline. The arrangement is shown in figure 6.5. Longitudinal direction of lines are identified by L and transverse or parallel lines to the shoreline are identified by T. The elevations along every line in 1989 are compared to elevations measured in 1977 (see figure 2.6). The different elevations are illustrated in figure 6.6, for line 1-L and 2-L, and the

remaining lines can be found in appendix B, figure B.2. Based on the deposition within the investigated area (3.25 x 3.00 km), the total volume can be found. Deposition per km^2 can be determined easily by the total volume divided by the area under investigation. Finally, the mean increment of the delta in front of the shortcut mouth can be estimated by the mean deposition per area divided by time (1977 to 1989). The result is 23.7 cm/year (see table 6.9).

Table 6.9 Estimation of Mean annual Deposition on the Brantas Delta

Area under investigation : 3 x 3.25 km = 9.75 km^2				
Line	Area(m^2)	Average(m^2)	Distance(m)	Volume(m^3)
1-L	9492.89			
		8425.61	750	6319207.5
2-L	7358.33			
		9810.46	750	7357841.3
3-L	12262.58			
		11047.30	750	8285475.0
4-L	9832.02			
		7670.05	750	5752533.8
5-L	5508.07			
Total volume of the deposition : 27715057.5 m^3 Volume per area : 2842570.0 m^3/km^2 Annual volume of the deposition : 236880.8 m^3/km^2/year Mean annual increment on the delta: 23.7 cm/year				

To determine the volume of active sediment within the surf zone during these years, longitudinal and lateral limits of the subaqueous buffer zone are required. According to section 5.3.2, the seaward limit of significant transport was about 5.10 km from the low water level (LWL) or 7.35 km from the shore. The lateral limits were estimated by evaluating topographic and aero-photo maps. The limit was found to be about 9.3 km ; 3.6 km at the south side and 5.7 km at the north side of the shortcut central axis. The area of the active delta is calculated by taking the mean distance from

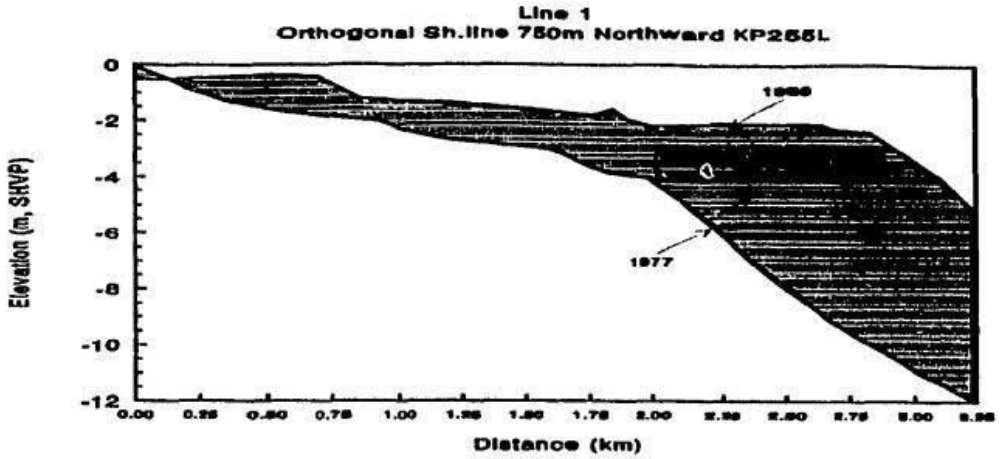

Fig.6.6-1 Longitudinal Deposition of the Brantas Delta (1977-1989), Line 1-L

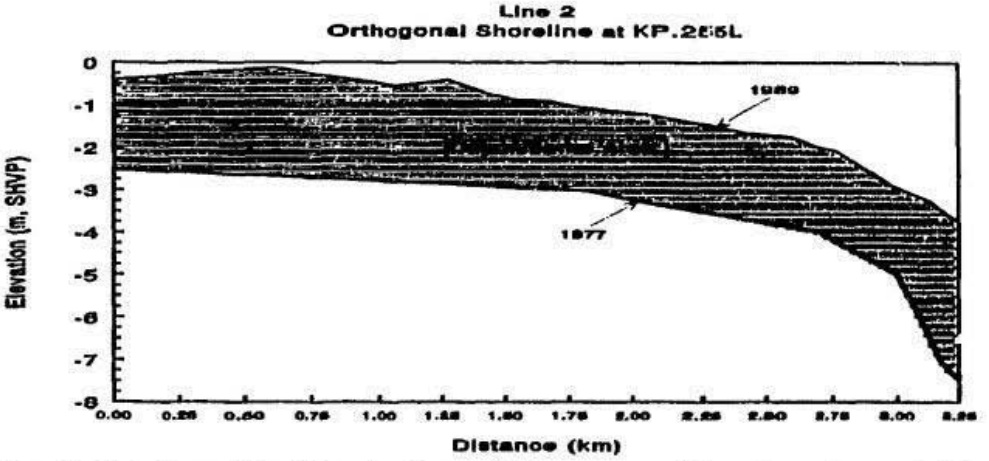

Fig.6.6-2 Longitudinal Deposition on the Brantas Delta (1977-1989), Line 2-L

the sea limit to the shoreline along the transverse width with about 0.5 km distance between two lines and then multiplying by the transverse distance. The estimation is illustrated in figure 6.7 where the mean distance from the sea limit to the shoreline was about 7.08 km. Hence the area of active sediment is 65.84 km^2.

If the deposition is assumed to be distributed evenly over the area, the mean deposition found in table 6.9 (0.237 m/year) can be applied. Finally, the total volume of

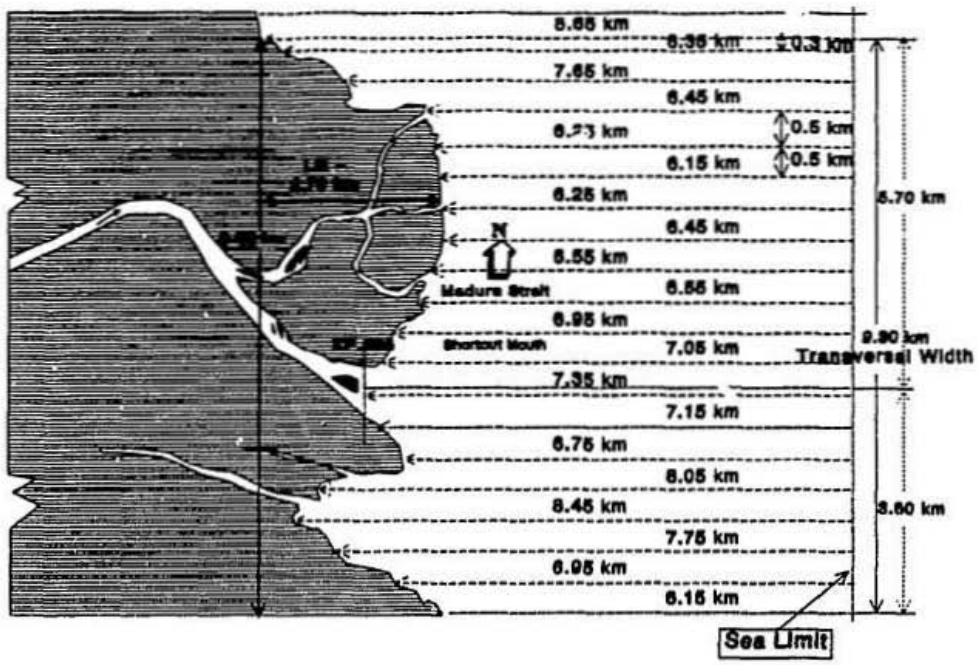

Fig.6.7 Estimation of Active Sediment Area for Determining Mean Annual Deposition on the Delta

the deposition within the subaqueous buffer zone will be 15,605,000 m^3/year. This amount is a valuable factor of the sediment budget within the estuary.

6.2.5 River Mouth Processes and Shoreline Geometry

This section deals with the distribution of sediment within the area surrounding the shortcut mouth. An evaluation of shoreline geometry is made related to the relative strengths of fluvial and marine forces. As mentioned in section 3.5.3 sediment distribution and shoreline configuration can be expected to reflect morphologic patterns and dominant forces that primarily determine the delta formation.

To evaluate the effluent mechanism of the fresh water discharge, the nature of the flow (i.e laminar, turbulent, transition) for any given discharge within the mouth should be known. In section 6.2.2, it was shown that the most significant contribution of sediment to deposition within the estuary and the delta is obtained mainly from the dominant discharge (712 m^3/sec). Thus, the condition of the flow will be examined under that discharge. A critical condition of the fresh water flow at the entrance occurs if the densimetric Froude number is equal to one (F_d = 1). A calculation similar to that mentioned in section 6.1.2 can be made. However, in this case, the fresh water discharge is obtained by trial and error using discharges for which F_d will be equal to 1. The interface height (h_0) is calculated by equation 3-9. Based on the three conditions of tides; spring, mean and neap tide, the discharges were found to be 685.5, 526.0 and 416.0 m^3/s, respectively (see table 6.10). Two important things should be pointed out from the table: when the fresh water velocity is equal to the densimetric velocity (given by eq. 3-7), the height of interface from the bed (h_0) is very small relative to the water depth (d). It can, therefore, be neglected and it can be assumed that the fresh water depth is dominant within the entire depth and no density contrast (homopycnal) occurs. The second thing is that the three discharges were found to be less than the dominant discharge (712 m^3/sec) for which the flow is turbulent. This condition (i.e turbulent flow at dominant discharge) will be examined by using the Reynolds number in the following paragraph.

Table 6.10 Estimation of Fresh Water discharge for Densimetric Froude Number =1

Data :
Fresh water discharge : various
Mean temperature : 29 °C
Salinity of sea water : 32 ppt
Density of salt water (ρ_s) : 1020 kg/m^3
Density of fresh water (ρ_f): 1000 kg/m^3
$\Delta\rho = \rho_s - \rho_f = 20$ kg/m^3
Average density $= (\rho_s - \rho_f)/2 = 1010$ kg/m^3

Tide condition	Spring Tide	Mean Tide	Neap Tide
Elevation (m,SHVP)	+0.385	-0.010	-0.385
Water depth (m)	3.985	3.590	3.215
Cross area (m^2)	751.6	632.6	528.5
Fresh w.discharge(m^3/s)	658.5	526.0	416.0
Fresh w.velocity(V_r=m/s)	0.876	0.832	0.787
Densimetric vel.(V_d=m/s)	0.88	0.83	0.79
Densimetric Froude number (F_d= V_r/V_d)	1.000	1.000	1.000
Height of interface/ /water depth (h_0/d)	0.003	0.003	0.003
h_0 (from the river bed = m)	0.011	0.011	0.010

As mentioned in the explanation of equation 3-54, the jet structure will be controlled by the ratio of inertial to viscous forces indexed by the Reynolds number. In order to check the value of Reynolds number with respect to the dominant discharge, the mean velocity of fresh water at the entrance (KP.250) should be estimated. Since the dominant discharge is higher than that for the critical condition of the flow, the mean velocity in such a condition is influenced purely by the fresh water discharge regardless of the tidal elevations. The calculation can be made as follows.

The first step is that the relationship between water elevation (h) and the water

area (A) for KP.250 should be expanded by the relationships between water elevation and hydraulic radius (R) given by the ratio of area (A) to wetted perimeter (P). The result is presented in figure 6.8.

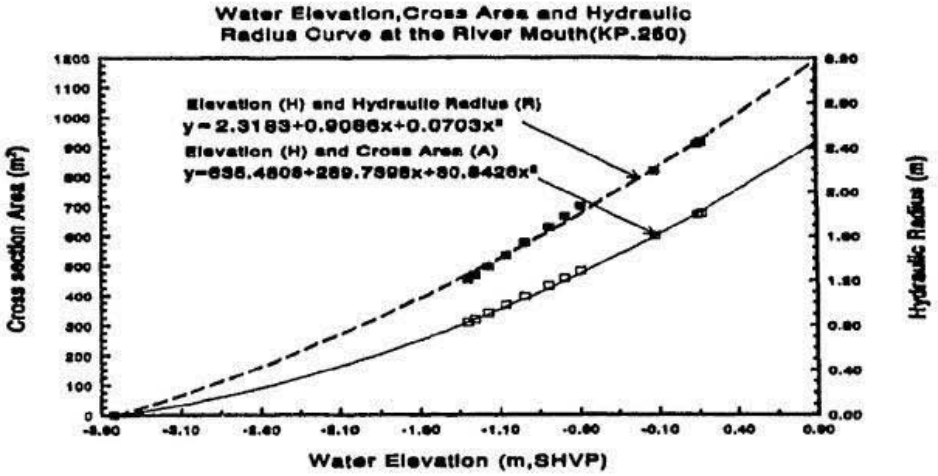

Fig.6.8 Relationships Between Water Elevation, Cross Area and Hydraulic Radius at KP.250

The second step is that other hydraulic factors at the station should be known. Those are the width of the channel (b), mean gradient of the river bed (S_0) and the Manning's roughness coefficient (n). The width of the channel and the mean gradient can be taken directly from the previous data, see table 6.1 and table 5.3. They were 253 m and 0.00029 respectively. The roughness factor (n) was observed by the Brantas experts in 1966 and 1990 (Design Calculations on the Kali Porong Project, 1966, and Porong River Rehabilitation Project, Design Report, 1990). They calculated n on the basis of water level data at two stations, Permisan and Porong station shown in figure 4.4. The calculation was started from the Permisan station by using gradually varied flow theory and the result was then compared to the actual water level of the Porong station at the same time. The result showed that the best approximate value of n was 0.025.

The final step is to calculate the velocity at the dominant discharge by using the Manning equation (Chadwick and Morfet, 1986). It can be given by

$$V = 1/n\ R^{2/3}\ S_0^{1/2} \qquad \textbf{(6-7)}$$

Where V = velocity (m/sec)

R = hydraulic radius (m)

S_0= bottom gradient of the channel

Since the known factors are the dominant discharge (Q = 712 m^3/sec) and S_0 = 0.00029 (see table 5.3), so a graphic showing relationship between water depth (y) and K, given by $Q/S_0^{1/2}$, can be made by using data in figure 6.8. The graph is presented in figure 6.9. For a value of K = 41,810 , the water elevation will be -0.086 m, SHVP. The results are summarized as follows:

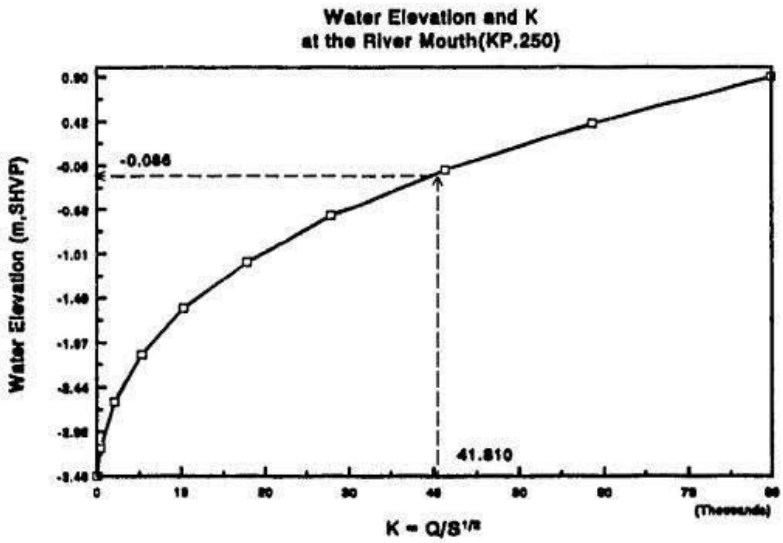

Fig.6.9 Graphic Relationship Between Water Elevation and K at KP.250

- Water elevation (h) : - 0.086 m,SHVP
- Water depth (d) : 3.51 m

- Hydraulic radius (R) : 2.24 m (using fig.6-8)

- Cross section area (A): 610.79 m^2(using fig.6-8)

- Velocity (V) : 1.17 m/sec

- Reynolds number (R_n): 30,048,729 (using equation 3-54) This shows that the Reynolds number of 3,000 is greatly exceeded, so the flow condition in that discharge will be fully turbulent.

To evaluate the condition of the flow (i.e laminar or turbulent or transitional, downstream from KP.250, an evaluation should be made for each of the fixed sections that have been shown in figure 6.5. Along the river section between KP.250 and KP.255, the lateral expansion of the turbulent flow is examined based on the geometry. This indicates that the funnel shape of the channel is established by the turbulent flow along the region which is dominated by the velocity of the fresh water discharge. There are two important geometric factors to be recognized; the width of the channel and the form of the cross sections (see figures 6.10-1 & 6.10-4). The width of the channel at KP.250 and KP.255 is about 253 m and 940.8 m, respectively. This is the largest difference in channel width over only 1 km distance and significant sediment deposition was found around KP.255. Without any maintenance work the depositional process seems to be continuous throughout the year. The different width along the channel represents the rate of jet expansion (ϵ) which is equal to $d(b/2)/d_x$ (see eq. 3-57), where x represents the distance between KP.250 and KP.255 (1 km). The variation in half width of the channels can be found in figure 6.11. The value of ϵ at the Brantas river mouth is given by

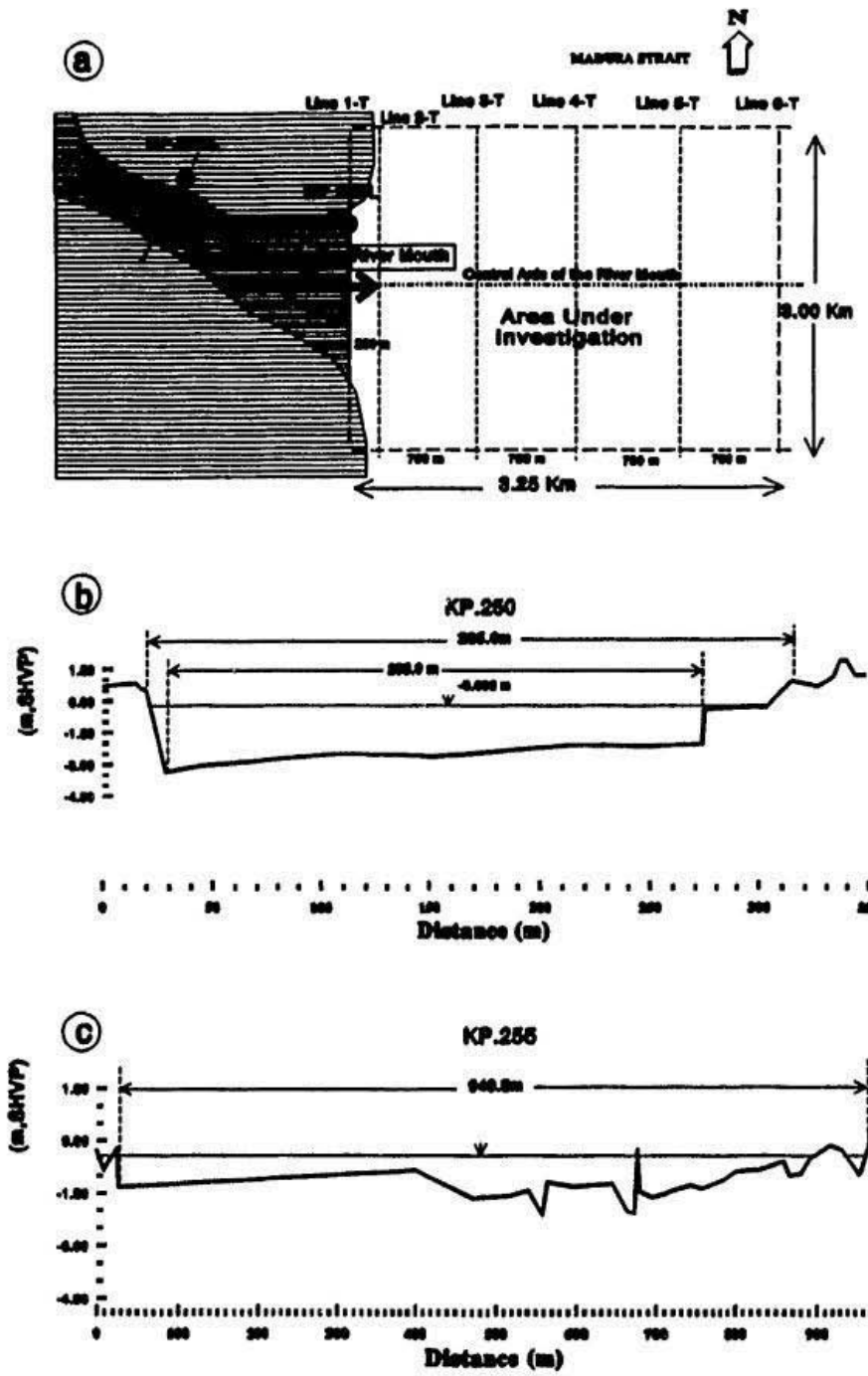

Fig.6.10 1.Schematic Plan of the Brantas River Mouth;
2.Cross Section of KP.250 (1 km of the Mouth)
3.Cross Section of KP.255 (at the River Mouth)

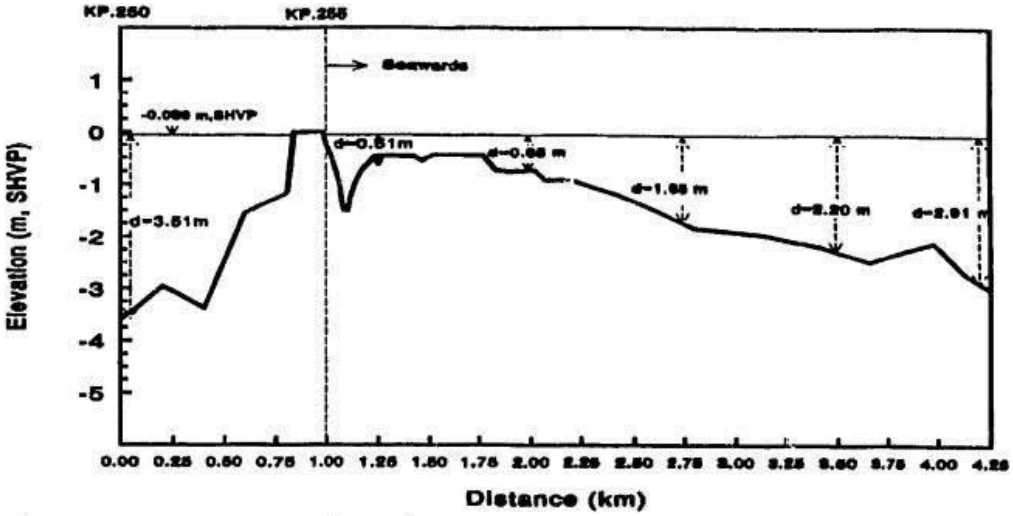

Figure 6.10-4 Longitudinal Section of the Brantas River Mouth from KP.250 to 4.25 Km Seaward

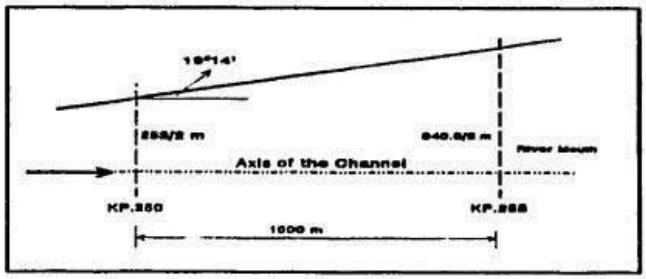

Fig.6.11 Variation in Half Width of the River Mouth

$$\varepsilon = \frac{d[(b/2)]}{dx}$$

$$\varepsilon = \frac{(940.8-253)/2}{1000}$$

Hence, the value of ϵ shall be 0.344. This means that the angle of separation between the centreline and the jet boundary will be approximately 19°14'.

Referring to equation 3-58, the maximum (U_{max}) velocity within a turbulent flow will experience a progressive longitudinal decrease inversely proportional to ϵ. Maximum velocity is also influenced by the integral of the similarity function for transverse velocity

distribution (I). Bates (1953) suggested a value of 0.316. The distance x in equation 3-58 may be taken as 1000 m. The maximum velocity at KP.255 will be about 1.36 m/s. It is a little bit higher than the mean velocity of KP.250 (1.17 m/s) but on average, the velocity along the section can be assumed to be equal and it is recognized as a zone of flow establishment. Turbulent eddies may be developed around KP.255 and a longitudinal diminished velocity occurs in the downstream area of this section. In such a condition, friction effects should normally be considered. However since the area of KP.255 is still dominated by fresh water and there is no density stratification, the latter factor can be neglected. By using the result of the previous section, the lateral expansion of the Brantas mouth under the dominant discharge will now be estimated.

The following paragraph discusses the condition of the flow, especially the lateral expansion of the flow within the area downstream of KP.255. This area is a zone of established flow and is divided into five main sections: KP.255+250 m, KP.255+1 km, KP.255+1.75 km, KP.255+2.5 km and KP.255+3.25 km (see figure 6.10.a). The estimation of KP.255+250 m is presented in table 6.11. The table shows that the velocity decreases markedly between KP.255 and KP.255+250 m. It will influence the tractive force upon the sediment. Coarse particles begin to settle in this region. The table also shows that the densimetric Froude number (F_d) is almost equal to 1. This infers that the turbulent flow decreases and buoyant expansion prevails. Therefore, beginning from KP.255+250 m seaward the evaluation will be applied to the buoyant principal as

Table 6.11 Estimation of Condition and Lateral Expansion of Flow within KP.255 and 250 m Seaward

Section : KP.255 -> KP.255 + 250 m
Data :
River discharge (Q) = 712 m^3/s
River mouth width, KP.255, (b_0) = 940.80 m
Mean depth at the mouth (d_0) = 1.10 m
Velocity at the mouth (U_0) = 1.36 m/s
Chezy coefficient (C) = 45.76 $m^{0.5}/s$
$K = g/C^2$ = 0.048 m/s
Average depth along this section = 0.92 m
The depth of KP.255+250 m = 0.51 m

Description	Estimation	Remark
Vel.at the mouth/Vel at KP.255+250 m (U_x/U_0)	0.29	Eq.3-54
Vel.at KP.255+250 m (U_x = m/s)	0.40	
Densimetric Froude- number at KP.255+250 m (F_d)	1.10	Eq.3-50
Rate of expansion (ϵ)	0.344	Previous paragraph
Width at KP.255+250 ($b_x = 2 \times b_0 \times 250 \times \epsilon$) m2	1,113	

Table 6.12 Estimation of Expansion Lateral Between KP.255+250 m to KP.255+3.25 km Using Buoyant Principal

Section : From KP.255 to boundaries stated below
Data :
Width of the mouth (b_0) = 940.8 m
Water discharge (Q) = 712 m^3/s
W.depth at KP.250+250 m = 0.51 m

Description	KP.255+ 1 km	KP.255+1. 75 km	KP.255+2. 5 km	KP.255+3.25 km	Remarks
B_e	0.41	0.41	0.41	0.41	Eq.3-61
a	0.0003	0.0003	0.0003	0.0003	Eq.3-60
h_x'/h_0'	0.83	0.75	0.68	0.63	Eq.3-59
h'(m)	0.43	0.38	0.35	0.32	
b_x/b_0 .	1.2	1.34	1.47	11.60	Eq.3-58
b_x (m)	1,129	1,260	1,384	1,504	

mentioned in section 3.5.2. The result is given in table 6.11.

Reference is now made to the investigations which have been done by Wright and Coleman (1971), namely that the configurations of shoreline and geometric form can reflect the morphological process of the delta regarding the relative importance of marine and river forces. On the basis of the results, the configuration of the shoreline and the

delta geometry of the Brantas will be examined.

The first factor to be examined is the crenulation index (C_i) which is a ratio of the shoreline length (L_s) to delta width (W) i.e $C_i = L_s/W$ (see equation 3-72). The width of the delta was obtained from figure 6.7 and is equal to 9.3 km. The shoreline length can be found by a measurement on a topographic map made by the Brantas Office in 1989 on the basis of an aerial photo map made in 1985. The result was 15.9 km and hence, the crenulation index is 1.67.

The second factor of the shoreline configuration is the protrusion index (P_i) as mentioned in equation 3-71. It is the ratio of the protrusion length (L_m) which is normal to the shoreline and the delta width (W). The protrusion length can be taken also from the topographical map. A schematic map has been introduced in figure 6.7 and the value of L_m was shown to be 2.7 km and the width (W) was 9.3 Km. Hence, the value of P_i is 0.29.

The next two factors to be examined are factors that deal with the geometry of the deposition within the delta. They are called the skewness index (S_k) and subaqueous hypsometric integral (HI). A detailed explanation of these factors can be found in section 3.5.3, equation 3-73 and 3-74. Basically, the skewness index will represent the distribution of sediment either to the right or left hand side of the river mouth. It will also reflect a dominant direction and influence of the longshore drift. The subaqueous hypsometric integral (HI) indicates the relative strength between marine and river forces. If the marine forces are dominant, the form of deposition of the delta front will be concave but if river forces are dominant, the delta front will be convex. The main reason for this is that the volume of sediment inflow to the delta area is large relative to the

available marine forces to rework the particles, and therefore, the accumulation of sediment will happen mainly on the delta front area to built a convex form.

Based on the topographical map of the delta area mentioned in appendix B, figure B.5-1 through figure B.5-9, both forces will be evaluated. Since the subaqueous hypsometric integral is focused on the delta front, the estimation is made only for certain boundaries that can reflect the configuration of the delta front. The boundaries are illustrated in figure 6.12 and a copy of the original contour map can be found in appendix B, figures 5-1 to 5-9.

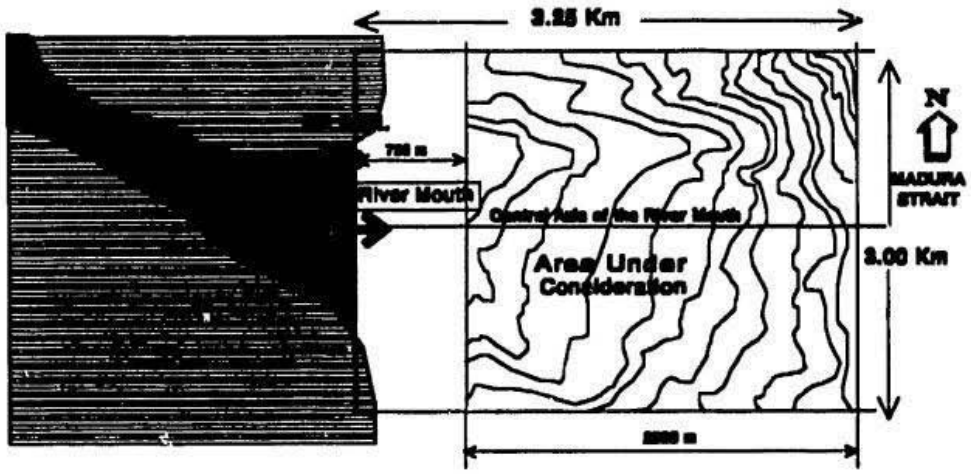

Fig.6.12 Area Under Consideration for Determining Subaqueous Hypsometric Integral of the Brantas Delta

The estimation is made based on the different volume of deposition in every 0.25 m increment beginning from elevation -4.50 m to -0.50. The volume in every layer represents a contribution to the entire form of the deposition and the total contribution will indicate the form of the delta front. If the value of the hypsometric integral, HI, is more than 0.5 the form is dominantly convex and if it is less than 0.5 the form is concave. In fact, the result is 0.642 (see table 6.13) and an inference can be drawn that

the river forces are more dominant than the marine forces through out the year.

For an evaluation of the skewness index, the volume of sediment within the area considered will be calculated on the basic reference of the different elevations between 1977 and 1989. To get an accurate estimation, the area is divided into segments, see figure 6.5, on longitudinal and transverse directions. Drawings of the longitudinal

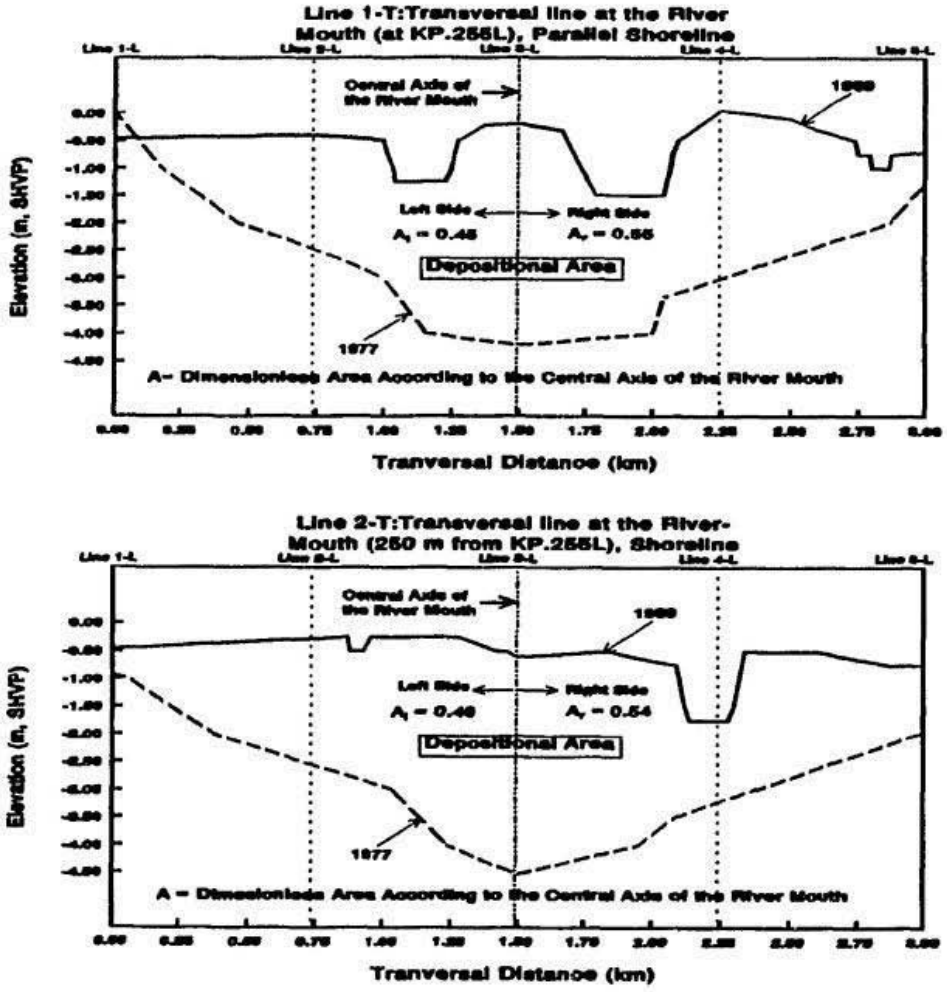

Fig.6.13 Transversal Sections of the Brantas Delta

Table 6.13

Estimation of Subaqueous Hypsometric Integral (HI)

No.	Elevation (m, SHVP)	Area (a= m2)	Average Area (m2)	Vertical Distanc (z= m)	a.z (m3)	HI a.z/A.Z
1	-0.50	127,760				
			308,627	0.25	77,157	0.003
2	-0.75	489,493				
			716,703	0.25	179,176	0.006
3	-1.00	943,913				
			1,361,305	0.25	340,326	0.012
4	-1.25	1,778,697				
			2,178,537	0.25	544,634	0.019
5	-1.50	2,578,377				
			2,967,161	0.25	741,790	0.026
6	-1.75	3,355,945				
			3,661,305	0.25	915,326	0.032
7	-2.00	3,966,665				
			4,258,137	0.25	1,064,534	0.037
8	-2.25	4,549,609				
			4,806,185	0.25	1,201,546	0.042
9	-2.50	5,062,761				
			5,336,041	0.25	1,334,010	0.047
10	-2.75	5,609,321				
			5,889,257	0.25	1,472,314	0.052
11	-3.00	6,169,193				
			6,460,409	0.25	1,615,102	0.057
12	-3.25	6,751,625				
			6,858,437	0.25	1,714,609	0.060
13	-3.50	6,965,248				
			6,986,848	0.25	1,746,712	0.062
14	-3.75	7,008,448				
			7,023,248	0.25	1,755,812	0.062
15	-4.00	7,038,048				
			7,062,528	0.25	1,765,632	0.062
16	-4.25	7,087,008				
			7,093,728	0.25	1,773,432	0.062
17	-4.50	7,100,448				
A=	7,100,448	; Z =	4.00 m and	Total	a.z/A.Z =	0.642

HI = 0.642 --> More than 0.5 --> Riverine forces are dominant

directions have been given in figure 6.6 and two of the six transverse drawings are presented in figure 6.13 while the others can be found in appendix B, figure B.3. The total volume of sediment with respect to the left and right central axis of the river mouth will illustrate the skewness distribution of the sediment outflow from the river mouth.

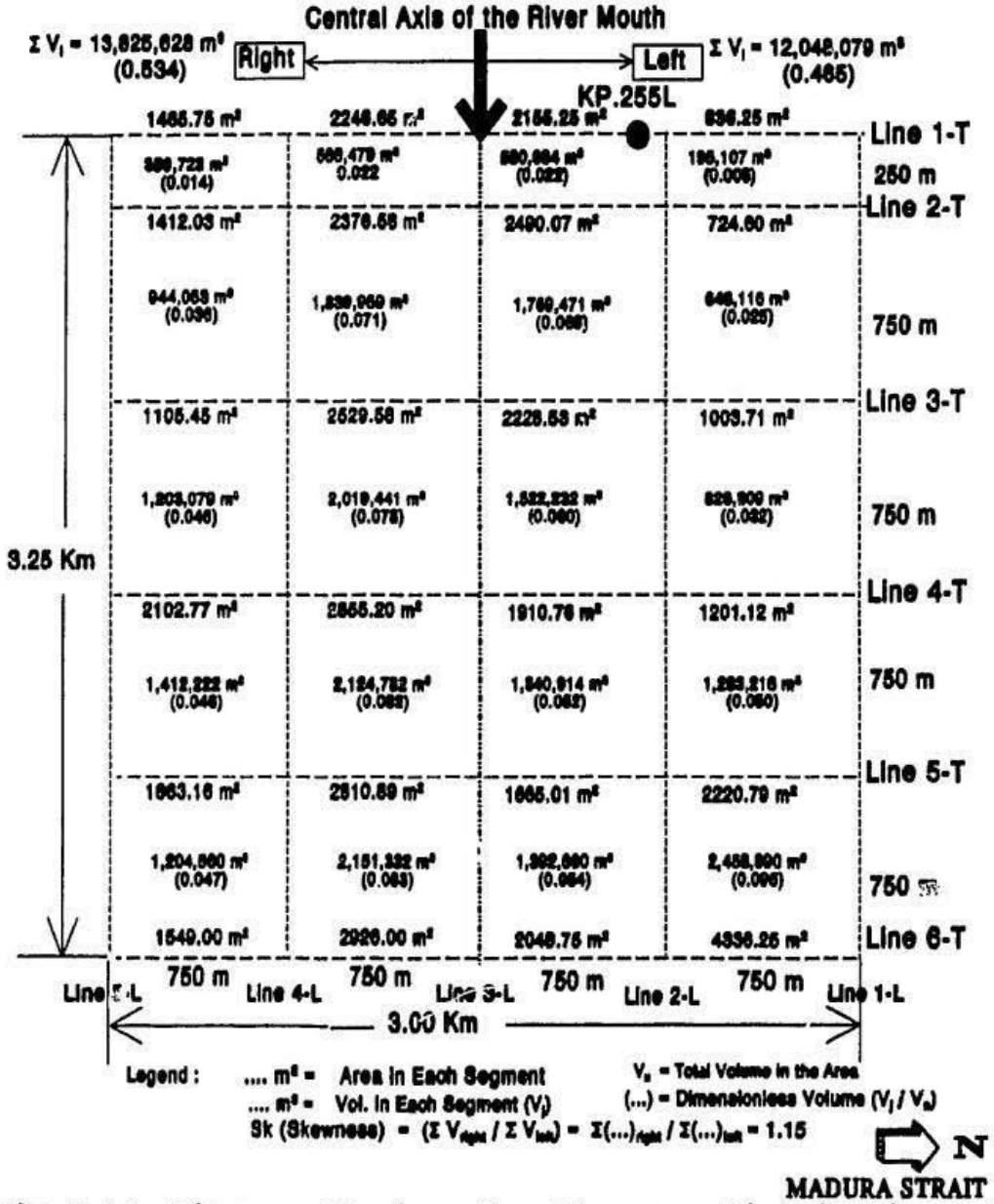

Fig.6.14 Diagram Showing the Skewness Distribution of Sediment Outflow from the River Mouth

As a result, a diagram can be made as in figure 6.14.

The result shows that the sediment volume on the right side of the axis mouth is higher than that on the left side, 53 % is in the right side and 47 % is in the left side. Hence, the skewness index is 1.15. If a similar evaluation is made for other distances from the river mouth or made for every section, the result may be different. This case means that the distribution of the sediment on the both sides of the central axis is unequal from place to place.

An estimation of dominant rates of deposition through out the year can be made from the surveys carried out in 1977 and 1989. The differences between transverse profiles (i.e at right angles central axis of the river mouth, see figure 6.13) in these years give total deposition between 1977 and 1987. The percentages of deposition to the left and to the right of the central axis were calculated and were shown in figure 6.13 and appendix B, figure B.3 while the widths of the expansion flow at the fixed sections caused by dominant discharge were given in table 6.11 and 6.12. If these percentages and the widths of the expansion flow are assumed as dominant distribution of the water and the sediment throughout the year, the direction of flow and its sediment distribution are illustrated in figure 6.15.

Another significant case to be considered is the direction of flow at the river mouth area when the discharge is equal to or less than the mean discharge of the dry season (equal to or less than 62 m^3/sec). Under the discharges, the flow seems totally to go the right side of the central axis of the river mouth. This condition can be traced directly from the topographic map (see original copy of the map in appendix B, figure B.5-1

through B.5-9) or from a schematic map showing rough contours of this area is illustrated in figure 6.16.

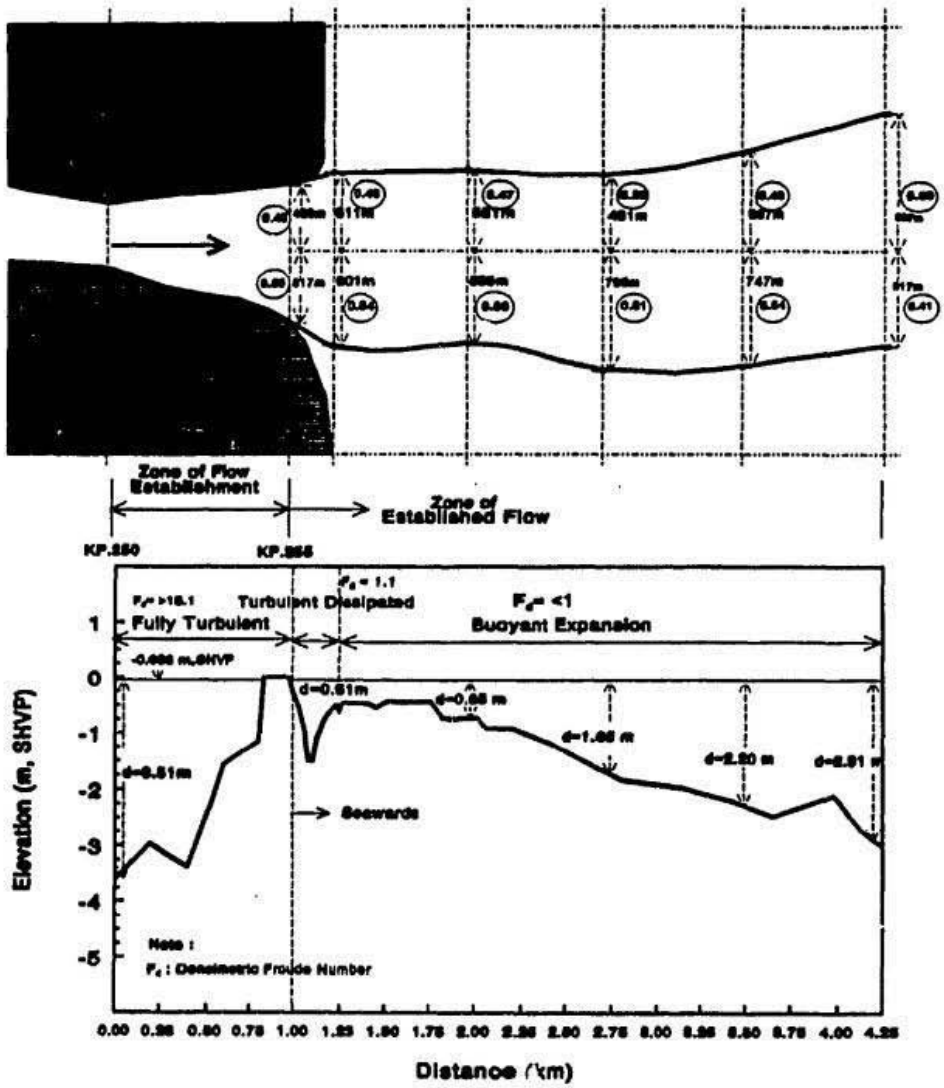

Fig.6.15 Direction of Flow and Sediment Distribution within the Brantas River Mouth at the Dominant Discharge (712 m^3/s)

An inference can be drawn from the estimations of shoreline configurations and

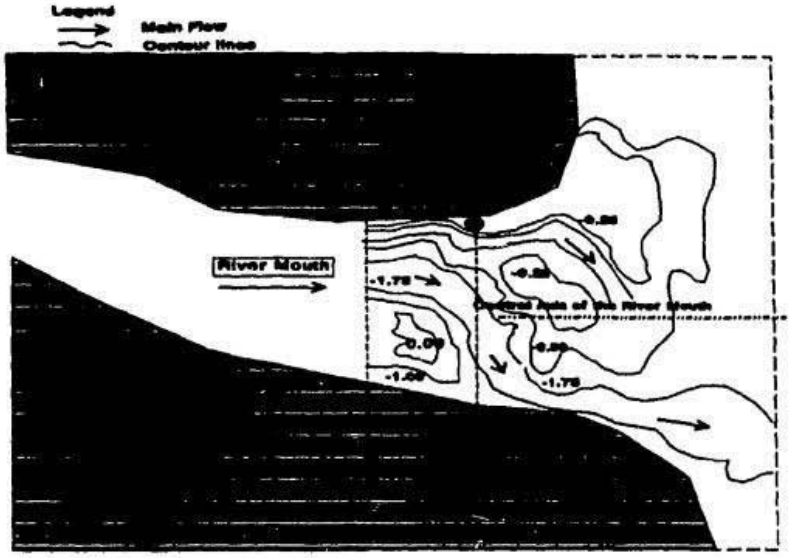

Fig.6.16 Directional Flow at the Brantas River Mouth at a Low Discharge (less than 63 m^3/s)

delta geometry of the Brantas River when compared to the morphometry of seven river deltas (see table 3.2). Table 6.14 compares the geometry of the Brantas to seven other river deltas and shows obviously that the Brantas delta may be categorized as a river delta.

Table 6.14 Morphometry of Seven Deltas & the Brantas Delta

Rivers	$C_l = L_e/W$	$P_i = L_m/W$	$S_k = V_r/V_l$	HI	Dominant Forces
Mississippi	5.20	0.35	0.85	0.59	River
Danube	1.46	0.30	1.13	0.51	River
Ebro	3.51	0.64	1.05	0.50	River & Marine
Niger	1.29	0.34	1.39	0.48	River & Marine
Nile	1.22	0.23	1.21	0.37	Marine
Sao Francisco	1.08	0.26	0.74	0.34	Marine
Senegal	1.02	None	None	0.26	Marine
Brantas	**1.67**	**0.29**	**1.15**	**0.64**	**River**

6.3 Pattern of Sediment Budget on the Brantas Estuary

Unfortunately, there is no recent geometric data of the original river that can be used to estimate the distribution of the sediment inflow through the original and the shortcut channel. However, based on the field survey carried out in the dry season of 1991, an estimate that 30 % of the sediment enters the original river seems to be reasonable.

In the rainy season, when the river discharge is greater than the mean discharge (301 m^3/sec), the suspended sediment inflow will be greater than 2.2 million m^3/yr for about 70 days duration (see figure 6.1). Corresponding values for the dominant discharge are 712 m^3/sec water discharge and 4.0 million m^3/yr for only about 30 days duration. The water flows directly to the surf zone with deposition of about 47 % and 53 % to the left and right hand side of the central axis respectively. A large amount of the wash load sediment floats continuously within the sea area which is considered to be a marine sink. Dredging works are also considered as another sink because the works have been done routinely since 1978. Even though the dredging volume seems to be insignificant compared to total amount of sediment inflow, however, the work is necessary for maintaining the shortcut channel from deposition by tidal currents during the dry season. This phenomenon is illustrated in figure 6.17.

In the dry season, when water discharge is relatively low, the river flow coming out from the upper area will flow dominantly to the shortcut channel rather. than to the original river. It is important to note under this condition that the flow at the river mouth

(KP.255) tends to go to the right hand side and by combination with the longshore currents and wave energy, a revolving stage of currents will be established. Based on the velocity estimation mentioned in table 6.3 and field observation in table 5.15.d, the mean velocity of the river flow and the mean longshore currents were 0.12 and 0.14 m/s, respectively. Therefore, both currents are almost balanced. An eddy may occur and the deposition will focus on the right hand side of the shortcut central axis. This case can be presented in figure 6.18. In addition, if the river discharge is less than 20 m^3/sec, the tidal action is dominant. This induces the fine grained sediment to flow to the estuarine area. Deposition also occurs mainly on the right side of the channel as illustrated in figure 6.19.

A general pattern of the sediment budget throughout the year is presented in figure 6.20 and summarized in table 6.15. A prediction of changing geometry caused by the depositional process on the delta and the shortcut channel can be made (see figure 6.21). Since the deposition on the right side is larger than that of on the left side, the flow will bend gradually to the left side. It will scour the left bank and finally, without any maintenance work, the alignment of the shortcut channel will bend to the left hand side and tend to go back to the original river. This phenomenon means that a manmade channel will change back slowly to a natural form similar to the original river.

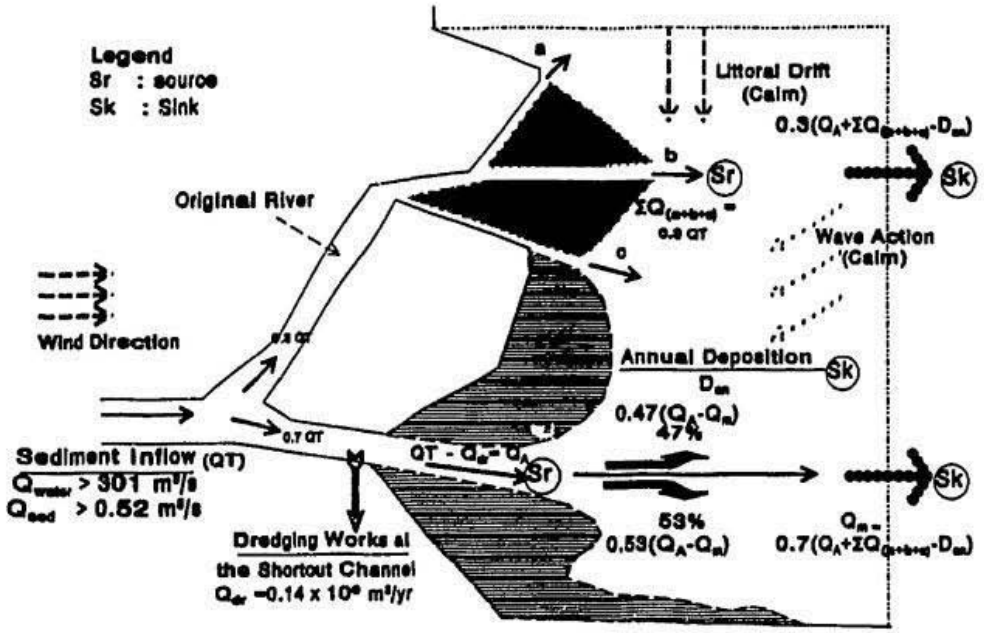

Fig.6.17 Pattern of Sediment Budget on the Rainy Season

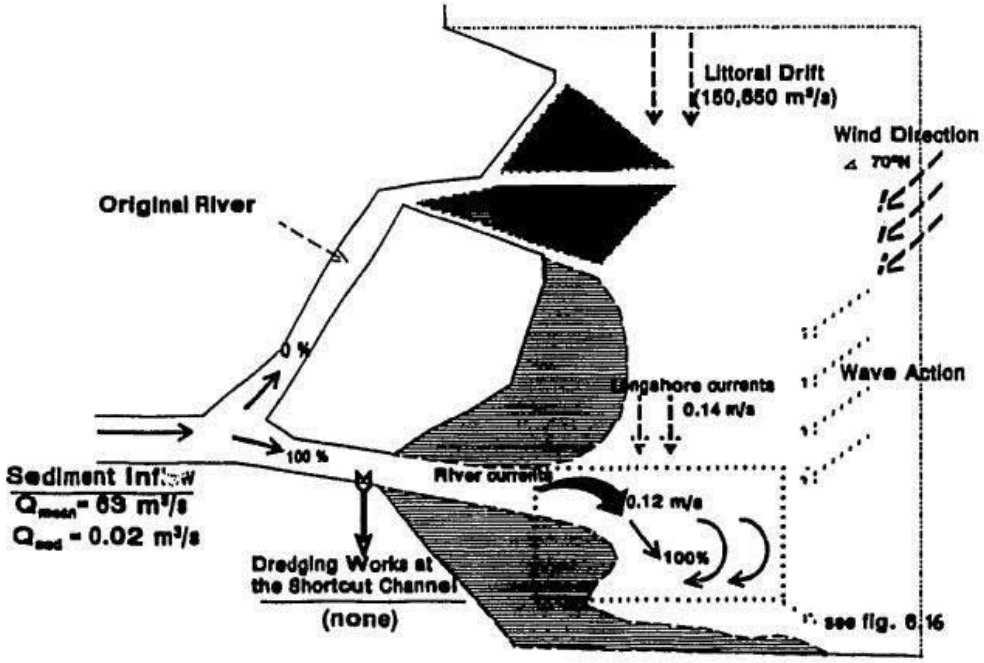

Fig.6.18 Pattern of Sediment Budget on the Dry Season

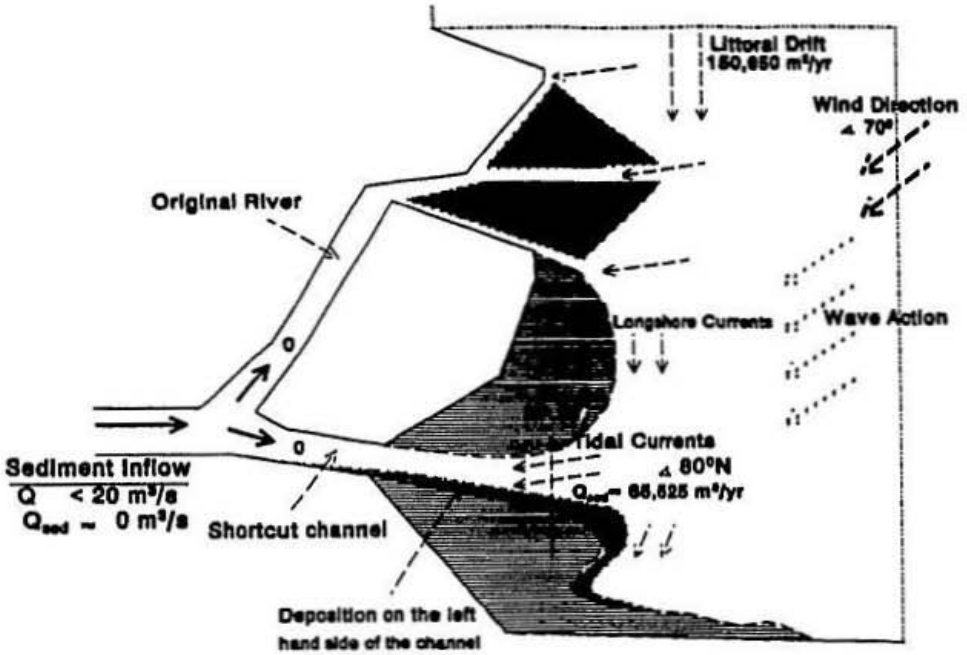

Fig.6.19 Pattern of Sediment Buget When River Discharge less than 20 m^3/sec

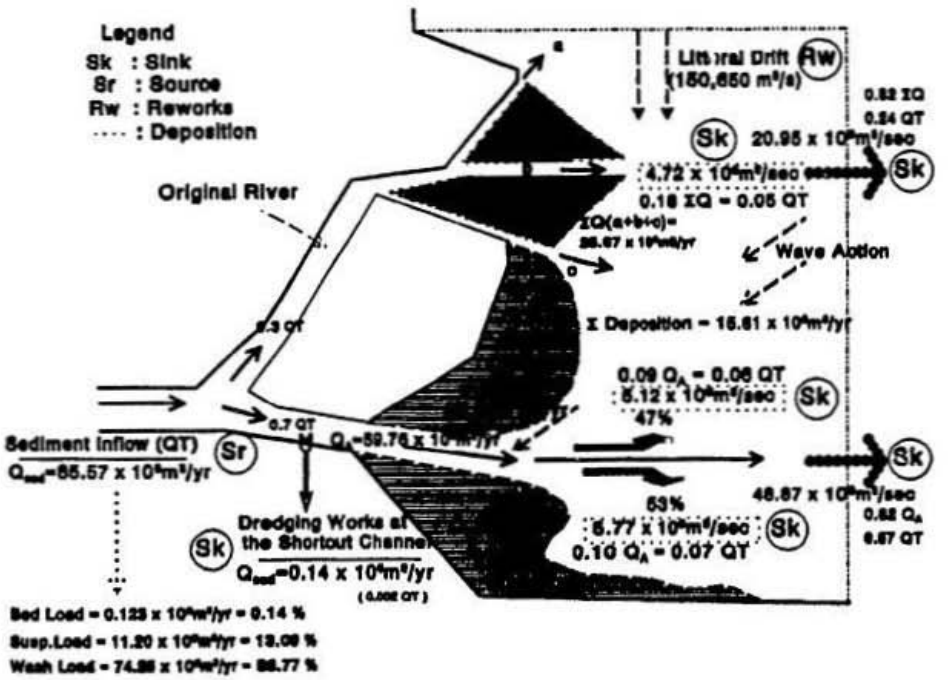

Fig.6.20 General Pattern of Sediment Budget throughout the year

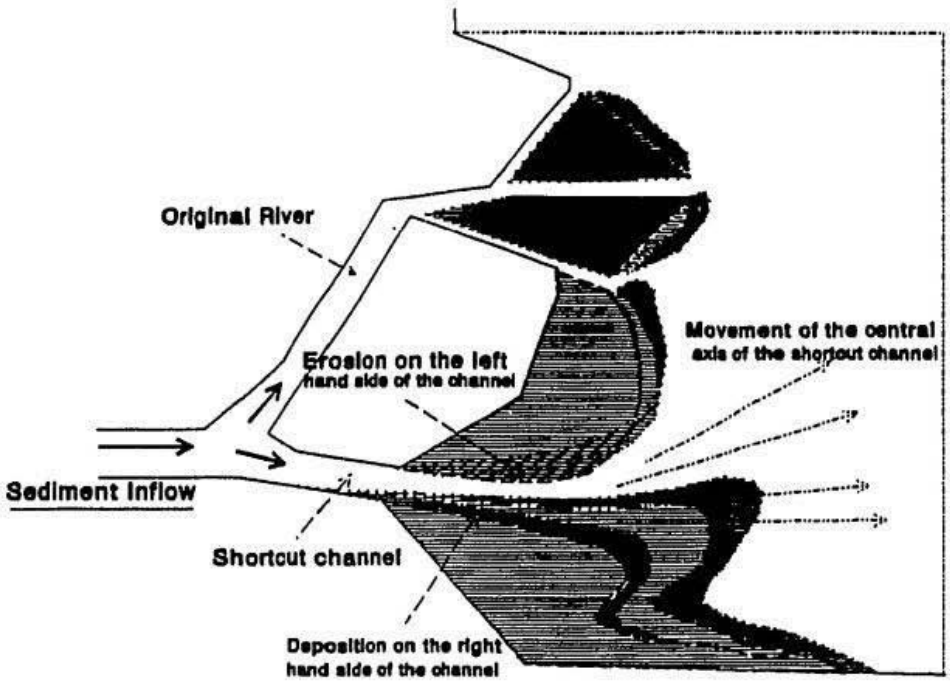

Fig.6.21 Prediction of Changing Alignment of the Shortcut Channel and Deposition on the Delta

Table 6.15 Summary of the Sediment Budget

Sources	m^3/year	Remarks
Brantas River	85.57×10^6	Main Source
Ocean	-	Low energy
Longshore drift	0.15×10^6	Reworks of the main source
Tidal Currents	0.07×10^6	Reworks of the main source
Total	85.57×10^6	
Sinks	m^3/year	
Deposition	4.72×10^6	In front of the org.mouths Northern
	5.12×10^6	shortcut mouth Southern shortcut
	5.77×10^6	mouth
Dredging work	0.14×10^6	
Marine sink	69.82×10^6	Mainly wash load
Total	85.57×10^6	

Chapter 7

Conclusions and Recommendations

Chapter 7

Conclusions and Recommendations

7.1 General Conclusions

Sediment entering the Brantas Estuary from the fresh water river system constitutes a main source of the delta formation. During the dry season, when the fresh water discharge is low, fine sediment is brought by tidal currents to the estuarine region and settles mainly along the shortcut channel and the original river. However, total sediment from the river water discharge is significant in the total deposition either on the Brantas Estuary and its delta. The quantity of dredged material at the shortcut channel is small relative to the total annual deposition but dredging work is needed to maintain the channel from decreasing its capacity to accommodate flood discharge rapidly to the sea.

According to Davis and Hayes (quoted in Kennish, M.J, 1986, see section 3.1.1) an estuary is classified as a microtidal estuary if the average tidal range is less than 2.00 m. The Brantas Estuary is, therefore, classified as a microtidal estuary since the average tidal range at the shortcut river mouth is only about 1.09 m (see table 5.2). According to Rusnak (quoted in Kennish, M.J, 1986), the Brantas Estuary is a positive estuary because the sediment comes primarily from the river while, during the dry season, sediment that enters the estuary originates also from the river and is reworked by the tidal

currents.

The rising and falling tide on the Brantas estuary occurs twice a day with unequal height. Spring and neap tides occur twice a month. Therefore, the tidal type is a mixed tide (see section 3.2.1) with bimonthly spring and neap tides.

Tidal period and tidal range were found to be unequal between any one station and the others. In general, however, the tidal range within the Brantas estuary decreases exponentially landward. Asymmetric periods between the rise and fall of the tide become significant at the upper places (see table 5.2).

Circulation and sedimentation within the Brantas estuary vary considerably between the rainy and the dry season. This is caused by variable discharge throughout the year. During the rainy season and the dry season, the average water discharges through the Porong river are about 301 m^3/sec and 63 m^3/sec, respectively. However, the maximum discharge between 1977 and 1989 was about 1,466 m^3/sec. Within the dry season, the discharge will be less than 20 m^3/sec or even 0 m^3/sec when the fresh water discharge is totally diverted to the Surabaya river for drinking and industrial water supply purposes. Consequently, the relative strength between marine and river forces is always variable and this causes circulation and sediment patterns also to vary considerably throughout the year.

During the rainy season, the fresh water discharges are largely dominant over the tidal action and the circulation pattern is mostly highly stratified. The tip of the wedge is located around 1.4 to 2.3 km upstream of the shortcut mouth (see section 6.1.2) if the fresh water is 301 m^3/sec (mean discharge of the rainy season). However, if the fresh

water is at the dominant discharge (712 m^3/sec) the tip of wedge will be pushed down as far as the shortcut mouth (KP.255). Significant deposition occurs at the area surrounding the shortcut mouth. This infers that the location of the tip of the saline wedge is found mostly in that point.

During the dry season, when the fresh water discharge is less than 20 m^3/sec, the circulation will be slightly stratified or well mixed. In this condition, tidal action is dominant. Sediment which has settled in the nearshore area will be reworked by the tidal currents and brought to the estuarine region. Based on the integration method in a unit tidal range developed for this thesis, it has been shown that the deposition occurs along the shortcut channel and the original river only (see figure 6.4). In the region just upstream of the split (KP.236), erosion will occur regularly in this condition. An inference can be drawn that the tidal current can only bring the sediment as far as 3 km upstream from the shortcut mouth. In addition, certain other features of sediment fluctuation during a tidal flood and ebb have been found. The highest sediment discharge happens at about 80 to 85% of the flood time. On the other hand, during the ebb process, the sediment will reach the maximum discharge at about 30% to 35% of the ebb time (see section 6.2.3).

Sediment measurements carried out during the dry season of 1991 implied that the intrusion length was about 9 km from the river mouth within this season. Attempts were made to fit a suitable formulae for calculating the intrusion length. Field data showed that Keulegan's (1966) formula (equation 3-5) is valid in the Brantas river for discharges greater than 105 m^3/sec. Thus

$$\frac{L_A}{d} = \left[\frac{0.88}{280(R_d)^{-1} + 0.148(R_d)^{-1/4}}\right](2F_d)^{-5/2} \quad \textbf{(3-5)}$$

All variables are as previously defined

For fresh water discharges between 65 m^3/sec and 105 m^3/sec it has been shown that Ozturk's formula (1970) can be used with modified constants. Thus

$$\frac{L_A}{d} = 1.435(R_d)^{1/4}(2F_d)^{-5/2} \quad \textbf{(6-3)}$$

For fresh water discharge less than 65 m^3/sec the estuary may be slightly stratified and neither formula is valid.

Analysis of distribution of sediment outflow from the river mouth showed that it is skewed and that more sediment is deposited on the right side of the central axis. In the rainy season the sediment is distributed 53% to the right side and 47% to the left side. However, during the dry season, the sediment distribution will be 100 % to the right side of the central axis. This can be traced from the contours around the area of the shortcut mouth and the dominant direction of the longshore currents (see figure 6.18). Both factors imply that throughout this season the flow goes completely to the right side of the central axis.

Analysis of the delta configuration and other geometric data showed that river forces are more important than marine forces. Since the sediment mainly comes from the river, accumulation of sediment occurs regularly throughout the year and the delta is formed continuously. Finally, without any maintenance work, the shortcut channel will tend to revert to the original channel (see figure 6.21).

7.2 Recommendations for Future Work

The maintenance dredging work that has been done by the Brantas Project is technically correct for maintaining the shortcut channel. However, this thesis has shown that the volume of the average annual dredging work is larger than the annual sediment that enters the estuary by the tidal current during dry season. In addition, it is known that the channel is increasing in size (see figure 4.10). If it is assumed that little deposition occurs during the wet season (because sediments are flushed to the sea) too much dredging may be being carried out. This possibility should be checked by measuring sediment deposition during the rainy season in order to obtain an accurate sediment budget. Furthermore, the location of the dredging should be changed with the direction being more focused on the right side of the channel. Dredging should maintain the channel with a flat bed rather than deepening one side as is current practice because the deepening will increase the landward penetration of the saline water and, in turn, will facilitate the transport of material to the shortcut channel region (see section 3.1.1, in salt wedge or highly stratified estuaries). This is reflected in an increase in the dredged quantity in the shortcut channel.

Additional field observations similar to those carried out by the author should be taken during the rainy season to obtain an understanding of the circulation patterns and sediment movements throughout the year. Methods similar to those used here may then be applied to develop detailed annual sediment budgets and circulation patterns in order to solve the general sediment problems of the Brantas Estuary.

References

References

Allen, J.H. (1962). "Hydraulics Studies in the Estuary of the River Tyne," *Ph.D thesis*, University Durham (King's College), 231 p.

An Open University Course Team. (1989). *Waves, Tides and Shallow Water Processes*, Pergamon Press, Oxford, 107p.

Bates, C.C. (1953)."Rational theory of delta formation,". *The American Association of Petroleum Geologists Bulletin*, v.37, p.2119-2161.

Bogardi, J.L. (1978). *Sediment Transport in Alluvial Streams*, Akademiai Kiado, Budapest., 774 p.

Bondar, (1968)."Hydraulical and Hydrological Conditions of the Black Sea Waters Penetration into the Danube Mouth" *Hydrological Study*, no.25, pp.103-120.

Borichansky, L. S., and Mikhailov, V. N. (1966). "Interaction of River and Sea Water in the Absence of Tides," *Scientific Problem of the Humid Tropical Zone Deltas and Their Implication*, UNESCO, p.175-180.

Brantas River Basin Development Executing Agency. (1966). *Design Calculations on Kali Porong Project*, Nippon Koei Co.,Ltd., 121 p.

Brantas River Basin Development Executing Agency. (1990)."Porong River Rehabilitation Project," *Design Report*, Nippon Koei Co.,Ltd., 37 p.

Bretschneider, C.L., and Reid, R.O. (1954)." Modification of Wave Height Due to Bottom Friction, Percolation and Refraction," *U.S Army Corp Engineering Beach Erosion Board Tech*, Memo, no. 45, 36 p.

Cameron, W.M. and Pritchard, D.W. (1963). "Estuaries," *The Sea, Vol. 2*, ed. Hill, M.L., Wiley International, New York, 306 p.

Chadwick, A.J., and Morfett, J.C. (1986). *Hydraulics in Civil Engineering*, Allen & Unwin Ltd., London., 492 p.

Crowley, W.P. (1968)."A Global Numerical Ocean Model": Part 1, *J. Comp. Phys.* no.3. pp.111-147

Coleman, J.M. (1982). *Deltas : The Processes of Deposition and Models for Exploration*, 2nd ed., International Human Resources Development Corporation, Boston, MA., 124 p.

Dyer, K.R. (1986). *Coastal and Estuarine Sediment Dynamics*, John Wiley and Sons, Chichester, Sussex (UK), 342 p.

Folk, R.L., and Ward, W.C. (1972)."Brazos River Bar. A Study in the Significances 6 Grain Size Parameters," *Journal of Sedimentary Petrology*, Vol. 27, pp. 3-26.

Hayashi, J., and Shuto, N. (1967)."Diffusion of Warm Water Jets Discharge Horizontally at the Water Surface," *Internat. Assoc. Hydraulic Research. 12 th Cong.*, Proc., v.4, pp.47-59.

Hayashi,J., and Shuto, N. (1968)." Diffusion of Warm cooling Water Discharged from a Power Plant," *Conf. Coastal Eng.*, Council Wave Research, 11 th, London, Proc. 48 p.

Ippen, A.T., (1966)" Estuary and Coastline Hydrodynamics," McGraw-Hill Book Company, New York. 744 p.

Ippen, A.T., and Harleman, D.R.F. (1966). "Tidal Dynamics in Estuaries," *Estuary and Coastline Hydrodynamics*, ed. A.T. Ippen, McGraw-Hill Book Company, pp. 493-545.

Kennish, M.J. (1986). *Ecology of Estuaries : Physical and Chemical Aspects*, CRC Press, Inc., Boca Raton, Florida, 254 p.

Keulegan, G.H. (1966). "The Mechanism of an Arrested Saline Wedge," *Estuary and Coastline Hydrodynamics*, ed. A.T. Ippen, McGraw-Hill Book Company, New York pp. 545-573.

Krumbein, W.C. (1936)."Application of Logarithmic Moments to Size Frequency Distribution of Sediments," *Journal of Sedimentary Petrology*, Vol. 6, no. 1., pp. 35-47

Lavelle, J.W., Mofjeld, H.O. and Baker, E.T. (1984)."An in-situ Erosion Rate for a Fine-grained Marine Sediment," *J. Geophys. Res.*, no. 89, pp. 5643-52

Longuet-Higgins, M.S. (1970) "Longshore Currents Generated by Obliquely Incident Waves, 1," *Journal of Geophysical Research*, Vol.75, No.33, Nov. 1970, pp.6788-6801.

Madsen, O.S. (1976). "Wave Climate of the Continental Margin: Elements of its Mathematical Description," *Marine Sediment Transport and Environmental Management*, ed. Daniel Jean Stanley and Donald J.P. Swift, John Wiley & Sons, New York, NY., pp. 65-87.

Neumann, G., and W. J. Pierson. (1966). *Principles of Physical Oceanography*, Prentice-hall, Englewood Cliffs, NJ, 545 p.

Pickard, G.L. (1975). *Descriptive Physical Oceanography*, 2nd ed. Pergamon Press, Inc., Oxford, U.K. 214 p.

Pritchard, D.W. (1955) "Estuarine Circulation Patterns," *Proc. Am. Soc. Civil Engs.*, Vol.81, paper no 717, pp 1-11.

Owen, M.W. (1976). "Problems in the Modelling of Transport, Erosion, and Deposition of Cohesive Sediments," *The Sea*, Vol. 6, Wiley-Interscience , New York, pp. 515-537.

Resio, D.T., and Vincent, C.L. (1977). "Estimation of Wind Over the Great Lakes," *Journal of the Waterway, Port, Coastal and Ocean Division, Proceedings of the American Society of Civil Engineers*, Vol. 103, No. WW2, p.265.

Roberson, J.A., Cassidy, J.J., and Chaudhry, M.H. (1988). *Hydraulic Engineering*, Houghton Mifflin Company, Boston, 662 p.

Sheng , Y.P., and Lick, W. (1979)."The Transport and Resuspension of Sediments in a Shallow Lake," *J. Geophys. Res.*, no. 84, pp. 1809-26.

Silvester, R. (1974). *Coastal Engineering, 2 : Sedimentation, Estuaries, Tides, Effluents, and Modelling*, Elsevier Scientific Publishing Co., Amsterdam, 338 p.

Simiu, E., and Scanlan, R.N., (1978) "Wind Effect on Structures: An introduction to Wind Engineering," New York, Wiley, p.62.

U.S Army CERC (1984). "Coastal Engineering Research Center," *Shore Protection Manual*, Vol. 1 & 2, Government Printing Office, Washington DC.

Wright, L.D., and Coleman, J.M. (1971). "The Discharge/wave-power climate and the morphology of delta coast," *Assoc. American Geographers Proc.*, v.3, p.186-189.

Wright, L.D., and Coleman, J.M. (1973). "Variation in Morphology of Major Deltas as Functions of Ocean Wave and River Discharge Regimes," *The American Association of Petroleum Geologists Bulletin*, Vol. 57, no. 2, pp 370-398.

Wright, L.D., and Coleman, J.M. (1974). "Mississippi River Mouth Processes : Effluent Dynamics and Morphologic Development," *Journal of Geology*, Vol. 82, pp 751-778.

Appendix A

Supplementary Tables to Calculations

Table A.1-1
TIDAL DATA at KP.242

Location : Shortcut channel, Porong River
Tidal Gauge : KP.242 (2.6 Km Upward from the Shortcut Mouth)
Recording period : From June 6, 1991 to July 12,1991

Date	High Water		Low Water		Duration		Range		Mean Level	
	Time	Elevation m,SHVP	Tim	Elevation m,SHVP	Fall hrs	Rise hrs	Fall m	Rise m	m,SHVP	
Jun 6	8	-0.122	14	-0.602	6.0	4.0	0.48	0.38	-0.362	-0.412
	18	-0.222	1	-0.722	7.0	6.0	0.50	0.98	-0.472	-0.257
7	7	0.208	15	-0.782	8.0	4.0	0.99	0.56	-0.287	-0.502
	19	-0.222	1	-0.722	6.0	7.0	0.50	1.02	-0.472	-0.212
8	8	0.298	16	-0.822	8.0	4.0	1.12	0.60	-0.262	-0.522
	20	-0.222	2	-0.712	6.0	6.0	0.49	1.19	-0.467	-0.117
9	8	0.478	16	-0.882	8.0	6.0	1.36	0.68	-0.202	-0.541
	22	-0.199	3	-0.692	5.0	5.0	0.49	1.29	-0.446	-0.047
10	8	0.598	17	-0.912	9.0	6.0	1.51	0.71	-0.157	-0.555
	23	-0.198	4	-0.722	5.0	5.0	0.52	1.55	-0.46	0.053
11	9	0.828	18	-0.922	9.0	5.0	1.75	0.82	-0.047	-0.512
	23	-0.102	5	-0.722	6.0	4.0	0.62	1.64	-0.412	0.098
12	9	0.918	18	-0.912	9.0	6.0	1.83	0.84	0.003	-0.492
13	24	-0.072	5	-0.712	5.0	5.0	0.64	1.71	-0.392	0.145
	10	1.002	19	-0.822	9.0	6.0	1.82	0.80	0.09	-0.422
14	1	-0.022	6	-0.742	5.0	5.0	0.72	1.67	-0.382	0.093
	11	0.928	20	-0.882	9.0	5.0	1.81	0.86	0.023	-0.45
15	1	-0.018	7	-0.622	6.0	4.0	0.60	1.50	-0.32	0.128
	11	0.878	20	-0.822	9.0	6.0	1.70	0.90	0.028	-0.372
16	2	0.078	8	-0.602	6.0	4.0	0.68	1.38	-0.262	0.088
	12	0.778	21	-0.722	9.0	5.0	1.50	0.84	0.028	-0.302
17	2	0.118	8	-0.592	6.0	6.0	0.71	1.11	-0.237	-0.037
	14	0.518	22	-0.652	8.0	5.0	1.17	0.84	-0.067	-0.232
18	3	0.188	9	-0.502	6.0	6.0	0.69	0.86	-0.157	-0.072
	15	0.358	23	-0.612	8.0	5.0	0.97	0.89	-0.127	-0.167
19	4	0.278	10	-0.422	6.0	6.0	0.70	0.60	-0.072	-0.122
	16	0.178	24	-0.562	8.0	5.0	0.74	0.79	-0.192	-0.167
20	5	0.228	11	-0.486	6.0	7.0	0.71	0.46	-0.129	-0.254
	18	-0.022	1	-0.592	7.0	4.0	0.57	0.87	-0.307	-0.157
21	5	0.278	11	-0.596	6.0	7.0	0.87	0.60	-0.159	-0.298
	18	0	2	-0.496	8.0	4.0	0.50	0.95	-0.248	-0.019
22	6	0.458	12	-0.642	6.0	7.0	1.10	0.62	-0.092	-0.332
	19	-0.022	3	-0.582	8.0	4.0	0.56	1.06	-0.302	-0.052
23	7	0.478	13	-0.752	6.0	7.0	1.23	0.72	-0.137	-0.39
	20	-0.028	4	-0.572	8.0	4.0	0.54	1.11	-0.3	-0.017
Jun 24	8	0.538	14	-0.812	6.0	7.0	1.35	0.83	-0.137	-0.395
	21	0.022	5	-0.612	8.0	4.0	0.63	1.19	-0.295	-0.017

(next page)

(Table A.1-1 Continued)

Date	High Water		Low Water		Duration		Range		Mean Level	
	Time	Elevation m,SHVP	Tim	Elevation m,SHVP	Fall hrs	Rise hrs	Fall m	Rise m	m,SHVP	
Jun 25	9	0.578	15	-0.892	6.0	6.0	1.47	0.94	-0.157	-0.42
26	21	0.052	5	-0.562	8.0	5.0	0.61	1.18	-0.255	0.028
	10	0.618	16	-0.882	6.0	6.0	1.50	0.97	-0.132	-0.395
27	22	0.092	6	-0.622	8.0	5.0	0.71	1.32	-0.265	0.038
	11	0.698	17	-0.902	6.0	6.0	1.60	1.01	-0.102	-0.395
28	23	0.112	6	-0.602	7.0	5.0	0.71	1.26	-0.245	0.028
	11	0.658	18	-0.922	7.0	6.0	1.58	0.97	-0.132	-0.435
29	24	0.052	6	-0.682	6.0	5.0	0.73	1.26	-0.315	-0.052
	11	0.578	19	-0.922	8.0	5.0	1.50	0.90	-0.172	-0.472
30	24	-0.022	7	-0.702	7.0	5.0	0.68	1.22	-0.362	-0.092
	12	0.518	20	-0.872	8.0	5.0	1.39	0.85	-0.177	-0.447
July 1	1	-0.022	8	-0.682	7.0	5.0	0.66	1.16	-0.352	-0.102
	13	0.478	21	-0.722	8.0	5.0	1.20	0.60	-0.122	-0.422
2	2	-0.122	8	-0.612	6.0	6.0	0.49	0.87	-0.367	-0.177
	14	0.258	21	-0.722	7.0	5.0	0.98	0.63	-0.232	-0.407
3	2	-0.092	9	-0.552	7.0	6.0	0.46	0.73	-0.322	-0.187
	15	0.178	21	-0.552	6.0	6.0	0.73	0.72	-0.187	-0.192
4	3	0.168	10	-0.492	7.0	5.0	0.66	0.42	-0.162	-0.282
	15	-0.072	22	-0.552	7.0	6.0	0.48	0.75	-0.312	-0.177
5	4	0.198	11	-0.552	7.0	5.0	0.75	0.55	-0.177	-0.277
	16	-0.002	22	-0.692	6.0	6.0	0.69	0.95	-0.347	-0.217
6	4	0.258	12	-0.792	8.0	5.0	1.05	0.79	-0.267	-0.396
	17	0.001	23	-0.592	6.0	7.0	0.59	0.95	-0.296	-0.117
7	6	0.358	13	-0.822	7.0	5.0	1.18	0.82	-0.232	-0.411
	18	0.001	24	-0.602	6.0	7.0	0.60	1.01	-0.301	-0.097
8	7	0.408	14	-0.872	7.0	5.0	1.28	0.86	-0.232	-0.442
	19	-0.012	1	-0.612	6.0	7.0	0.60	1.09	-0.312	-0.067
9	8	0.478	15	-0.892	7.0	5.0	1.37	0.86	-0.207	-0.462
	20	-0.032	2	-0.622	6.0	7.0	0.59	1.15	-0.327	-0.047
10	9	0.528	16	-0.912	7.0	5.0	1.44	0.86	-0.192	-0.482
	21	-0.052	3	-0.592	6.0	7.0	0.54	1.35	-0.322	0.083
11	10	0.758	17	-0.982	7.0	5.0	1.74	0.79	-0.112	-0.587
	22	-0.192	4	-0.622	6.0	7.0	0.43	1.45	-0.407	0.103
July 12	11	0.828	18	-0.902	7.0	-	1.73	-	-0.037	-
Average		0.245		-0.705	6.9	5.5	0.95	0.95	-0.23	-0.23

Table A.1-2
TIDAL DATA at KP.236

Location : Porong River, Upper Shortcut Tributary
Tidal Gauge : KP.236 (3.8 Km Upward from the Shortcut Mouth)
Recording period : From June 6, 1991 to July 12,1991

Date	High Water		Low Water		Duration		Range		Mean Level	
	Time	Elevation m,SHVP	Time	Elevation m,SHVP	Fall hrs	Rise hrs	Fall m	Rise m	m,SHVP	
Jun 6	8	0.061	14	-0.401	6.0	4.0	0.46	0.37	-0.17	-0.216
	18	-0.031	1	-0.481	7.0	6.0	0.45	0.86	-0.256	-0.05
7	7	0.381	15	-0.501	8.0	4.0	0.88	0.46	-0.06	-0.27
	19	-0.038	1	-0.421	6.0	7.0	0.38	0.87	-0.23	0.016
8	8	0.453	16	-0.521	8.0	4.0	0.97	0.52	-0.034	-0.261
	20	-0.001	2	-0.386	6.0	6.0	0.39	1.03	-0.194	0.130
9	8	0.646	16	-0.521	8.0	6.0	1.17	0.56	0.063	-0.24
	22	0.041	3	-0.411	5.0	5.0	0.45	1.24	-0.185	0.210
10	8	0.831	17	-0.581	9.0	6.0	1.41	0.67	0.125	-0.245
	23	0.091	4	-0.381	5.0	5.0	0.47	1.39	-0.145	0.315
11	9	1.011	18	-0.581	9.0	5.0	1.59	0.73	0.215	-0.215
	23	0.151	5	-0.381	6.0	4.0	0.53	1.45	-0.115	0.345
12	9	1.071	18	-0.591	9.0	6.0	1.66	0.76	0.240	-0.21
13	24	0.171	5	-0.401	5.0	5.0	0.57	1.58	-0.115	0.390
	10	1.181	19	-0.571	9.0	6.0	1.75	0.76	0.305	-0.19
14	1	0.191	6	-0.361	5.0	5.0	0.55	1.52	-0.085	0.400
	11	1.161	20	-0.501	9.0	5.0	1.66	0.76	0.330	-0.12
15	1	0.261	7	-0.301	6.0	4.0	0.56	1.39	-0.02	0.395
	11	1.091	20	-0.491	9.0	6.0	1.58	0.77	0.300	-0.105
16	2	0.281	8	-0.251	6.0	4.0	0.53	1.12	0.015	0.310
	12	0.871	21	-0.481	9.0	5.0	1.35	0.85	0.195	-0.055
17	2	0.371	8	-0.241	6.0	6.0	0.61	0.90	0.065	0.210
	14	0.661	22	-0.391	8.0	5.0	1.05	0.84	0.135	0.03
18	3	0.451	9	-0.221	6.0	6.0	0.67	0.76	0.115	0.160
	15	0.541	23	-0.331	8.0	5.0	0.87	0.83	0.105	0.085
19	4	0.501	10	-0.231	6.0	6.0	0.73	0.61	0.135	0.075
	16	0.381	24	-0.311	8.0	5.0	0.69	0.86	0.035	0.120
20	5	0.551	11	-0.231	6.0	7.0	0.78	0.55	0.160	0.045
	18	0.321	1	-0.301	7.0	4.0	0.62	0.76	0.01	0.080
21	5	0.461	11	-0.291	6.0	7.0	0.75	0.54	0.085	-0.02
	18	0.251	2	-0.211	8.0	4.0	0.46	0.87	0.02	0.225
22	6	0.661	12	-0.351	6.0	7.0	1.01	0.57	0.155	-0.065
	19	0.221	3	-0.201	8.0	4.0	0.42	0.93	0.01	0.265
23	7	0.731	13	-0.455	6.0	7.0	1.19	0.69	0.138	-0.112
	20	0.231	4	-0.191	8.0	4.0	0.42	1.08	0.020	0.350
Jun 24	8	0.891	14	-0.491	6.0	7.0	1.38	0.75	0.200	-0.115
	21	0.261	5	-0.251	8.0	4.0	0.51	1.10	0.005	0.300

(next page)

(Table A.1-2 Continued)

Date	High Water		Low Water		Duration		Range		Mean Level	
	Time	Elevation m,SHVP	Time	Elevation m,SHVP	Fall hrs	Rise hrs	Fall m	Rise m	m,SHVP	
Jun 25	9	0.851	15	-0.491	6.0	6.0	1.34	0.68	0.180	-0.15
26	21	0.191	5	-0.251	8.0	5.0	0.44	1.14	-0.03	0.320
	10	0.891	16	-0.501	6.0	6.0	1.39	0.69	0.195	-0.155
27	22	0.191	6	-0.261	8.0	5.0	0.45	1.31	-0.035	0.395
	11	1.051	17	-0.511	6.0	6.0	1.56	0.81	0.270	-0.105
28	23	0.301	6	-0.201	7.0	5.0	0.50	1.21	0.050	0.405
	11	1.011	18	-0.501	7.0	6.0	1.51	0.69	0.255	-0.155
29	24	0.191	6	-0.271	6.0	5.0	0.46	1.19	-0.04	0.325
	11	0.921	19	-0.491	8.0	5.0	1.41	0.69	0.215	-0.145
30	24	0.201	7	-0.291	7.0	5.0	0.49	1.18	-0.045	0.300
	12	0.891	20	-0.471	8.0	5.0	1.36	0.75	0.210	-0.097
July 1	1	0.277	8	-0.231	7.0	5.0	0.51	0.9[illegible]	0.023	0.265
	13	0.761	21	-0.376	8.0	5.0	1.14	0.[illegible]7	0.193	-0.093
2	2	0.191	8	-0.201	6.0	6.0	0.39	0.75	-0.005	0.176
	14	0.552	21	-0.391	7.0	5.0	0.94	0.58	0.081	-0.1
3	2	0.191	9	-0.193	7.0	6.0	0.38	0.66	-0.001	0.139
	15	0.471	21	-0.241	6.0	6.0	0.71	0.66	0.115	0.09
4	3	0.421	10	-0.181	7.0	5.0	0.60	0.38	0.120	0.010
	15	0.201	22	-0.291	7.0	6.0	0.49	0.71	-0.045	0.065
5	4	0.421	11	-0.291	7.0	5.0	0.71	0.49	0.065	-0.045
	16	0.201	22	-0.401	6.0	6.0	0.60	0.91	-0.1	0.055
6	4	0.511	12	-0.471	8.0	5.0	0.98	0.66	0.020	-0.14
	17	0.191	23	-0.301	6.0	7.0	0.49	0.90	-0.055	0.150
7	6	0.601	13	-0.501	7.0	5.0	1.10	0.68	0.050	-0.162
	18	0.178	24	-0.391	6.0	7.0	0.57	1.18	-0.107	0.200
8	7	0.791	14	-0.561	7.0	5.0	1.35	0.84	0.115	-0.14
	19	0.281	1	-0.271	6.0	7.0	0.55	1.03	0.005	0.245
9	8	0.761	15	-0.571	7.0	5.0	1.33	0.77	0.095	-0.185
	20	0.201	2	-0.311	6.0	7.0	0.51	1.11	-0.055	0.245
10	9	0.801	16	-0.481	7.0	5.0	1.28	0.69	0.160	-0.135
	21	0.211	3	-0.301	6.0	7.0	0.51	1.34	-0.045	0.370
11	10	1.041	17	-0.481	7.0	5.0	1.52	0.68	0.280	-0.14
	22	0.201	4	-0.201	6.0	7.0	0.40	1.30	0	0.450
July 12	11	1.101	18	-0.571	7.0	-	1.67	0.57	0.265	-
Average		0.487		-0.3756	6.93	5.46	0.86	0.90	0.056	0.060

Table A.1-3
TIDAL DATA at SB.5

Location : Original River
Tidal Gauge : SB.5 (750m. downstream of tributary)
Recording period : From June 6, 1991 to July 12,1991

Date	High Water		Low Water		Duration		Range		Mean Level	
	Time	Elevation m,SHVP	Time	Elevation m,SHVP	Fall hrs	Rise hrs	Fall m	Rise m	m,SHVP	
June 6	8	-0.145	14	-0.625	6.0	4.0	0.48	0.30	-0.385	-0.475
	18	-0.325	1	-0.855	7.0	6.0	0.53	0.86	-0.59	-0.425
7	7	0.005	15	-0.825	8.0	4.0	0.83	0.54	-0.41	-0.555
	19	-0.285	1	-0.945	6.0	7.0	0.66	1.03	-0.615	-0.43
8	8	0.085	16	-1.055	8.0	4.0	1.14	0.74	-0.485	-0.685
	20	-0.315	2	-0.875	6.0	6.0	0.56	1.19	-0.595	-0.28
9	8	0.315	16	-1.095	8.0	6.0	1.41	0.78	-0.39	-0.705
	22	-0.315	3	-0.875	5.0	5.0	0.56	1.34	-0.595	-0.205
10	8	0.465	17	-1.045	9.0	6.0	1.51	0.75	-0.29	-0.67
	23	-0.295	4	-0.915	5.0	5.0	0.62	1.57	-0.605	-0.13
11	9	0.655	18	-1.195	9.0	5.0	1.85	0.93	-0.27	-0.73
	23	-0.265	5	-0.915	6.0	4.0	0.65	1.62	-0.59	-0.105
12	9	0.705	18	-1.185	9.0	6.0	1.89	0.93	-0.24	-0.72
13	24	-0.255	5	-0.915	5.0	5.0	0.66	1.67	-0.585	-0.08
	10	0.755	19	-1.145	9.0	6.0	1.90	0.90	-0.195	-0.695
14	1	-0.245	6	-0.875	5.0	5.0	0.63	1.64	-0.56	-0.055
	11	0.765	20	-1.135	9.0	5.0	1.90	0.94	-0.185	-0.665
15	1	-0.195	7	-0.815	6.0	4.0	0.62	1.56	-0.505	-0.035
	11	0.745	20	-1.115	9.0	6.0	1.86	0.93	-0.185	-0.65
16	2	-0.185	8	-0.721	6.0	4.0	0.54	1.30	-0.453	-0.073
	12	0.575	21	-0.975	9.0	5.0	1.55	0.82	-0.2	-0.565
17	2	-0.155	8	-0.785	6.0	6.0	0.63	1.25	-0.47	-0.16
	14	0.465	22	-0.915	8.0	5.0	1.38	0.81	-0.225	-0.51
18	3	-0.105	9	-0.665	6.0	6.0	0.56	0.98	-0.385	-0.175
	15	0.315	23	-0.785	8.0	5.0	1.10	0.94	-0.235	-0.315
19	4	0.155	10	-0.645	6.0	6.0	0.80	0.53	-0.245	-0.382
	16	-0.119	24	-0.805	8.0	5.0	0.69	0.93	-0.462	-0.34
20	5	0.125	11	-0.655	6.0	7.0	0.78	0.45	-0.265	-0.43
	18	-0.205	1	-0.805	7.0	4.0	0.60	0.96	-0.505	-0.325
21	5	0.155	11	-0.705	6.0	7.0	0.86	0.46	-0.275	-0.475
	18	-0.245	2	-0.835	8.0	4.0	0.59	1.13	-0.54	-0.27
22	6	0.295	12	-0.915	6.0	7.0	1.21	0.68	-0.31	-0.575
	19	-0.235	3	-0.745	8.0	4.0	0.51	1.10	-0.49	-0.195
23	7	0.355	13	-1.005	6.0	7.0	1.36	0.76	-0.325	-0.625
	20	-0.245	4	-0.775	8.0	4.0	0.53	1.12	-0.51	-0.215
June 24	8	(' 345	14	-1.035	6.0	7.0	1.38	0.82	-0.345	-0.625
	21	-0.215	5	-0.805	8.0	4.0	0.59	1.21	-0.51	-0.2

(next page)

(Table A.1-3 Continued)

Date		High Water		Low Water		Duration		Range		Mean Level	
		Time	Elevation m,SHVP	Time	Elevation m,SHVP	Fall hrs	Rise hrs	Fall m	Rise m	m,SHVP	
June	25	9	0.405	15	-1.105	6.0	6.0	1.51	0.90	-0.35	-0.655
	26	21	-0.205	5	-0.805	8.0	5.0	0.60	1.30	-0.505	-0.155
		10	0.495	16	-1.115	6.0	6.0	1.61	0.91	-0.31	-0.66
	27	22	-0.205	6	-0.835	8.0	5.0	0.63	1.39	-0.52	-0.14
		11	0.555	17	-1.135	6.0	6.0	1.69	0.92	-0.29	-0.675
	28	23	-0.215	6	-0.825	7.0	5.0	0.61	1.32	-0.52	-0.165
		11	0.495	18	-1.105	7.0	6.0	1.60	0.85	-0.305	-0.68
	29	24	-0.255	6	-0.885	6.0	5.0	0.63	1.28	-0.57	-0.245
		11	0.395	19	-1.1	8.0	5.0	1.50	0.82	-0.353	-0.693
	30	24	-0.285	7	-0.855	7.0	5.0	0.57	1.25	-0.57	-0.23
		12	0.395	20	-1.055	8.0	5.0	1.45	0.74	-0.33	-0.685
July	1	1	-0.315	8	-0.805	7.0	5.0	0.49	1.07	-0.56	-0.27
		13	0.265	21	-1.025	8.0	5.0	1.29	0.61	-0.38	-0.72
	2	2	-0.415	8	-0.785	6.0	6.0	0.37	0.85	-0.6	-0.36
		14	0.065	21	-0.955	7.0	5.0	1.02	0.53	-0.445	-0.69
	3	2	-0.425	9	-0.825	7.0	6.0	0.40	0.80	-0.625	-0.425
		15	-0.025	21	-0.805	6.0	6.0	0.78	0.69	-0.415	-0.46
	4	3	-0.115	10	-0.811	7.0	5.0	0.70	0.39	-0.463	-0.618
		15	-0.425	22	-0.855	7.0	6.0	0.43	0.71	-0.64	-0.5
	5	4	-0.145	11	-0.805	7.0	5.0	0.66	0.45	-0.475	-0.58
		16	-0.355	22	-0.905	6.0	6.0	0.55	0.80	-0.63	-0.505
	6	4	-0.105	12	-1.025	8.0	5.0	0.92	0.63	-0.565	-0.71
		17	-0.395	23	-0.885	6.0	7.0	0.49	1.01	-0.64	-0.38
	7	6	0.125	13	-1.105	7.0	5.0	1.23	0.78	-0.49	-0.715
		18	-0.325	24	-0.915	6.0	7.0	0.59	1.15	-0.62	-0.34
	8	7	0.235	14	-1.175	7.0	5.0	1.41	0.87	-0.47	-0.74
		19	-0.305	1	-0.905	6.0	7.0	0.60	1.21	-0.605	-0.3
	9	8	0.305	15	-1.215	7.0	5.0	1.52	0.86	-0.455	-0.785
		20	-0.355	2	-0.905	6.0	7.0	0.55	1.31	-0.63	-0.25
	10	9	0.405	16	-1.211	7.0	5.0	1.62	0.85	-0.403	-0.788
		21	-0.365	3	-0.885	6.0	7.0	0.52	1.45	-0.625	-0.16
	11	10	0.565	17	-1.215	7.0	5.0	1.78	0.84	-0.325	-0.795
		22	-0.375	4	-0.845	6.0	7.0	0.47	1.52	-0.61	-0.085
July	12	11	0.675	18	-1.225	7.0	-	1.90	-	-0.275	-
Average :			0.038		-0.928	6.9	5.5	0.97	0.96	-0.445	-0.442

Table A.1-4
TIDAL DATA at KP.180

Location : Porong River
Tidal Gauge : KP.180 (15 Km Upward from the Shortcut Mouth)
Recording period : From June 6, 1991 to July 12,1991

Date	High Water		Low Water		Duration		Range		Mean Level	
	Time	Elevation m,SHVP	Time	Elevation m,SHVP	Fall hrs	Rise hrs	Fall m	Rise m	m,SHVP	
Jun 6	9	1.056	17	0.625	8.0	3.0	0.43	0.22	0.841	0.736
	20	0.846	4	0.656	8.0	4.0	0.19	0.54	0.751	0.924
7	8	1.192	18	0.595	10.0	3.0	0.60	0.29	0.894	0.741
	21	0.886	3	0.656	6.0	6.0	0.23	0.72	0.771	1.014
8	9	1.371	19	0.571	10.0	3.0	0.80	0.35	0.971	0.744
	22	0.916	5	0.666	7.0	4.0	0.25	0.80	0.791	1.066
9	9	1.465	20	0.526	11.0	3.0	0.94	0.44	0.996	0.746
	23	0.966	6	0.676	7.0	3.0	0.29	0.95	0.821	1.151
10	9	1.625	21	0.515	12.0	3.0	1.11	0.50	1.070	0.766
	24	1.016	7	0.676	7.0	3.0	0.34	1.11	0.846	1.231
11	10	1.786	21	0.516	11.0	4.0	1.27	0.51	1.151	0.771
12	1	1.026	8	0.686	7.0	2.0	0.34	1.16	0.856	1.266
	10	1.846	22	0.506	12.0	4.0	1.34	0.58	1.176	0.796
13	2	1.086	8	0.696	6.0	3.0	0.39	1.13	0.891	1.261
	11	1.826	22	0.516	11.0	4.0	1.31	0.58	1.171	0.806
14	2	1.096	8	0.686	6.0	4.0	0.41	1.09	0.891	1.231
	12	1.776	23	0.556	11.0	4.0	1.22	0.58	1.166	0.846
15	3	1.136	9	0.706	6.0	4.0	0.43	1.01	0.921	1.211
	13	1.716	24	0.596	11.0	3.0	1.12	0.56	1.156	0.876
16	3	1.156	10	0.756	7.0	4.0	0.40	0.90	0.956	1.206
	14	1.656	1	0.646	11.0	3.0	1.01	0.55	1.151	0.921
17	4	1.196	11	0.856	7.0	4.0	0.34	0.67	1.026	1.191
	15	1.526	1	0.686	10.0	4.0	0.84	0.53	1.106	0.951
18	5	1.216	12	0.796	7.0	4.0	0.42	0.62	1.006	1.106
	16	1.416	2	0.716	10.0	4.0	0.70	0.63	1.066	1.031
19	6	1.346	13	0.816	7.0	4.0	0.53	0.38	1.081	1.006
	17	1.196	3	0.766	10.0	4.0	0.43	0.56	0.981	1.046
20	7	1.326	14	0.766	7.0	5.0	0.56	0.34	1.046	0.936
	19	1.106	4	0.896	9.0	3.0	0.21	0.55	1.001	1.171
21	7	1.446	15	0.776	8.0	5.0	0.67	0.35	1.111	0.951
	20	1.126	5	0.696	9.0	3.0	0.43	0.81	0.911	1.101
22	8	1.506	16	0.746	8.0	5.0	0.76	0.38	1.126	0.936
	21	1.126	6	0.846	9.0	3.0	0.28	0.74	0.986	1.216
23	9	1.586	17	0.656	8.0	5.0	0.93	0.48	1.121	0.896
	22	1.136	7	0.706	9.0	3.0	0.43	0.98	0.921	1.196
Jun 24	10	1.686	18	0.586	8.0	5.0	1.10	0.45	1.136	0.812
	23	1.038	8	0.706	9.0	3.0	0.33	1.04	0.872	1.226

(next page)

(Table A.1.4 Continued)

Date	High Water		Low Water		Duration		Range		Mean Level	
	Time	El. m,SHVP	Time	El. m,SHVP	Fall hrs	Rise hrs	Fall m	Rise m	m,SHVP	
Jun 25	11	1.746	19	0.526	8.0	4.0	1.22	0.53	1.136	0.791
26	23	1.056	8	0.696	9.0	4.0	0.36	1.10	0.876	1.246
	12	1.796	20	0.526	8.0	4.0	1.27	0.54	1.161	0.796
27	24	1.066	9	0.696	9.0	3.0	0.37	1.11	0.881	1.251
	12	1.806	21	0.506	9.0	4.0	1.30	0.55	1.156	0.781
28	1	1.056	9	0.716	8.0	3.0	0.34	1.03	0.886	1.231
	12	1.746	22	0.536	10.0	4.0	1.21	0.51	1.141	0.791
29	2	1.046	10	0.716	8.0	3.0	0.33	0.87	0.881	1.151
	13	1.586	23	0.586	10.0	3.0	1.00	0.44	1.086	0.806
30	2	1.026	10	0.726	8.0	3.0	0.30	0.76	0.876	1.106
	13	1.486	24	0.616	11.0	3.0	0.87	0.38	1.051	0.806
July 1	3	0.996	11	0.716	8.0	3.0	0.28	0.68	0.856	1.058
	14	1.4	24	0.716	10.0	4.0	0.68	0.25	1.058	0.843
2	4	0.97	11	0.736	7.0	4.0	0.23	0.54	0.853	1.006
	15	1.276	1	0.696	10.0	3.0	0.58	0.27	0.986	0.831
3	4	0.966	12	0.746	8.0	4.0	0.22	0.53	0.856	1.011
	16	1.276	1	0.705	9.0	4.0	0.57	0.26	0.991	0.836
4	5	0.966	13	0.756	8.0	3.0	0.21	0.34	0.861	0.926
	16	1.096	2	0.686	10.0	4.0	0.41	0.61	0.891	0.992
5	6	1.298	14	0.686	8.0	3.0	0.61	0.33	0.992	0.851
	17	1.016	2	0.706	9.0	4.0	0.31	0.75	0.861	1.081
6	6	1.456	15	0.656	9.0	4.0	0.80	0.37	1.056	0.841
	19	1.026	3	0.696	8.0	4.0	0.33	0.83	0.861	1.111
7	7	1.526	16	0.636	9.0	4.0	0.89	0.45	1.081	0.861
	20	1.086	4	0.676	8.0	4.0	0.41	1.00	0.881	1.176
8	8	1.676	17	0.606	9.0	4.0	1.07	0.48	1.141	0.846
	21	1.086	5	0.666	8.0	4.0	0.42	1.08	0.876	1.206
9	9	1.746	18	0.586	9.0	4.0	1.16	0.52	1.166	0.846
	22	1.106	6	0.756	8.0	4.0	0.35	1.05	0.931	1.281
10	10	1.806	19	0.546	9.0	4.0	1.26	0.58	1.176	0.836
	23	1.126	7	0.686	8.0	4.0	0.44	1.13	0.906	1.251
11	11	1.816	20	0.526	9.0	4.0	1.29	0.56	1.171	0.806
	24	1.086	8	0.696	8.0	4.0	0.39	1.12	0.891	1.256
July 12	12	1.816	21	0.518	9.0	-	1.30	-	1.167	-
Averag		1.316		0.666	8.7	3.7	0.65	0.65	0.991	0.994

Table A. 2-1

Longitudinal Observed Data: Salinity, Velocity and Temperature Distribution Including Calcuiation of Density and Density Index

(During an Flood Tide, Second Observation)

Date : June 27,1991
Location : From the shortcut mouth through 15 Km upward.
Station : KP.250 to KP.180

No	Time	Station & Total Depth (No..& m)	Water Depth (m)	Velocity (m/sec)	Salinity (ppt)	Temp. (C)	Density (gr/cm3)	Density index (Sigma-t)	Note
1	05.20 a.m	KP.250	0.00	0.343	23.0	26.2	1.0140	14.0	Beginning of the rising tide
			0.39	0.360	23.0	26.2	1.0140	14.0	
		1.55	0.78	0.259	23.1	26.4	1.0140	14.0	
			1.16	0.133	23.2	26.5	1.0141	14.1	
			1.55	0.000	23.3	26.6	1.0141	14.1	
2	05.45 a.m	KP.245	0.00	0.303	9.8	26.8	1.0039	3.9	
			0.43	0.373	9.8	26.8	1.0039	3.9	
		2.57	0.86	0.393	11.1	27.1	1.0048	4.8	
			1.29	0.379	12.9	27.4	1.0061	6.1	
			1.71	0.354	14.8	27.5	1.0075	7.5	
			2.14	0.198	19.1	27.6	1.0107	10.7	
			2.57	0.000	21.6	27.9	1.0124	12.4	
3	06.00 a.m	KP.240	0.00	0.244	7.1	27.4	1.0018	1.8	
			0.43	0.269	7.1	27.4	1.0018	1.8	
		2.55	0.85	0.348	7.1	27.6	1.0017	1.7	
			1.28	0.322	8.4	27.6	1.0027	2.7	
			1.70	0.250	13.5	27.6	1.0065	6.5	
			2.13	0.153	15.5	27.7	1.0079	7.9	
			2.55	0.000	19.4	27.8	1.0108	10.8	
4	06.15 a.m	KP.235	0.00	0.472	8.2	26.5	1.0028	2.8	
			0.46	0.354	8.2	26.5	1.0028	2.8	
		2.76	0.92	0.299	8.8	27.0	1.0031	3.1	
			1.38	0.266	12.7	27.1	1.0060	6.0	
			1.84	0.208	14.9	27.1	1.0077	7.7	
			2.30	0.135	16.6	27.1	1.0089	8.9	
			2.76	2.000	19.0	27.1	1.0107	10.7	
5	06.30 a.m	KP.230	0.00	0.337	5.2	27.2	1.0004	0.4	
			0.56	0.373	5.2	27.2	1.0004	0.4	
		3.34	1.11	0.472	5.2	27.3	1.0004	0.4	
			1.67	0.408	7.6	27.5	1.0021	2.1	
			2.23	0.299	9.0	27.8	1.0031	3.1	
			2.78	0.253	11.5	27.8	1.0049	4.9	
			3.34	0.000	12.9	27.9	1.0059	5.9	
6	06.45 a.m	KP.225	0.00	0.506	5.1	27.5	1.0002	0.2	
			0.33	0.408	5.1	27.5	1.0002	0 2	
		2.00	0.67	0.337	6.0	27.8	1.0008	0.8	
			1.00	0.276	6.8	28.0	1.0014	1.4	
			1.33	0.000	7.0	28.0	1.0015	1.5	
7	07.00 a.m	KP.220	0.00	0.408	5.1	27.8	1.0002	0 2	The tide is still rising
			0.48	0.354	5.1	27.8	1.0002	0.2	
		2.90	0.97	0.373	5.3	28.0	1.0002	0.2	
			1.45	0.343	6.1	28.0	1.0008	0.8	
			1.93	0.247	6.6	28.1	1.0012	1.2	
			2.42	0.176	7.4	28.2	1.0018	1.8	
			2.90	0.000	7.5	28.3	1.0018	1.8	

(continued)

Table A. 2-1 Continued

No	Time	Station & Total Depth (No..& m)	Water Depth (m)	Velocity (m/sec)	Salinity (ppt)	Temp. (C)	Density (gr/cm3)	Density index (Sigma-t)	Note
8	07.15 a.m	KP.215	0.00	0.472	5.1	27.9	1.0001	0.1	The tide is still rising
			0.52	0.386	5.1	27.9	1.0001	0.1	
		3.10	1.03	0.343	5.1	28.0	1.0001	0.1	
			1.55	0.287	5.1	28.2	1.0000	0.0	
			2.07	0.226	5.1	28.2	1.0000	0.0	
			2.58	0.299	5.3	28.3	1.0002	0.2	
			3.10	0.000	5.3	28.3	1.0002	0.2	
9	07.30 a.m	KP.210	0.00	0.506	5.0	28.3	1.0000	0.0	
			0.43	0.472	5.0	28.3	1.0000	0.0	
		2.60	0.87	0.425	5.0	28.5	1.0000	0.0	
			1.30	0.360	5.0	28.6	1.0000	0.0	
			1.73	0.206	5.0	28.7	1.0000	0.0	
			2.17	0.185	5.0	28.7	1.0000	0.0	
			2.60	0.000	5.0	28.8	1.0000	0.0	
10	07.50 a.m	KP.205	0.00	0.416	5.0	28.4	1.0000	0.0	
			0.48	0.452	5.0	28.4	1.0000	0.0	
		2.90	0.97	0.416	5.0	28.5	1.0000	0.0	
			1.45	0.366	5.0	28.5	1.0000	0.0	
			1.93	0.312	5.0	28.6	1.0000	0.0	
			2.42	0.269	5.0	28.8	1.0000	0.0	
			2.90	0.000	5.0	28.9	1.0000	0.0	
11	08.05 a.m	KP.200	0.00	0.506	5.0	28.5	1.0000	0.0	
			0.39	0.425	5.0	28.5	1.0000	0.0	
		2.32	0.77	0.416	5.0	28.8	1.0000	0.0	
			1.16	0.393	5.0	28.9	1.0000	0.0	
			1.55	0.287	5.0	28.9	1.0000	0.0	
			1.93	0.241	5.0	29.0	1.0000	0.0	
			2.32	0.000	5.0	29.0	1.0000	0.0	
12	08.20 a.r	KP.195	0.00	0.518	5.0	28.8	1.0000	0.0	
			0.28	0.625	5.0	28.8	1.0000	0.0	
		1.65	0.55	0.462	5.0	28.9	1.0000	0.0	
			0.83	0.348	5.0	29.0	1.0000	0.0	
			1.10	0.000	5.0	29.0	1.0000	0.0	
13	08.30 a.m	KP.190	0.00	0.574	5.0	28.6	1.0000	0.0	
			0.23	0.531	5.0	28.6	1.0000	0.0	
		1.36	0.45	0.483	5.0	28.6	1.0000	0.0	
			0.68	0.416	5.0	28.7	1.0000	0.0	
			0.91	0.000	5.0	28.7	1.0000	0.0	
14	08.40 a.m	KP.185	0.00	0.643	5.0	28.3	1.0000	0.0	
			0.33	0.599	5.0	28.3	1.0000	0.0	
		1.30	0.65	0.505	5.0	28.4	1.0000	0.0	
			0.98	0.324	5.0	28.4	1.0000	0.0	
			1.30	0.000	5.0	28.5	1.0000	0.0	
15	08.55 a.m	KP.180	0.00	0.411	5.0	28.2	1.0000	0.0	The tide is still rising
			0.41	0.416	5.0	28.2	1.0000	0.0	
		1.65	0.83	0.402	5.0	28.3	1.0000	0.0	
			1.24	0.327	5.0	28.3	1.0000	0.0	
			1.65	0.000	5.0	28.3	1.0000	0.0	

Table A. 2-2

Longitudinal Observed Data: Salinity, Velocity and Temperature Distribution Including Calculation of Density and Density Index

(During an Ebb Tide, First Observation)

Date : June 25,1991
Location : From 15 Km upstream to the shortcut mouth (downward)
Station : KP.180 to KP.250

No	Time	Station & Total Depth (No..& m)	Water Depth (m)	Velocity (m/sec)	Salinity (ppt)	Temp. (C)	Density (gr/cm3)	Density Index (Sigma-t)	Note
1	09.30 a.m	KP.180	0.00	0.146	5.0	28.5	1.0000	0.0	Beginning of the falling tide
			0.44	0.183	5.0	28.5	1.0000	0.0	
		1.75	0.88	0.204	5.0	28.5	1.0000	0.0	
			1.31	0.200	5.0	28.4	1.0000	0.0	
			1.75	0.000	5.0	28.3	1.0000	0.0	
2	09.45 a.m	KP.185	0.00	0.269	5.0	28.6	1.0000	0.0	
			0.36	0.327	5.0	28.6	1.0000	0.0	
		1.45	0.73	0.282	5.0	28.6	1.0000	0.0	
			1.09	0.259	5.0	28.6	1.0000	0.0	
			1.45	0.000	5.0	28.6	1.0000	0.0	
3	10.00 a.m	KP.190	0.00	0.361	5.0	29.0	1.0000	0.0	
			0.39	0.368	5.0	29.1	1.0000	0.0	
		1.55	0.78	0.354	5.0	29.1	1.0000	0.0	
			1.16	0.302	5.0	29.1	1.0000	0.0	
			1.55	0.000	5.0	29.1	1.0000	0.0	
4	10.10 a.m	KP.195	0.00	0.785	5.0	29.1	1.0000	0.0	
			0.40	0.804	5.0	29.1	1.0000	0.0	
		2.40	0.80	0.752	5.0	29.2	1.0000	0.0	
			1.20	0.707	5.0	29.3	1.0000	0.0	
			1.60	0.643	5.0	29.3	1.0000	0.0	
			2.00	0.520	5.0	29.3	1.0000	0.0	
			2.40	0.000	5.0	29.3	1.0000	0.0	
5	10.20 a.m	KP.200	0.00	0.276	5.0	29.3	1.0000	0.0	
			0.50	0.366	5.0	29.3	1.0000	0.0	
		2.00	1.00	0.330	5.0	29.4	1.0000	0.0	
			1.50	0.322	5.0	29.5	1.0000	0.0	
			2.00	0.000	5.0	29.5	1.0000	0.0	
6	10.30 a.m	KP.205	0.00	0.324	5.0	29.0	1.0000	0.0	
			0.43	0.354	5.0	29.0	1.0000	0.0	
		2.60	0.87	0.324	5.0	29.1	1.0000	0.0	
			1.30	0.302	5.0	29.2	1.0000	0.0	
			1.73	0.268	5.0	29.3	1.0000	0.0	
			2.17	0.264	5.0	29.3	1.0000	0.0	
			2.60	0.000	5.0	29.3	1.0000	0.0	
7	10.45 a.m	KP.210	0.00	0.416	5.0	29.2	1.0000	0.0	
			0.39	0.389	5.0	29.2	1.0000	0.0	
		2.35	0.78	0.393	5.0	29.2	1.0000	0.0	
			1.18	0.368	5.0	29.2	1.0000	0.0	
			1.57	0.340	5.0	29.2	1.0000	0.0	
			1.96	0.280	5.0	29.2	1.0000	0.0	
			2.35	0.000	5.0	29.2	1.0000	0.0	
8	10.55 a.m	KP.215	0.00	0.411	5.0	28.9	1.0000	0.0	The tide is still falling
			0.45	0.416	5.0	28.9	1.0000	0.0	
		2.70	0.90	0.402	5.0	28.9	1.0000	0.0	
			1.35	0.390	5.0	28.9	1.0000	0.0	
			1.80	0.327	5.0	28.9	1.0000	0.0	
			2.25	0.292	5.0	28.9	1.0000	0.0	
			2.70	0.000	5.0	28.8	1.0000	0.0	

(continued)

Table A. 2-2 Continued

No	Time	Station & Total Depth (No..& m)	Water Depth (m)	Velocity (m/sec)	Salinity (ppt)	Temp. (C)	Density (gr/cm3)	Density Index (Sigma-t	Note
9	11.05 a.m	KP.220	0.00	0.426	5.0	28.7	1.0000	0.0	The tide
			0.48	0.411	5.0	28.7	1.0000	0.0	is still falling
		2.90	0.97	0.402	5.0	28.7	1.0000	0.0	
			1.45	0.330	5.0	28.6	1.0000	0.0	
			1.93	0.256	6.0	28.5	1.0006	0.6	
			2.42	0.119	8.1	28.3	1.0023	2.3	
			2.90	0.000	8.3	28.1	1.0025	2.5	
10	11.20 a.m	KP.225	0.00	0.478	5.0	28.8	1.0000	0.0	
			0.44	0.491	5.0	28.8	1.0000	0.0	
		1.77	0.89	0.368	6.4	28.5	1.0009	0.9	
			1.33	0.215	7.2	28.4	1.0016	1.6	
			1.77	0.000	8.3	28.2	1.0024	2.4	
11	11.30 a.m	KP.230	0.00	0.376	7.3	28.6	1.0016	1.6	
			0.43	0.421	7.3	28.6	1.0016	1.6	
		2.55	0.85	0.389	7.9	28.5	1.0020	2.0	
			1.28	0.368	7.9	28.5	1.0020	2.0	
			1.70	0.287	8.2	28.4	1.0023	2.3	
			2.13	0.212	8.5	28.4	1.0025	2.5	
			2.55	0.000	9.3	28.3	1.0031	3.1	
12	11.40 a.m	KP.235	0.00	0.437	8.2	28.6	1.0022	2.2	
			0.38	0.478	8.2	28.6	1.0022	2.2	
		2.27	0.76	0.384	9.4	28.3	1.0032	3.2	
			1.14	0.276	10.0	28.1	1.0037	3.7	
			1.51	0.230	10.6	28.1	1.0042	4.2	
			1.89	0.104	11.2	28.0	1.0047	4.7	
			2.27	0.000	12.3	27.8	1.0055	5.5	
13	11.50 a.m	KP.240	0.00	0.544	9.7	28.3	1.0034	3.4	
			0.38	0.459	9.7	28.3	1.0034	3.4	
		2.28	0.76	0.453	10.7	28.1	1.0042	4.2	
			1.14	0.343	11.6	28.1	1.0049	4.9	
			1.52	0.290	12.3	27.9	1.0055	5.5	
			1.90	0.199	13.4	27.6	1.0064	6.4	
			2.28	0.000	14.0	27.5	1.0069	6.9	
14	12.00 (noon)	KP.245	0.00	0.580	11.9	28.1	1.0051	5.1	
			0.50	0.520	11.9	28.1	1.0051	5.1	
		2.00	1.00	0.411	12.5	28.1	1.0056	5.6	
			1.50	0.310	13.0	28.0	1.0060	6.0	
			2.00	0.000	13.6	27.8	1.0065	6.5	
15	00.15 p.m	KP.250	0.00	0.340	14.4	28.1	1.0070	7.0	The tide
			0.48	0.357	14.4	28.1	1.0070	7.0	is still falling
		1.90	0.95	0.274	16.2	27.8	1.0084	8.4	
			1.43	0.236	17.9	27.2	1.0099	9.9	
			1.90	0.000	18.8	27.0	1.0106	10.6	

Table A. 2-3

Longitudinal Observed Data: Salinity, Velocity and Temperature Distribution Including Calculation of Density and Density Index

(During an Ebb Tide, Second Observation)

Date : June 25,1991
Location : From 11 Km upstream to the shortcut mouth (downward)
Station : KP.200 to KP 250

No	Time	Station & Total Depth (No. & m)	Water Depth (m)	Velocity (m/sec)	Salinity (ppt)	Temp (C)	Density (gr/cm3)	Density Index (Sigma-t)	Note
1	01.00 p.m	KP 200	0.00	0.108	4.9	29.6	1.0000	0.0	Beginning of the falling tide
			0.33	0.113	4.9	29.6	1.0000	0.0	
		1.30	0.65	0.130	4.9	29.7	1.0000	0.0	
			0.98	0.094	4.9	29.7	1.0000	0.0	
			1.30	0.000	4.9	29.8	1.0000	0.0	
2	01.15 p.m	KP 205	0.00	0.153	5.0	29.2	1.0000	0.0	
			0.49	0.156	5.0	29.2	1.0000	0.0	
		1.93	0.97	0.148	5.0	29.3	1.0000	0.0	
			1.45	0.120	5.0	29.4	1.0000	0.0	
			1.93	0.000	5.0	29.5	1.0000	0.0	
3	01.30 p.m	KP.210	0.00	0.136	5.0	29.2	1.0000	0.0	
			0.40	0.128	5.0	29.2	1.0000	0.0	
		1.60	0.80	0.119	5.0	29.3	1.0000	0.0	
			1.20	0.113	5.0	29.4	1.0000	0.0	
			1.60	0.000	5.0	29.5	1.0000	0.0	
4	01.40 p.m	KP.215	0.00	0.136	5.0	29.5	1.0000	0.0	
			0.36	0.106	5.0	29.5	1.0000	0.0	
		2.14	0.71	0.088	5.0	29.6	1.0000	0.0	
			1.07	0.061	5.0	29.7	1.0000	0.0	
			1.43	0.053	5.0	29.8	1.0000	0.0	
			1.78	0.035	5.0	29.8	1.0000	0.0	
			2.14	0.000	5.0	29.8	1.0000	0.0	
5	01.50 p.m	KP.220	0.00	0.206	5.0	29.2	1.0000	0.0	
			0.36	0.144	5.0	29.2	1.0000	0.0	
		2.14	0.71	0.130	5.0	29.5	1.0000	0.0	
			1.07	0.140	5.0	29.5	1.0000	0.0	
			1.43	0.155	5.0	29.6	1.0000	0.0	
			1.78	0.109	3.0	29.6	1.0000	0.0	
			2.14	0.000	5.0	29.6	1.0000	0.0	
6	02.00 p.m	KP.225	0.00	0.126	5.0	29.1	1.0000	0.0	
			0.38	0.173	5.0	29.1	1.0000	0.0	
		1.50	0.75	0.153	5.0	29.3	1.0000	0.0	
			1.13	0.123	5.0	29.4	1.0000	0.0	
			1.50	0.000	5.0	29.5	1.0000	0.0	
7	02.10 p.m	KP.230	0.00	0.134	5.0	28.9	1.0000	0.0	
			0.37	0.135	5.0	28.9	1.0000	0.0	
		2.20	0.73	0.136	5.0	29.0	1.0000	0.0	
			1.10	0.170	5.0	29.1	1.0000	0.0	
			1.47	0.160	5.0	29.2	1.0000	0.0	
			1.83	0.163	5.0	29.2	1.0000	0.0	
			2.20	0.000	6.0	29.3	1.0004	0.4	
8	02.20 p.m	KP.235	0.00	0.142	5.0	28.9	1.0000	0.0	
			0.50	0.183	5.0	28.9	1.0000	0.0	
		2.00	1.00	0.108	5.0	29.0	1.0000	0.0	
			1.50	0.000	6.7	29.0	1.0010	1.0	
			2.00	0.000	7.5	29.0	1.0016	1.6	
9	02.30 p.m	KP.240	0.00	0.197	5.0	28.7	1.0000	0.0	
			0.44	0.217	5.0	28.7	1.0000	0.0	
		1.77	0.88	0.137	5.7	28.8	1.0003	0.3	
			1.33	0.119	6.0	28.8	1.0005	0.5	
			1.77	0.256	7.1	28.8	1.0014	1.4	
10	02.45 p.m	KP.245	0.00	0.262	5.8	28.5	1.0005	0.5	
			0.36	0.283	5.8	28.5	1.0005	0.5	
		1.45	0.73	0.269	6.4	28.7	1.0009	0.9	
			1.09	0.171	6.5	28.9	1.0009	0.9	
			1.45	0.000	9.2	28.9	1.0029	2.9	
11	03.00 p.m	KP.250	0.00	0.182	7.8	28.5	1.0020	2.0	The tide is still falling
			0.35	0.259	7.8	28.5	1.0020	2.0	
		1.40	0.70	0.250	8.7	28.6	1.0026	2.6	
			1.05	0.187	9.4	28.6	1.0031	3.1	
			1.40	0.000	10.2	28.6	1.0037	3.7	

Table A.3-1

Calculation of Tidal Area at KP.242

Location : 25 Km Upward from the Estuary Mouth
Tidal Gauge : KP.242
Recording period : From June 6, 1951 to July 24, 1951

Date		Elevation		Cross Area		Tidal Area	
		HWL	LWL	HWL	LWL	Fall	Rise
		m,SHVP	m,SHVP	m2	m2	m2	m2
June	6	-0.122	-0.602	327.91	263.96	63.95	50.16
		-0.222	-0.722	314.12	248.85	65.27	126.30
	7	0.208	-0.782	375.15	241.43	133.72	72.68
		-0.222	-0.722	314.12	248.85	65.27	139.65
	8	0.298	-0.822	388.50	236.54	151.97	77.58
		-0.222	-0.712	314.12	250.10	64.02	165.70
	9	0.478	-0.882	415.80	229.26	186.54	88.00
		-0.199	-0.692	317.27	252.60	64.67	181.84
	10	0.598	-0.912	434.44	225.66	208.78	91.74
		-0.198	-0.722	317.41	248.85	68.55	222.30
	11	0.828	-0.922	471.15	224.47	246.69	106.23
		-0.102	-0.722	330.70	248.85	81.84	237.02
	12	0.918	-0.912	485.87	225.66	260.21	109.23
	13	-0.072	-0.712	334.89	250.10	84.80	249.69
		1.002	-0.822	499.79	236.54	263.25	105.41
	14	-0.022	-0.742	341.94	246.37	95.57	241.15
		0.928	-0.882	487.52	229.26	258.26	113.24
	15	-0.018	-0.622	342.51	261.42	81.09	217.89
		0.878	-0.822	479.31	236.54	242.77	119.69
	16	0.078	-0.602	356.22	263.96	92.27	199.10
		0.778	-0.722	463.06	248.85	214.21	113.15
	17	0.118	-0.592	362.00	265.23	96.77	156.74
		0.518	-0.652	421.97	257.62	164.35	114.59
	18	0.188	-0.502	372.22	276.81	95.40	120.70
		0.358	-0.612	397.51	262.68	134.83	122.84
	19	0.278	-0.422	385.52	287.28	98.25	83.47
		0.178	-0.562	370.75	269.07	101.68	109.03
	20	0.228	-0.486	378.10	278.89	99.21	63.05
		-0.022	-0.592	341.94	265.23	76.71	120.29
	21	0.278	-0.596	385.52	264.72	120.80	80.34
		0.000	-0.496	345.06	277.59	67.47	135.14
	22	0.458	-0.642	412.73	258.88	153.85	83.06
		-0.022	-0.582	341.94	266.51	75.43	149.29
	23	0.478	-0.752	415.80	245.13	170.67	95.96
		-0.028	-0.572	341.09	267.79	73.31	157.29
June	24	0.538	-0.812	425.08	237.76	187.32	110.44
		0.022	-0.612	348.20	262.68	85.51	168.62

(next page)

(Table A3-1 Continued)

Date		Elevation		Cross Area		Tidal Area	
		HWL m,SHVP	LWL m,SHVP	HWL m2	LWL m2	Fall m2	Rise m2
June	25	0.578	-0.892	431.31	228.06	203.25	124.43
	26	0.052	-0.562	352.49	269.07	83.42	168.51
		0.618	-0.882	437.58	229.26	208.32	128.98
	27	0.092	-0.622	358.24	261.42	96.83	188.83
		0.698	-0.902	450.24	226.86	223.38	134.27
	28	0.112	-0.602	361.13	263.96	97.18	179.93
		0.658	-0.922	443.89	224.47	219.43	128.02
	29	0.052	-0.682	352.49	253.85	98.64	177.46
		0.578	-0.922	431.31	224.47	206.84	117.48
	30	-0.022	-0.702	341.94	251.35	90.60	170.63
		0.518	-0.872	421.97	230.47	191.50	111.47
July	1	-0.022	-0.682	341.94	253.85	88.09	161.95
		0.478	-0.722	415.80	248.85	166.95	79.05
	2	-0.122	-0.612	327.91	262.68	65.22	119.86
		0.258	-0.722	382.55	248.85	133.69	83.24
	3	-0.092	-0.552	332.09	270.35	61.74	100.39
		0.178	-0.552	370.75	270.35	100.39	98.93
	4	0.168	-0.492	369.29	278.11	91.17	56.78
		-0.072	-0.552	334.89	270.35	64.54	103.33
	5	0.198	-0.552	373.68	270.35	103.33	74.42
		-0.002	-0.692	344.78	252.60	92.18	129.95
	6	0.258	-0.792	382.55	240.21	142.34	105.00
		0.001	-0.592	345.21	265.23	79.97	132.28
	7	0.358	-0.822	397.51	236.54	160.98	108.67
		0.001	-0.602	345.21	263.96	81.25	141.13
	8	0.408	-0.872	405.09	230.47	174.62	112.89
		-0.012	-0.612	343.36	262.68	80.67	153.12
	9	0.478	-0.892	415.80	228.06	187.74	112.47
		-0.032	-0.622	340.53	261.42	79.11	162.11
	10	0.528	-0.912	423.52	225.66	197.86	112.04
		-0.052	-0.592	337.71	265.23	72.47	194.61
	11	0.758	-0.982	459.84	217.34	242.50	100.89
		-0.192	-0.622	318.23	261.42	56.81	209.74
July	12	0.828	-0.902	471.15	226.86	244.29	-
Average :		0.245	-0.705	381.96	251.22	130.74	131.16

Table A 3-2

Calculation of Tidal Area at KP.236

Location [illegible]
Tidal Gauge [illegible]
According period [illegible]

Date		Elevation		Cross Area		Tidal Area	
		HWL m,SHVP	LWL m,SHVP	HWL m2	LWL m2	Fall m2	Rise m2
June	6	0.061	-0.401	351.33	273.96	77.37	61.24
		-0.031	-0.481	335.20	261.48	73.72	148.71
	7	0.381	-0.501	410.19	258.40	151.79	75.59
		-0.038	-0.421	333.99	270.82	63.18	153.21
	8	0.453	-0.521	424.03	255.34	168.69	85.08
		-0.001	-0.386	340.42	276.33	64.09	185.87
	9	0.646	-0.521	462.21	255.34	206.87	92.45
		0.041	-0.411	347.79	272.39	75.41	227.89
	10	0.831	-0.581	500.27	246.26	254.02	110.41
		0.091	-0.381	356.66	277.13	79.54	261.57
	11	1.011	-0.581	538.70	246.26	292.44	121.19
	12	0.151	-0.381	367.45	277.13	90.32	274.69
		1.071	-0.591	551.81	244.76	307.05	126.32
	13	0.171	-0.401	371.08	273.96	97.11	302.28
		1.181	-0.571	576.24	247.76	328.48	126.96
	14	0.191	-0.361	374.72	280.30	94.42	291.46
		1.161	-0.501	571.76	258.40	313.36	129.21
	15	0.261	-0.301	387.61	289.95	97.67	266.27
		1.091	-0.491	556.21	259.94	296.28	131.39
	16	0.281	-0.251	391.33	298.09	93.24	210.60
		0.871	-0.481	508.70	261.48	247.22	146.81
	17	0.371	-0.241	408.29	299.74	108.55	165.50
		0.661	-0.391	465.24	275.54	189.70	148.10
	18	0.451	-0.221	423.64	303.03	120.61	138.21
		0.541	-0.331	441.24	285.11	156.14	148.27
	19	0.501	-0.231	433.38	301.38	132.00	108.81
		0.381	-0.311	410.19	288.33	121.86	154.89
	20	0.551	-0.231	443.22	301.38	141.84	97.44
		0.321	-0.301	398.83	289.95	108.88	135.64
	21	0.461	-0.291	425.58	291.57	134.02	94.19
		0.251	-0.211	385.76	304.69	81.07	160.55
	22	0.661	-0.351	465.24	281.90	183.34	98.32
		0.221	-0.201	380.22	306.35	73.87	173.17
	23	0.731	-0.455	479.52	265.51	214.01	116.55
		0.231	-0.191	382.06	308.01	74.05	204.92
June	24	0.891	-0.491	512.93	259.94	252.99	127.67
		0.261	-0.251	387.61	298.09	89.52	206.38

(next page)

(Table A3-2 Continued)

Date		Elevation		Cross Area		Tidal Area	
		HWL m,SHVP	LWL m,SHVP	HWL m2	LWL m2	Fall m2	Rise m2
June	25	0.851	-0.491	504.48	259.94	244.54	114.78
	26	0.191	-0.251	374.72	298.09	76.63	214.84
		0.891	-0.501	512.93	258.40	254.53	116.32
	27	0.191	-0.261	374.72	296.46	78.26	250.97
		1.051	-0.511	547.42	256.87	290.55	138.20
	28	0.301	-0.201	395.07	306.35	88.72	232.35
		1.011	-0.501	538.70	258.40	280.30	116.32
	29	0.191	-0.271	374.72	294.82	79.90	224.40
		0.921	-0.491	519.32	259.94	259.38	116.61
	30	0.201	-0.291	376.55	291.57	84.98	221.36
		0.891	-0.471	512.93	263.03	249.91	127.56
July	1	0.277	-0.231	390.59	301.38	89.20	184.32
		0.761	-0.376	485.70	277.92	207.78	96.80
	2	0.191	-0.201	374.72	306.35	68.37	137.07
		0.552	-0.391	443.42	275.54	167.88	99.18
	3	0.191	-0.193	374.72	307.68	67.04	119.85
		0.471	-0.241	427.53	299.74	127.79	118.12
	4	0.421	-0.181	417.85	309.68	108.17	66.87
		0.201	-0.291	376.55	291.57	84.98	126.29
	5	0.421	-0.291	417.85	291.57	126.29	84.98
		0.201	-0.401	376.55	273.96	102.59	161.38
	6	0.511	-0.471	435.34	263.03	172.31	111.70
		0.191	-0.301	374.72	289.95	84.78	163.22
	7	0.601	-0.501	453.17	258.40	194.76	113.95
		0.178	-0.391	372.35	275.54	96.81	216.38
	8	0.791	-0.561	491.92	249.27	242.65	142.07
		0.281	-0.271	391.33	294.82	96.51	190.88
	9	0.761	-0.571	485.70	247.76	237.94	128.79
		0.201	-0.311	376.55	288.33	88.22	205.68
	10	0.801	-0.481	494.00	261.48	232.52	116.90
		0.211	-0.301	378.38	289.95	88.44	255.29
	11	1.041	-0.481	545.24	261.48	283.76	115.07
		0.201	-0.201	376.55	306.35	70.20	252.07
July	12	1.101	-0.571	558.42	247.76	310.66	-
Average :		0.487	-0.376	433.12	278.30	154.82	155.55

Table A3-3

Calculation of Tidal Area at SB.5

Location: [illegible] River
Tidal Range: [illegible] 7.50 m Downward
Recording period: [illegible] June 6, 1991 to [illegible]

Date		Elevation		Cross Area		Tidal Area	
		HWL m,SHVP	LWL m,SHVP	HWL m2	LWL m2	Fall m2	Rise m2
June	6	-0.145	-0.625	41.02	21.58	19.44	11.60
		-0.325	-0.855	33.18	13.94	19.25	34.13
	7	0.005	-0.825	48.07	14.87	33.19	20.00
		-0.285	-0.945	34.87	11.24	23.63	40.77
	8	0.085	-1.055	52.01	8.17	43.84	25.44
		-0.315	-0.875	33.60	13.32	20.28	50.75
	9	0.315	-1.095	64.07	7.11	56.96	26.49
		-0.315	-0.875	33.60	13.32	20.28	59.20
	10	0.465	-1.045	72.52	8.43	64.09	26.01
		-0.295	-0.915	34.44	12.12	22.32	71.77
	11	0.655	-1.195	83.89	4.61	79.28	31.11
		-0.265	-0.915	35.72	12.12	23.60	74.88
	12	0.705	-1.185	87.00	4.85	82.15	31.30
	13	-0.255	-0.915	36.15	12.12	24.03	78.05
		0.755	-1.145	90.17	5.83	84.33	30.75
	14	-0.245	-0.875	36.59	13.32	23.26	77.48
		0.765	-1.135	90.81	6.09	84.72	32.69
	15	-0.195	-0.815	38.78	15.19	23.59	74.34
		0.745	-1.115	89.53	6.59	82.94	32.63
	16	-0.185	-0.721	39.22	18.26	20.96	60.75
		0.575	-0.975	79.01	10.38	68.64	30.20
	17	-0.155	-0.785	40.57	16.15	24.42	56.38
		0.465	-0.915	72.52	12.12	60.41	30.74
	18	-0.105	-0.665	42.86	20.18	22.68	43.90
		0.315	-0.785	64.07	16.15	47.92	39.42
	19	0.155	-0.645	55.57	20.88	34.69	21.34
		-0.119	-0.805	42.21	15.51	26.71	38.52
	20	0.125	-0.655	54.03	20.52	33.50	17.81
		-0.205	-0.805	38.34	15.51	22.83	40.06
	21	0.155	-0.705	55.57	18.80	36.77	17.79
		-0.245	-0.835	36.59	14.56	22.03	48.42
	22	0.295	-0.915	62.98	12.12	50.86	24.90
		-0.235	-0.745	37.02	17.46	19.56	48.82
	23	0.355	-1.005	66.28	9.53	56.75	27.06
		-0.245	-0.775	36.59	16.47	20.11	49.25
June	24	0.345	-1.035	65.73	8.71	57.02	29.19
		-0.215	-0.805	37.90	15.51	22.39	53.58

(next page)

(Table A3-3 Continued)

Date		Elevation		Cross Area		Tidal Area	
		HWL m,SHVP	LWL m,SHVP	HWL m2	LWL m2	Fall m2	Rise m2
June	25	0.405	-1.105	69.09	6.85	62.24	31.49
	26	-0.205	-0.805	38.34	15.51	22.83	58.76
		0.495	-1.115	74.27	6.59	67.68	31.74
	27	-0.205	-0.835	38.34	14.56	23.78	63.26
		0.555	-1.135	77.82	6.09	71.73	31.81
	28	-0.215	-0.825	37.90	14.87	23.02	59.40
		0.495	-1.105	74.27	6.85	67.42	29.30
	29	-0.255	-0.885	36.15	13.02	23.14	55.51
		0.395	-1.100	68.52	6.98	61.54	27.89
	30	-0.285	-0.855	34.87	13.94	20.93	54.59
		0.395	-1.055	68.52	8.17	60.36	25.44
July	1	-0.315	-0.805	33.60	15.51	18.09	45.85
		0.265	-1.025	61.36	8.98	52.38	20.53
	2	-0.415	-0.785	29.51	16.15	13.36	34.86
		0.065	-0.955	51.01	10.95	40.06	18.16
	3	-0.425	-0.825	29.11	14.87	14.24	31.75
		-0.025	-0.805	46.62	15.51	31.11	26.89
	4	-0.115	-0.811	42.40	15.32	27.08	13.80
		-0.425	-0.855	29.11	13.94	15.18	27.09
	5	-0.145	-0.805	41.02	15.51	25.52	16.43
		-0.355	-0.905	31.94	12.42	19.52	30.44
	6	-0.105	-1.025	42.86	8.98	33.88	21.33
		-0.395	-0.885	30.31	13.02	17.29	41.01
	7	0.125	-1.105	54.03	6.85	47.18	26.33
		-0.325	-0.915	33.18	12.12	21.06	47.64
	8	0.235	-1.175	59.75	5.09	54.66	28.93
		-0.305	-0.905	34.02	12.42	21.60	51.11
	9	0.305	-1.215	63.53	4.14	59.39	27.80
		-0.355	-0.905	31.94	12.42	19.52	56.67
	10	0.405	-1.211	69.09	4.23	64.86	27.30
		-0.365	-0.885	31.53	13.02	18.51	65.40
	11	0.565	-1.215	78.41	4.14	74.28	26.99
		-0.375	-0.845	31.12	14.25	16.88	70.88
July	12	0.675	-1.225	85.13	3.90	81.23	-
Average :		0.038	-0.928	51.01	11.98	39.03	39.06

Table A.3-4

Calculation of Tidal Area at KP.180

Location : 1.5 Km Upward from the River Mouth
Tidal Gauge : KP.180
Recording period : From June 6, 1991 to July [illegible]

Date		Elevation		Cross Area		Tidal Area	
		HWL m,SHVP	LWL m,SHVP	HWL m2	LWL m2	Fall m2	Rise m2
June	6	1.056	0.625	245.06	199.91	45.15	22.84
		0.846	0.656	222.75	203.07	19.67	56.76
	7	1.192	0.595	259.83	196.86	62.97	30.09
		0.886	0.656	226.95	203.07	23.88	76.58
	8	1.371	0.571	279.66	194.43	85.22	35.69
		0.916	0.666	230.12	204.10	26.02	86.14
	9	1.465	0.526	290.24	189.90	100.34	45.53
		0.966	0.676	235.43	205.12	30.30	103.41
	10	1.625	0.515	308.53	188.79	119.74	51.97
		1.016	0.676	240.77	205.12	35.64	122.17
	11	1.786	0.516	327.29	188.89	138.40	52.95
	12	1.026	0.686	241.84	206.15	35.69	128.22
		1.846	0.506	334.37	187.89	146.48	60.41
	13	1.086	0.696	248.30	207.18	41.12	124.83
		1.826	0.516	332.01	188.89	143.11	60.49
	14	1.096	0.686	249.38	206.15	43.23	119.97
		1.776	0.556	326.12	192.92	133.20	60.80
	15	1.136	0.706	253.72	208.20	45.52	110.89
		1.716	0.596	319.09	196.96	122.13	58.93
	16	1.156	0.756	255.90	213.37	42.53	98.75
		1.656	0.646	312.12	202.05	110.07	58.22
	17	1.196	0.856	260.27	223.80	36.47	73.38
		1.526	0.686	297.17	206.15	91.03	56.32
	18	1.216	0.796	262.47	217.52	44.94	67.19
		1.416	0.716	284.71	209.23	75.47	67.63
	19	1.346	0.816	276.86	219.61	57.25	40.66
		1.196	0.766	260.27	214.40	45.87	60.23
	20	1.326	0.766	274.63	214.40	60.23	36.06
		1.106	0.896	250.46	228.01	22.46	60.09
	21	1.446	0.776	288.09	215.44	72.65	37.19
		1.126	0.696	252.63	207.18	45.46	87.72
	22	1.506	0.746	294.90	212.33	82.56	40.30
		1.126	0.846	252.63	222.75	29.89	81.30
	23	1.586	0.656	304.04	203.07	100.97	50.65
		1.136	0.706	253.72	208.20	45.52	107.40
June	24	1.686	0.586	315.60	195.95	119.65	47.18
		1.038	0.706	243.13	208.20	34.92	114.39

(next page)

(Table A.3-4 Continued)

Date		Elevation		Cross Area		Tidal Area	
		HWL m,SHVP	LWL m,SHVP	HWL m2	LWL m2	Fall m2	Rise m2
June	25	1.746	0.526	322.60	189.90	132.70	55.17
	26	1.056	0.696	245.06	207.18	37.89	121.29
		1.796	0.526	328.47	189.90	138.57	56.24
	27	1.066	0.696	246.14	207.18	38.96	122.47
		1.806	0.506	329.65	187.89	141.76	57.17
	28	1.056	0.716	245.06	209.23	35.83	113.36
		1.746	0.536	322.60	190.90	131.70	53.08
	29	1.046	0.716	243.99	209.23	34.75	94.81
		1.586	0.586	304.04	195.95	108.09	45.89
	30	1.026	0.726	241.84	210.27	31.57	82.36
		1.486	0.616	292.62	199.00	93.63	39.63
July	1	0.996	0.716	238.63	209.23	29.39	73.68
		1.400	0.716	282.91	209.23	73.68	26.62
	2	0.970	0.736	235.85	211.30	24.55	57.78
		1.276	0.696	269.08	207.18	61.91	28.25
	3	0.966	0.746	235.43	212.33	23.09	56.75
		1.276	0.736	269.08	208.10	60.98	27.32
	4	0.966	0.756	235.43	213.37	22.06	36.01
		1.096	0.686	249.38	206.15	43.23	65.37
	5	1.298	0.686	271.52	206.15	65.37	34.62
		1.016	0.706	240.77	208.20	32.56	81.02
	6	1.456	0.656	289.22	203.07	86.15	38.76
		1.026	0.696	241.84	207.18	34.66	90.00
	7	1.526	0.636	297.17	201.03	96.14	47.27
		1.086	0.676	248.30	205.12	43.18	109.32
	8	1.676	0.606	314.44	197.98	116.46	50.32
		1.086	0.666	248.30	204.10	44.20	118.50
	9	1.746	0.586	322.60	195.95	126.65	54.51
		1.106	0.756	250.46	213.37	37.10	116.28
	10	1.806	0.546	329.65	191.91	137.74	60.72
		1.126	0.686	252.63	206.15	46.49	124.68
	11	1.816	0.526	330.83	189.90	140.93	58.40
		1.086	0.696	248.30	207.18	41.12	123.65
July	12	1.816	0.518	330.83	189.09	141.73	-
Average :		1.316	0.666	274.17	204.16	70.01	70.21

Table A. 4-1

Calculation of Tidal Volume (KP.242 - KP.236)

Location : Between KP.242 and KP.236
Distance : 1.2 km
Recording period : From June 6, 1991 to July 12,1991

Date		Tidal Area				Tidal Volume	
		KP.242		KP.250		KP.242 --> KP.236	
		Fall m2	Rise m2	Fall m2	Rise m2	Fall m3	Rise m3
June	6	63.95	50.16	77.37	61.24	84,790	66,842
		65.27	126.30	73.72	148.71	83,394	165,008
	7	133.72	72.68	151.79	75.59	171,307	88,965
		65.27	139.65	63.18	153.21	77,065	175,720
	8	151.97	77.58	168.69	85.08	192,396	97,599
		64.02	165.70	64.09	185.87	76,866	210,946
	9	186.54	88.00	206.87	92.45	236,042	108,274
		64.67	181.84	75.41	227.89	84,047	245,838
	10	208.78	91.74	254.02	110.41	277,678	121,290
		68.55	222.30	79.54	261.57	88,854	290,324
	11	246.69	106.23	292.44	121.19	323,478	136,452
		81.84	237.02	90.32	274.69	103,298	307,023
	12	260.21	109.23	307.05	126.32	340,358	141,331
	13	84.80	249.69	97.11	302.28	109,146	331,183
		263.25	105.41	328.48	126.96	355,042	139,420
	14	95.57	241.15	94.42	291.46	113,993	319,565
		258.26	113.24	313.36	129.21	342,970	145,473
	15	81.09	217.89	97.67	266.27	107,257	290,496
		242.77	119.69	296.28	131.39	323,427	150,649
	16	92.27	199.10	93.24	210.60	111,303	245,823
		214.21	113.15	247.22	146.81	276,854	155,975
	17	96.77	156.74	108.55	165.50	123,194	193,347
		164.35	114.59	189.70	148.10	212,431	157,618
	18	95.40	120.70	120.61	138.21	129,607	155,346
		134.83	122.84	156.14	148.27	174,580	162,665
	19	98.25	83.47	132.00	108.81	138,144	115,369
		101.68	109.03	121.86	154.89	134,126	158,356
	20	99.21	63.05	141.84	97.44	144,628	96,295
		76.71	120.29	108.88	135.64	111,355	153,556
	21	120.80	80.34	134.02	94.19	152,889	104,720
		67.47	135.14	81.07	160.55	89,123	177,411
	22	153.85	83.06	183.34	98.32	202,310	108,827
		75.43	149.29	73.87	173.17	89,583	193,476
	23	170.67	95.96	214.01	116.55	230,807	127,510
		73.31	157.29	74.05	204.92	88,413	217,323
June	24	187.32	110.44	252.99	127.67	264,186	142,867
		85.51	168.62	89.52	206.38	105,017	225,003

(next page)

(Table A 4-1 Continued)

Date		Tidal Area				Tidal Volume	
		KP.242		KP.250		KP.242 --> KP.236	
		Fall m2	Rise m2	Fall m2	Rise m2	Fall m3	Rise m3
June	25	203.25	124.43	244.54	114.78	268,671	143,525
	26	83.42	168.51	76.63	214.84	96,026	230,008
		208.32	128.98	254.53	116.32	277,707	147,178
	27	96.83	188.83	78.26	250.97	105,055	263,876
		223.38	134.27	290.55	138.20	308,362	163,486
	28	97.18	179.93	88.72	232.35	111,540	247,370
		219.43	128.02	280.30	116.32	299,834	146,604
	29	98.64	177.46	79.90	224.49	107,122	241,172
		206.84	117.48	259.38	116.61	279,732	140,453
	30	90.60	170.63	84.98	221.36	105,348	235,196
		191.50	111.47	249.91	127.56	264,845	143,421
July	1	88.09	161.95	89.20	184.32	106,379	207,761
		166.95	79.05	207.78	96.80	224,838	105,514
	2	65.22	119.86	68.37	137.07	80,157	154,158
		133.69	83.24	167.88	99.18	180,942	109,451
	3	61.74	100.39	67.04	119.85	77,267	132,144
		100.39	98.93	127.79	118.12	136,910	130,228
	4	91.17	56.78	108.17	66.87	119,607	74,191
		64.54	103.33	84.98	126.29	89,714	137,770
	5	103.23	74.42	126.29	84.98	137,770	95,645
		92.18	129.95	102.59	161.38	116,862	174,796
	6	142.34	105.00	172.31	111.70	188,793	130,017
		79.97	132.28	84.78	163.22	98,850	177,302
	7	160.98	108.67	194.76	113.95	213,445	133,570
		81.25	141.13	96.81	216.38	106,834	214,508
	8	174.62	112.89	242.65	142.07	250,365	152,973
		80.67	153.12	96.51	190.88	106,312	206,397
	9	187.74	112.47	237.94	128.79	255,408	144,754
		79.11	162.11	88.22	205.68	100,401	220,671
	10	197.86	112.04	232.52	116.90	258,231	137,369
		72.47	194.61	88.44	255.29	96,548	269,940
	11	242.50	100.89	283.76	115.07	315,754	129,575
		56.81	209.74	70.20	252.07	76,209	277,087
July	12	244.29	-	310.66	-	332,974	-
Average :		130.74	131.16	154.82	155.55	171,335	172,029

Table A 4-2

Calculation of Tidal Volume (KP.236 - KP.180)

Location : Between KP.236 and KP.180
Distance : 11.2 km
Recording period : From June 6, 1991 to July 12,1991

Date		Tidal Area				Tidal Volume	
		KP.236		KP.180		KP.236 --> KP.180	
		Fall m2	Rise m2	Fall m2	Rise m2	Fall m3	Rise m3
June	6	77.37	61.24	45.15	22.84	686,094	470,839
		73.72	148.71	19.67	56.76	523,026	1,150,633
	7	151.79	75.59	62.97	30.09	1,202,660	591,808
		63.18	153.21	23.88	76.58	487,497	1,286,863
	8	168.69	85.08	85.22	35.69	1,421,929	676,312
		64.09	185.87	26.02	86.14	504,625	1,523,300
	9	206.87	92.45	100.34	45.53	1,720,386	772,697
		75.41	227.89	30.30	103.41	591,968	1,855,275
	10	254.02	110.41	119.74	51.97	2,093,057	909,330
		79.54	261.57	35.64	122.17	645,016	2,148,963
	11	292.44	121.19	138.40	52.95	2,412,715	975,161
		90.32	274.69	35.69	128.22	705,664	2,256,295
	12	307.05	126.32	146.48	60.41	2,539,803	1,045,673
	13	97.11	302.28	41.12	124.83	774,124	2,391,828
		328.48	126.96	143.11	60.49	2,640,947	1,049,714
	14	94.42	291.46	43.23	119.97	770,829	2,303,988
		313.36	129.21	133.20	60.80	2,500,740	1,064,075
	15	97.67	266.27	45.52	110.89	801,826	2,112,090
		296.28	131.39	122.13	58.93	2,343,071	1,065,843
	16	93.24	210.60	42.53	98.75	760,309	1,732,370
		247.22	146.81	110.07	58.22	2,000,774	1,148,142
	17	108.55	165.50	36.47	73.38	812,137	1,337,732
		189.70	148.10	91.03	56.32	1,572,056	1,144,749
	18	120.61	138.21	44.94	67.19	927,090	1,150,208
		156.14	148.27	75.47	67.63	1,297,027	1,209,045
	19	132.00	108.81	57.25	40.66	1,059,792	837,035
		121.86	154.89	45.87	60.23	939,292	1,204,669
	20	141.84	97.44	60.23	36.06	1,131,555	747,606
		108.88	135.64	22.46	60.09	735,493	1,096,053
	21	134.02	94.19	72.65	37.19	1,157,329	735,739
		81.07	160.55	45.46	87.72	708,543	1,390,313
	22	183.34	98.32	82.56	40.30	1,489,053	776,274
		73.87	173.17	29.89	81.30	581,038	1,425,002
	23	214.01	116.55	100.97	50.65	1,763,887	936,323
		74.05	204.92	45.52	107.40	669,565	1,748,956
June	24	252.99	127.67	119.65	47.18	2,086,794	979,154
		89.52	206.38	34.92	114.39	696,860	1,796,350

(next page)

(Table A 4-2 Continued)

Date		Tidal Area				Tidal Volume	
		KP.236		KP.180		KP.236 --> KP.180	
		Fall m2	Rise m2	Fall m2	Rise m2	Fall m3	Rise m3
June	25	244.54	114.78	132.70	55.17	2,112,545	951,706
	26	76.63	214.84	37.89	121.29	641,272	1,882,327
		254.53	116.32	138.57	56.24	2,201,369	966,348
	27	78.26	250.97	38.96	122.47	656,481	2,091,255
		290.55	138.20	141.76	57.17	2,420,945	1,094,099
	28	88.72	232.35	35.83	113.36	697,478	1,936,000
		280.30	116.32	131.70	53.08	2,307,166	948,657
	29	79.90	224.49	34.75	94.81	642,043	1,788,097
		259.38	116.61	108.09	45.89	2,057,834	909,991
	30	84.98	221.36	31.57	82.36	652,710	1,700,841
		249.91	127.56	93.63	39.63	1,923,783	936,275
July	1	89.20	184.32	29.39	73.68	664,132	1,444,758
		207.78	96.80	73.68	26.62	1,576,164	691,149
	2	68.37	137.07	24.55	57.78	520,378	1,091,168
		167.88	99.18	61.91	28.25	1,286,777	713,602
	3	67.04	119.85	23.09	56.75	504,751	988,930
		127.79	118.12	60.98	27.32	1,057,104	814,467
	4	108.17	66.87	22.06	36.01	729,289	576,137
		84.98	126.29	43.23	65.37	718,006	1,073,287
	5	126.29	84.98	65.37	34.62	1,073,287	669,763
		102.59	161.38	32.56	81.02	756,833	1,357,412
	6	172.31	111.70	86.15	38.76	1,447,384	842,567
		84.78	163.22	34.66	90.00	668,852	1,418,029
	7	194.76	113.95	96.14	47.27	1,629,075	902,801
		96.81	216.38	43.18	109.32	783,912	1,823,895
	8	242.65	142.07	116.46	50.32	2,011,033	1,077,358
		96.51	190.88	44.20	118.50	787,987	1,732,528
	9	237.94	128.79	126.65	54.51	2,041,702	1,026,497
		88.22	205.68	37.10	116.28	701,779	1,802,948
	10	232.52	116.90	137.74	60.72	2,073,463	994,712
		88.44	255.29	46.49	124.68	755,569	2,127,825
	11	283.76	115.07	140.93	58.40	2,378,238	971,442
		70.20	252.07	41.12	123.65	623,413	2,104,059
July	12	310.66	-	141.73	-	2,533,421	-
Average :		154.82	155.55	70.01	70.21	1,259,025	1,264,248

Table A. 4-3

Calculation of Tidal Volume (KP.180 - Td. Limit)

Location : [illegible] KP.180 and Tidal Limit [illegible]
Distance : [illegible]
Recording period : From June 6, 1991 to July 12,1991

Date		Tidal Area		Range		Tidal Volume	
		KP.180		KP.180		KP.180 --> LIMIT	
		Fall	Rise	Fall	Rise	Fall	Rise
		m2	m2	m	m	m3	m3
June	6	45.15	22.84	0.43	0.22	139,000	36,049
		19.67	56.76	0.19	0.54	26,699	217,303
	7	62.97	30.09	0.60	0.29	268,524	62,543
		23.88	76.58	0.23	0.72	39,227	391,117
	8	85.22	35.69	0.80	0.35	486,998	87,943
		26.02	86.14	0.25	0.80	46,467	491,635
	9	100.34	45.53	0.94	0.44	673,028	143,090
		30.30	103.41	0.29	0.95	62,770	700,985
	10	119.74	51.97	1.11	0.50	949,384	185,990
		35.64	122.17	0.34	1.11	86,562	968,633
	11	138.40	52.95	1.27	0.51	1,255,483	192,871
		35.69	128.22	0.34	1.16	86,674	1,062,433
	12	146.48	60.41	1.34	0.58	1,402,053	250,266
	13	41.12	124.83	0.39	1.13	114,557	1,007,570
		143.11	60.49	1.31	0.58	1,339,145	250,592
	14	43.23	119.97	0.41	1.09	126,608	934,042
		133.20	60.80	1.22	0.58	1,160,739	251,898
	15	45.52	110.89	0.43	1.01	139,800	799,986
		122.13	58.93	1.12	0.56	977,035	235,738
	16	42.53	98.75	0.40	0.90	121,517	634,828
		110.07	58.22	1.01	0.55	794,047	228,715
	17	36.47	73.38	0.34	0.67	88,581	351,167
		91.03	56.32	0.84	0.53	546,159	213,201
	18	44.94	67.19	0.42	0.62	134,828	297,539
		75.47	67.63	0.70	0.63	377,375	304,326
	19	57.25	40.66	0.53	0.38	216,745	110,369
		45.87	60.23	0.43	0.56	140,876	240,911
	20	60.23	36.06	0.56	0.34	240,911	87,571
		22.46	60.09	0.21	0.55	33,686	236,053
	21	72.65	37.19	0.67	0.35	347,682	92,977
		45.46	87.72	0.43	0.81	139,620	507,526
	22	82.56	40.30	0.76	0.38	448,203	109,389
		29.89	81.30	0.28	0.74	59,771	429,706
	23	100.97	50.65	0.93	0.48	670,721	173,643
		45.52	107.40	0.43	0.98	139,800	751,770
June	24	119.65	47.18	1.10	0.45	940,104	152,310
		34.92	114.39	0.33	1.04	82,814	849,790

(next page)

(Table A 4-3 Continued)

Date		Tidal Area KP.180		Range KP.180		Tidal Volume KP.180 --> LIMIT	
		Fall m2	Rise m2	Fall m	Rise m	Fall m3	Rise m3
June	25	132.70	55.17	1.22	0.53	1,156,406	208,840
	26	37.89	121.29	0.36	1.10	97,422	953,020
		138.57	56.24	1.27	0.54	1,257,048	216,937
	27	38.96	122.47	0.37	1.11	102,976	971,024
		141.76	57.17	1.30	0.55	1,316,318	224,605
	28	35.83	113.36	0.34	1.03	87,011	834,042
		131.70	53.08	1.21	0.51	1,138,236	193,376
	29	34.75	94.81	0.33	0.87	81,915	589,172
		108.09	45.89	1.00	0.44	772,094	144,217
	30	31.57	82.36	0.30	0.76	67,654	447,082
		93.63	39.63	0.87	0.38	581,827	107,567
July	1	29.39	73.68	0.28	0.68	58,782	359,958
		73.68	26.62	0.68	0.25	359,958	48,291
	2	24.55	57.78	0.23	0.54	41,039	222,879
		61.91	28.25	0.58	0.27	256,468	54,482
	3	23.09	56.75	0.22	0.53	36,289	214,837
		60.98	27.32	0.57	0.26	248,713	50,940
	4	22.06	36.01	0.21	0.34	33,086	87,459
		43.23	65.37	0.41	0.61	126,608	285,767
	5	65.37	34.62	0.61	0.33	285,767	81,598
		32.56	81.02	0.31	0.75	72,100	434,030
	6	86.15	38.76	0.80	0.37	492,277	102,445
		34.66	90.00	0.33	0.83	81,703	533,567
	7	96.14	47.27	0.89	0.45	611,191	151,928
		43.18	109.32	0.41	1.00	126,445	780,827
	8	116.46	50.32	1.07	0.48	890,081	172,525
		44.20	118.50	0.42	1.08	132,603	914,152
	9	126.65	54.51	1.16	0.52	1,049,375	202,477
		37.10	116.28	0.35	1.05	92,739	872,095
	10	137.74	60.72	1.26	0.58	1,239,641	251,572
		46.49	124.68	0.44	1.13	146,096	1,006,331
	11	140.93	58.40	1.29	0.56	1,298,567	233,608
		41.12	123.65	0.39	1.12	114,557	989,207
July	12	141.73	-	1.30	-	1,314,069	-
Average :		70.01	70.21	0.65	0.65	431,990	385,476

Table A 4-4

Calculation of Tidal Volume (Org. River Mouth - SB.5)

Location : Between Original river Mouth & SB.5
Distance : 6 km
Recording period : From June 6, 1991 to July 12,1991

Date		Tidal Area				Tidal Volume	
		River Mouth		SB.5		River Mouth --> SB.5	
		Fall	Rise	Fall	Rise	Fall	Rise
		m2	m2	m2	m2	m3	m3
June	6	80.57	63.28	19.44	11.60	250,016	187,194
		89.06	167.78	19.25	34.13	270,762	504,769
	7	169.10	90.38	33.19	20.00	505,728	275,935
		81.06	174.08	23.63	40.77	261,730	537,132
	8	189.94	98.48	43.84	25.44	584,465	309,778
		87.96	219.03	20.28	50.75	270,598	674,442
	9	237.14	107.63	56.96	26.49	735,268	335,316
		90.84	246.48	20.28	59.20	277,808	764,214
	10	263.40	118.76	64.09	26.01	818,728	361,931
		100.52	281.78	22.32	71.77	307,107	883,875
	11	306.36	139.51	79.28	31.11	964,105	426,562
		113.60	298.26	23.60	74.88	343,004	932,866
	12	325.44	140.77	82.15	31.30	1,018,965	430,179
	13	112.26	300.93	24.03	78.05	340,743	947,439
		331.94	161.29	84.33	30.75	1,040,675	480,110
	14	122.20	292.84	23.26	77.48	363,651	925,814
		321.71	154.39	84.72	32.69	1,016,077	467,709
	15	107.55	272.87	23.59	74.34	327,841	868,015
		315.99	174.35	82.94	32.63	997,312	517,464
	16	135.43	237.81	20.96	60.75	390,997	746,421
		270.25	162.73	68.64	30.20	847,211	482,313
	17	116.01	208.05	24.42	56.38	351,087	661,069
		249.38	174.77	60.41	30.74	774,463	513,759
	18	130.56	168.00	22.68	43.90	383,114	529,755
		206.89	176.45	47.92	39.42	637,029	539,675
	19	141.87	97.40	34.69	21.34	441,413	296,834
		121.16	162.13	26.71	38.52	369,668	501,630
	20	141.22	82.18	33.50	17.81	436,801	249,991
		100.36	171.74	22.83	40.06	307,969	529,497
	21	173.11	90.47	36.77	17.79	524,692	270,630
		82.18	184.60	22.03	48.42	260,518	582,553
	22	220.84	128.07	50.86	24.90	679,265	382,422
		90.43	196.02	19.56	48.82	274,973	612,110
	23	243.88	141.53	56.75	27.06	751,581	421,467
		90.87	200.63	20.11	49.25	277,460	624,699
June	24	251.29	141.53	57.02	29.19	770,771	426,807
		93.67	214.64	22.39	53.58	290,151	670,568

(next page)

(Table A. 4 Continued)

Date		Tidal Area				Tidal Volume	
		River Mouth		SB.5		River Mouth --> SB.5	
		Fall m2	Rise m2	Fall m2	Rise m2	Fall m3	Rise m3
June	25	265.02	153.87	62.24	31.49	1,832,672	1,038,000
	26	100.69	221.30	22.83	58.76	691,722	1,568,331
		275.73	155.12	67.68	31.74	1,923,068	1,046,459
	27	102.09	236.08	23.78	63.26	704,882	1,676,314
		289.11	156.77	71.73	31.81	2,020,734	1,056,071
	28	106.53	225.49	23.02	59.40	725,529	1,595,369
		271.96	149.71	67.42	29.30	1,900,507	1,002,453
	29	107.40	212.71	23.14	55.51	730,996	1,501,979
		255.01	144.79	61.54	27.89	1,772,713	967,003
	30	102.48	207.12	20.93	54.59	691,130	1,465,582
		243.07	130.31	60.36	25.44	1,699,195	872,183
July	1	94.37	186.94	18.09	45.85	629,775	1,303,649
		219.03	116.83	52.38	20.53	1,519,882	769,225
	2	81.98	148.63	13.36	34.86	533,882	1,027,532
		171.70	101.87	40.06	18.16	1,185,864	672,194
	3	77.41	111.51	14.24	31.75	513,226	802,223
		121.16	116.19	31.11	26.89	852,744	801,249
	4	105.14	74.43	27.08	13.80	740,438	494,072
		78.60	127.70	15.18	27.09	525,157	866,828
	5	123.53	90.43	25.52	16.43	834,672	598,418
		108.26	160.20	19.52	30.44	715,606	1,067,614
	6	180.01	115.24	33.88	21.33	1,197,766	764,809
		90.02	170.53	17.29	41.01	600,928	1,184,624
	7	204.71	133.79	47.18	26.33	1,410,583	896,711
		102.33	196.52	21.06	47.64	691,011	1,367,274
	8	236.76	139.36	54.66	28.93	1,631,945	942,379
		99.12	207.47	21.60	51.11	676,041	1,448,064
	9	247.71	142.57	59.39	27.80	1,719,768	954,088
		102.33	229.78	19.52	56.67	682,385	1,604,120
	10	272.49	141.83	64.86	27.30	1,889,149	947,118
		103.17	256.66	18.51	65.40	681,397	1,803,537
	11	296.56	144.67	74.28	26.99	2,076,682	961,246
		98.00	275.24	16.88	70.88	643,327	1,938,279
July	12	320.67	0.00	81.23	-	2,250,615	-
Average :		168.45	168.90	39.03	39.06	821,968	812,542

Table A 4-5

Calculation of Tidal Volume (SB.5 - KP.23€)

Location : Between SB.5 and KP.236
Distance : 0.75 km
Recording period : From June 6, 1991 to July 12,1991

Date		Tidal Area				Tidal Volume	
		SB.5		KP.236		SB.5 --> SB.5	
		Fall m2	Rise m2	Fall m2	Rise m2	Fall m3	Rise m3
June	6	19.44	11.60	77.37	61.24	36,303	27,315
		19.25	34.13	73.72	148.71	34,864	68,566
	7	33.19	20.00	151.79	75.59	69,369	35,845
		23.63	40.77	63.18	153.21	32,552	72,745
	8	43.84	25.44	168.69	85.08	79,701	41,445
		20.28	50.75	64.09	185.87	31,638	88,735
	9	56.96	26.49	206.87	92.45	98,937	44,604
		20.28	59.20	75.41	227.89	35,882	107,659
	10	64.09	26.01	254.02	110.41	119,291	51,156
		22.32	71.77	79.54	261.57	38,199	125,004
	11	79.28	31.11	292.44	121.19	139,395	57,113
		23.60	74.88	90.32	274.69	42,722	131,088
	12	82.15	31.30	307.05	126.32	145,951	59,108
	13	24.03	78.05	97.11	302.28	45,430	142,623
		84.33	30.75	328.48	126.96	154,806	59,142
	14	23.26	77.48	94.42	291.46	44,130	138,353
		84.72	32.69	313.36	129.21	149,280	60,714
	15	23.59	74.34	97.67	266.27	45,472	127,729
		82.94	32.63	296.28	131.39	142,205	61,510
	16	20.96	60.75	93.24	210.60	42,826	101,758
		68.64	30.20	247.22	146.81	118,445	66,376
	17	24.42	56.38	108.55	165.50	49,865	83,204
		60.41	30.74	189.70	148.10	93,789	67,065
	18	22.68	43.90	120.61	138.21	53,734	68,290
		47.92	39.42	156.14	148.27	76,523	70,384
	19	34.69	21.34	132.00	108.81	62,507	48,804
		26.71	38.52	121.86	154.89	55,714	72,530
	20	33.50	17.81	141.84	97.44	65,753	43,221
		22.83	40.06	108.88	135.64	49,392	65,886
	21	36.77	17.79	134.02	94.19	64,043	41,991
		22.03	48.42	81.07	160.55	38,661	78,365
	22	50.86	24.90	183.34	98.32	87,826	46,208
		19.56	48.82	73.87	173.17	35,037	83,247
	23	56.75	27.06	214.01	116.55	101,536	53,854
		20.11	49.25	74.05	204.92	35,311	95,314
June	24	57.02	29.19	252.99	127.67	116,255	58,824
		22.39	53.58	89.52	206.38	41,965	97,487

(next page)

(Table A. 4-5 Continued)

Date		Tidal Area				Tidal Volume	
		SB.5		KP.236		SB.5 --> SB.5	
		Fall m2	Rise m2	Fall m2	Rise m2	Fall m3	Rise m3
June	25	62.24	31.49	244.54	114.78	115,041	54,851
	26	22.83	58.76	76.63	214.84	37,296	102,600
		67.68	31.74	254.53	116.32	120,827	55,524
	27	23.78	63.26	78.26	250.97	38,266	117,834
		71.73	31.81	290.55	138.20	135,857	63,755
	28	23.02	59.40	88.72	232.35	41,905	109,405
		67.42	29.30	280.30	116.32	130,394	54,609
	29	23.14	55.51	79.90	224.49	38,638	105,000
		61.54	27.89	259.38	116.61	120,346	54,188
	30	20.93	54.59	84.98	221.36	39,718	103,482
		60.36	25.44	249.91	127.56	116,349	57,374
July	1	18.09	45.85	89.20	184.32	40,237	86,314
		52.38	20.53	207.78	96.80	97,561	44,000
	2	13.36	34.86	68.37	137.07	30,650	64,474
		40.06	18.16	167.88	99.18	77,977	44,003
	3	14.24	31.75	67.04	119.85	30,480	56,848
		31.11	26.89	127.79	118.12	59,588	54,377
	4	27.08	13.80	108.17	66.87	50,720	30,250
		15.18	27.09	84.98	126.29	37,560	57,516
	5	25.52	16.43	126.29	84.98	56,927	38,031
		19.52	30.44	102.59	161.38	45,791	71,931
	6	33.88	21.33	172.31	111.70	77,322	49,886
		17.29	41.01	84.78	163.22	38,276	76,587
	7	47.18	26.33	194.76	113.95	90,729	52,605
		21.06	47.64	96.81	216.38	44,202	99,006
	8	54.66	28.93	242.65	142.07	111,493	64,122
		21.60	51.11	96.51	190.88	44,293	90,746
	9	59.39	27.80	237.94	128.79	111,499	58,723
		19.52	56.67	88.22	205.68	40,404	98,380
	10	64.86	27.30	232.52	116.90	111,518	54,076
		18.51	65.40	88.44	255.29	40,106	120,257
	11	74.28	26.99	283.76	115.07	134,262	53,271
		16.88	70.88	70.20	252.07	32,654	121,108
July	12	81.23	-	310.66	-	146,958	-
Average :		39.03	39.06	154.82	155.55	72,692	72,977

Table A 5-1

Estimation of Sediment Transport through KP.242 &
Relationships between Sediment Deposit, Tidal Range & Water Discharge
Recording period : From June 6, 1991 to July 12,1991

Date	Range		Duration		Mean Discharge		Sediment Discharge		Sediment
	Fall	Rise	Fall	Rise	Fall	Rise	Fall	Rise	Deposit
	m	m	hrs	hrs	m3/s	m3/s	Kg	Kg	Kg
June 6	0.48	0.38	6.0	4.0	38.77	38.32	46,817	148,509	101,692
	0.50	0.98	7.0	6.0	26.08	68.26	56,896	574,497	517,601
7	0.99	0.56	8.0	4.0	53.90	51.29	128,748	218,856	90,108
	0.50	1.02	6.0	7.0	29.10	68.43	48,768	697,604	648,836
8	1.12	0.60	8.0	4.0	67.22	58.97	145,654	234,489	88,834
	0.49	1.19	6.0	6.0	30.15	96.87	47,793	697,604	649,811
9	1.36	0.68	8.0	6.0	84.19	45.50	176,866	400,389	223,523
	0.49	1.29	5.0	5.0	40.93	142.88	40,071	630,188	590,117
10	1.51	0.71	9.0	6.0	92.00	52.81	220,920	418,562	197,642
	0.52	1.55	5.0	5.0	45.33	171.76	42,591	757,203	714,612
11	1.75	0.82	9.0	5.0	110.08	69.54	256,033	400,585	144,552
	0.62	1.64	6.0	4.0	41.53	227.97	60,473	640,936	580,463
12	1.83	0.84	9.0	6.0	117.68	62.43	267,737	492,426	224,689
13	0.64	1.71	5.0	5.0	53.82	187.47	52,019	837,320	785,301
	1.82	0.80	9.0	6.0	119.49	64.13	266,859	468,977	202,118
14	0.72	1.67	5.0	5.0	55.19	179.74	58,522	815,825	757,303
	1.81	0.86	9.0	5.0	111.69	77.38	264,811	422,080	157,268
15	0.60	1.50	6.0	4.0	46.09	204.08	58,912	586,222	527,310
	1.70	0.90	9.0	6.0	103.34	65.83	248,718	527,599	278,882
16	0.68	1.38	6.0	4.0	46.24	168.25	66,325	539,324	472,999
	1.50	0.84	9.0	5.0	87.23	80.95	219,457	410,355	190,898
17	0.71	1.11	6.0	6.0	46.18	85.12	69,251	650,706	581,455
	1.17	0.84	8.0	5.0	77.75	81.53	152,157	410,355	258,198
18	0.69	0.86	6.0	6.0	52.77	71.33	67,300	504,151	436,851
	0.97	0.89	8.0	5.0	62.26	88.90	126,147	434,781	308,634
19	0.70	0.60	6.0	6.0	62.18	45.64	68,275	351,733	283,458
	0.74	0.79	8.0	5.0	39.85	84.70	96,236	385,929	289,693
20	0.71	0.46	6.0	7.0	65.45	34.02	69,641	317,341	247,700
	0.57	0.87	7.0	4.0	34.39	101.16	64,862	340,009	275,147
21	0.87	0.60	6.0	7.0	72.81	34.61	85,247	407,619	322,373
	0.50	0.95	8.0	4.0	30.05	133.01	64,504	372,837	308,333
22	1.10	0.62	6.0	7.0	94.20	39.53	107,290	424,034	316,744
	0.56	1.06	8.0	4.0	25.29	133.37	72,827	414,263	341,436
23	1.23	0.72	6.0	7.0	114.03	47.58	119,970	495,162	375,192
	0.54	1.11	8.0	4.0	29.42	167.13	70,746	433,804	363,058
June 24	1.35	0.83	6.0	7.0	135.40	48.89	131,674	570,394	438,720
	0.63	1.19	8.0	4.0	29.58	176.91	82,451	465,069	382,618

(next page)

(Table A. 5-1 Continued)

Date	Range		Duration		Mean Discharge		Sediment Discharge		Sediment
	Fall	Rise	Fall	Rise	Fall	Rise	Fall	Rise	Deposits
	m	m	hrs	hrs	m3/s	m3/s	Kg	Kg	Kg
June 25	1.47	0.94	6.0	6.0	177.77	77.68	143,378	553,393	410,015
26	0.61	1.18	8.0	5.0	38.01	184.19	79,850	576,451	496,602
	1.50	0.97	6.0	6.0	187.32	78.83	146,305	570,980	424,675
27	0.71	1.32	8.0	5.0	39.08	199.12	92,855	644,844	551,989
	1.60	1.01	6.0	6.0	201.00	84.32	156,058	594,429	438,371
28	0.71	1.26	7.0	5.0	46.21	183.64	81,248	615,533	534,285
	1.58	0.97	7.0	6.0	160.45	76.02	179,792	570,980	391,188
29	0.73	1.26	6.0	5.0	51.87	164.32	71,592	615,533	543,941
	1.50	0.90	8.0	5.0	121.59	86.17	195,073	439,666	244,593
30	0.68	1.22	7.0	5.0	43.24	153.70	77,379	595,992	518,613
	1.39	0.85	8.0	5.0	111.47	82.32	180,767	415,240	234,473
July 1	0.66	1.16	7.0	5.0	41.65	132.32	75,103	566,681	491,578
	1.20	0.60	8.0	5.0	91.84	64.48	156,058	293,111	137,053
2	0.49	0.87	6.0	6.0	39.09	82.97	47,793	510,013	462,220
	0.98	0.63	7.0	5.0	83.00	61.98	111,517	307,766	196,250
3	0.46	0.73	7.0	6.0	32.28	71.13	52,345	427,942	375,597
	0.73	0.72	6.0	6.0	76.32	59.99	71,202	422,080	350,878
4	0.66	0.42	7.0	5.0	46.48	49.08	75,103	205,178	130,075
	0.48	0.75	7.0	6.0	41.58	78.46	54,620	439,666	385,046
5	0.75	0.55	7.0	5.0	66.35	57.69	85,344	268,685	183,341
	0.69	0.95	6.0	6.0	55.33	100.65	67,300	556,911	489,610
6	1.05	0.79	8.0	5.0	82.72	73.49	136,551	387,395	250,844
	0.59	0.95	6.0	7.0	48.24	94.17	57,839	649,729	591,890
7	1.18	0.82	7.0	5.0	109.86	83.13	134,275	402,050	267,775
	0.60	1.01	6.0	7.0	56.79	119.04	58,814	690,764	631,950
8	1.28	0.86	7.0	5.0	135.97	93.70	145,654	420,126	274,471
	0.60	1.09	6.0	7.0	56.62	122.00	58,522	745,479	686,957
9	1.37	0.86	7.0	5.0	143.83	92.81	155,896	420,126	264,230
	0.59	1.15	6.0	7.0	52.43	127.73	57,546	786,514	728,968
10	1.44	0.86	7.0	5.0	154.78	92.74	163,861	420,126	256,264
	0.54	1.35	6.0	7.0	55.73	148.00	52,670	923,299	870,629
11	1.74	0.79	7.0	5.0	172.32	91.36	197,999	385,929	187,930
	0.43	1.45	6.0	7.0	48.29	150.83	41,941	991,692	949,751
July 12	1.73	-	7.0	-	182.72	-	196,861	-	-

Total Suspended Sediment Inflow During 36.88 days (kg)	27,626,220
Mean Sediment Inflow / day (kg/day)	749,084
Spesific Gravity = 2,770 kg/m3	
Volume of Sediment inflow (m3/day)	270
Bulk Volume = Volume of Particles /(1-Porosity)	
Porosity = 0.4	
Bulk Volume (m3/day)	451

Table A. 5-2

Estimation of Sediment Transport through KP.236 &
Relationships between Sediment Deposit, Tidal Range & Water Discharge
Recording period : From June 6, 1991 to July 12,1991

Date	Range		Duration		Mean Discharge		Sediment Discharge		Sediment
	Fall	Rise	Fall	Rise	Fall	Rise	Fall	Rise	Deposit
	m	m	hrs	hrs	m3/s	m3/s	Kg	Kg	Kg
June 6	0.46	0.37	6.0	4.0	38.20	35.20	23,966	7,172	(16,794)
	0.45	0.86	7.0	6.0	21.81	63.33	27,234	25,063	(2,171)
7	0.88	0.46	8.0	4.0	51.08	45.44	61,004	8,975	(52,029)
	0.38	0.87	6.0	7.0	24.39	66.59	19,868	29,647	9,780
8	0.97	0.52	8.0	4.0	66.28	53.07	67,367	10,079	(57,287)
	0.39	1.03	6.0	6.0	25.51	93.28	19,971	30,006	10,034
9	1.17	0.56	8.0	6.0	83.10	42.40	80,716	16,340	(64,375)
	0.45	1.24	5.0	5.0	36.37	142.01	19,539	30,093	10,554
10	1.41	0.67	9.0	6.0	93.90	50.71	109,869	19,539	(90,330)
	0.47	1.39	5.0	5.0	40.64	173.20	20,404	33,728	13,324
11	1.59	0.73	9.0	5.0	113.22	64.89	123,875	17,736	(106,139)
	0.53	1.45	6.0	4.0	36.68	230.47	27,597	28,145	548
12	1.66	0.76	9.0	6.0	121.66	60.00	129,322	22,155	(107,166)
13	0.57	1.58	5.0	5.0	49.37	188.86	24,727	38,331	13,605
	1.75	0.76	9.0	6.0	122.84	60.20	136,325	22,155	(114,169)
14	0.55	1.52	5.0	5.0	49.86	179.89	23,862	36,877	13,015
	1.66	0.76	9.0	5.0	113.01	73.11	129,322	18,463	(110,859)
15	0.56	1.39	6.0	4.0	43.59	202.23	29,153	26,982	(2,171)
	1.58	0.77	9.0	6.0	102.47	60.26	123,097	22,446	(100,651)
16	0.53	1.12	6.0	4.0	40.83	164.39	27,597	21,748	(5,848)
	1.35	0.85	9.0	5.0	86.26	76.49	105,200	20,644	(84,557)
17	0.61	0.90	6.0	6.0	41.70	78.19	31,747	26,226	(5,521)
	1.05	0.84	8.0	5.0	73.55	75.44	72,762	20,401	(52,361)
18	0.67	0.76	6.0	6.0	49.16	67.03	34,859	22,155	(12,704)
	0.87	0.83	8.0	5.0	58.14	84.08	60,312	20,159	(40,153)
19	0.73	0.61	6.0	6.0	59.10	43.86	37,972	17,794	(20,178)
	0.69	0.86	8.0	5.0	37.51	80.31	47,862	20,886	(26,976)
20	0.78	0.55	6.0	7.0	63.54	33.14	40,565	18,725	(21,841)
	0.62	0.76	7.0	4.0	30.52	92.51	37,643	14,770	(22,873)
21	0.75	0.54	6.0	7.0	69.68	32.89	39,009	18,385	(20,624)
	0.46	0.87	8.0	4.0	29.45	131.79	31,954	16,903	(15,052)
22	1.01	0.57	6.0	7.0	89.69	35.15	52,496	19,403	(33,093)
	0.42	0.93	8.0	4.0	22.25	128.80	29,188	18,066	(11,122)
23	1.19	0.69	6.0	7.0	112.71	44.05	61,522	23,270	(38,252)
	0.42	1.08	8.0	4.0	28.10	173.66	29,188	20,973	(8,215)
June 24	1.38	0.75	6.0	7.0	140.13	44.90	71,690	25,509	(46,181)
	0.51	1.10	8.0	4.0	27.07	183.76	35,413	21,361	(14,052)

(next page)

(table A. 5-2 continued)

Date	Range		Duration		Mean Discharge		Sediment Discharge		Sediment
	Fall	Rise	Fall	Rise	Fall	Rise	Fall	Rise	Deposits
	m	m	hrs	hrs	m3/s	m3/s	Kg	Kg	Kg
June 25	1.34	0.68	6.0	6.0	151.34	53.73	69,615	19,829	(49,785)
26	0.44	1.14	8.0	5.0	25.65	157.52	30,571	27,670	(2,901)
	1.39	0.69	6.0	6.0	160.11	54.78	72,208	20,120	(52,088)
27	0.45	1.31	8.0	5.0	26.37	170.13	31,263	31,789	526
	1.56	0.81	6.0	6.0	173.02	61.05	81,027	23,609	(57,418)
28	0.50	1.21	7.0	5.0	31.13	153.89	30,381	29,366	(1,015)
	1.51	0.69	7.0	6.0	136.72	52.87	91,506	20,120	(71,385)
29	0.46	1.19	6.0	5.0	33.52	132.07	23,966	28,882	4,916
	1.41	0.69	8.0	5.0	98.26	58.57	97,661	16,767	(80,894)
30	0.49	1.18	7.0	5.0	28.59	119.33	29,776	28,639	(1,136)
	1.36	0.75	8.0	5.0	87.00	57.99	94,203	18,124	(76,079)
July 1	0.51	0.99	7.0	5.0	28.69	100.26	30,744	24,036	(6,708)
	1.14	0.57	8.0	5.0	67.23	41.08	78,641	13,738	(64,903)
2	0.39	0.75	6.0	6.0	25.99	60.84	20,335	21,894	1,559
	0.94	0.58	7.0	5.0	61.24	42.67	57,070	14,102	(42,968)
3	0.38	0.66	7.0	6.0	21.47	55.73	23,240	19,306	(3,933)
	0.71	0.66	6.0	6.0	60.45	40.07	36,934	19,248	(17,686)
4	0.60	0.38	7.0	5.0	30.25	36.87	36,433	9,256	(27,177)
	0.49	0.71	7.0	6.0	33.52	62.92	29,776	20,702	(9,074)
5	0.71	0.49	7.0	5.0	53.93	41.74	43,090	11,921	(31,169)
	0.60	0.91	6.0	6.0	38.38	82.94	31,228	26,517	(4,711)
6	0.98	0.66	8.0	5.0	67.35	52.50	67,920	16,040	(51,880)
	0.49	0.90	6.0	7.0	34.75	77.44	25,522	30,597	5,075
7	1.10	0.68	7.0	5.0	88.90	58.60	66,693	16,452	(50,241)
	0.57	1.18	6.0	7.0	42.15	103.36	29,516	40,095	10,579
8	1.35	0.84	7.0	5.0	115.12	69.44	81,822	20,401	(61,421)
	0.55	1.03	6.0	7.0	42.62	105.03	28,634	35,007	6,372
9	1.33	0.77	7.0	5.0	122.66	68.28	80,612	18,705	(61,907)
	0.51	1.11	6.0	7.0	36.78	106.15	26,559	37,721	11,161
10	1.28	0.69	7.0	5.0	131.47	69.24	77,586	16,767	(60,819)
	0.51	1.34	6.0	7.0	41.74	124.37	26,559	45,522	18,963
11	1.52	0.68	7.0	5.0	145.90	66.95	92,111	16,525	(75,586)
	0.40	1.30	6.0	7.0	34.17	132.75	20,853	44,166	23,312
July 12	1.67	0.57	7.0	-	152.68	-	101,189	-	-

Total Suspended Sediment Inflow During 36.88 days (kg)	(2,113,306)
Mean Sediment Inflow / day (kg/day)	(57,302)
Spesific Gravity = 2,770 kg/m3	
Volume of Sediment inflow (m3/day)	(21)
Bulk Volume = Volume of Particles /(1-Porosity)	
Porosity = 0.4	
Bulk Volume (m3/day)	(34)

Table A 5-3

Estimation of Sediment Transport through SB.5 &
Relationships between Sediment Deposit, Tidal Range & Water Discharge
Recording period : From June 6, 1991 to July 12,1991

Date	Range		Duration		Mean Discharge		Sediment Discharge		Sediment
	Fall	Rise	Fall	Rise	Fall	Rise	Fall	Rise	Deposit
	m	m	hrs	hrs	m3/s	m3/s	Kg	Kg	Kg
June 6	0.48	0.30	6.0	4.0	15.34	15.12	2,080	886	(1,195)
	0.53	0.86	7.0	6.0	9.99	26.75	2,680	3,809	1,129
7	0.83	0.54	8.0	4.0	21.29	19.95	4,796	1,594	(3,202)
	0.66	1.03	6.0	7.0	11.06	27.03	2,860	5,322	2,462
8	1.14	0.74	8.0	4.0	26.62	22.85	6,588	2,185	(4,403)
	0.56	1.19	6.0	6.0	11.50	38.04	2,427	5,271	2,844
9	1.41	0.78	8.0	6.0	33.27	17.81	8,148	3,455	(4,693)
	0.56	1.34	5.0	5.0	15.79	56.40	2,023	4,946	2,923
10	1.51	0.75	9.0	6.0	36.64	20.83	9,817	3,322	(6,495)
	0.62	1.57	5.0	5.0	17.46	68.11	2,239	5,795	3,555
11	1.85	0.93	9.0	5.0	43.86	27.21	12,027	3,433	(8,594)
	0.65	1.62	6.0	4.0	16.05	90.50	2,817	4,783	1,966
12	1.89	0.93	9.0	6.0	46.95	24.60	12,287	4,119	(8,168)
13	0.66	1.67	5.0	5.0	21.01	74.57	2,384	6,164	3,780
	1.90	0.90	9.0	6.0	47.62	24.98	12,352	3,986	(8,366)
14	0.63	1.64	5.0	5.0	21.58	71.32	2,275	6,053	3,778
	1.90	0.94	9.0	5.0	44.35	30.31	12,352	3,469	(8,883)
15	0.62	1.56	6.0	4.0	18.09	80.59	2,687	4,603	1,919
	1.86	0.93	9.0	6.0	40.75	25.58	12,092	4,119	(7,973)
16	0.54	1.30	6.0	4.0	17.92	66.48	2,323	3,827	1,504
	1.55	0.82	9.0	5.0	34.46	31.78	10,077	3,027	(7,050)
17	0.63	1.25	6.0	6.0	18.14	32.89	2,730	5,536	2,806
	1.38	0.81	8.0	5.0	30.09	31.79	7,975	2,990	(4,985)
18	0.56	0.98	6.0	6.0	20.77	27.67	2,427	4,341	1,913
	1.10	0.94	8.0	5.0	24.05	34.67	6,357	3,469	(2,887)
19	0.80	0.53	6.0	6.0	24.24	18.17	3,467	2,330	(1,138)
	0.69	0.93	8.0	5.0	15.76	33.00	3,964	3,433	(532)
20	0.78	0.45	6.0	7.0	25.70	13.51	3,381	2,325	(1,055)
	0.60	0.96	7.0	4.0	13.39	39.10	3,034	2,835	(199)
21	0.86	0.46	6.0	7.0	28.46	13.81	3,727	2,377	(1,350)
	0.59	1.13	8.0	4.0	11.87	52.25	3,409	3,337	(73)
22	1.21	0.68	6.0	7.0	36.74	15.21	5,244	3,514	(1,730)
	0.51	1.10	8.0	4.0	9.86	52.34	2,947	3,248	301
23	1.36	0.76	6.0	7.0	44.84	18.53	5,894	3,927	(1,967)
	0.53	1.12	8.0	4.0	11.59	66.81	3,063	3,307	244
June 24	1.38	0.82	6.0	7.0	54.06	19.17	5,981	4,237	(1,744)
	0.59	1.21	8.0	4.0	11.67	70.62	3,409	3,573	163

(next page)

(Table A. 5-3 Continued)

Date	Range		Duration		Mean Discharge		Sediment Discharge		Sediment
	Fall	Rise	Fall	Rise	Fall	Rise	Fall	Rise	Deposite
	m	m	hrs	hrs	m3/s	m3/s	Kg	Kg	Kg
June 25	1.51	0.90	6.0	6.0	57.90	23.11	6,544	3,988	(2,558)
26	0.60	1.30	8.0	5.0	11.18	59.96	3,467	4,798	1,331
	1.61	0.91	6.0	6.0	60.99	23.56	6,978	4,031	(2,947)
27	0.63	1.39	8.0	5.0	11.63	65.16	3,641	5,130	1,490
	1.69	0.92	6.0	6.0	65.91	25.87	7,325	4,075	(3,250)
28	0.61	1.32	7.0	5.0	13.78	59.52	3,084	4,872	1,788
	1.60	0.85	7.0	6.0	52.55	22.85	8,090	3,765	(4,326)
29	0.63	1.28	6.0	5.0	15.16	52.48	2,730	4,724	1,994
	1.50	0.82	8.0	5.0	38.91	25.60	8,639	3,008	(5,631)
30	0.57	1.25	7.0	5.0	12.79	48.32	2,882	4,614	1,732
	1.45	0.74	8.0	5.0	35.04	25.13	8,379	2,731	(5,648)
July 1	0.49	1.07	7.0	5.0	12.69	41.29	2,478	3,949	1,472
	1.29	0.61	8.0	5.0	27.96	18.47	7,455	2,251	(5,203)
2	0.37	0.85	6.0	6.0	11.58	25.37	1,604	3,765	2,161
	1.02	0.53	7.0	5.0	25.45	18.73	5,158	1,956	(3,201)
3	0.40	0.80	7.0	6.0	9.54	22.52	2,023	3,543	1,521
	0.78	0.69	6.0	6.0	24.22	17.83	3,381	3,056	(324)
4	0.70	0.39	7.0	5.0	13.64	15.21	3,519	1,425	(2,095)
	0.43	0.71	7.0	6.0	13.43	25.10	2,174	3,145	970
5	0.66	0.45	7.0	5.0	21.44	17.75	3,337	1,661	(1,676)
	0.55	0.80	6.0	6.0	16.80	32.72	2,384	3,543	1,160
6	0.92	0.63	8.0	5.0	26.66	22.71	5,316	2,325	(2,991)
	0.49	1.01	6.0	7.0	14.88	30.22	2,124	5,219	3,095
7	1.23	0.78	7.0	5.0	35.07	25.10	6,219	2,879	(3,340)
	0.59	1.15	6.0	7.0	17.54	39.20	2,557	5,942	3,385
8	1.41	0.87	7.0	5.0	44.27	29.05	7,130	3,211	(3,918)
	0.60	1.21	6.0	7.0	17.61	39.80	2,600	6,252	3,652
9	1.52	0.86	7.0	5.0	46.89	28.54	7,686	3,174	(4,512)
	0.55	1.31	6.0	7.0	15.76	40.84	2,384	6,769	4,385
10	1.62	0.85	7.0	5.0	50.05	28.61	8,171	3,123	(5,049)
	0.52	1.45	6.0	7.0	17.14	47.88	2,254	7,493	5,239
11	1.78	0.84	7.0	5.0	56.15	27.69	9,000	3,100	(5,900)
	0.47	1.52	6.0	7.0	14.21	47.93	2,037	7,854	5,817
July 12	1.90	-	7.0	-	58.93	-	9,607	-	-

Total Suspended Sediment Inflow During 36.88 days (kg)	(76,773)
Mean Sediment Inflow / day (kg/day)	(2,082)
Spesific Gravity = 2,780 kg/m3	
Volume of Sediment inflow (m3/day)	-0.75
Bulk Volume = Volume of Particles /(1-Porosity)	
Porosity = 0.4	
Bulk Volume (m3/day)	-1.25

Appendix B

Supplementary Figures

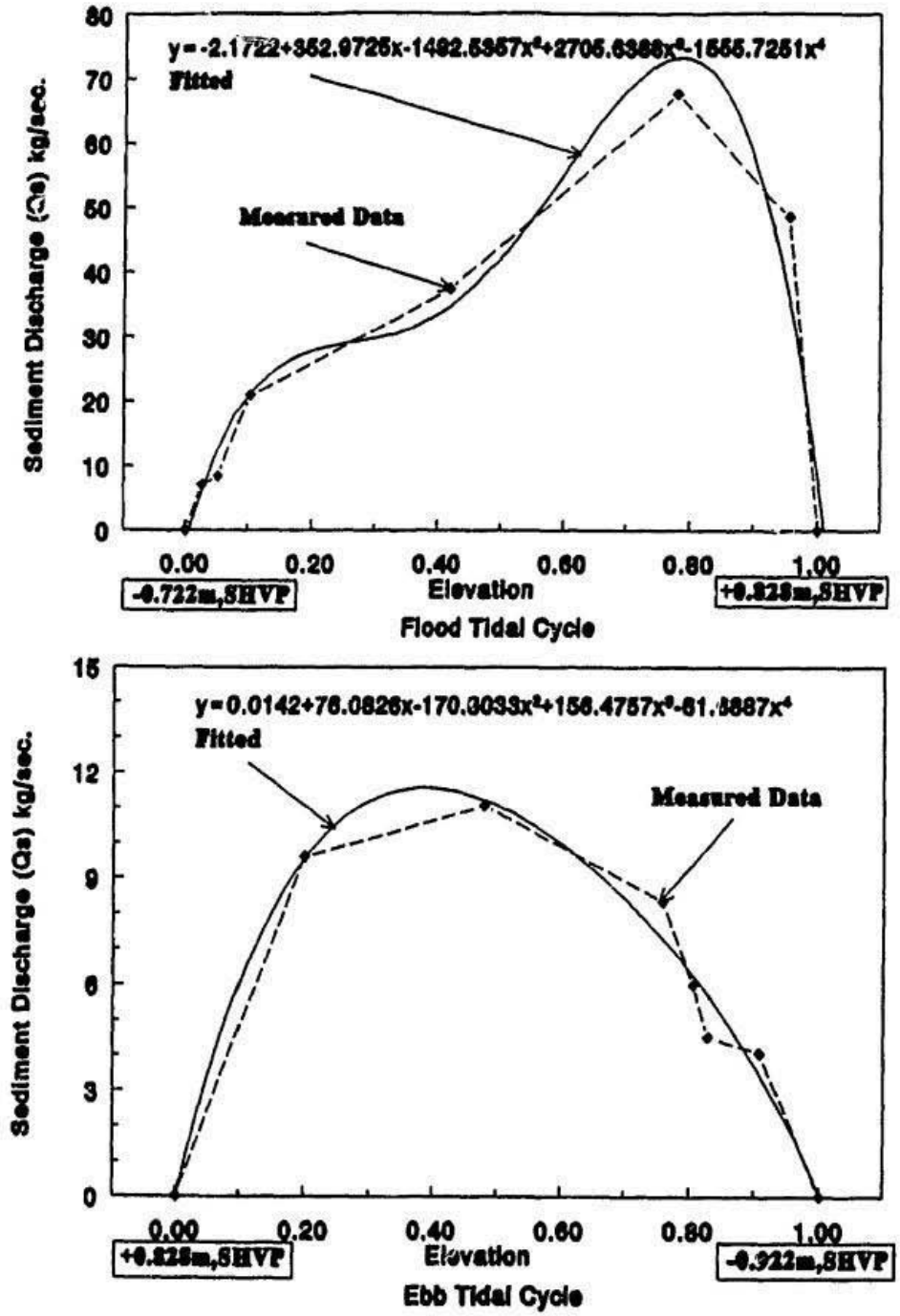

Fig.B.1-1 Phenomena of Suspended Sediment Discharge at KP.242 during a Tidal Cycle

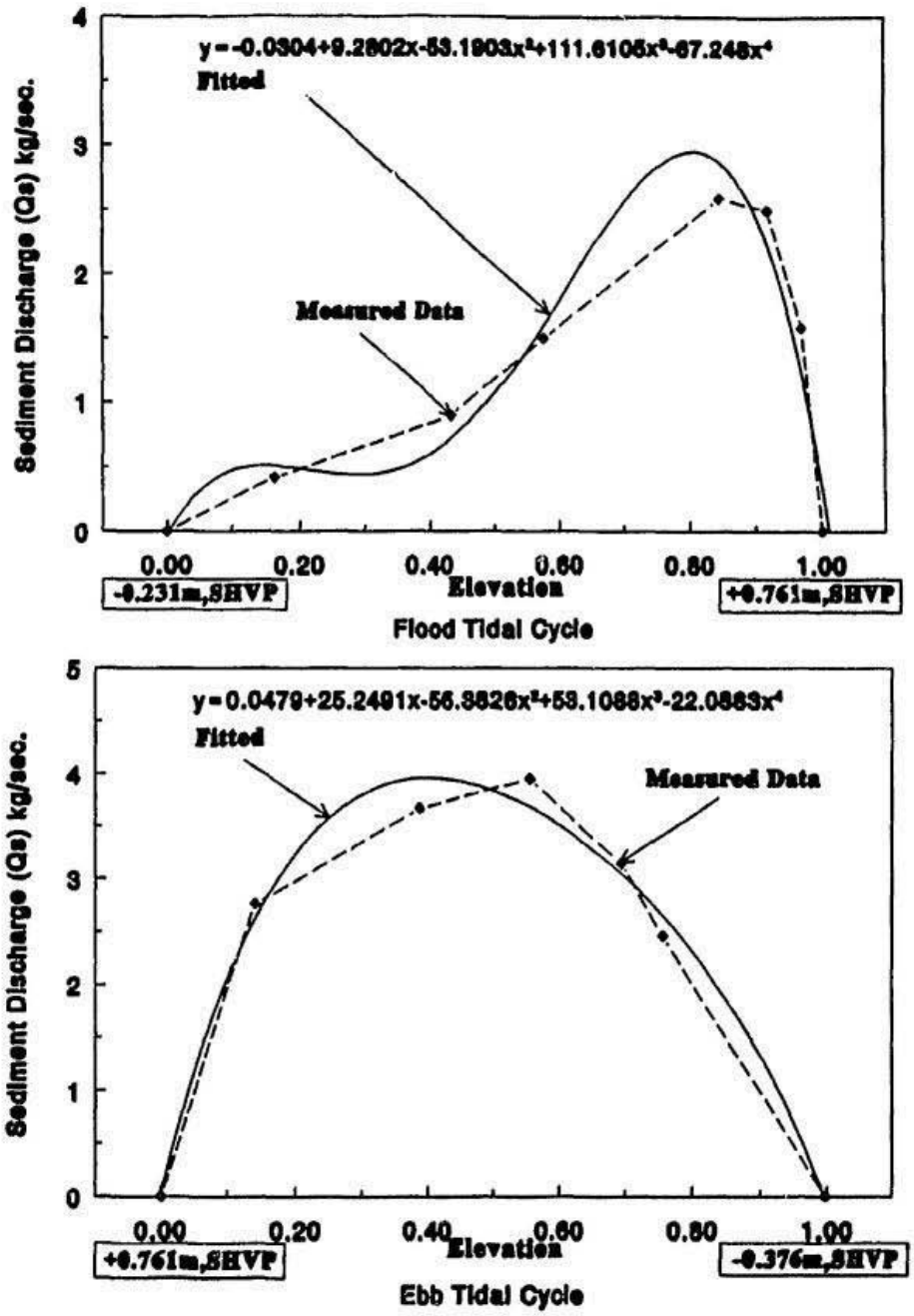

Fig.B.1-2 Phenomena of Suspended Sediment Discharge at KP.236 during a Tidal Cycle

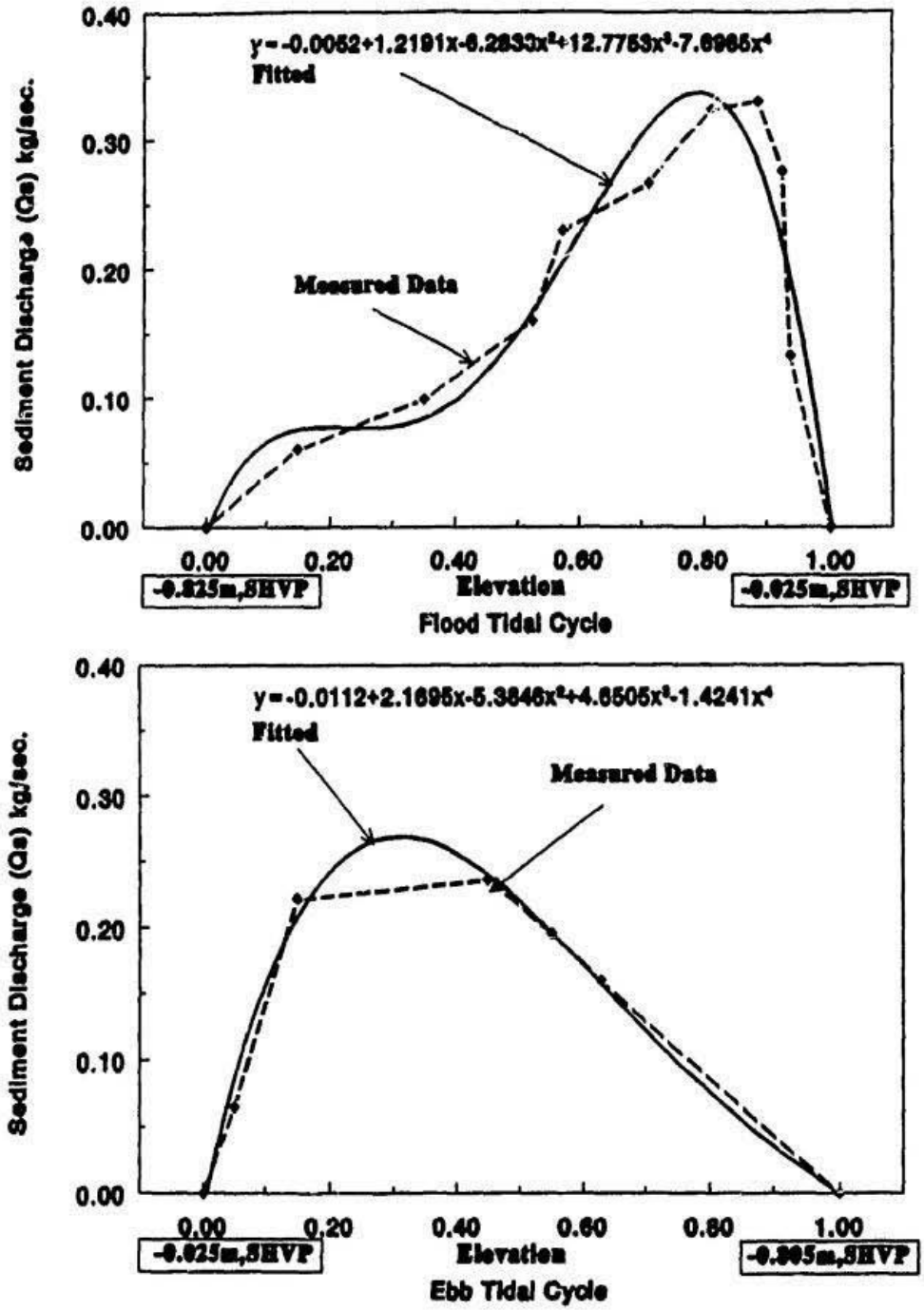

Fig.B.1-3 Phenomena of Suspended Sediment Discharge at SB.5 during a Tidal Cycle

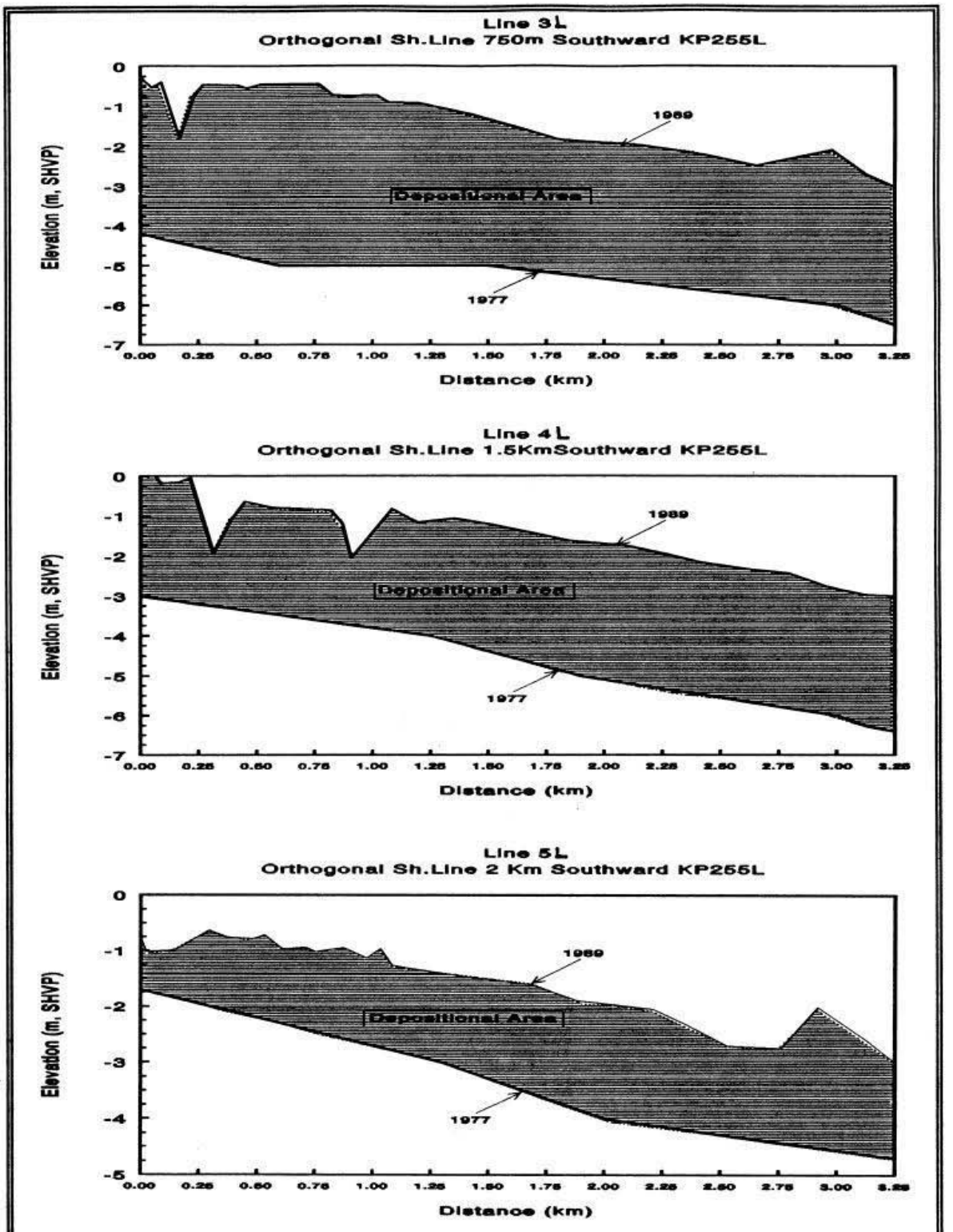

Fig.B.2 Longitudinal Deposition of the Brantas Delta (1977-1989)

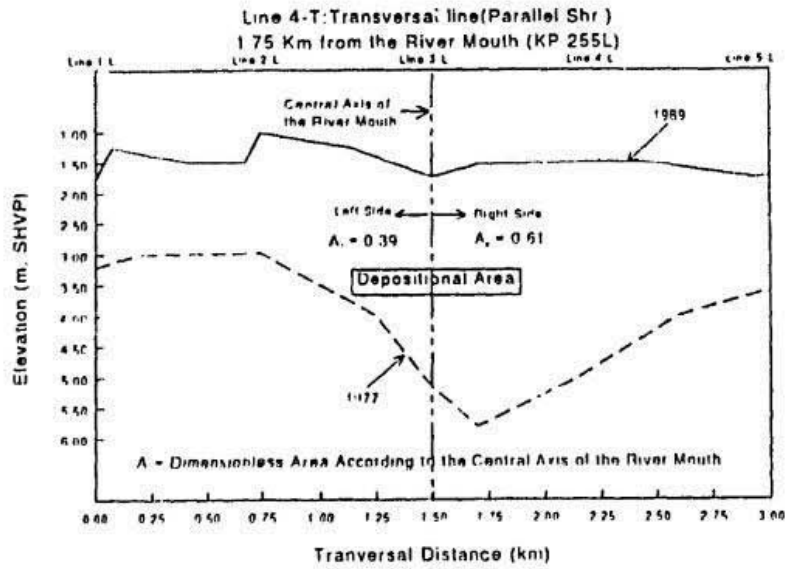

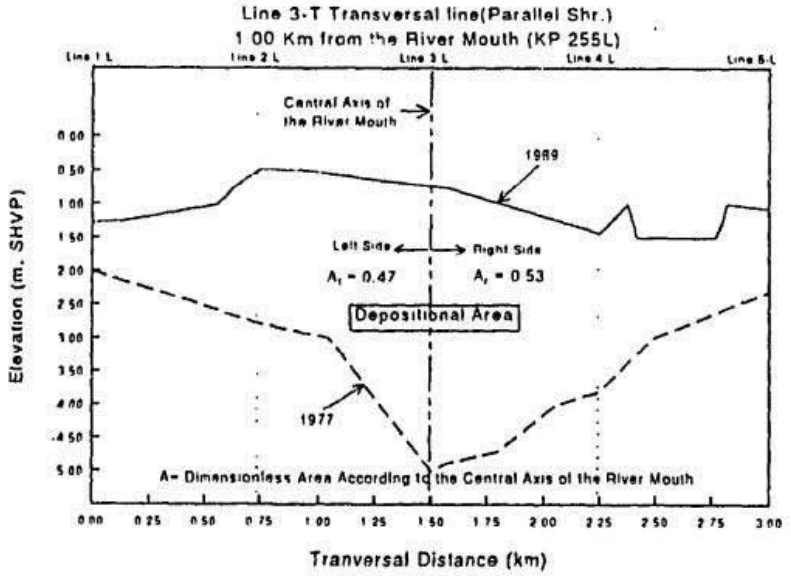

Figure B.3 Tranversal Deposition of the Brantas Delta (1977-1989)

Figure B.3 (continued)

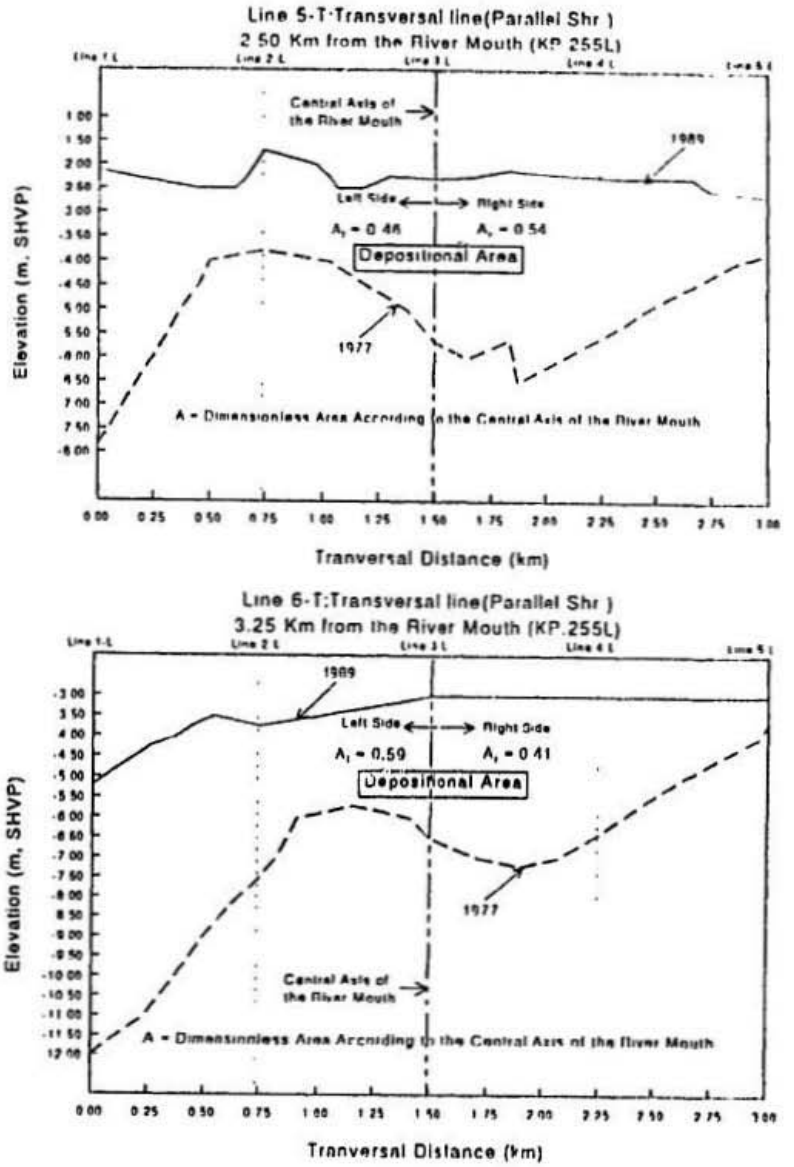

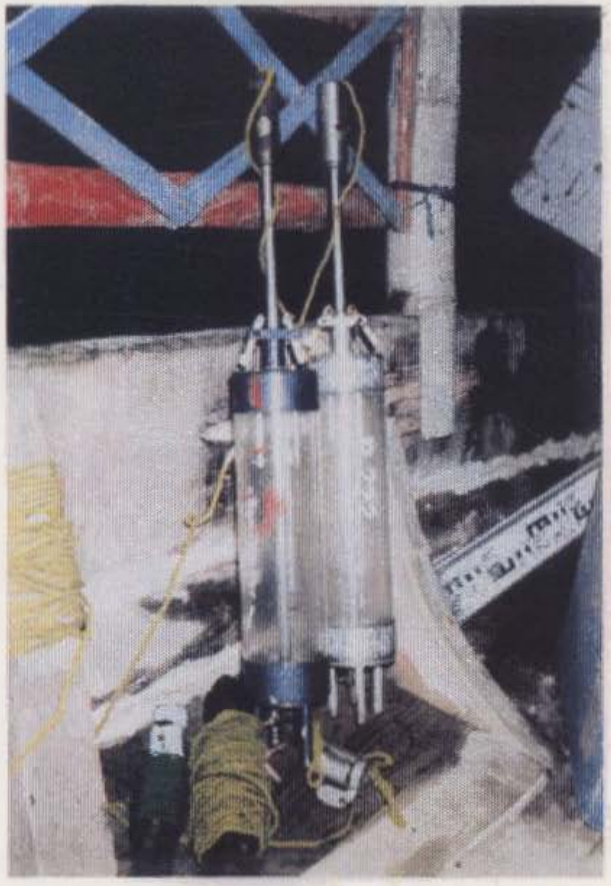

Fig.B.4-1 Photo of Suspended Sediment Samplers

Fig.B.4-2 Working with the Bed Load Sampler

Fig.B.4-3 Photo of Current Meter Used (Diameter 5")

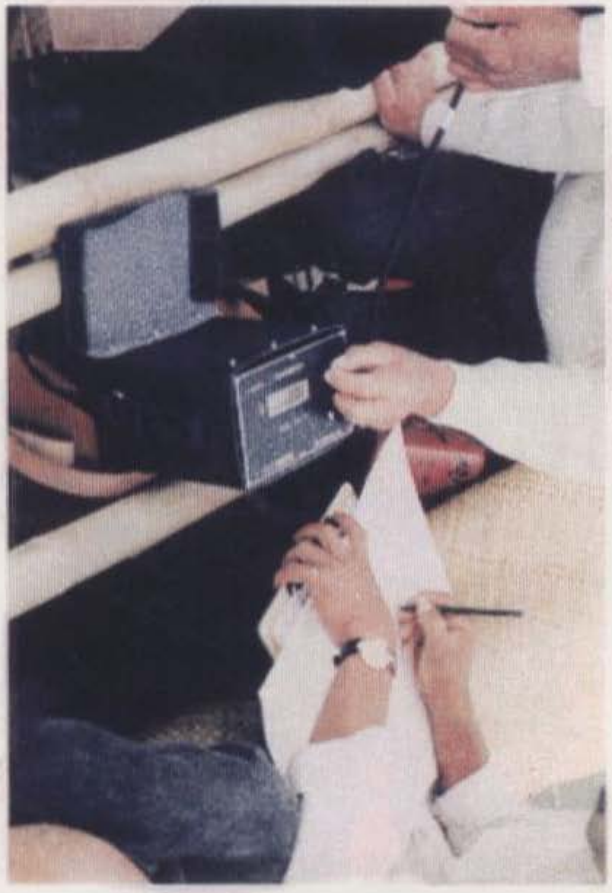

Fig.B.4-4 Photo of Salinometer (Type STC-2D)

Fig.B.4-5 **Photo of Anemometer Using in the Field Observations along the Shoreline and the Surf Zone**

Fig.B.4-6 **Photo of Dredging at the Shortcut Channel of the Brantas Estuary**

Copy Original Maps of the Delta Contours

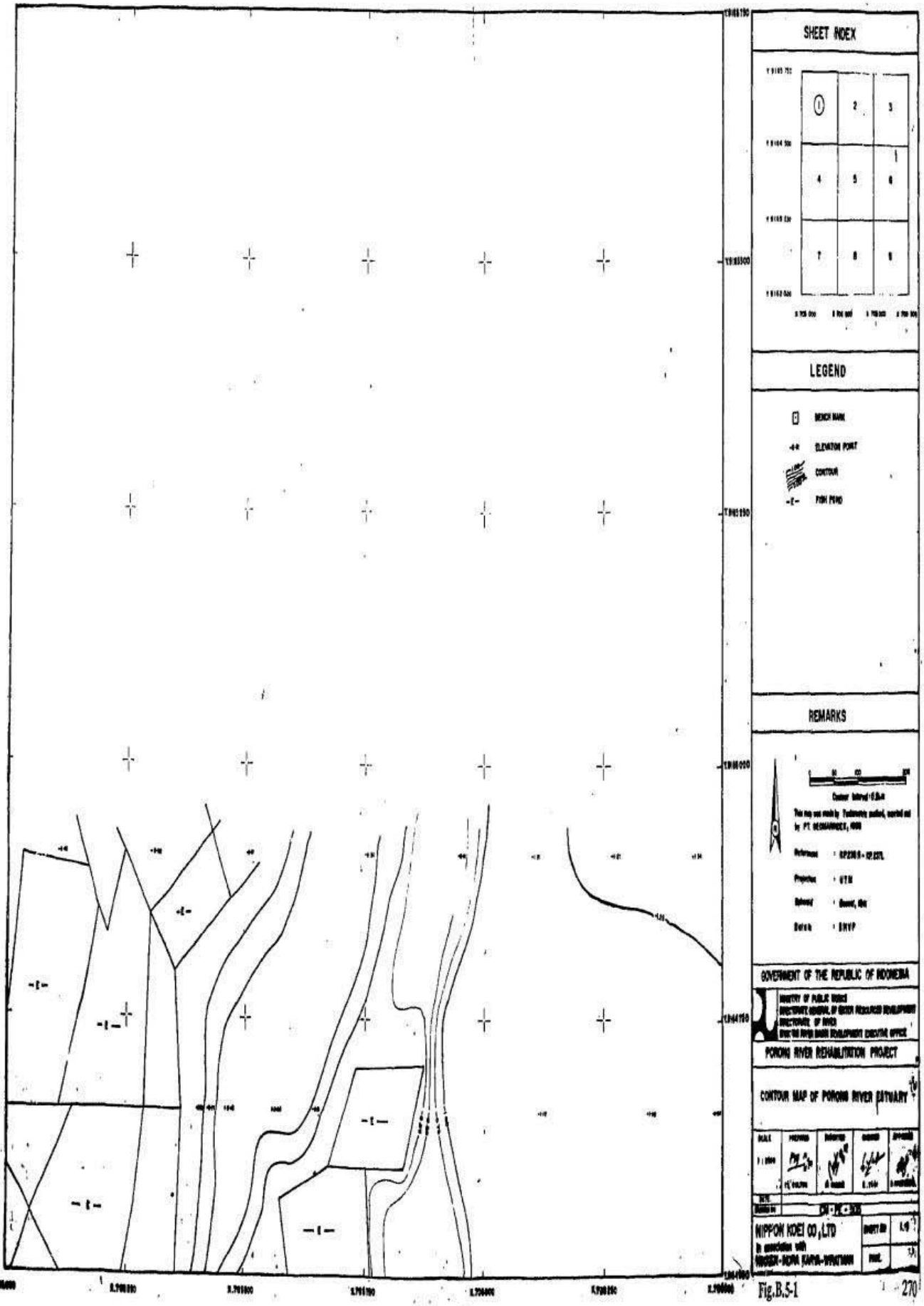
SHEET INDEX
LEGEND
BENCH MARK
ELEVATION POINT
CONTOUR
FISH POND
REMARKS
GOVERNMENT OF THE REPUBLIC OF INDONESIA
PORONG RIVER REHABILITATION PROJECT
CONTOUR MAP OF PORONG RIVER ESTUARY
NIPPON KOEI CO.,LTD
in association with
KRIDER-NORA KAPSA-WIRATAMA

Fig.B.5-1

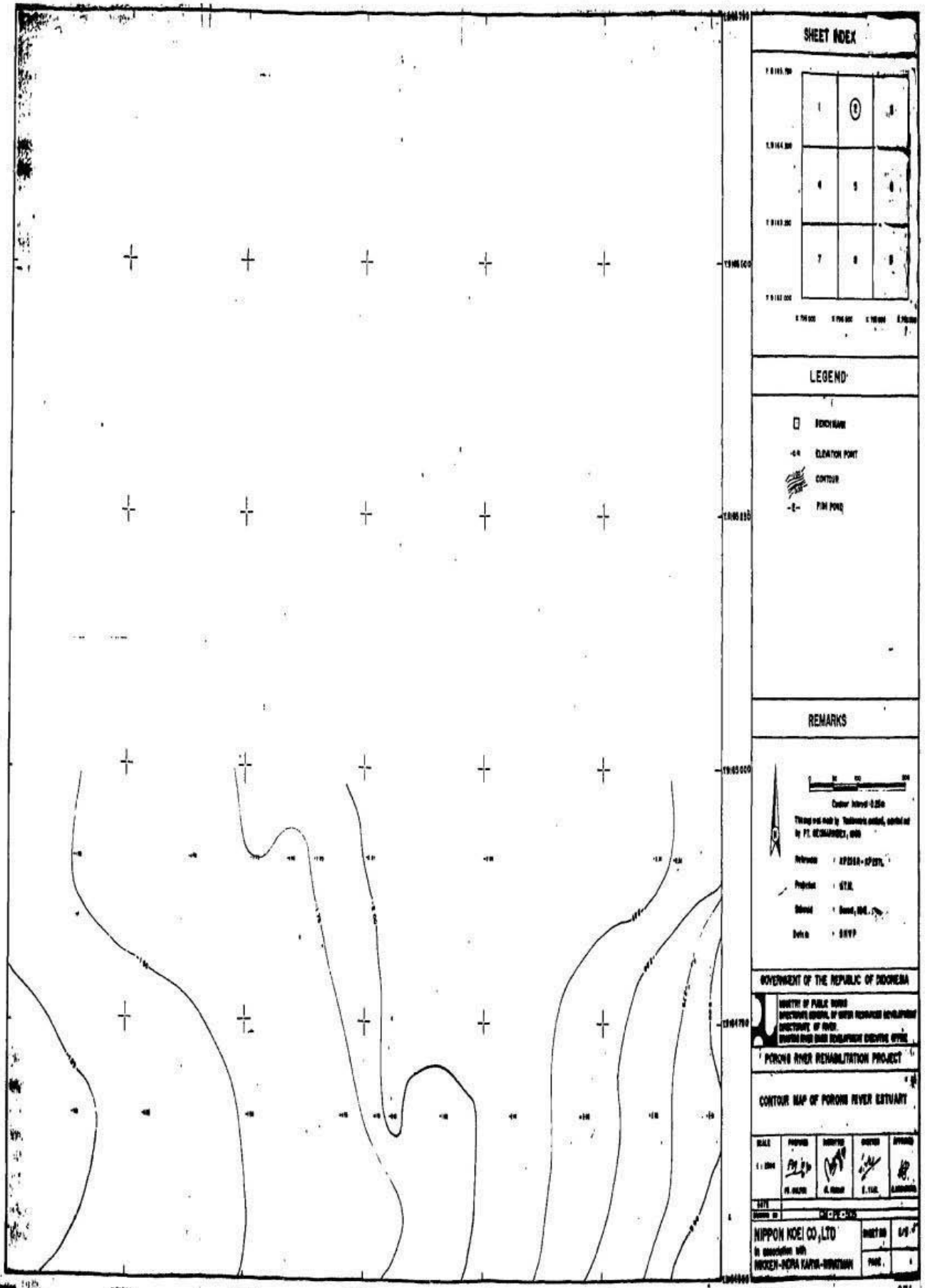
SHEET INDEX
LEGEND
BENCHMARK
ELEVATION POINT
CONTOUR
FISH POND
REMARKS
GOVERNMENT OF THE REPUBLIC OF INDONESIA
PORONG RIVER REHABILITATION PROJECT
CONTOUR MAP OF PORONG RIVER ESTUARY
NIPPON KOEI CO.,LTD
in association with
NIKKEN-NOPA KARYA-BINATAMA

Fig.B.5-2

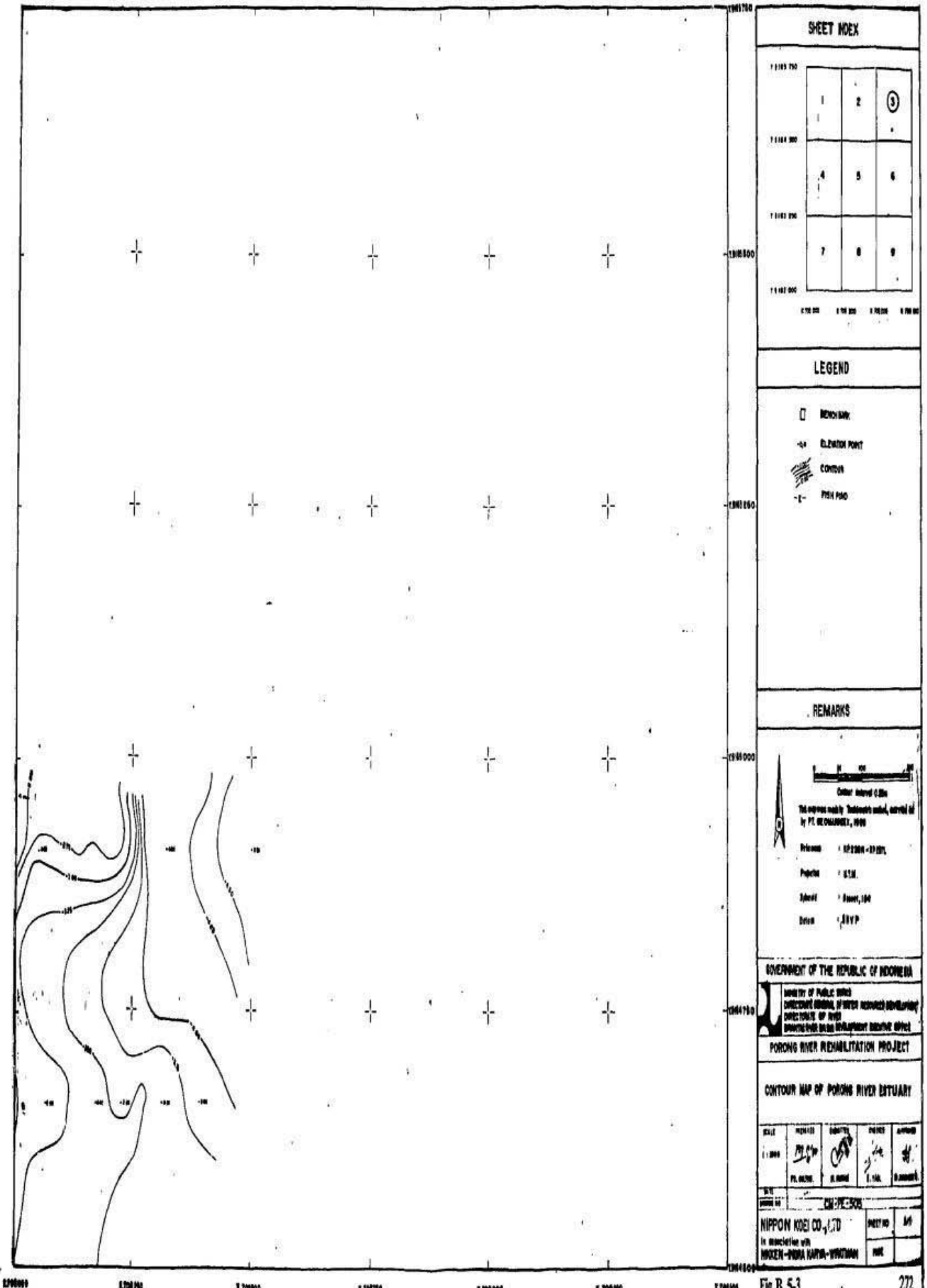
SHEET INDEX
1
2
3
4
5
6
7
8
9
LEGEND
BENCH MARK
ELEVATION POINT
CONTOUR
FISH POND
REMARKS
GOVERNMENT OF THE REPUBLIC OF INDONESIA
PORONG RIVER REHABILITATION PROJECT
CONTOUR MAP OF PORONG RIVER ESTUARY
NIPPON KOEI CO., LTD
in association with
NIKKEN-PRIMA KARYA-WINDIMAN

Fig.B.5-3

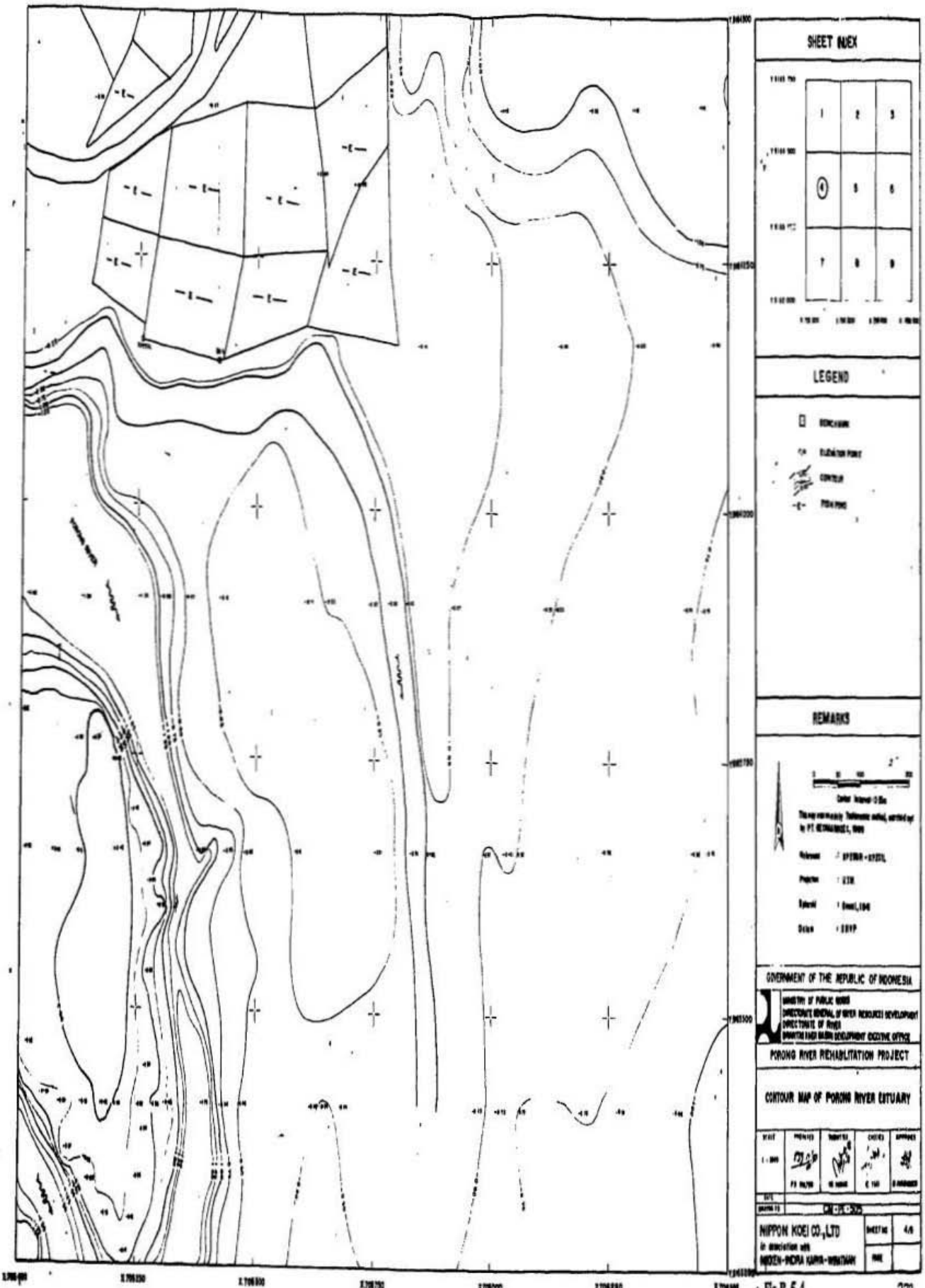
SHEET INDEX
LEGEND
REMARKS
GOVERNMENT OF THE REPUBLIC OF INDONESIA
PORONG RIVER REHABILITATION PROJECT
CONTOUR MAP OF PORONG RIVER ESTUARY
NIPPON KOEI CO.,LTD

Fig.B.5-4

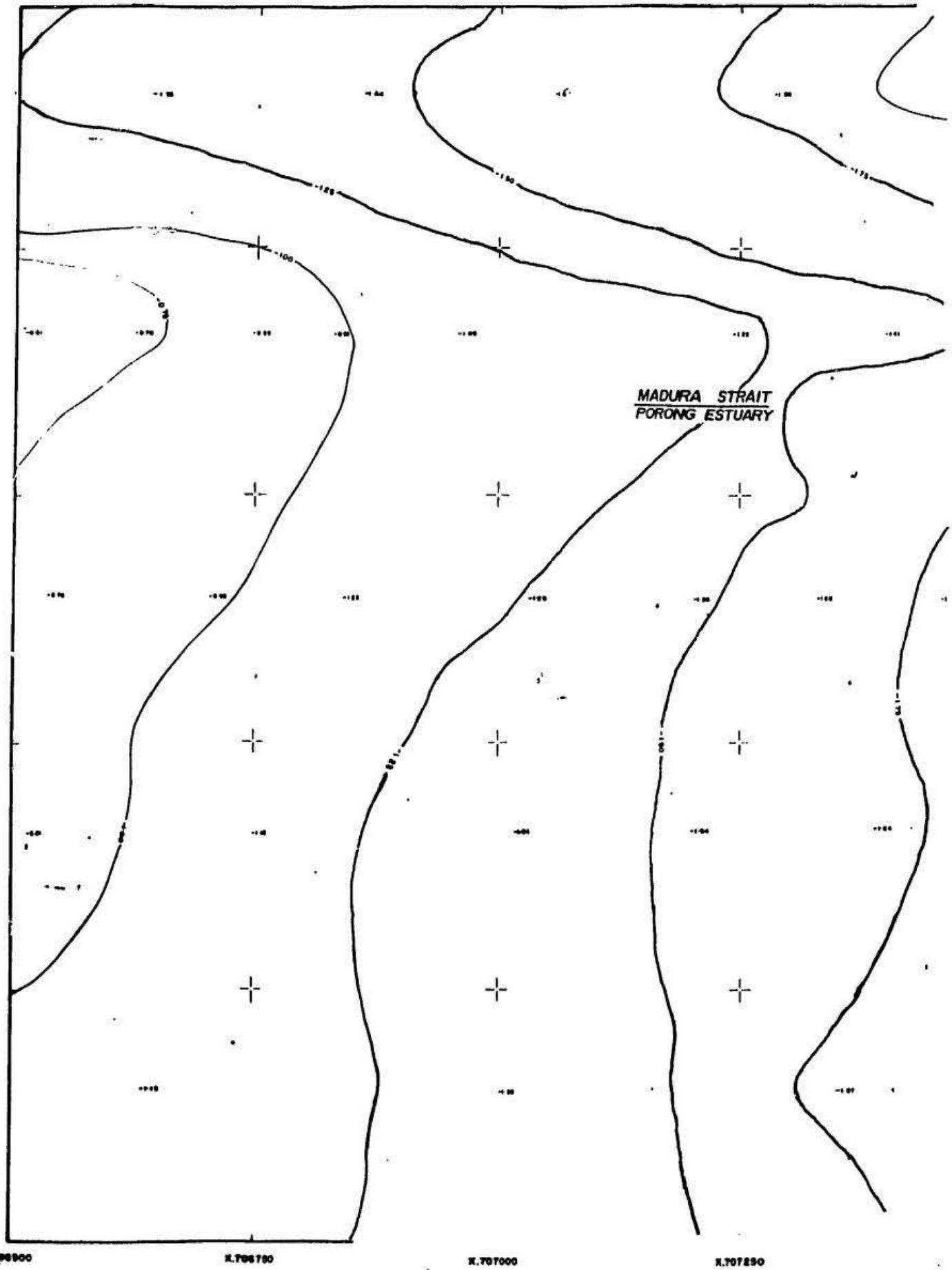
MADURA STRAIT
PORONG ESTUARY
X.706500
X.706750
X.707000
X.707250

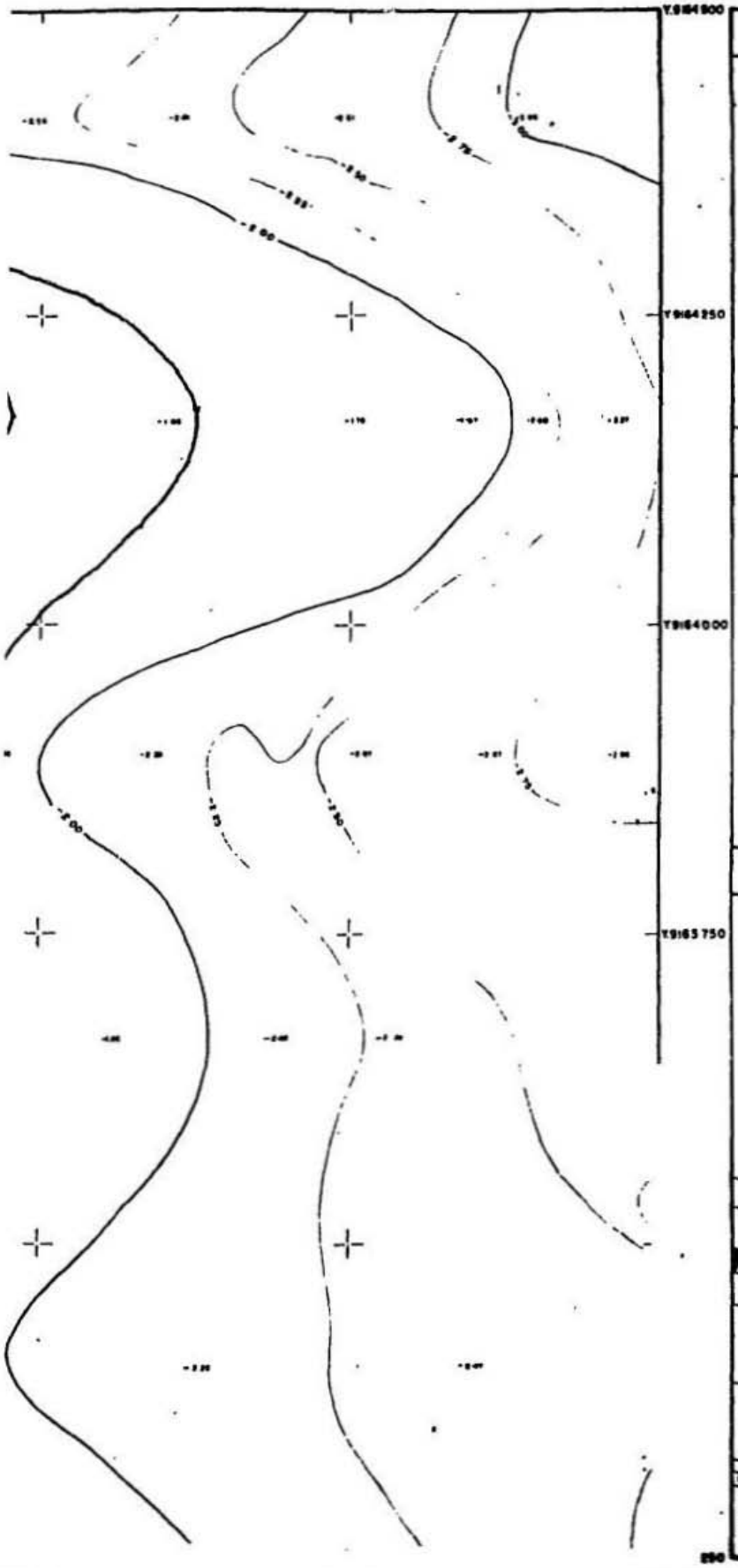

SHEET INDEX

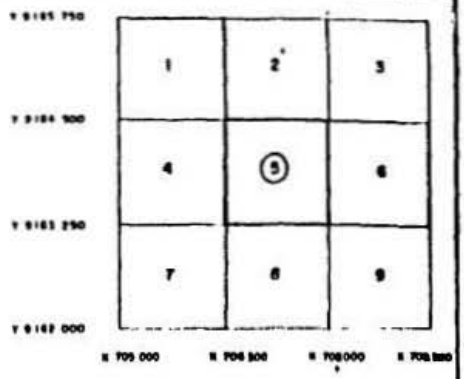

LEGEND

- BENCH MARK
- ELEVATION POINT
- CONTOUR
- FISH POND

REMARKS

Contour Interval : 0.25m

This map was made by Tachimetric method, carried out by PT. GEOMARINDO, 1990

Reference : KP 235R – KP 237L

Projection : UTM

Spheroid : Everest, 1830

Datum : SKVP

GOVERNMENT OF THE REPUBLIC OF INDONESIA

MINISTRY OF PUBLIC WORKS
DIRECTORATE GENERAL OF WATER RESOURCES DEVELOPMENT
DIRECTORATE OF RIVER
BRANTAS RIVER BASIN DEVELOPMENT EXECUTIVE OFFICE

PORONG RIVER REHABILITATION PROJECT

CONTOUR MAP OF PORONG RIVER ESTUARY

SCALE	PREPARED	DRAWN	CHECKED	APPROVED
1 : 2500				

DRAWING NO : CM - PE - 505

NIPPON KOEI CO.,LTD
in association with
RACHEN - SUMA KARYA - WIRATMAN

SHEET NO 8/9

PAGE

Fig.B.5-5

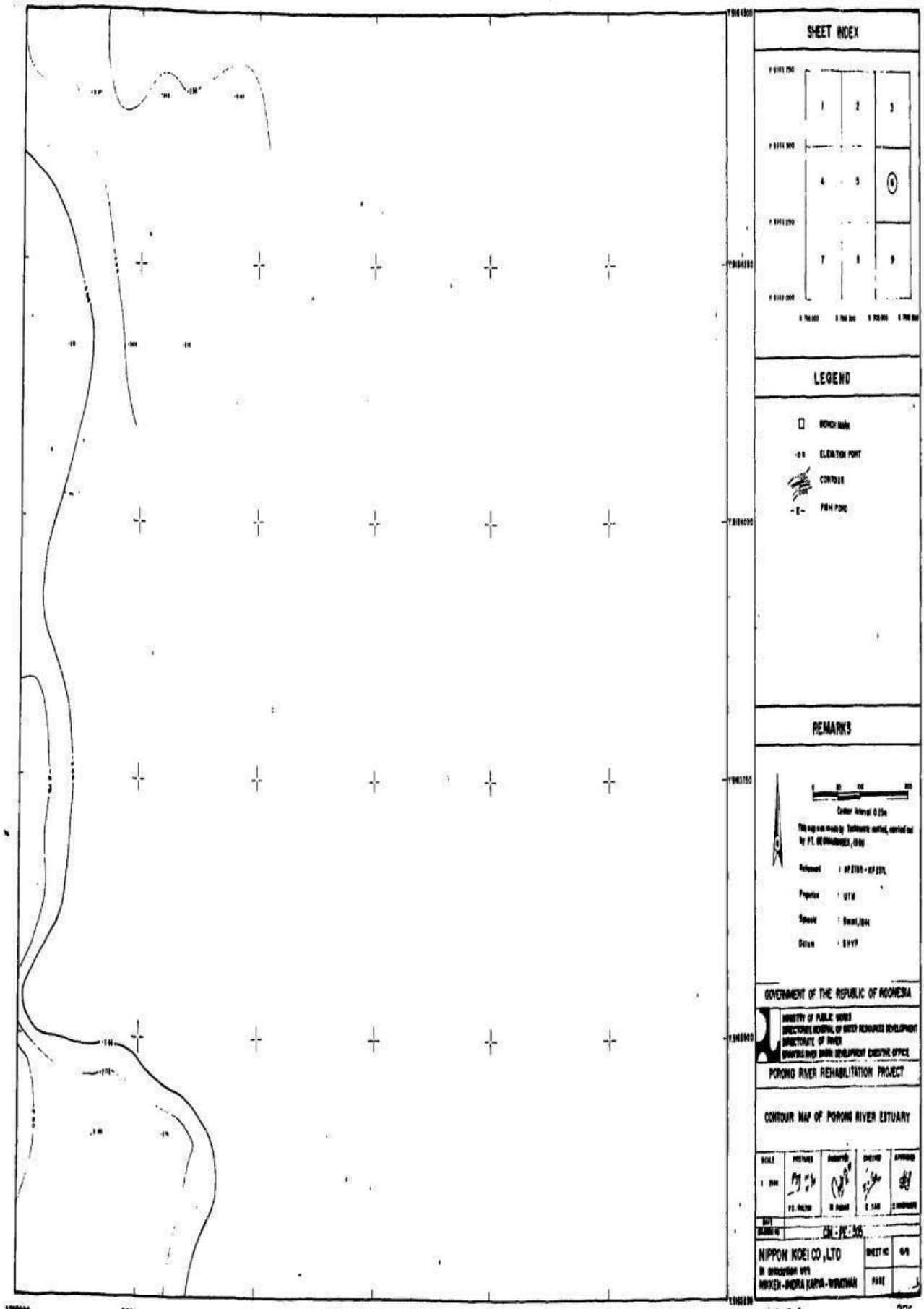
SHEET INDEX
1
2
3
4
5
6
7
8
9
LEGEND
BENCH MARK
ELEVATION POINT
CONTOUR
BOUNDARY POINT
REMARKS
Contour Interval 0.25m
Reference : WGS 1984
Projection : UTM
Spheroid : Bessel 1841
Datum : EVEREST
GOVERNMENT OF THE REPUBLIC OF INDONESIA
MINISTRY OF PUBLIC WORKS
DIRECTORATE GENERAL OF WATER RESOURCES DEVELOPMENT
DIRECTORATE OF RIVER
BRANTAS RIVER BASIN DEVELOPMENT EXECUTIVE OFFICE
PORONG RIVER REHABILITATION PROJECT
CONTOUR MAP OF PORONG RIVER ESTUARY
SCALE
1 : 2000
DRAWN
CHECKED
APPROVED
DRAWING NO.
CH - PE - 5.5
NIPPON KOEI CO., LTD
In association with
NIKKEN - INDRA KARYA - WINDHAM
SHEET NO.
6/9
PAGE
X 790000
X 790250
X 790500
X 790750
X 791000
X 791250
X 791500
Y 9164500
Y 9164250
Y 9164000
Y 9163750
Y 9163500

Fig.B.5-6

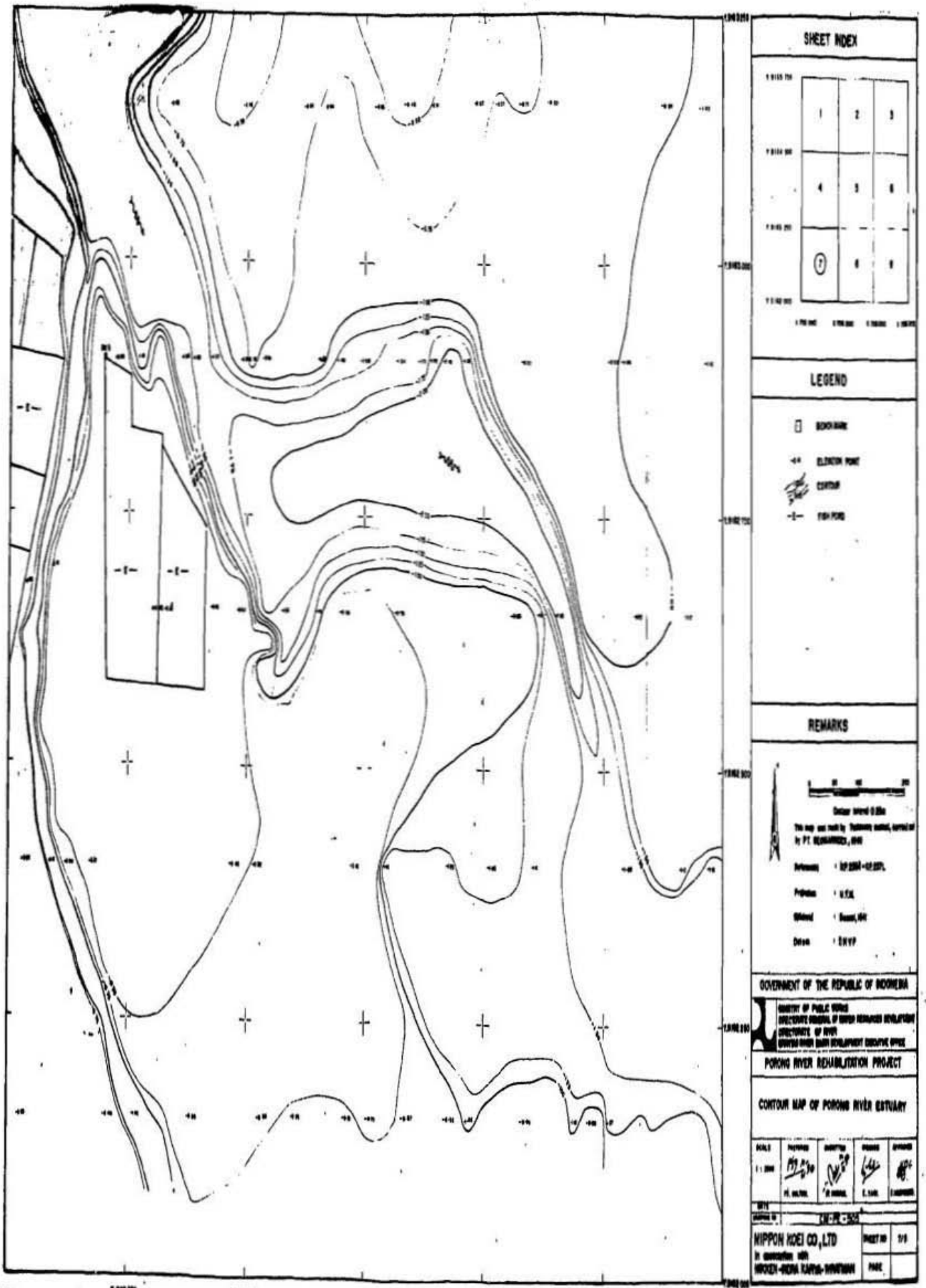
SHEET INDEX
1
2
3
4
5
6
7
8
9
LEGEND
REMARKS
GOVERNMENT OF THE REPUBLIC OF INDONESIA
PORONG RIVER REHABILITATION PROJECT
CONTOUR MAP OF PORONG RIVER ESTUARY
NIPPON KOEI CO.,LTD

Fig.B.5-7

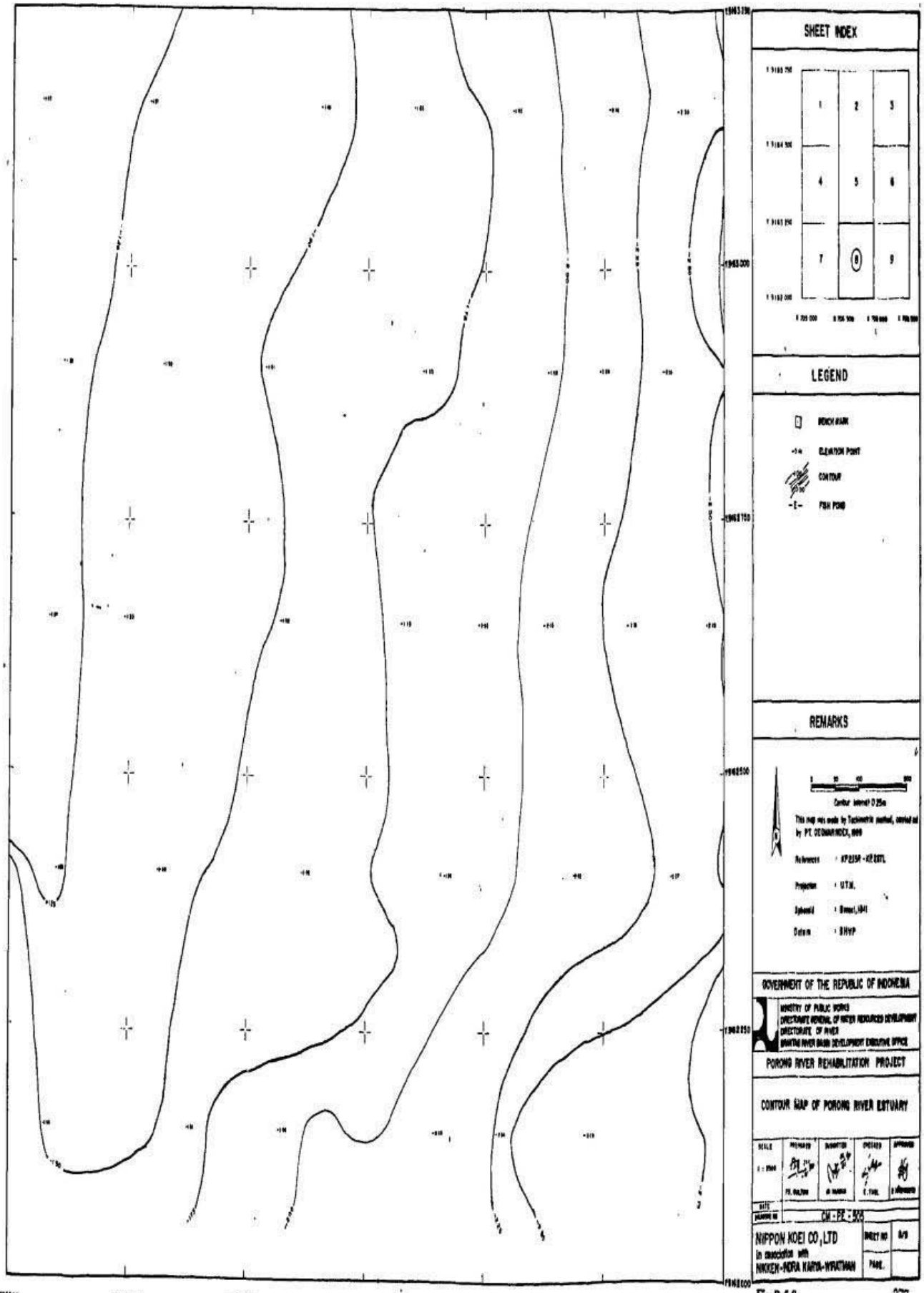
SHEET INDEX
1
2
3
4
5
6
7
8
9
LEGEND
BENCH MARK
ELEVATION POINT
CONTOUR
FISH POND
REMARKS
Contour interval 0.25m
This map was made by Tachometric method, carried out by PT. DESHARINDO, 1989
Reference : KP.0154 - KP.0371
Projection : U.T.M.
Spheroid : Bessel, 1841
Datum : BHVP
GOVERNMENT OF THE REPUBLIC OF INDONESIA
MINISTRY OF PUBLIC WORKS
DIRECTORATE GENERAL OF WATER RESOURCES DEVELOPMENT
DIRECTORATE OF RIVER
BANTEN RIVER BASIN DEVELOPMENT EXECUTIVE OFFICE
PORONG RIVER REHABILITATION PROJECT
CONTOUR MAP OF PORONG RIVER ESTUARY
SCALE
1 : 2500
PREPARED
CHECKED
APPROVED
DATE
DRAWING NO
CM - PE - 506
NIPPON KOEI CO, LTD
in association with
NIKKEN - NORA KARYA - WIRATMAN
SHEET NO
8/9
PAGE

Fig.B.5-8

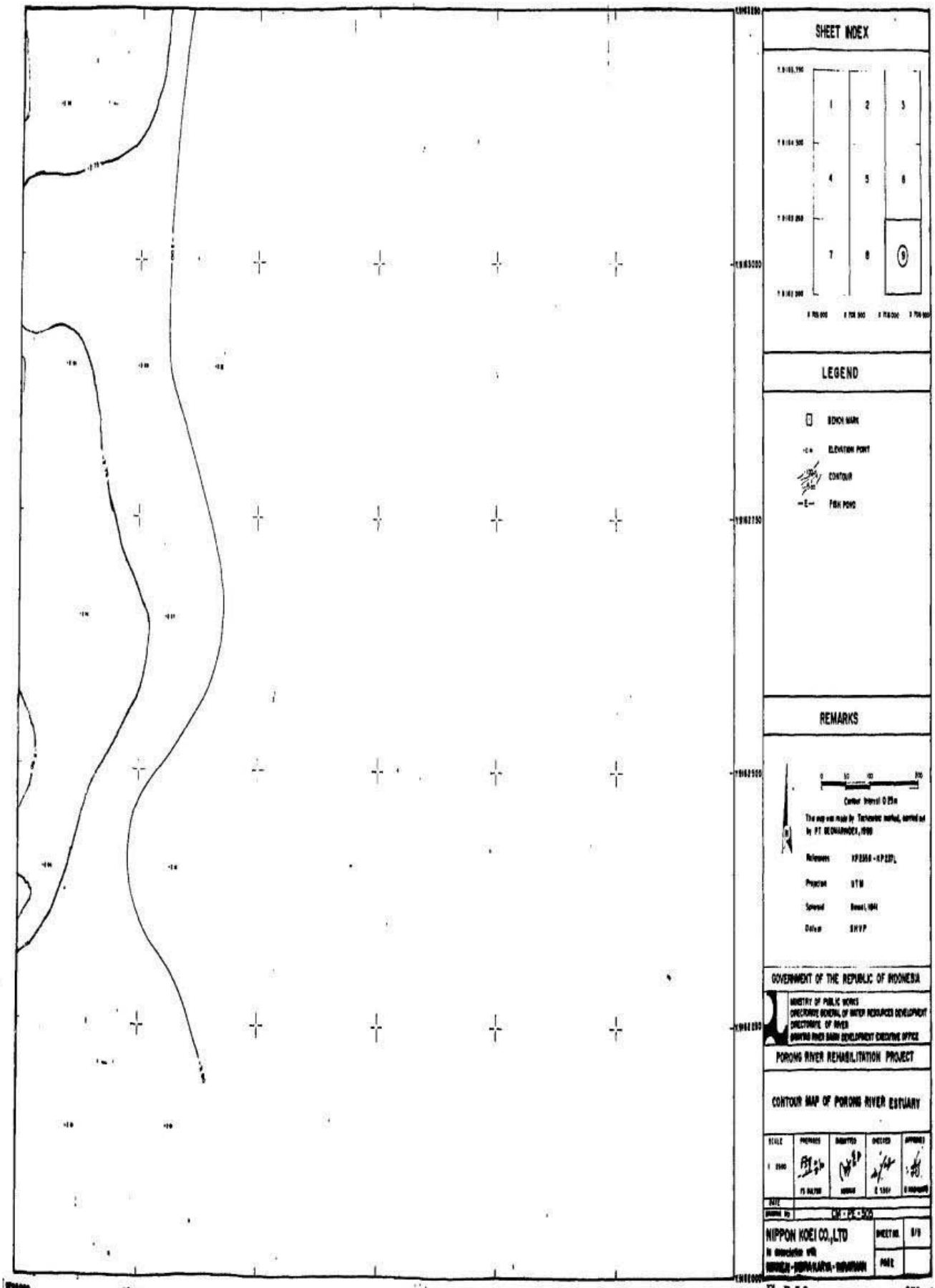
SHEET INDEX
1
2
3
4
5
6
7
8
9
LEGEND
BENCH MARK
ELEVATION POINT
CONTOUR
FISH POND
REMARKS
Contour Interval 0.25m
The map was made by Tachometer method, carried out by PT. BEDJAMARDJA, 1990
Projection UTM
Spheroid Bessel 1841
Datum SKYP
GOVERNMENT OF THE REPUBLIC OF INDONESIA
MINISTRY OF PUBLIC WORKS
DIRECTORATE GENERAL OF WATER RESOURCES DEVELOPMENT
DIRECTORATE OF RIVER
BRANTAS RIVER BASIN DEVELOPMENT EXECUTIVE OFFICE
PORONG RIVER REHABILITATION PROJECT
CONTOUR MAP OF PORONG RIVER ESTUARY
SCALE
1 : 2500
PREPARED
CHECKED
APPROVED
DATE
DRAWING No. CM - PR - 505
NIPPON KOEI CO., LTD
In association with
SHEET NO. 8/9
PAGE

Fig.B.5-9